

Copper-Catalyzed Borylation of Hemiaminal Ethers and Ruthenium-Catalyzed Tandem Reactions of Nitrogen-Tethered Dienes

Author: Lu Xiao

Persistent link: <http://hdl.handle.net/2345/bc-ir:107234>

This work is posted on [eScholarship@BC](#),
Boston College University Libraries.

Boston College Electronic Thesis or Dissertation, 2016

Copyright is held by the author, with all rights reserved, unless otherwise noted.

Boston College
The Graduate School of Arts and Sciences
Department of Chemistry

**COPPER-CATALYZED BORYLATION OF HEMIAMINAL
ETHERS AND RUTHENIUM-CATALYZED TANDEM
REACTIONS OF NITROGEN-TETHERED DIENES**

A dissertation

By

LU XIAO

Submitted in partial fulfillment of the requirements

for the degree of

Doctor of Philosophy

October 2016

© Copyright by LU XIAO

2016

COPPER-CATALYZED BORYLATION OF HEMIAMINAL ETHERS AND RUTHENIUM-CATALYZED TANDEM REACTIONS OF NITROGEN- TETHERED DIENES

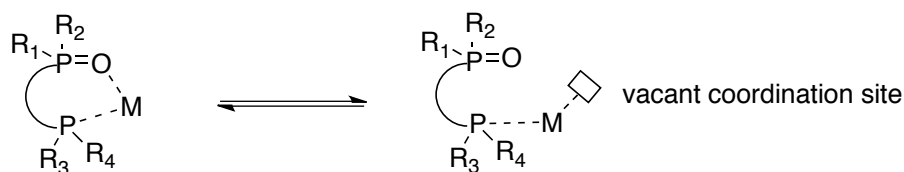
Lu Xiao

Dissertation Advisor: Professor Marc L. Snapper

Abstract

Chapter 1

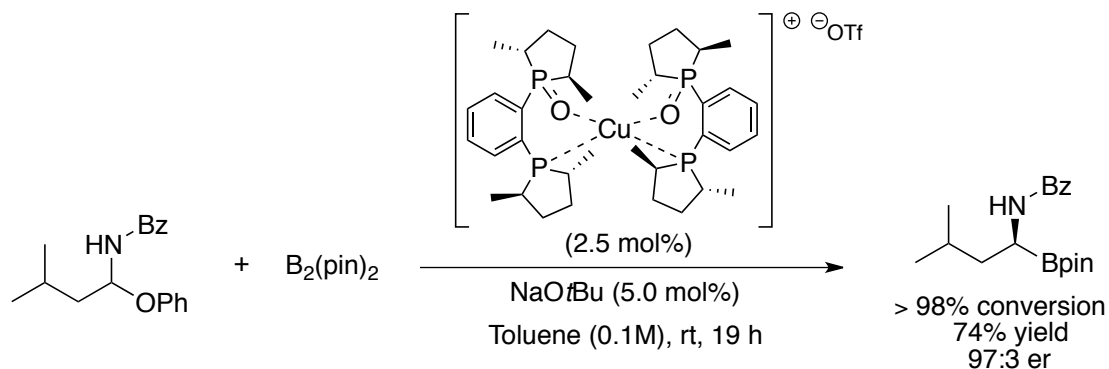
Bisphosphine monoxides have unique coordinating capabilities with transition metals. Several research groups have independently reported transition metal-catalyzed highly stereoselective reactions by using chiral bisphosphine monoxides as the ligands. A review of recent works in this field is provided in this chapter to showcase the features of this class of ligand.



Chapter 2

We have developed a copper-catalyzed borylation method to synthesize α -aminoboronic esters, which are biologically interesting molecules in enzyme inhibitions. Employment of hemiaminal ethers as substrates to *in situ* generate the corresponding aldimines obviated purification of the unstable aldimines and potential imine-enamine tautomerization. By using a chiral bisphosphine monoxide ligand in our copper-catalyzed

borylation conditions, we successfully synthesized a variety of enantioenriched alkyl-substituted α -aminoboronic esters in good yields and with good enantioselectivity.



Chapter 3

A ruthenium-catalyzed three-step tandem sequence was established to prepare nitrogen-protected 2,3-dihydroxypyrrolidines and 2,3-dihydroxypiperidines. This tandem sequence includes ring-closing metathesis, olefin isomerization and olefin dihydroxylation, and utilizes the second-generation Grubbs' catalyst as the initial ruthenium precatalyst. Readily accessible nitrogen-tethered dienes were used as the substrates to prepare the heterocyclic compounds in an efficient fashion. Through optimization, we discovered the optimal conditions for ruthenium-catalyzed dihydroxylation of ene-carbamates and ene-sulfonamides, which were the challenging substrates in the previous methods.

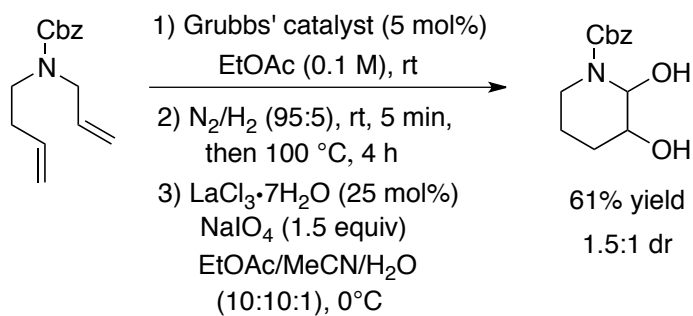


Table of Contents

List of Tables	vi
List of Schemes.....	viii
List of Figures	x
List of Equations	xii
List of Abbreviations	xiv

Chapter 1

Literature Review: Recent Examples of Using Chiral Bisphosphine

Monoxide Ligands in Transition Metal-Catalyzed Asymmetric

Reactions.....	1
1.1 General introduction	1
1.2 DuPhos-based chiral BPMOs	2
1.3 BINAP and SDP-based chiral BPMOs	12
1.4 QuinoxP*-based chiral BPMO	24
1.5 Conclusion	26

Chapter 2

Borylation of Hemiaminal Ethers: An Approach of Making

Enantioenriched Aliphatic α -Amino Boronates..... 27

2.1 General Introduction	27
--------------------------------	----

2.2 Precedents of enantioselective synthesis of α -aminoboronic esters	31
2.2.1 Substrate-controlled processes	31
2.2.2 Catalyst-controlled processes	35
2.2.3 Organocatalytic asymmetric syntheses of α -aminoboronic esters	41
2.3 Proposed catalytic synthesis of α -amido boronates with hemiaminal ethers	43
2.4 Development of copper-catalyzed borylation of hemiaminal ethers	45
2.4.1 Borylation of phenyl-substituted hemiaminal methyl ether	45
2.4.2 Copper-catalyzed borylation of alkyl-substituted hemiaminal ethers	50
2.4.3 Development of enantioselective borylation of aliphatic hemiaminal ethers ..	54
2.5 Conclusion	61
2.6 Experimental Procedures and Characterization	62

Chapter 3

Ruthenium-Catalyzed Tandem Reactions for Constructing N-Protected

2,3-Dihydroxypyrrolidines and 2,3-Dihydroxypiperidines..... 184

3.1 General Introduction	184
3.2 Background	190
3.2.1 Tandem RCM/olefin isomerization process	190
3.2.2 Ruthenium tetroxide-catalyzed dihydroxylation of olefins	197
3.2.3 Low-valent Ruthenium oxide-catalyzed dihydroxylation of olefins	201
3.2.4 Tandem RCM/olefin dihydroxylation reactions	202
3.3 Modification of previously established RCM/olefin isomerization condition	205

3.4 Development of tandem RCM/olefin isomerization/olefin dihydroxylation sequence	209
3.5 Conclusion	218
3.6 Experimental Procedures and Characterizations	218

List of Tables

Table 1.1 Optimization of catalyst and ligand loadings and additives	3
Table 1.2 Control experiments for ligand identification.....	4
Table 1.3 Ligand effect on the reactivity and stereoselectivity	9
Table 1.4 Effect of different Lewis hard groups on the reactivity and stereoselectivity ..	10
Table 1.5 Ligand effect on arylation of 2,3-dihydrofuran	15
Table 1.6 Ligand effect on arylation of cyclopentene	16
Table 1.7 Effect of the substrate structure on the reactivity and stereoselectivity	22
Table 2.1 The influence of base loading ^b	46
Table 2.2 Screening of different copper precatalysts ^c	48
Table 2.3 Further studies of other variables in the borylation reactions ^d	49
Table 2.4 Optimization of the reaction condition of synthesis of 2.54 ^e	51
Table 2.5 Influence of temperature and substrate structure on the reactivity ^c	53
Table 2.6 Ligand screening in enantioselective borylation	55
Table 2.7 Further optimization of the borylation condition.....	57
Table 2.8 A time study of the borylation reaction	58
Table 3.1 N ₂ /H ₂ mixture as the hydride source in tandem RCM/olefin isomerization....	196
Table 3.2 RuO ₄ -catalyzed olefin dihydroxylation in a solvent mixture.....	198
Table 3.3 Influence of different additives on chemoselectivity and yield of dihydroxylation	199
Table 3.4 Influence of CeCl ₃ as an additive on pH and redox potential.....	200

Table 3.5 Representative examples of Blechert's tandem RCM/olefin dihydroxylation	203
Table 3.6 Representative examples of Snapper's tandem RCM/olefin dihydroxylation	204
Table 3.7 Solvent effect on tandem RCM/olefin isomerization reaction	205
Table 3.8 Optimization of the olefin isomerization step	206
Table 3.9 Optimization of the olefin isomerization step	207
Table 3.10 Optimization of olefin isomerization step	208
Table 3.11 Exploration of key factors in the olefin dihydroxylation step	210
Table 3.12 Kobayashi's study of dihydroxylation of ene-carbamate 3.80	212
Table 3.13 Further optimization of the olefin dihydroxylation step	214
Table 3.14 Substrate scope of tandem RCM/olefin isomerization/olefin dihydroxylation	216

List of Schemes

Scheme 1.1 <i>in situ</i> Generated alkyl imines in copper-catalyzed nucleophilic addition.....	6
Scheme 1.2 Proposed model for the stereoselectivity in Hayashi's arylation	14
Scheme 1.3 Synthetic application of Zhou's arylation method	17
Scheme 1.4 Proposed coordination equilibrium assisted by a functional group	22
Scheme 1.5 Proposed coordination equilibrium assisted by a hemilabile ligand	23
Scheme 1.6 Proposed catalytic cycle of the designed amination reaction.....	25
Scheme 2.1 α -aminoboronic esters in enantiospecific Suzuki-Miyaura cross-coupling...	29
Scheme 2.2 The first example of enantioselective synthesis of α -amino boronic esters .	32
Scheme 2.3 Industrial synthesis of Bortezomib.....	32
Scheme 2.4 Tandem diboration/pivaloylation of aromatic N-(trimethylsilyl) aldimines.	40
Scheme 2.5 1,2-boryl rearrangement of non-protected α -amino boronic acid pinacol esters	45
Scheme 2.6 Two possible pathways of the aldimine intermediate in the nucleophilic addition	47
Scheme 2.7 Proposed NaOMe-mediated borylation of aldimine 2.50	47
Scheme 2.8 Preparation of an alkyl-substituted hemiaminal ether 2.53	50
Scheme 2.9 Proposed dissociation equilibrium of deprotonated substrate 2.53	52
Scheme 2.10 Preparation of the new hemiaminal ether 2.58.....	53
Scheme 3.1 Proposed tandem RCM/olefin isomerization/dihydroxylation sequence.....	185
Scheme 3.2 Racemic 2,3-dihydropiperidine in Wittig reaction.....	187
Scheme 3.3 Enantioselective synthesis of 2,3-dihydropiperidine diacetate	187

Scheme 3.4 2,3-Dihydropiperidine diacetate as an acyliminium ion precursor	188
Scheme 3.5 2,3-Dihydropyrrolidine in Petasis borono-Mannich addition	189
Scheme 3.6 The proposed pathway of epimerization of the hydroxyl group at C-2 position.....	213

List of Figures

Figure 1.1 Representative chelation mode of hemilabile ligands with transition metals ...	1
Figure 1.2 Methyl-DuPhos and Methyl-DuPhos monoxide	2
Figure 1.3 (<i>R</i>)-BINAP and (<i>R</i>)-BINAP monoxide, (<i>R</i>)-Xyl-SDP and (<i>R</i>)-Xyl-SDP monoxide.....	12
Figure 1.4 (<i>R</i>)-Xyl-SDP(O) in enantioselective intermolecular Heck reaction	17
Figure 1. 5 Scope of triflates in intermolecular cyclization reactions	19
Figure 1.6 Aryl halides in enantioselective intermolecular Heck reaction	21
Figure 1.7 Ligand effect on the stereoselectivity of desymmetrization of 1,6-diene	23
Figure 1.8 Ligand effect on the stereoselectivity of desymmetrization of 1,6- and 1,4- dienes	23
Figure 1.9 Quinox* and Quinox* monoxide	24
Figure 1.10 Structure of Elbasvir.....	25
Figure 2.1 Examples of α -aminoboronic acid-based enzyme inhibitors.....	28
Figure 2.2 Proposed models for observed diastereoselectivity.....	34
Figure 2.3 Cu(I)/chiral sulfoxide-phosphine complex in borylation of N-Boc-imines	37
Figure 2.4 The deuterium-labeling experiment in Tang's hydroboration study	41
Figure 2.5 Proposed catalytic cycle of borylation of hemiaminal ethers.....	44
Figure 2.6 Single crystal x-ray structure of enantioenriched compound 2.54	59
Figure 2.7 Substrate scope of the enantioselective borylation of hemiaminal ethers	60
Figure 2.8 Preparation of hemiaminal phenyl ethers	70
Figure 3.1 Commercially available Grubbs' catalysts.....	185

Figure 3.2 A general mechanism of transition metal hydride-catalyzed olefin isomerization.....	190
Figure 3.3 Additive-free strategy for tandem RCM/olefin isomerization	191
Figure 3.4 NaH and NaBH ₄ as the hydride source in tandem RCM/olefin isomerization	192
Figure 3.5 Triethylsilane as the hydride source in tandem RCM/olefin isomerization ..	193
Figure 3.6 <i>i</i> -Propanol/NaOH as the additive in tandem RCM/olefin isomerization.....	194
Figure 3.7 Energy diagram of oxidative olefin cleavage via RuO ₄ and OsO ₄	197
Figure 3.8 Proposed catalytic cycle of RuO ₄ -catalyzed olefin dihydroxylation.....	200
Figure 3.9 Proposed transition states of β -hydride elimination.....	209

List of Equations

Equation 1.1 Cu(OTf) ₂ /Methyl-DuPhos catalyzed nucleophilic addition of imines	3
Equation 1.2 New reaction condition based on Methyl-DuPhos monoxide ligand.....	5
Equation 1.3 Alkyl-substituted α -amino sulfones in nucleophilic addition	6
Equation 1.4 A one-pot condition of preparation of enantioenriched secondary amines ...	7
Equation 1.5 Preparation of trifluoromethyl-substituted hemiaminal ethyl ethers.....	8
Equation 1.6 Copper-catalyzed nucleophilic addition of hemiaminal ethyl ethers	8
Equation 1.7 Copper-catalyzed nucleophilic addition of diethylzinc to β -nitroalkenes...	11
Equation 1.8 Enantioselective reduction of β,β -disubstituted vinyl phenyl sulfones.....	12
Equation 1.9 Hayashi's catalyst system for arylation of 2,3-dihydrofuran	13
Equation 1.10 Norbornene in intermolecular cyclization reaction	19
Equation 1.11 Designed Buchwald-Hartwig amination reaction	25
Equation 2.1 α -sulfinamido trifluoroborates in Rh-catalyzed addition to trifluoromethyl ketones.....	30
Equation 2.2 NHC–Cu(I)-catalyzed borylation of <i>N-tert</i> -butanesulfinyl aldimines	33
Equation 2.3 A benzimidazole-derived NHC ligand in borylation of aldimines and ketimines	35
Equation 2.4 Chiral NHC-Cu(I)- catalyzed borylation of aromatic aldimines	36
Equation 2.5 α -Benzamido sulfones as substrates in enantioselective borylation	36
Equation 2.6 Cu(I)-catalyzed enantioselective hydroamination of alkenyl Bdan compounds	39

Equation 2.7 Rh(I)-catalyzed enantioselective hydroboration of α -aryl-N-Acylenamines	41
Equation 2.8 NHC-catalyzed hydroboration of (<i>R</i>)-N- <i>tert</i> -butanesulfinylaldimines and imines	42
Equation 2.9 Chiral diphosphines for enantioselective hydroboration of tosylaldimines	43
Equation 2.10 The initial evaluation of an alkyl hemiaminal ether in the borylation conditions	50
Equation 2.11 α -amido sulfone as the substrate in borylation reaction.....	54
Equation 2.12 The new reaction condition for borylation of hemiaminal ethers	59
Equation 3.1 NaOH as an additive in tandem RCM/olefin isomerization.....	195
Equation 3.2 N ₂ /H ₂ as the hydride source in tandem RCM/olefin isomerization.....	196
Equation 3.3 Ru(III)-catalyzed olefin dihydroxylation	202

List of Abbreviations

Å: angstrom	DABCO: 1,4-Diazabicyclo[2.2.2]octane
Ac: acetyl	DART: direct analysis in real time
Ar: aryl	dba: dibenylidene acetone
aq: aqueous	DBU: 1,8-diazabicyclo[5.4.0]undec-7-
BF ₃ : boron trifluoride	ene
BF ₄ : tetrafluoroborate	DCE: dichloroethane
BINAP: 2,2'-bis(diphenylphosphino)-	DFT: density functional theory
1,1'-binaphthalene	DMAP: 4-(Dimethylamino)pyridine
Bn: benzyl	DMF: N,N-dimethylformamide
Boc: <i>tert</i> -butoxycarbonyl	dr: diastereomeric ratio
B ₂ (pin) ₂ : bis(pinacolato)diboron	ee: enantiomeric excess
BPMO: bisphosphine monoxide	equiv: equivalent
Bu: butyl	er: enantiomeric ratio
Bz: benzoyl	(<i>R,R</i>)-EtDuPhos: 1,2-bis[(2 <i>R</i> , 5 <i>R</i>)-2,5-
Cbz: carboxybenzyl	diethylphospholano]benzene
CDI: carbonyl diimidazole	ESI: electrospray ionization
CDCl ₃ : deuterated chloroform	Et: ethyl
CD ₂ Cl ₂ : deuterated dichloromethane	Et ₂ O: diethyl ether
CM: cross metathesis	EtOAc: ethyl acetate
cod: cyclooctadiene	EtOH: ethanol
Cy: cyclohexyl	Et ₃ SiH: triethylsilane

Et ₃ Si: triethylsilyl	M.S.: molecular sieve
FTIR: Fourier transform infrared	MTBE: methyl <i>tert</i> -butyl ether
GLC: gas liquid chromatography	N: nitrogen
GI: Grubbs catalyst 1 st generation	NHC: N-heterocyclic carbene
GII: Grubbs catalyst 2 nd generation	NMO: 4-methylmorpholine N-oxide
h: hour(s)	NMR: nuclear magnetic resonance
HMDS: bis(trimethylsilyl)amine	OAc: acetate
HPLC: high performance liquid chromatography	OPh: phenoxy
HPFC: high performance flash chromatography	OTf: trifluoromethanesulfonate
HRMS: high resolution spectrometry	PCy ₃ : tricyclohexylphosphine
H ₂ SO ₄ : sulfuric acid	Ph: phenyl
<i>i</i> : isopropyl	PhH: benzene
L: ligand	PhMe: toluene
LiHMDS: lithium bis(trimethylsilyl) amide	PG: protecting group
M: molar	PPh ₃ : triphenylphosphine
Me: methyl	PMA: phosphomolybdic acid
MeCN: acetonitrile	PMP: <i>para</i> -methoxyphenyl
(<i>R,R</i>)-MeDuPhos: 1,2-bis[(2 <i>R</i> , 5 <i>R</i>)-2,5-dimethylphospholano]benzene	PTFE: polytetrafluoroethylene
MeOH: methanol	Pr: propyl
	Quinap: 1-(2-diphenylphosphino-1-naphthyl)isoquinoline
	R ₁ and R ₂ : alkyl group
	RCM: ring-closing metathesis

rt: room temperature

(*R*)-xyl-SDP: (*R*)-(+)-7,7'-bis[di(3,5-

dimethylphenyl)phosphino]-1,1'-

spirobiindane

SFC: supercritical fluid chromatography

TBS: *tert*-butyldimethylsilyl

TFA: trifluoroacetic acid

THF: tetrahydrofuran

TMSCl: trimethylsilyl chloride

Ts: *p*-toluenesulfonyl

(*R,R*)-QuinoxP*: (*R,R*)-(-)-2,3-bis(tert-

butylmethylphosphino)quinoxaline

(*R*)-(*R_p*)-Walpos (CF₃): (*R*)-1-{(*R_p*)-2-

[2-(diphenylphosphino)phenyl]-

ferrocenyl}ethylbis[3,5-

bis(trifluoromethyl)phenyl]phosphine

Chapter 1

Literature Review: Recent Examples of Using Chiral Bisphosphine Monoxide Ligands in Transition Metal- Catalyzed Asymmetric Reactions

1.1 General introduction

Since the concept of “hemilabile ligand” was proposed in the 1970s,¹ it has become an attractive direction in new ligand design. This class of ligand is consisted of a Lewis soft group, a Lewis hard group and the linker between these two fragments that possess distinctive coordinating capabilities. The soft moiety has strong affinity with a low-valent transition metal, but the hard moiety binds to the same metal in a relatively weak and reversible fashion. Compared to a conventional bidentate ligand, a hemilabile ligand can readily provide a vacant coordinating site on the chelated metal; compared to a monodentate ligand, a hemilabile ligand can contribute more stabilization to the chelated metal. This unique chelation mode sometimes leads to unexpected reactivity and/or selectivity in a transition metal-catalyzed reaction.

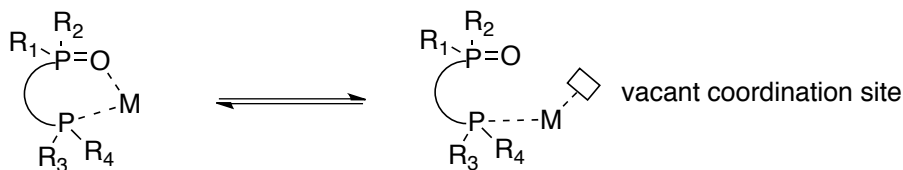


Figure 1.1 The representative chelation mode of hemilabile ligands with transition metals

¹ For reviews, see: (a) Bader, A.; Lindner, E. *Coord. Chem. Rev.* **1991**, *108*, 27-110. (b) Braunstein, P.; Naud, F. *Angew. Chem. Int. Ed.* **2001**, *40*, 680-699. (c) Bassetti, M. *Eur. J. Inorg. Chem.* **2006**, 4473-4482.

Bisphosphine monoxides (BPMOs) constitute a broad and important branch in the field of hemilabile ligand.² Their phosphine fragments can bind to various transition metals, whereas the phosphine oxide fragments serve as the labile coordinating sites. Recently, several groups separately reported highly enantioselective reactions employing chiral BPMO ligands. This chapter will provide a review of their studies.

1.2 DuPhos-based chiral BPMOs

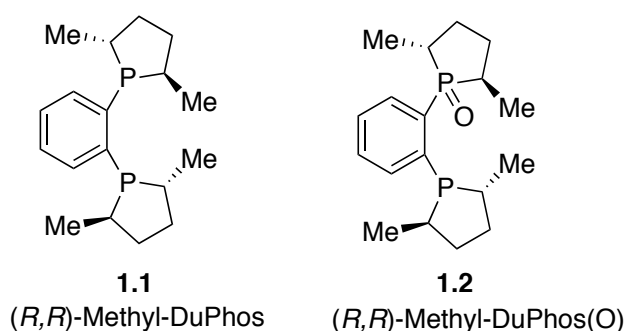


Figure 1.2 Methyl-DuPhos and Methyl-DuPhos monoxide

In the study of copper-catalyzed nucleophilic addition of dialkylzinc reagents to *N*-phosphinoylaldimines,³ Charette initially found that 5 mol% Cu(OTf)₂ and 5.5 mol% **1.1** served as the most effective catalyst system in the model reaction.^{3a} During optimization they found that the stereoselectivity could be further improved by using additives. Addition of 5 mol% Zn(OTf)₂ (entry 3, Table 1.1) or simply employing 10 mol% Cu(OTf)₂ (entry 4, Table 1.1) improved the enantioselectivity to 96% ee, but a comparable yield was only obtained in the latter case (entry 1 and 4, Table 1.1). With the optimal conditions Charette and coworkers tested a variety of aryl-substituted *N*-

² For a review, see: Grushin, V. *Chem. Rev.* **2004**, *104*, 1629-1662.

³ (a) Boezio, A. A.; Charette, A. B. *J. Am. Chem. Soc.* **2003**, *125*, 1692-1693. (b) Boezio, A. A.; Pytkowicz, J.; Côté, A.; Charette, A. B. *J. Am. Chem. Soc.* **2003**, *125*, 14260-14261.

phosphinoylimines in the reaction. High yields and enantioselectivities were obtained from almost all the surveyed substrates.

$\text{Ph-CH=N-P(=O)(Ph)2} \xrightarrow[\text{Et}_2\text{Zn (2.0 equiv)}]{\text{Cu(OTf)}_2 \text{ (x mol\%)} \text{ and } \mathbf{1.1} \text{ (y mol\%)}} \text{Ph-CH(Et)-NH-P(=O)(Ph)2}$

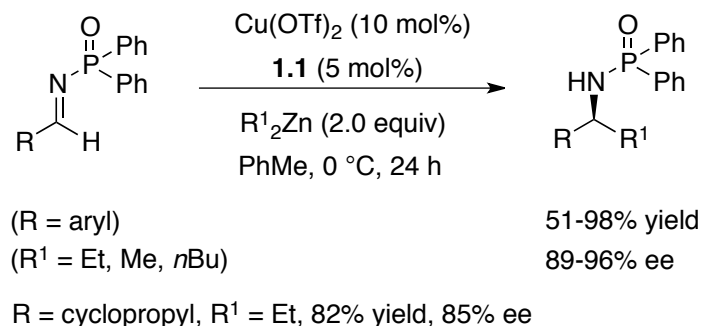
1.3 **1.4**

PhMe, 0 °C, 24 h

Entry	Cu(OTf) ₂ (mol%)	1.1 (mol%)	Additive (mol%)	Conversion (%) ^a	ee (%) ^b
1	5.0	5.5	—	96	93
2	8.0	8.5	—	96	96
3	5.0	5.5	Zn(OTf) ₂ (5.0)	86	96
4	10.0	5.0	—	95	95

^aDetermined by ¹H-NMR. ^bDetermined by chiral HPLC.

Table 1.1 Optimization of catalyst and ligand loadings and additives



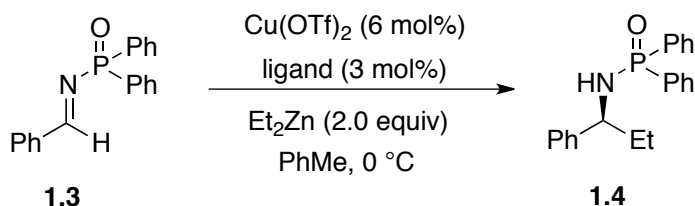
Equation 1.1 Cu(OTf)₂/Methyl-DuPhos Catalyzed nucleophilic addition of imines

Meanwhile, Charette's group conducted a mechanistic study of the reaction of Table 1.1.⁴ They observed that the addition sequence of required reagents is critical to the reaction outcome. If Cu(OTf)₂ (6 mol%) and ligand **1.1** (3 mol%) were mixed for 1 h before Et₂Zn (2.0 equiv) was added, 92% conversion and 89% ee were obtained (entry 1, Table 1.2). If Cu(OTf)₂ and Et₂Zn were mixed before the ligand was added, 38%

⁴ Côté, A.; Boezio, A. A.; Charette, A. B. *Angew. Chem. Int. Ed.* **2004**, *43*, 6525-6528.

conversion and a racemic product were obtained (entry 2, Table 1.2). According to these observations, Charette proposed that premixing $\text{Cu}(\text{OTf})_2$ and **1.1** caused the electron-rich phosphines to be oxidized by $\text{Cu}(\text{II})$, and that the *in situ* generated phosphine oxide species was the actual ligand responsible for high reactivity and enantiocontrol.

To test the hypothesis, Methyl-Duphos monoxide and bisoxide were synthesized and evaluated in the reaction respectively. The results of control experiments unambiguously indicated that **1.2** is a better ligand in the copper-catalyzed nucleophilic addition (entry 3 and 4, Table 1.2). With Methyl-DuPhos bisoxide the reaction still reached over 80% conversion, but produced no stereoselectivity. In addition, Charrete investigated oxidation of Methyl-DuPhos by different $\text{Cu}(\text{I})$ and $\text{Cu}(\text{II})$ salts. The results suggested that Methyl-DuPhos monoxide **1.2** is generated by mixing Methyl-DuPhos and $\text{Cu}(\text{OTf})_2$.



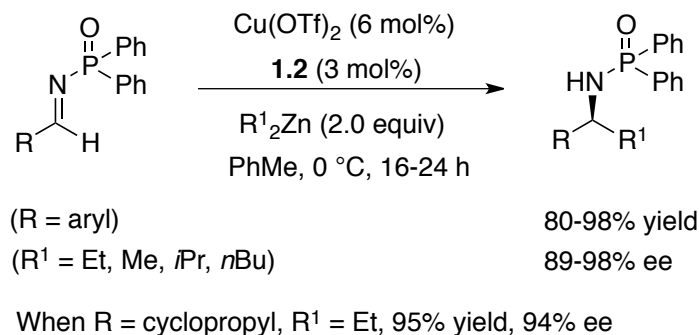
Entry	Ligand	Conversion (%) ^a	ee (%) ^b
1 ^c	1.1	92	89
2 ^d	1.1	38	0
3 ^d	1.2	100	97
4 ^d	1.2	100	97

^aDetermined by ^1H -NMR. ^bDetermined by chiral HPLC. ^c $\text{Cu}(\text{OTf})_2$ mixed with ligand, then Et_2Zn .

^d $\text{Cu}(\text{OTf})_2$ mixed with Et_2Zn , then ligand.

Table 1.2 Control experiments for ligand identification

As the actual ligand was identified Charette's group developed a three-step gram-scale synthesis to prepare **1.2**,^{3b} and then demonstrated its outstanding catalytic activity in the same type of reaction.



Equation 1.2 The new reaction conditions based on Methyl-DuPhos monoxide ligand

Encouraged by the success in aryl substrates, Charette and coworkers planned to extend the substrate scope to alkyl aldimines.⁵ A practical problem they had was lacking an efficient method to access alkyl-substituted *N*-phosphinoylaldimines, because these compounds usually are susceptible to hydrolysis and tend to undergo isomerization to the corresponding enamines. To overcome this issue, they introduced *N*-phosphinoyl α -amino sulfones to *in situ* generate corresponding aldimines in presence of excess dialkylzinc reagents.⁵ Under the initial conditions shown in Scheme 1.1 the 3-phenylpropanal derived model substrate gave 97% yield and 94% ee. To improve the enantioselectivity while retaining a high yield, they optimized the ratio of copper to ligand and discovered that approximate 1:1 ratio gave the most satisfying result (98% yield, 96% ee). Under the optimal conditions, other α -amino sulfone substrates also gave excellent yields and enantioselectivities. They proposed that EtZnOTf, generated from

⁵ Côté, A.; Boezio, A. A.; Charette, A. B. *Proc. Natl. Acad. Sci.* **2004**, *101*, 5405-5410.

Reaction scheme for the synthesis of **1.6** from **1.5**:

1.5 (a phosphoramidite derivative) reacts with Et-ZnEt (1.0 equiv) to form an intermediate (shown in brackets) and $\text{EtZnSO}_2\text{Tol}$. The intermediate then reacts with $\text{Cu}(\text{OTf})_2$ (**1.2**) and Et_2Zn (1.5 equiv) to yield **1.6** (a phosphoramidate derivative).

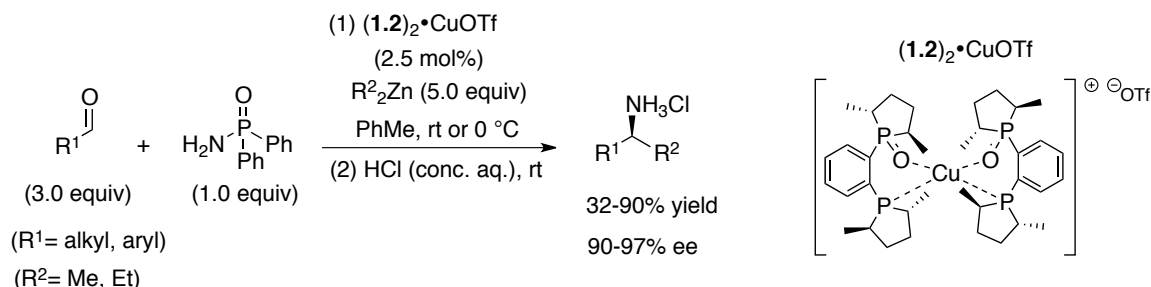
Cu(OTf)₂: 4.5 mol%, **1.2**: 5 mol% 98% yield, 96% ee

Cu(OTf)₂ (4.5 mol%)
1.2 (5 mol%)
 Et₂Zn (2.5 equiv)
 PhMe, -20 °C to rt, 16 h
 86-98% yield
 90-97% ee

⁶ (a) Porter, J. R.; Traverse, J. F.; Hoveyda, A. H.; Snapper, M. L. *J. Am. Chem. Soc.* **2001**, *123*, 10409-10410. (b) Akullian, L. C.; Snapper, M. L.; Hoveyda, A. H. *Angew. Chem. Int. Ed.* **2003**, *42*, 4244-4247. (c) Akullian, L. C.; Porter, J. R.; Traverse, J. F.; Snapper, M. L.; Hoveyda, A. H. *Adv. Synth. Catal.* **2005**, *347*, 417-425.

6

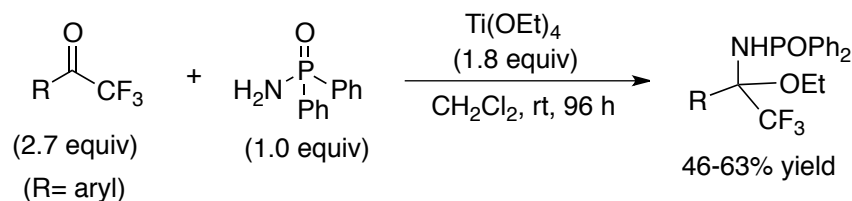
copper(I) species and electron-rich phosphines are usually oxygen-sensitive. With the established conditions, diphenylphosphinoylamine and a variety of aldehydes can be used directly as the starting materials to produce various enantioenriched secondary amines.



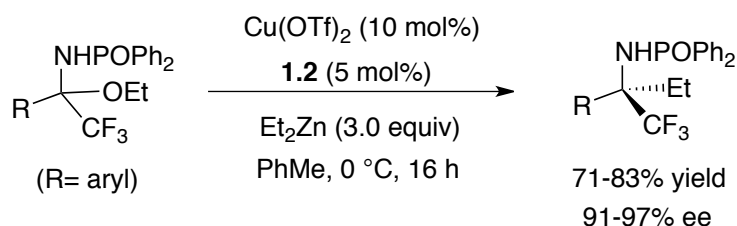
Equation 1.4 The one-pot conditions for preparation of enantioenriched secondary amines

In addition to using aldimines as the substrates, Charette and coworkers tried to apply their methodologies to trifluoromethyl-substituted ketimines to access corresponding enantioenriched tertiary amines.⁸ To circumvent the low reactivity of aryl trifluoromethyl ketones in condensation with *N*-diphenylphosphinoyl amide and the stability issue with the resulted ketimines, Charette employed the trifluoromethyl-substituted hemiaminal ethyl ethers, which were prepared through a Ti(OEt)₄-mediated three-component reaction (Equation 1.5),⁸ as the precursors of the corresponding ketimines in presence of excess dialkylzinc reagents. The synthesized hemiaminal ethers can be deprotonated by the dialkylzinc reagents to release the parent ketimines *in situ*,⁸ similar to the “decomposition” pathway of *N*-phosphinoyl α-amino sulfones in their previous studies.⁵ Under the optimal conditions established for the aldimine substrates, the trifluoromethyl-substituted hemiaminal ethyl ethers produced the desired tertiary amines in good yields and high enantioselectivities (Equation 1.6).

⁸ Lauzon, C.; Charette, A. B. *Org. Lett.* **2006**, 8(13), 2743-2745.



Equation 1.5 Preparation of trifluoromethyl-substituted hemiaminal ethyl ethers

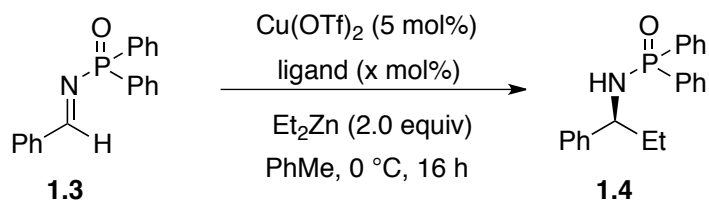


Equation 1.6 Copper-catalyzed nucleophilic addition of hemiaminal ethyl ethers

Back to the general principles of ligand design, Charette was interested in which phosphine-containing moiety in Methyl-DuPhos monoxide dominates stereocontrol in the abovementioned copper-catalyzed reactions.⁹ Unfortunately, the disproportionating nature of Cu(I) caused rapid equilibration between the paramagnetic Cu(0) and Cu(II) complexes, which complicated ³¹P-NMR of Methyl-DuPhos(O) under the reaction conditions. Alternatively, Charette's group conducted a series of control experiments with some analogues of ligand **1.2** that were synthesized separately.

The fact that ligand **1.7**, **1.8**, or a mixture of **1.7** and **1.8** gave the racemic product indicated the necessity of a bidentate ligand for enantioinduction. The results obtained from ligand **1.9**, **1.10** and **1.11** provided a clear clue to the “puzzle” they had. Ligand **1.10** exhibited slight enantioselectivity, but **1.11** gave the same level of enantioselectivity as **1.2**. This comparison demonstrated that the chiral structure of phosphinyl fragment in Methyl-DuPhos(O) is important for the stereochemical outcome.

⁹ Bonnaventure, I.; Charette, A. B. *J. Org. Chem.* **2008**, 73, 6330-6340.



Entry	Ligand (mol%)	Conversion (%) ^a	ee (%) ^b
1	1.2 (5)	85	96
2	1.7 (10)	85	0
3	1.8 (10)	81	0
4	1.7 + 1.8 (5 + 5)	92	0
5	1.9 (5)	65	60
6	1.10 (5)	99	13
7	1.11 (5)	95	96

^aDetermined by ¹H-NMR. ^bDetermined by chiral HPLC or SFC.

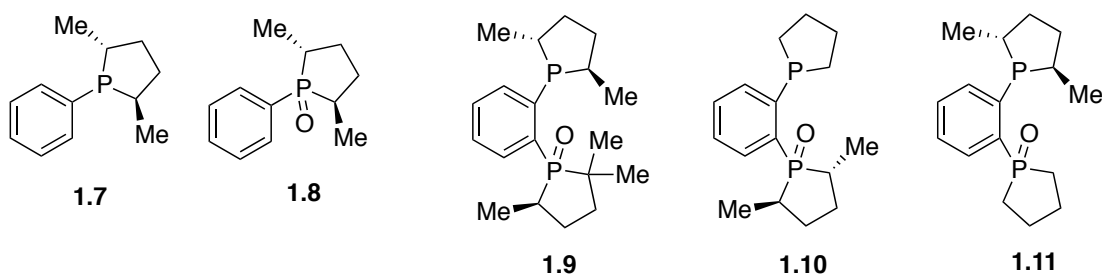
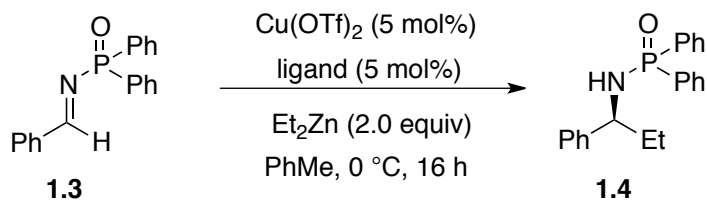


Table 1.3 Ligand effect on the reactivity and stereoselectivity

On the other hand, the significant difference in enantioselectivity produced by ligand **1.2** and **1.9** implied that the skeleton of phosphinoyl fragment also plays a role. In ligand **1.12**, **1.13**, **1.14**, **1.15**, and **1.16** the phosphinoyl group was replaced with another type of Lewis hard group, but they all gave low enantioselectivity (up to 29% ee) and mostly low conversions (up to 68%). This observation confirmed the importance of a suitable hemilabile group for good reactivity and selectivity. Focused on mixed phosphine-phosphine oxide ligands, Charette further studied the effect of different

phosphinoyl fragments on the reaction. To their delight, ligand **1.21** produced comparable conversion and enantioselectivity as the Methyl-DuPhos(O).



Entry	Ligand	Conversion (%) ^a	ee (%) ^b
1	1.2	85	96
2	1.17	75	90
3	1.18	10	0
4	1.19	36	60
5	1.20	91	86
6	1.21	84	94
7	1.22	49	38

^aDetermined by ¹H-NMR. ^bDetermined by chiral HPLC or SFC.

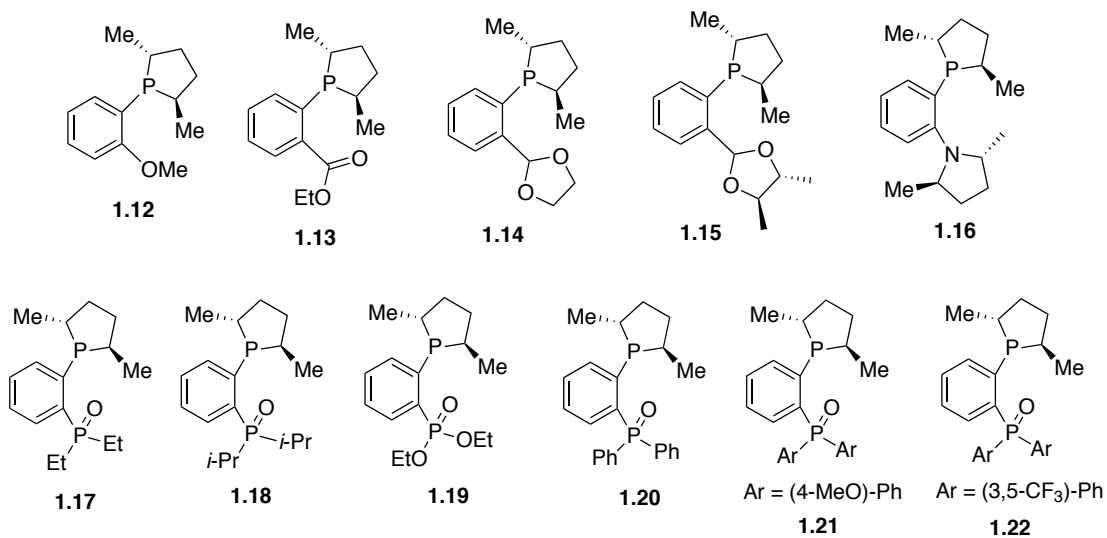
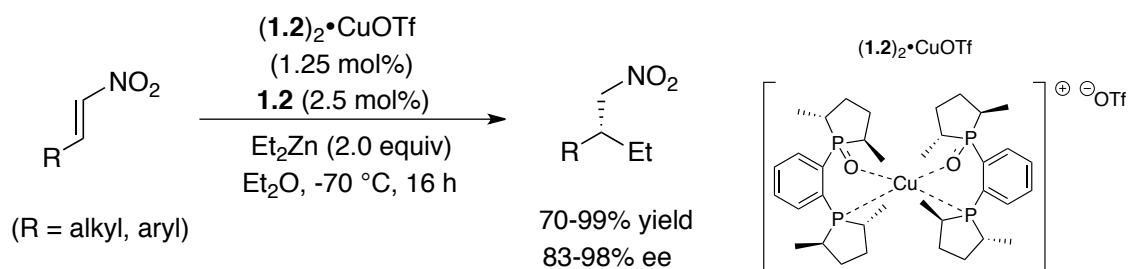


Table 1.4 Effect of different Lewis hard groups on the reactivity and stereoselectivity

As a conclusion, they proposed that the chiral skeleton of phosphine moiety in Methyl-DuPhos monoxide is an essential factor in stereocontrol, and that the Lewis

basicity of phosphine oxide moiety, manifested in bond length and polarizability, cooperatively poses impact on the shape of the chiral pocket and catalyst activity.⁵

Charette also studied the same type of reaction with β -nitroalkenes as the substrates.¹⁰ When excess ligand **1.2** was used, making the ratio of copper to ligand as 1:4, high yields and enantioselectivities were obtained from most of the substrates. High ligand loading suppressed polymerization of the substrates and disrupted the dimerization of $(\mathbf{1.2})_2\cdot\text{CuEt}$ complex to a non-selective form.¹¹



Equation 1.7 Copper-catalyzed nucleophilic addition of diethylzinc to β -nitroalkenes

Another type of reaction that Charette explored with Cu(I)/Methyl-DuPhos(O) catalyst system is enantioselective hydrosilylation of β,β -disubstituted vinyl phenyl sulfones in presence of a proton source,¹² which can serve as an alternative way of asymmetric hydrogenation of vinyl sulfones under mild conditions. Cu(I)/Methyl-DuPhos(O) complex exhibited impressive enantiocontrol. Use of a NaOH aqueous solution as the additive suppressed consumption of phenylsilane by water¹³ and hence drove the reaction to completion. More importantly, this additive improved the

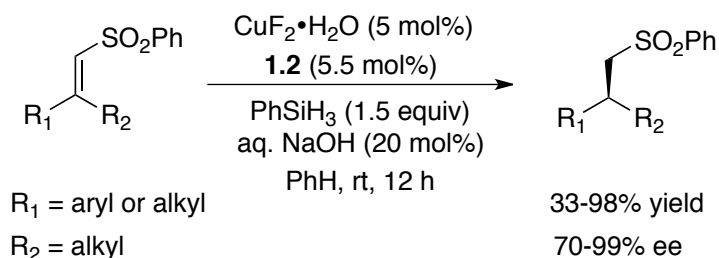
¹⁰ Côté, A.; Lindsay, V. N. G.; Charette, A. B. *Org. Lett.* **2007**, 9(1), 85-87.

¹¹ Charette, A. B.; Côté, A.; Desrosiers, J.-N.; Bonnaventure, I.; Lindsay, V. N. G.; Lauzon, C.; Tannous, J.; Boezio, A. A. *Pure Appl. Chem.* **2008**, 80(5), 881-890.

¹² Desrosiers, J.-N.; Charette, A. B. *Angew. Chem. Int. Ed.* **2007**, 46, 5955-5957.

¹³ Schubert, U.; Lorenz, C. *Inorg. Chem.* **1997**, 36, 1258-1259.

reproducibility of the reaction. Use of pure water or protic organic solvents as the additive led to low conversions.



Equation 1.8 Enantioselective reduction of β,β -disubstituted vinyl phenyl sulfones

1.3 BINAP and SDP-based chiral BPMOs

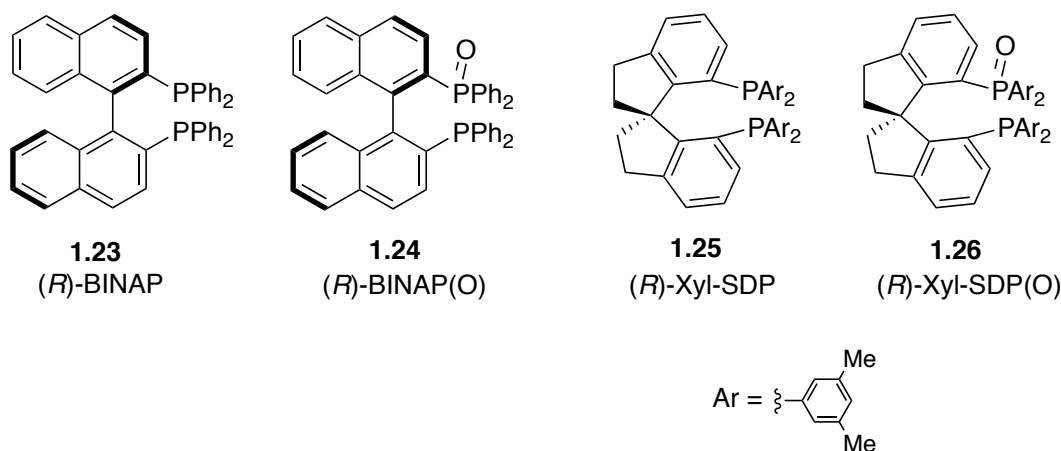


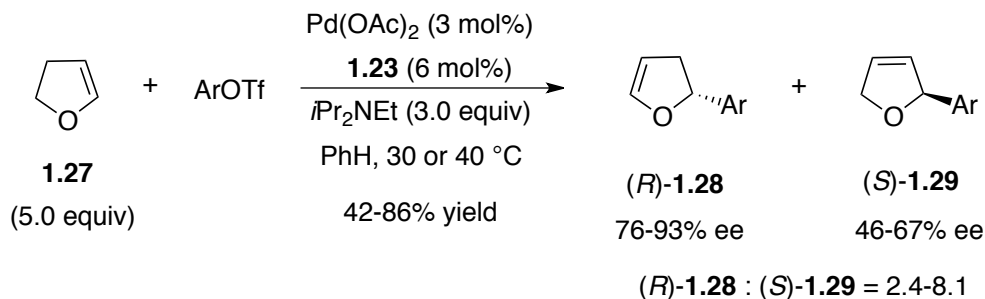
Figure 1.3 *(R)*-BINAP and *(R)*-BINAP monoxide, *(R)*-Xyl-SDP and *(R)*-Xyl-SDP monoxide

In situ reduction of Pd(II) to Pd(0) by excess phosphine ligands¹⁴ is a frequently used strategy in Pd(0)/phosphine complex-catalyzed reactions. The sacrificed phosphines are converted to phosphine oxides, which are less coordinating to Pd(0) and usually treated as inert species. Since Oestreich's group disclosed that chiral BINAP monoxides

¹⁴ (a) Ozawa, F.; Kubo, A.; Hayashi, T. *Chemistry Letters* **1992**, 2177-2180. (b) Amatore, C.; Carré, E.; Jutand, A.; M'Barki, M. A. *Organometallics* **1995**, 14, 1818-1826. (c) Csákai, Z.; Skoda-Földes, R.; Kollár, L. *Inorganica Chimica Acta* **1999**, 286, 93-97.

can behave as effective ligands in enantioselective Heck reactions,¹⁵ the catalytic utility of this class of ligand started receiving more attention.

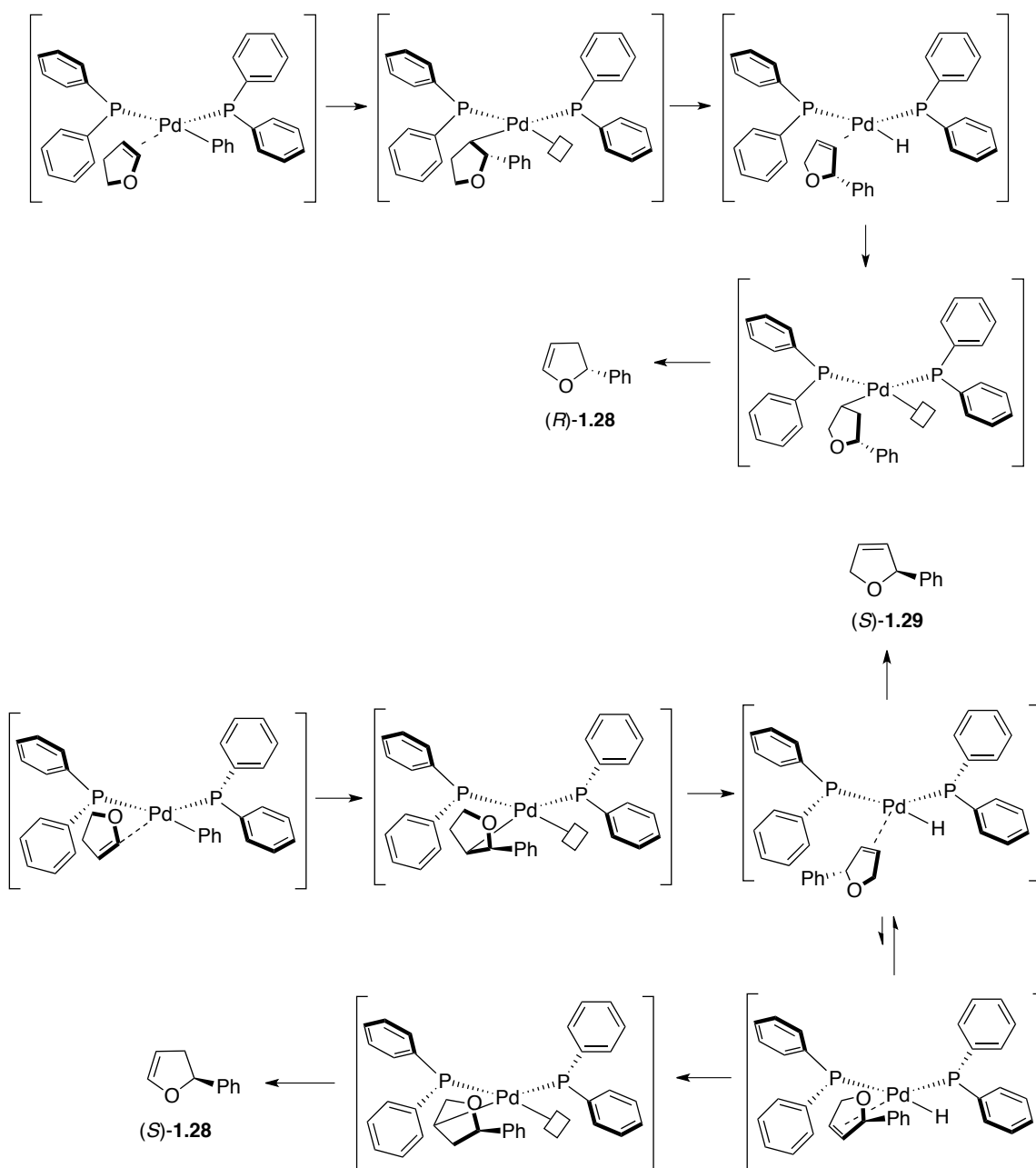
In the early 1990s Hayashi reported an enantioselective intermolecular Heck reaction of 2,3-dihydrofuran and aryl triflates by using Pd(OAc)₂ and (*R*)-BINAP (1:2 ratio of Pd to ligand) as the catalyst system.¹⁶ The enantioselectivity initially came from a stereoselective olefin insertion step where a suitable orientation of 2,3-dihydrofuran could avoid close interaction to the ligand (Scheme 1.2). Use of aryltriflates as the coupling partners is important to this step, because the cationic aryl-Pd(II) intermediate can strongly bind with the olefin substrates and suppress partial dissociation of (*R*)-BINAP from Pd(II) for olefin insertion. Otherwise, the insertion process will be much less stereoselective (aryl iodides resulted in racemic products).^{16a}



Equation 1.9 Hayashi's catalyst system for arylation of 2,3-dihydrofuran

¹⁵ (a) Wöste, T. H.; Oestreich, M. *Chem. Eur. J.* **2011**, *17*, 11914-11918. (b) Wöste, T. H.; Oestreich, M. *ChemCatChem* **2012**, *4*, 2096-2101.

¹⁶ (a) Ozawa, F.; Kubo, A.; Hayashi, T.; Nishioka, E.; Yanagi, K.; Moriguchi, K.-I. *J. Am. Chem. Soc.* **1991**, *113*, 1417-1419. (b) Ozawa, F.; Kubo, A.; Hayashi, T. *Tetrahedron Letters* **1992**, *33*(11), 1485-1488. (c) Ozawa, F.; Kobatake, Y.; Hayashi, T. *Tetrahedron Letters* **1993**, *34*(15), 2505-2508.

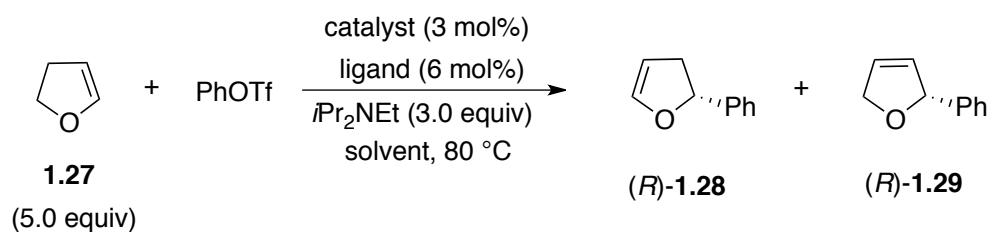


Scheme 1.2 Proposed model for the stereoselectivity in Hayashi's arylation

Furthermore, the observed enantioselectivity was also a consequence of a kinetic resolution process, in which the more energetically favorable pathway will lead to a

subsequent hydrometallation/ β -hydride elimination sequence (Scheme 1.2).¹⁷ As a net effect, this incorporated kinetic resolution enhanced enantiopurities of two final products through converting one enantiomer of the arylated compound to a different olefin isomer. The ratio of two olefin products is determined by the dissociation rate of the arylated olefin from a hydrido-Pd(II)-olefin complex (an associative mechanism is involved).¹⁷

In the same period, Hayashi also demonstrated that Pd(OAc)₂ can stoichiometrically oxidize BINAP to generate Pd(0) along with BINAP monoxide.^{14a} Intrigued by these two related studies, Oestreich evaluated (*R*)-BINAP(O) as a chiral ligand in the same type of reaction.^{15a}



Entry	Catalyst	Ligand	Solvent	Yield (%)	Ratio ^a (<i>R</i>)- 1.28 : (<i>R</i>)- 1.29	ee (%) ^b (<i>R</i>)- 1.28	ee (%) ^b (<i>R</i>)- 1.29
1	Pd(OAc) ₂	1.23	THF	68	100 : 0	66	—
2	Pd(OAc) ₂	1.24	THF	80	2 : 98	—	92
3	Pd(OAc) ₂	1.23	PhH	75	99 : 1	64	—
4	Pd(OAc) ₂	1.24	PhH	70	12 : 88	76	88
5	Pd(dba) ₂	1.23	PhH	56 ^c	99 : 1	66	—
6	Pd(dba) ₂	1.24	PhH	80	5 : 95	92	94

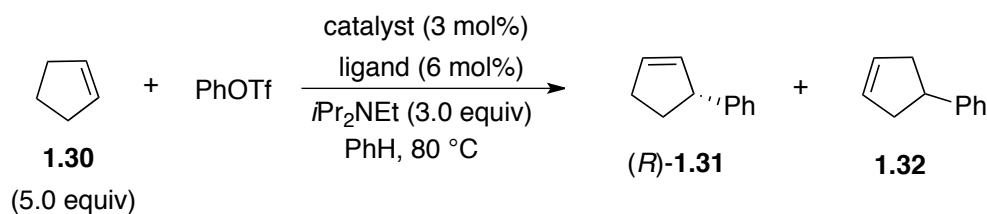
^aDetermined by achiral GLC. ^bDetermined by chiral GLC. ^cIncomplete conversion.

Table 1.5 Ligand effect on arylation of 2,3-dihydrofuran

¹⁷ For a detailed mechanistic study, see: Ozawa, F.; Kubo, A.; Matsumoto, Y.; Hayashi, T. *Organometallics*, **1993**, 12, 4188-4196.

Unexpectedly, they observed contrasting selectivities from control experiments (note: the unisomerized product contains (*R*)- instead of (*S*)-configuration, which is a different observation than Hayashi disclosed). With (*R*)-BINAP the thermodynamically more stable compound (*R*)-**1.28** was preferentially generated (entry 1, 3 and 5, Table 1.5). With (*R*)-BINAP(O) the unisomerized compound (*R*)-**1.29** was the major product (entry 2, 4 and 6, Table 1.5). This reversed product distribution indicated when chelated with (*R*)-BINAP(O) the hydrido-Pd(II)-olefin triflate complex tends to undergo reductive elimination to release Pd(0) rather than hydrometallate the coordinated olefin. Presumably, the less electron-donating phosphinoyl group provides less stabilization to Pd(II) and hence kinetically favors reductive elimination. From another aspect, the higher enantioselectivities produced by (*R*)-BINAP(O) suggested that the initial olefin insertion step was more stereoselective.

Oestreich also tested cyclopentene in the arylation conditions and found the same trend that with (*R*)-BINAP(O) olefin isomerization was minimized and products contained higher enantiopurities.



Entry	Catalyst	Ligand	Yield (%)	Ratio ^a (<i>R</i>)- 1.31 : 1.32	ee (%) ^b (<i>R</i>)- 1.31
1	Pd(OAc) ₂	1.23	41 ^c	74 : 26	6
2	Pd(OAc) ₂	1.24	75	90 : 10	80
3	Pd(dba) ₂	1.23	24 ^c	62 : 38	14
4	Pd(dba) ₂	1.24	75	94 : 6	86

^aDetermined by achiral GLC. ^bDetermined by chiral GLC. ^cIncomplete conversion.

Table 1.6 Ligand effect on arylation of cyclopentene

Zhou and coworkers also independently investigated different chiral bisphosphine monoxide ligands in Hayashi's olefin arylation reactions.¹⁸ They discovered that (*R*)-Xyl-SDP(O) is a versatile ligand toward a variety of olefin substrates. Excellent enantioselectivity and good to high olefin selectivity were obtained from most of the cases they surveyed.

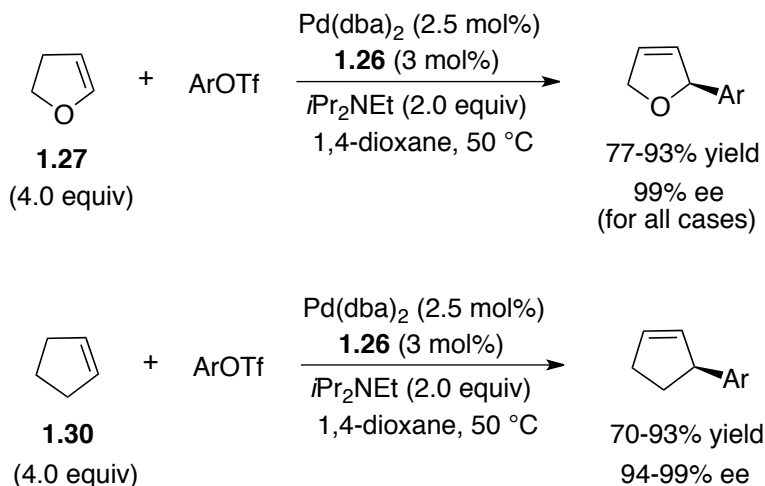
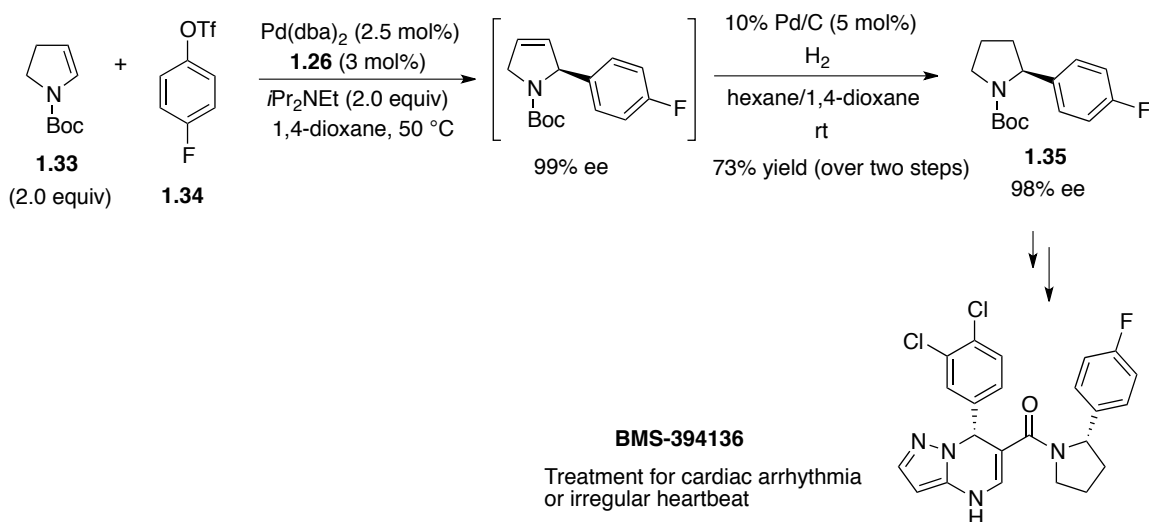


Figure 1.4 (*R*)-Xyl-SDP(O) in enantioselective intermolecular Heck reaction



Scheme 1.3 Synthetic application of Zhou's arylation method

¹⁸ Hu, J.; Lu, Y.; Li, Y.; Zhou, J. *Chem. Commun.* **2013**, 49, 9425-9427.

To gain some insight of the origin of the observed high stereoselectivity, Zhou first synthesized a [(**1.26**)(4-CF₃-phenyl)(I)Pd(II)] complex from (*R*)-Xyl-SDP(O), Pd₂(dba)₃ and 1-Iodo-4-(trifluoromethyl)benzene. The crystal structure of this complex shows that the aryl group is *cis* to the phosphinyl fragment of (*R*)-Xyl-SDP(O). A possible explanation for this orientation is that a *trans* configuration of two groups bearing strong trans effect would destabilize the palladium complex.¹⁸ Further, Zhou did DFT calculations of the transition state of the olefin insertion step. The results revealed that the bidentate coordinating mode of (*R*)-Xyl-SDP(O) with Pd(II) is energetically more favorable, and that the steric repulsion between the incoming olefin substrate and the phosphinoyl fragment of (*R*)-Xyl-SDP(O) plays an important role in stereocontrol. The energy difference between the favorable and unfavorable olefin orientations in the olefin insertion step is 2.6 kcal/mol.

This study elucidated that the Lewis hard moiety in a BPMO ligand is also important for enantioinduction rather than simply behaving as a labile coordination site. A hemilabile ligand can become better chelating, as the transition metal becomes more Lewis acidic in an oxidative addition.

After identified the catalytic utility of BPMOs, Zhou designed a Heck reaction-triggered intermolecular cyclization reaction with Pd(0)/(*R*)-BINAP(O) as the catalyst system.¹⁹ A vinyl group was installed at the *ortho*-position of aryl triflates, which can further react with the alkyl palladium intermediate before it undergoes β-hydride elimination. A 1,3-dienyl triflate **1.36** was tested to be an effective substrate as well. The scope of olefin substrates in this method includes simple cyclic alkenes, 2,3-dihydrofuran,

¹⁹ Hu, J.; Hirao, H.; Li, Y.; Zhou, J. *Angew. Chem. Int. Ed.* **2013**, *52*, 8676-8680.

N-Boc-2,3-dihydropyrrole and norbornenes. Cyclopentene, cycloheptene and cyclooctene gave decent yields (63-85%) and good to high enantioselectivities (88-99% ee), but no reaction occurred with cyclohexene. The proposed explanation is that the half-chair conformation of cyclohexene impeded its binding to Pd(II) center.¹⁹ The products from norbornene substrates contain good to excellent enantiopurity (up to 99% ee) and *exo*-configuration. To demonstrate the synthetic utility of this method, Zhou and coworkers also applied a cyclization product in a formal asymmetric synthesis of (-)-martinellic acid.¹⁹

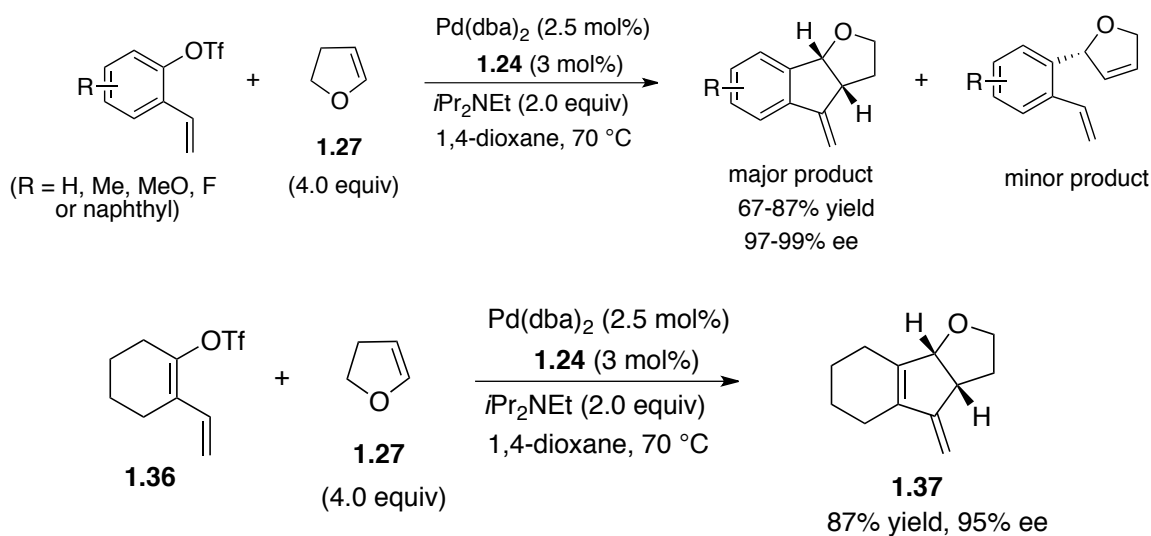
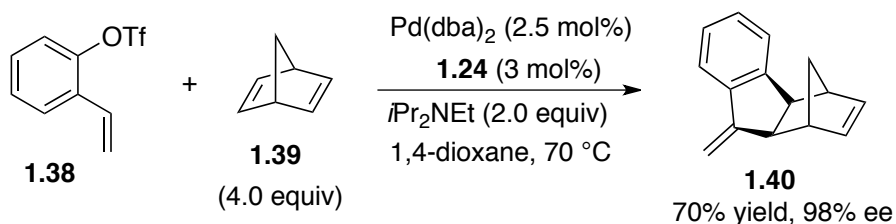
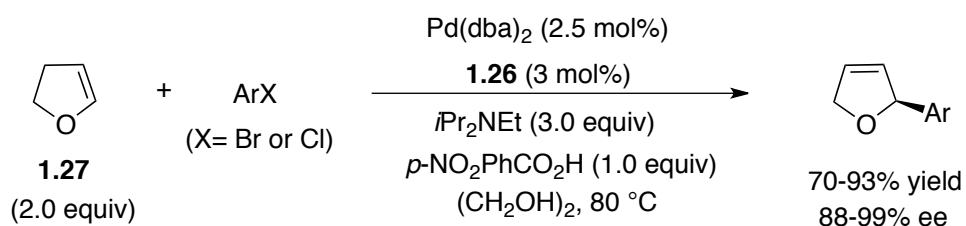


Figure 1. 5 Scope of triflates in the intermolecular cyclization reactions



Equation 1.10 Norbornene in the intermolecular cyclization reactions

More recently, Zhou discovered conditions for asymmetric intermolecular Heck reaction with aryl bromides or chlorides as the coupling partners.²⁰ To facilitate dissociation of halide anions from Pd(II) center for olefin insertion, Zhou tested different solvents and additives. Protic solvents were found to be crucial to achieve high reactivity, whereas with THF or 1,4-dioxane no reaction occurred. They proposed that the protic solvents, like MeOH, could accelerate departure of halide anions via hydrogen bond formation. Addition of silver salts as the halide scavengers could further improved the reactivity, but 4-nitrobenzoic acid turned to be a more effective additive that led to higher yields without loss of enantioselectivity. The *in situ* generated ammonium salt from 4-nitrobenzoic acid and Hünig's base may serve as the active species that benefits ionization of chlorine or bromine in the corresponding palladium-halogen bond.²⁰ Presumably, the tertiary ammonium cation can form an intimate ion pair with departed bromide or chloride anion. The principle behind this method is consistent with Hayashi's conclusion^{16a} that a cationic arylPd(II) complex is important for achieving high stereoselectivity, but it provides an opportunity of conducting asymmetric intermolecular Heck reaction without using expensive aryl triflates.



²⁰ Wu, C.; Zhou, J. *J. Am. Chem. Soc.* **2014**, *136*, 650-652.

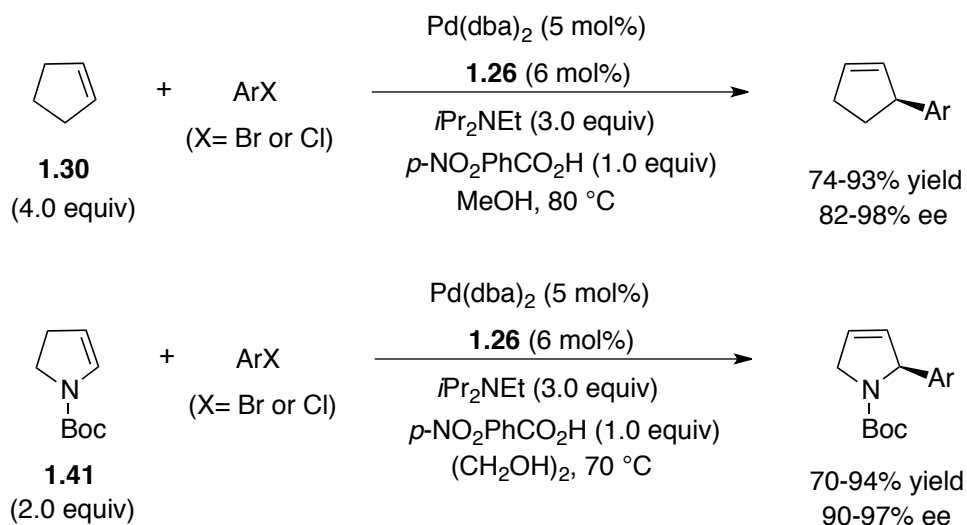
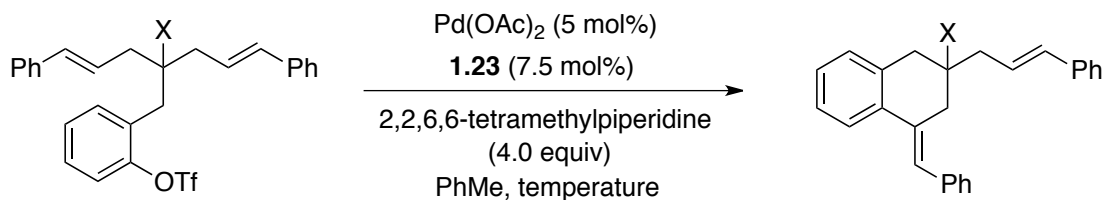


Figure 1.6 Aryl halides in the enantioselective intermolecular Heck reactions

BPMOs also found applications in intramolecular Heck reaction. Oestreich proposed utilizing the hemilability of this type of ligand to “manipulate” the coordinating mode of Pd(II) in a desymmetrizing cyclization process.^{15b} In 2007 Oestreich’s group reported Pd(0)/(*R*)-BINAP catalyzed intramolecular Heck reaction for desymmetrization of 1,6-dienes.²¹ They found that the existence of an oxygen-donor in the substrate caused dramatic increase in enantioselectivity (Table 1.7). The DFT calculations they conducted suggested that an oxygen-containing group can serve as a labile coordinating site to the 14-electron Pd(II) cation after dissociation of the coordinated alkenyl group (Scheme 1.4). This coordinating mode prolonged the lifetime of the Pd(II) intermediate and allowed an coordination equilibrium between two alkenyl side chains to be established prior to the enantioselectivity-determining migratory insertion.²¹ Without this substrate assistance, coordination of each alkenyl side chain to Pd(II) was fast and irreversible, and low

²¹ Machotta, A. B.; Straub, B. F.; Oestreich, M. *J. Am. Chem. Soc.* **2007**, *129*, 13455-13463.

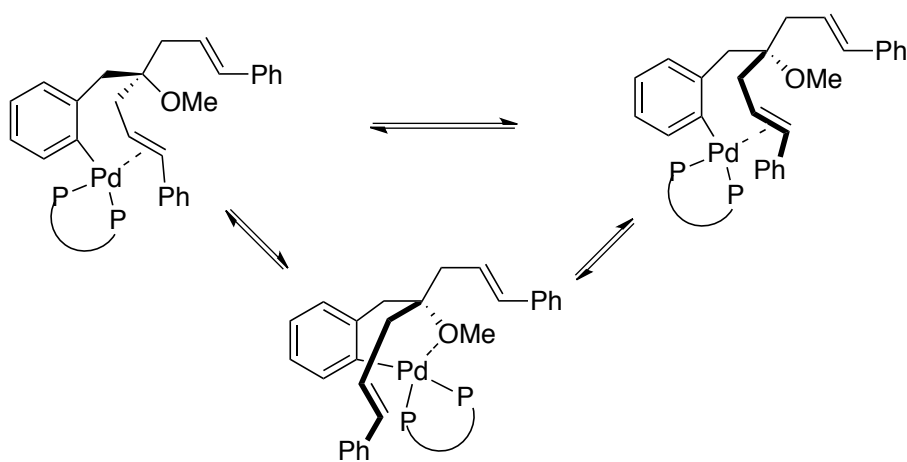
stereoselectivity was observed due to the low energy difference between the different transition states.



Entry	X	Temperature (°C)	Yield (%)	ee (%) ^a
1	MeO	50	98	97
2	H	80	86	8

^aDetermined by chiral GLC

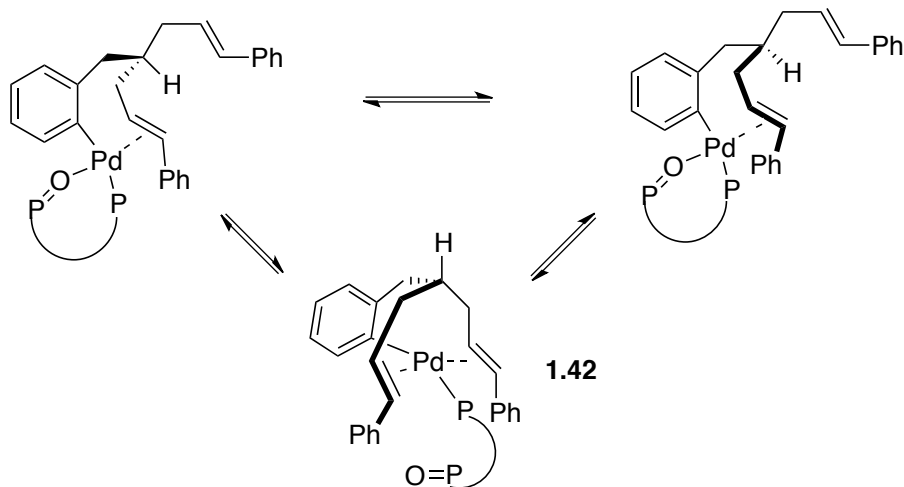
Table 1.7 Effect of the substrate structure on the reactivity and stereoselectivity



Scheme 1.4 Proposed coordination equilibrium assisted by a functional group

When a BPMP(O) was used as the ligand, the hemilability of the phosphine oxide fragment could “force” both alkenyl side chains in the substrate to coordinate with Pd(II) to form intermediate **1.42**. Through dissociation and reassociation of the phosphinoyl group in the ligand, the coordination of each side chain to Pd(II) can become interconvertible (Scheme 1.5) and then shift the migratory insertion to be the enantioselectivity-determining step.^{15b} Indeed, when (*R*)-BINAP(O) was employed the

obtained enantioselectivity was slightly higher than that (*R*)-BINAP produced (Figure 1.7). From another substrate **1.45**, Oestreich also observed the same trend that (*R*)-BINAP(O) exhibited better enantiocontrol than the parent (*R*)-BINAP (Figure 1.8).



Scheme 1.5 Proposed coordination equilibrium assisted by a hemilabile ligand

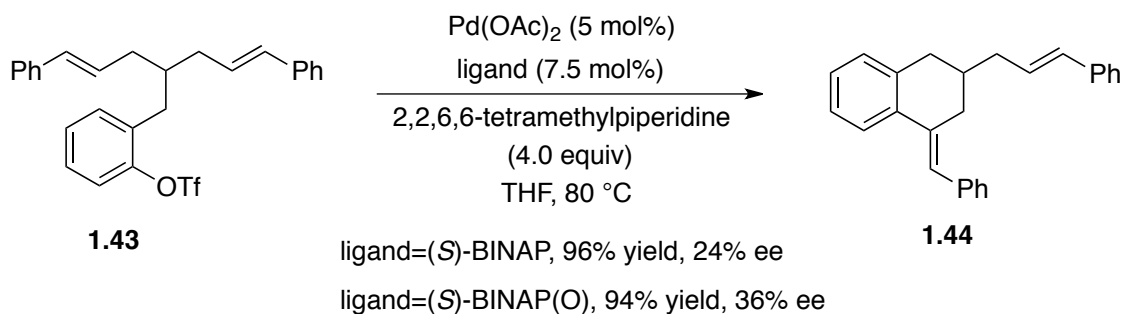


Figure 1.7 Ligand effect on the stereoselectivity of desymmetrization of 1,6-diene

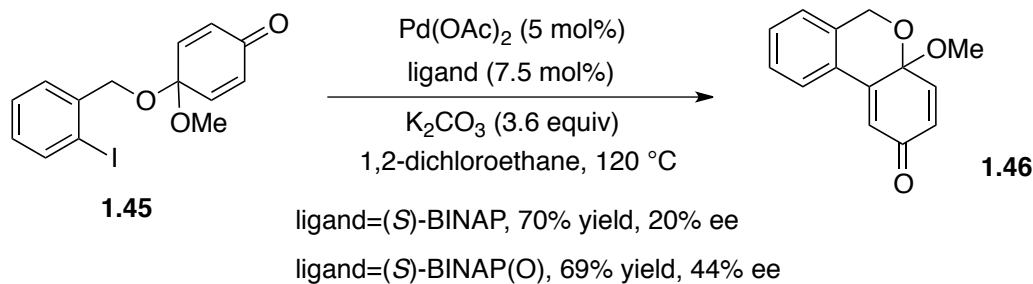


Figure 1.8 Ligand effect on the stereoselectivity of desymmetrization of 1,6- and 1,4-dienes

1.4 QuinoxP*-based chiral BPMO

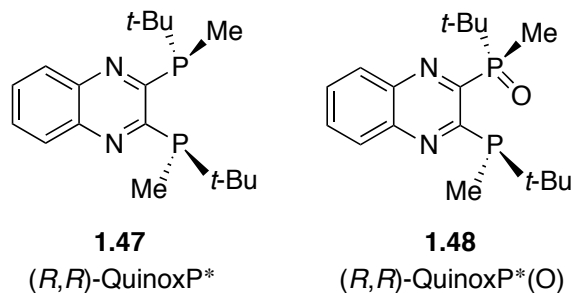


Figure 1.9 Quinoxp* and Quinoxp* monoxide

Elbasvir, a compound containing a chiral hemiaminal ether moiety, is a protease inhibitor used for treating hepatitis C virus infection.²² To synthesize this molecule a research group in Merck & Co. Inc. designed a Buchwald-Hartwig amination reaction to construct the indole fragment, while controlling the stereochemistry of the *in situ* formed hemiaminal ether with a Pd(0)/chiral phosphine complex.²³ Their exploration started with benzoxazine **1.49**, the stereogenic center of which is stereochemically labile due to a ring-opening and reclosing process.²³ During the screening of different palladium precatalysts and chiral phosphine ligands, they observed an interesting phenomena that when (*R,R*)-QuinoxP* combined with Pd(OAc)₂ was applied the reaction achieved full conversion along with 96% ee, but when the same ligand combined with Pd₂(dba)₃ the reaction reached less than 20% conversion and 80% ee. This considerable difference in their reactivities drove them to suspect that (*R,R*)-QuinoxP* may undergo *in situ* oxidation by Pd(OAc)₂ to generate the bisphosphine monoxide, which served as the actual ligand.

²² Coburn, C. A.; Meinke, P. T.; Chang, W.; Fandozzi, C. M.; Graham, D. J.; Hu, B.; Huang, Q.; Kargman, S.; Kozłowski, J.; Liu, R.; McCauley, J. A.; Momeir, A. A.; Soll, R. M.; Vacca, J. P.; Wang, D.; Wu, H.; Zhong, B.; Olsen, D. B.; Ludmerer, S. W. *ChemCatChem* **2013**, *8*, 1930-1940.

²³ Li, H.; Belyk, K. M.; Yin, J.; Chen, Q.; Hyde, A.; Ji, Y.; Oliver, S.; Tudge, M. T.; Campeau, L.-C.; Campos, K. R. *J. Am. Chem. Soc.* **2015**, *137*, 13728-13731.

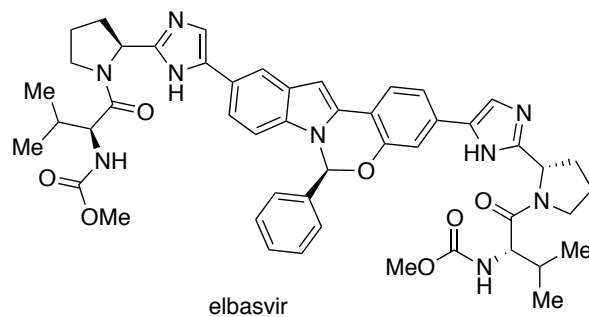
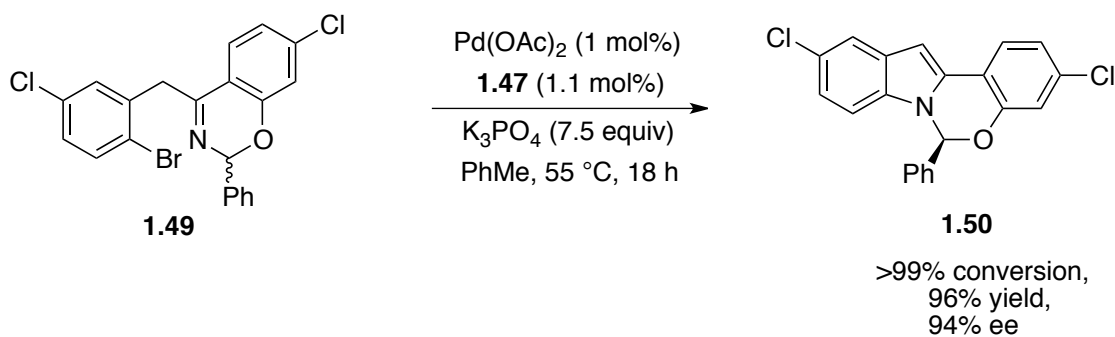
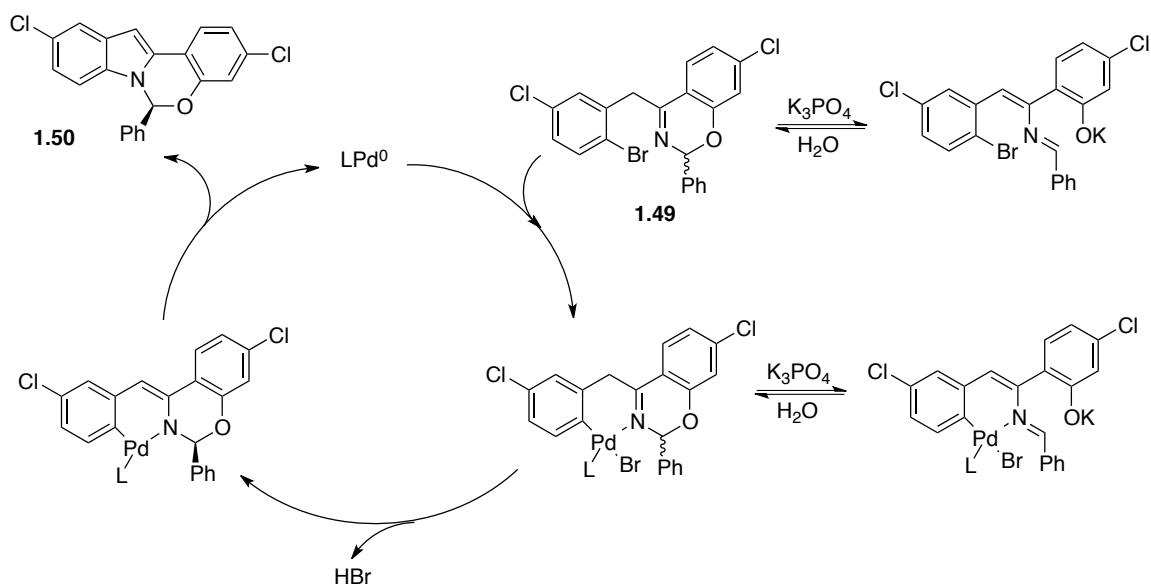


Figure 1.10 Structure of Elbasvir



Equation 1.11 Designed Buchwald-Hartwig amination reaction



Scheme 1.6 Proposed catalytic cycle of the designed amination reaction

To verify this possibility, two methods were employed. First, they synthesized (*R,R*)-QuinoxP*(O) separately and tested it with Pd₂(dba)₃ in the standard condition. The reaction gave almost full conversion and 89% ee. Next, they monitored ³¹P-NMR of the reaction carried with Pd(OAc)₂/*(R,R)*-QuinoxP*. The observed signals matched with that of the reaction conducted with Pd₂(dba)₃/*(R,R)*-QuinoxP*(O). Hence, the actual ligand that gave high reactivity and stereoselectivity in the model reaction was identified to be (*R,R*)-QuinoxP*(O). Under the standard condition a variety of substrates containing different aryl substituents or backbones gave high yields (86-96%) and high enantioselectivities (87-97% ee). As for making alkyl-substituted hemiaminal ethers, (*R,R*)-QuinoxP*(O) produced about 70% ee, but the stereoselectivity could be improved by switching to a Josiphos ligand.²³

1.5 Conclusion

In transition metal-catalyzed asymmetric reactions, chiral bisphosphine monoxide ligands may exhibit higher catalytic activity and selectivity than the parent bisphosphines. This type of hemilabile ligand is actually well known in organometallic studies, but their catalytic utilities are still under discovery. As more chiral bisphosphine monoxides have become commercially available, this field will create more opportunities for synthetic chemists to develop new and powerful catalyst systems.

Chapter 2

Borylation of Hemiaminal Ethers: An Approach of Making Enantioenriched Aliphatic α -Amino Boronates

2.1 General Introduction

α -Aminoboronic acids have unique biological activities in enzyme inhibitions.¹ Since 1990s chemical biologists have discovered this class of molecule as potential inhibitors targeting proteasome,² thrombin³ and β -lactamase.⁴ Application of α -aminoboronic acid-based organic compounds in clinic therapeutics leads to a new direction in drug discovery. A landmark in this field is that bortezomib (trade mark as Velcade®, by Millennium Pharmaceuticals, Inc. in 2003) was launched as the first proteasome inhibitor medicine on the market for treating myeloma and relapsed mantle cell lymphoma.⁵

¹ For reviews, see: (a) Yang, W.; Gao, X.; Wang, B. *Medicinal Research Reviews* **2003**, 23(3), 346-368. (b) Dembitsky, V. M.; Serbnik, M. *Tetrahedron* **2003**, 59, 579-593. (c) Matteson, D. S. *Medicinal Research Reviews* **2008**, 28(2), 233-246. (d) Baker, S. J.; Ding, C. Z.; Akama, T.; Zhang Y. K.; Hernandez, V.; Xia, Y. *Future Med. Chem.* **2009**, 1(7), 1275-1288. (e) Dick, L. R.; Fleming, P. E. *Drug Discovery Today* **2010**, 15, 243-249. (f) Touchet, S.; Carreaux, F.; Carboni, B.; Bouillon, A.; Boucher, J. L. *Chem. Soc. Rev.* **2011**, 40, 3895-3914. (g) Baker, S. J.; Tomsho, J. W.; Benkovic, S. J. *Chem. Soc. Rev.* **2011**, 40, 4279-4285. (h) Smounm, R.; Rubinstein, A.; Dembitsky, V. M.; Serbnik, M. *Chem. Rev.* **2012**, 112, 4156-4220.

² For representative examples, see: (a) Adams, J.; Behnke, M.; Chen, S.; Cruickshank, A. A.; Dick, L. R.; Grenier, L.; Klunder, J. M.; Ma, Y.-T.; Plamondon, L.; Stein, R. L. *Bioorganic & Medicinal Chemistry Letters* **1998**, 8, 333-338. (b) Milo, L. J.; Lai, J. H. Jr.; Wu, W.; Liu, Y.; Maw, H.; Li, H.; Jin, Z.; Shu, Y.; Poplawski, S. E.; Wu, Y.; Sanford, D. G.; Sudmeier, J. L.; Bachovchin, W. W. *J. Med. Chem.* **2011**, 54, 4365-4377. (c) Gallerani, E.; Zucchetti, M.; Brunelli, D.; Marangon, E.; Noberasco, C.; Hess, D.; Delmonte, A.; Martinelli, G.; Böhm, S.; Driessen, C.; De Braud, F.; Marsoni, S.; Cereda, R.; Sala, F.; D'Incalci, M.; Sessa, C. *Eur. J. Cancer*, **2013**, 49, 290.

³ Fevig, J. M.; Abelman, M. M.; Brittelli, D. R.; Rettner, C. A.; Knabb, R. M.; Weber, P. C. *Bioorg. Med. Chem. Lett.* **1996**, 6(3), 295-300.

⁴ Chen, Y.; Shoichet, B.; Bonnet, R. *J. Am. Chem. Soc.* **2005**, 127, 5423-5434.

⁵ www.velcade.com

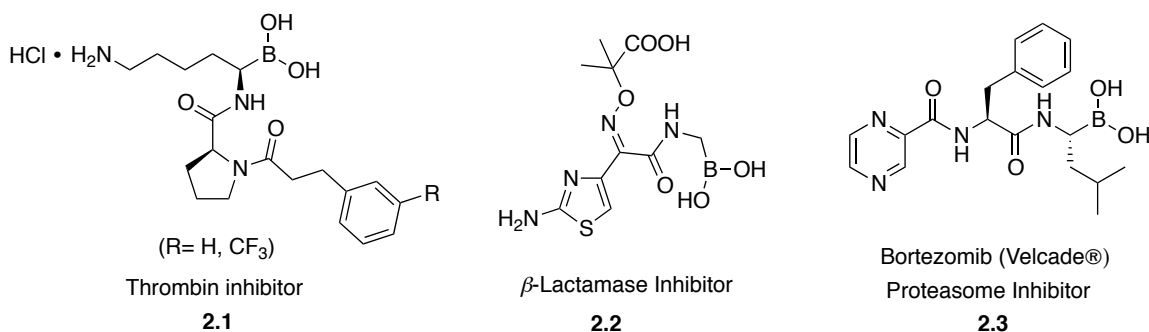


Figure 2.1 Selected examples of α -aminoboronic acid-based enzyme inhibitors

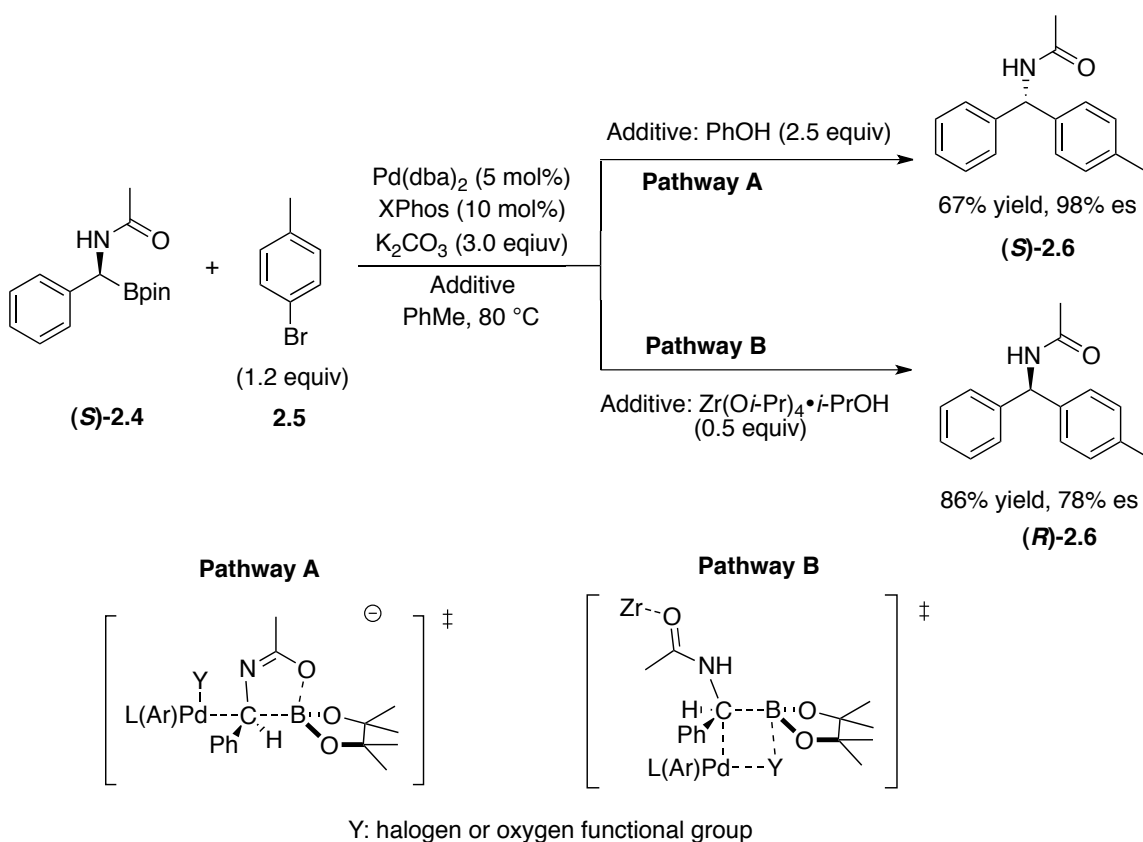
The distinctive biological activities of α -aminoboronic acids is featured in forming reversible coordination between the boron atom and specific hydroxyl or nitrogen-containing groups in an enzyme.^{1a,c} Once forming an anionic adduct with different Lewis bases, the boron atom will adopt a tetrahedral structure, which enables an α -aminoboronic acid to mimic an α -amino acid involved in different biological processes in the humane body.^{1a-c,g}

In synthetic chemistry, α -aminoboronic acids and related derivatives, like boronic esters or trifluoroborate salts, can be used as intermediates to synthesize amines. Suginome's group conducted a systematic study of chiral aryl-substituted α -amidoboronic esters in Pd-catalyzed Suzuki-Miyaura cross coupling reactions,⁶ which provides an alternative way to prepare enantioenriched benzhydryl amines.⁷ They demonstrated that the stereochemical outcome could be controlled by carefully choosing

⁶ (a) Ohmura, T.; Awano, T.; Suginome, M. *Chemistry Letters*, **2009**, 38(7), 664-665. (b) Ohmura, T.; Awano, T.; Suginome, M. *J. Am. Chem. Soc.* **2010**, 132, 13191-13193. (c) Awano, T.; Ohmura, T.; Suginome, M. *J. Am. Chem. Soc.* **2011**, 133, 20738-20741.

⁷ For arylstannanes mediated synthesis, see: (a) Hayashi, T.; Ishigedani, M. *J. Am Chem. Soc.* **2000**, 122, 976-977; for aryltitanium mediated synthesis, see: (b) Hayashi, T.; Kawai, M.; Tokunaga, N. *Angew. Chem. Int. Ed.* **2004**, 43, 6125-6128; for arylboroxines and arylboronic acids mediated syntheses, see: (c) Kuriyama, M.; Soeta, T.; Hao, X.; Chen, Q.; Tomioka, K. *J. Am Chem. Soc.* **2004**, 126, 8128-8129; (d) Tokunaga, N.; Otomaru, Y.; Okamoto, K.; Ueyama, K.; Shintani, R.; Hayashi, T. *J. Am Chem. Soc.* **2004**, 126, 13584-13585; (e) Duan, H.-F.; Jia, Y.-X.; Wang, L.-X.; Zhou, Q.-L. *Org. Lett.* **2006**, 8, 2567-2569.

different additives. When 2.5 equivalents phenol was used, products were generated in high stereospecificity with inverted stereochemistry.^{6c} When substoichiometric amount of $\text{Zr}(\text{O}i\text{-Pr})_4 \cdot i\text{-PrOH}$ (0.5 equivalents) was used, the stereochemistry of the α -aminoboronic esters was retained in the products.^{6c}

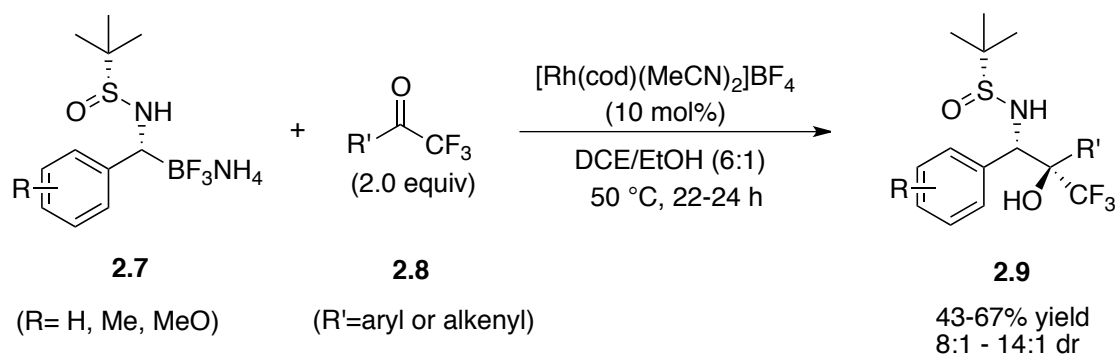


Scheme 2.1 α -aminoboronic esters in enantiospecific Suzuki-Miyaura cross-coupling

Ellman studied Rh-catalyzed nucleophilic addition of α -sulfinamido trifluoroborates to aryl or alkenyl trifluoromethyl ketones.⁸ 1,2-Amino alcohols were generated with retentive stereochemistry from the diastereopure trifluoroborates. For α,β -unsaturated ketones, only 1,2-addition products were observed. However, the substrate scope of α -sulfinamido trifluoroborates in the method was relatively narrow. Aliphatic

⁸ Buesking, A. W.; Ellman, J. *Chem. Sci.* **2014**, 5, 1983-1987.

trifluoroborates were not effective in the reaction, and aromatic trifluoroborates containing an electron-deficient aryl group were ineffective as well.



Equation 2.1 Rh-Catalyzed addition of α -sulfinamido trifluoroborates to trifluoromethyl ketones

In light of their emerging importance in biological and medicinal studies, several research groups have developed enantioselective catalytic reactions to prepare nonracemic α -aminoboronic esters (for an extensive introduction of the published works, please see Section 2.2 in this chapter). Unfortunately, according to the literature, synthesis of enantioenriched aliphatic α -aminoboronic esters is still a challenge to a catalyst-controlled reaction. Herein, we aim to develop a Cu(I)-catalyzed enantioselective borylation reaction to synthesize these biologically interesting compounds.

2.2 Precedents of enantioselective synthesis of α -aminoboronic esters⁹

2.2.1 Substrate-controlled processes

In the 1980s Matteson utilized (+)-pinanediol boronic ester as a chiral auxiliary and developed the first enantioselective synthesis of α -amido boronic acid esters.¹⁰ The key step in his method is a diastereoselective homologation reaction.¹¹ The obtained α -chloromethyl boronic ester was *in situ* treated with LiHMDS to introduce bis(trimethylsilyl)amino group at the α -position. In presence of acetic acid, the silylamine reacted with acetic anhydride to generate the desired product. The industrial synthesis¹² of bortezomib employs an enhanced Matteson homologation reaction,¹³ in which ZnCl₂ (0.7 equiv) is added as a promoter. ZnCl₂ has dual functions¹⁴ in the migration step: (1) facilitating departure of the chloride ion via coordination; (2) improving diastereoselectivity through chelating with an oxygen atom in boronic ester fragment and a chlorine atom in dichloromethyl fragment.

⁹ For racemic syntheses, see: (a) Mann, G.; John, K. D.; Baker, R. T. *Org. Lett.* **2000**, 2, 2105-2108. (b) Kawamorita, S.; Miyazaki, T.; Iwai, T.; Ohmiya, H.; Sawamura, M. *J. Am. Chem. Soc.* **2012**, 134, 12924-12927. (c) Li, Q.; Liskey, C. W.; Hartwig, J. F. *J. Am. Chem. Soc.* **2014**, 136, 8755-8765.

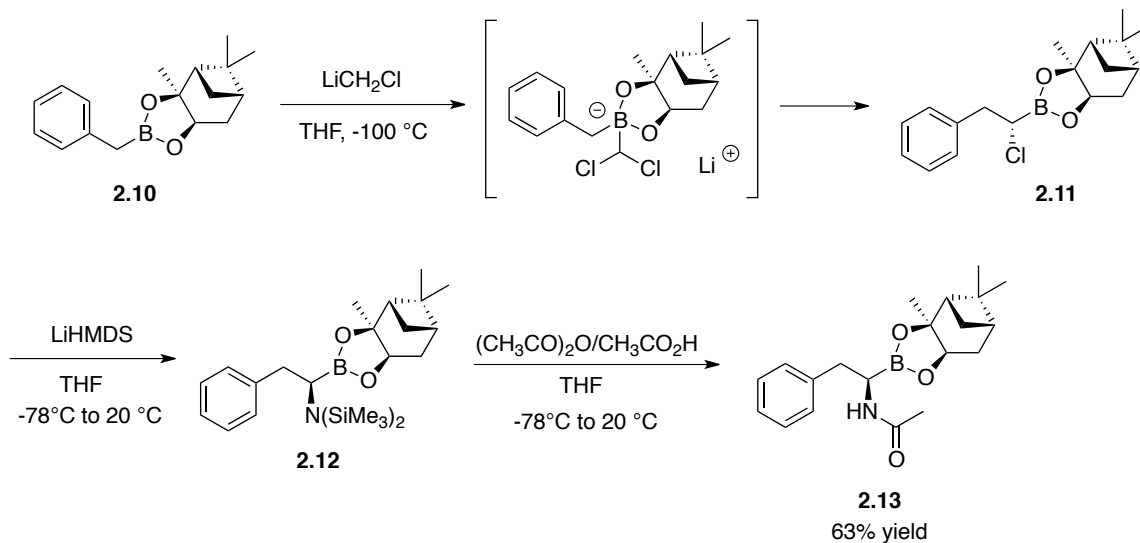
¹⁰ Matteson, D. S.; Sadhu, K. M. *J. Am. Chem. Soc.* **1981**, 103, 5241-5242.

¹¹ For reviews of Matteson homologation reaction, see: (a) Matteson, D. S. *J. Org. Chem.* **2013**, 78, 10009-10023; (b) Matteson, D. S. *Chem. Rev.* **1989**, 89, 1535-1551.

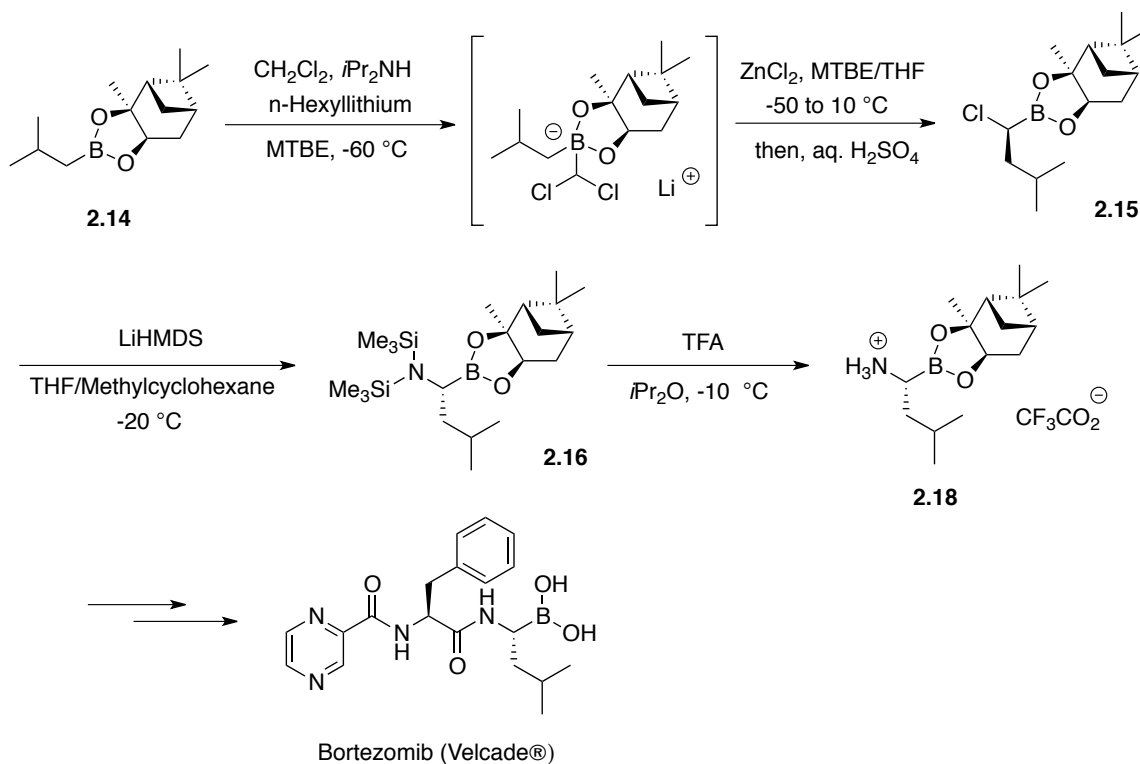
¹² Pickersgill, I. F.; Bishop, J.; Koellner, C.; Gomez, J.-M.; Geiser, A.; Hett, R.; Am-moscato, V.; Munk, S.; Lo, Y.; Chui, F.-T.; Kulkarni, V. R. **WO Patent Appl. 097,809, 2005**.

¹³ (a) Matteson, D. S.; Sadhu, K. M.; Peterson, M. L. *J. Am. Chem. Soc.* **1986**, 108, 810-819. (b) Matteson, D. S.; Sadhu, K. M. *J. Am. Chem. Soc.* **1983**, 105, 2077-2078.

¹⁴ Thomas, S. P.; French, R. M.; Jheengut, V.; Aggarwal, V. K. *The Chemical Record* **2009**, 9, 24-39.

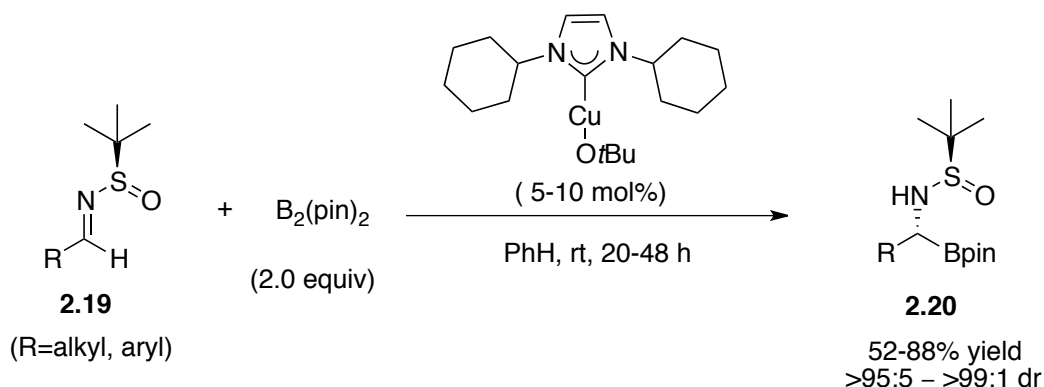


Scheme 2.2 The first example of enantioselective synthesis of α -amino boronic esters



Scheme 2.3 Industrial synthesis of Bortezomib

The amino-protecting group can also play a role in enantioinduction. Ellman employed Sadighi's catalyst,¹⁵ a NHC-Copper complex, in cross additions of B₂(pin)₂ to (*R*)-*N*-*tert*-butanesulfinyl aldimines.¹⁶ α -Sulfinamido boronates were produced in moderate to good yields and with high diastereoselectivity; aryl- and enolizable alkyl-substituted aldimines were both effective substrates in the reaction. The nonracemic *tert*-butylsulfinyl group acted as an amino protecting group and as the chiral auxiliary, which can be removed under acidic conditions. In 2014, Ellman reported greener and operationally simpler conditions¹⁷ for the same type of reaction, in which CuSO₄ and PCy₃ (added in form of HBF₄ salt) were used as the catalyst and ligand, respectively. The reactions were conducted in aqueous toluene in open air with BnNH₂ as the Lewis base. Ketimines were also tested to be suitable substrates in the new conditions to make tertiary α -amino boronates with good diastereoselectivity.



Equation 2.2 NHC–Cu(I)-catalyzed borylation of *N*-*tert*-butanesulfinyl aldimines

¹⁵ Laitar, D. S.; Tsui, E. Y.; Sadihi, J. P. *J. Am. Chem. Soc.* **2006**, *128*, 11036-11037.

¹⁶ Beenen, M. A.; An, C.; Ellman, J. A. *J. Am. Chem. Soc.* **2008**, *130*, 6910-6911.

¹⁷ Buesking, A. W.; Bacauanu, V.; Cai, I.; Ellman, J. A. *J. Org. Chem.* **2014**, *79*, 3671-3677.

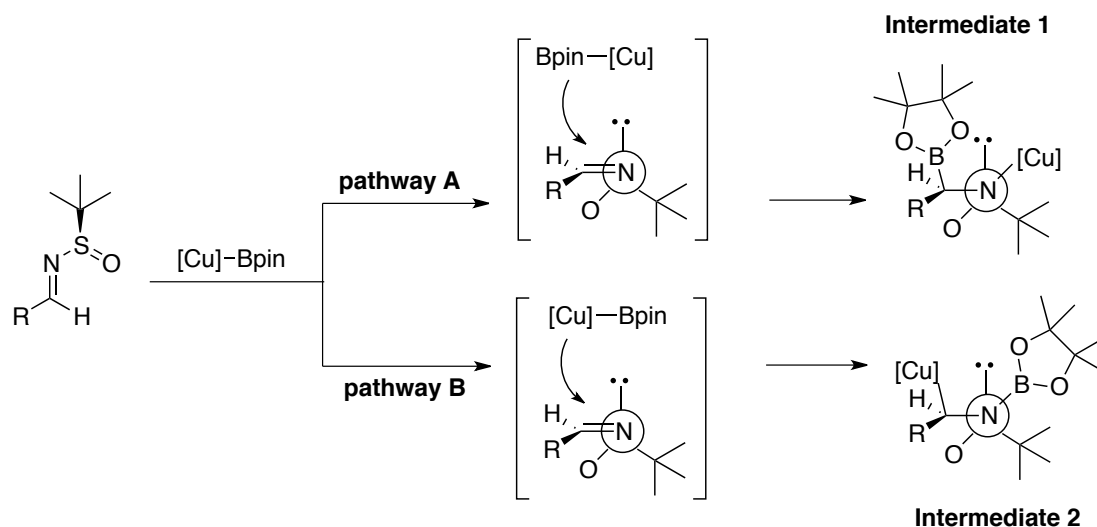
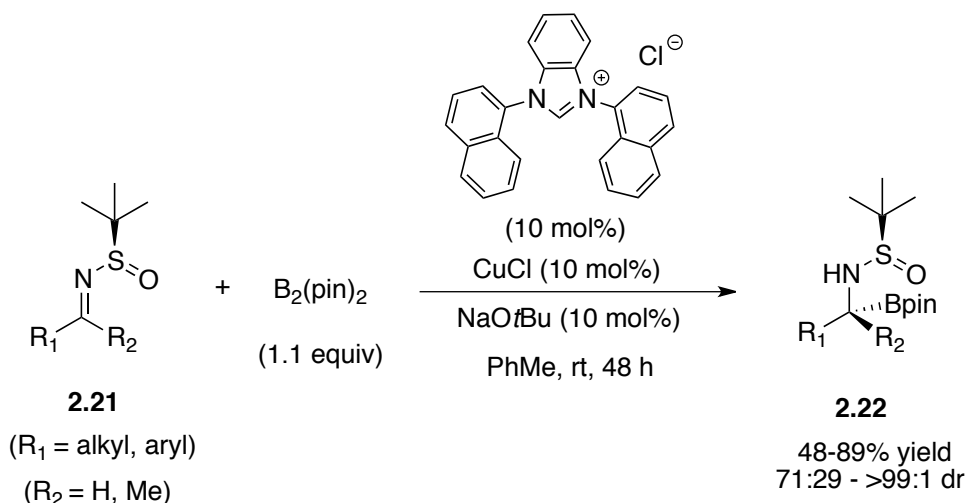


Figure 2.2 Proposed models for observed diastereoselectivity

Sun and coworkers evaluated different types of NHC ligands in the above-mentioned Ellman's borylation strategy, and developed a one-pot procedure for making α -sulfinamido boronates.¹⁸ They found that a *N,N'*-dinaphthyl benzimidazole-derived NHC was a robust ligand for high reactivity, and that the NHC-Cu(I) catalyst could be preformed in the reaction vessel under argon without using a glovebox. Ketimine substrates were also investigated in the standard reaction conditions, but only modest diastereoselectivity was obtained.

¹⁸ Wen, K.; Wang, H.; Chen, J.; Zhang, H.; Cui, X.; Wei, C.; Fan, E.; Sun, Z. *J. Org. Chem.* **2013**, 78, 3405-3409.



Equation 2.3 A benzimidazole-derived NHC ligand in borylation of aldimines and ketimines

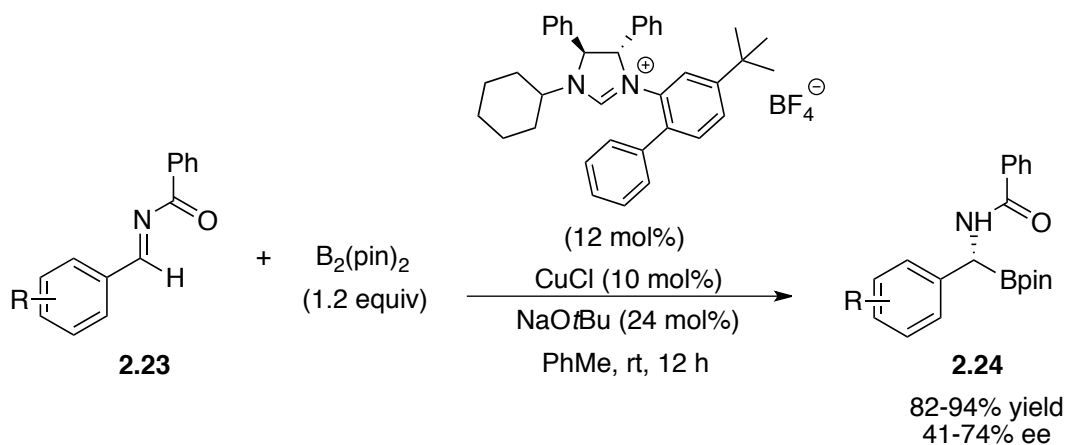
2.2.2 Catalyst-controlled processes

Transition metal-catalyzed borylation reactions provide an effective and tunable method to make boron-containing compounds. Enantioenriched α -amino boronates can be synthesized by using a chiral ligand in the reaction.

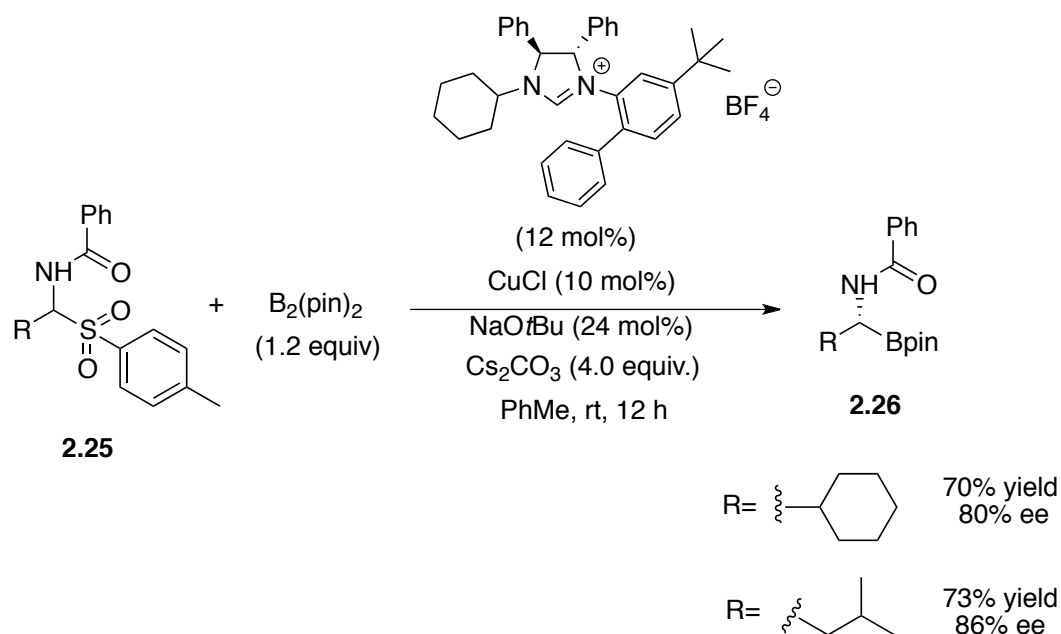
Lin and co-workers investigated chiral NHC-Cu(I)-catalyzed cross addition of $\text{B}_2(\text{pin})_2$ to benzamide-derived aldimines.¹⁹ Through screening different imidazolium salts (the precursors of NHC ligands), they found that a (*N*-alkyl, *N'*-aryl)-hybrid NHC ligand gave good reactivity and high stereoselectivity. While aryl aldimines underwent borylation smoothly, two alkyl aldimines they tested produced low yields (up to 40%). It should be mentioned that these two alkyl substrates gave good stereoselectivity (80% and 84% ee). They attributed the mass loss to the instability of alkyl aldimines under the reaction conditions. To avoid this issue, they employed α -benzamido sulfones as the

¹⁹ Zhang, S.-S.; Zhao, Y.-S.; Tian, P.; Lin, G.-Q. *Synlett* **2013**, 24, 437-442.

substrates to generate the corresponding aldimines *in situ* in presence of excess Cs_2CO_3 , and successfully achieved reasonable yields without loss of stereoselectivity.



Equation 2.4 Chiral NHC-Cu(I)- catalyzed borylation of aromatic aldimines



Equation 2.5 α -Benzamido sulfones as substrates in enantioselective borylation reactions

Liao's group applied a chiral sulfoxide-phosphine ligand in the borylation of *N*-Boc-protected aryl aldimines.²⁰ They found that either a cationic Cu(I) salt or CuCl was an effective precatalyst, and that using a less coordinating solvent, like *t*BuOMe, benefited the stereoselectivity. Unfortunately, the borylated products were not stable under the purification conditions they used. Although the NMR yields they obtained were above 80% in most of cases, the isolated yields were in the range of 40% to 65%. The alkyl substrate **2.29** gave low stereoselectivity under the standard conditions.

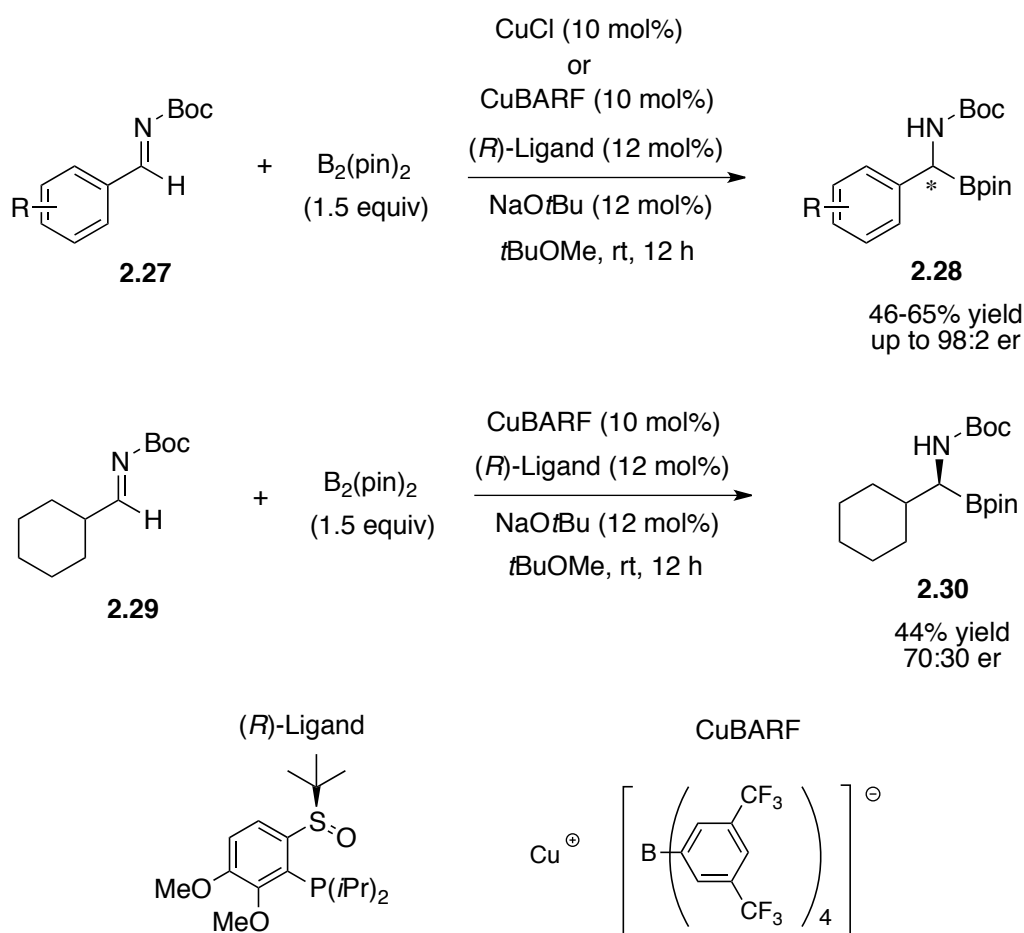
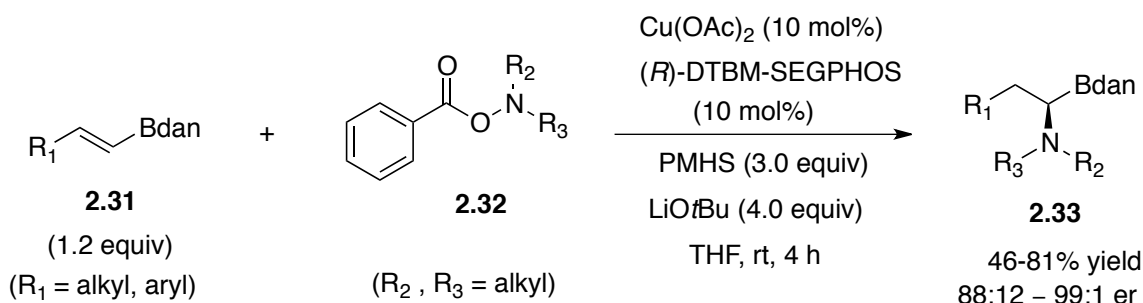


Figure 2.3 Use of Cu(I)/chiral sulfoxide-phosphine complex in borylation of *N*-Boc-imines

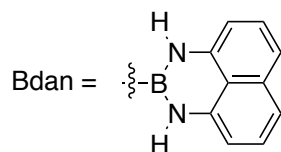
²⁰ Wang, D.; Cao, P.; Wang, B.; Jia, T.; Lou, Y.; Wang, M.; Liao, J. *Org. Lett.* **2015**, *17*, 2420-2423.

More recently, Hirano and Miura developed a $\text{Cu}(\text{OAc})_2$ -catalyzed enantioselective hydroamination reaction of alkenyl Bdan compounds (Bdan = 1,8-diaminonaphthyl boronate).²¹ In presence of polymethylhydrosiloxane (as the hydride source) and sodium *tert*-butoxide, $\text{Cu}(\text{OAc})_2$ was *in situ* converted to Cu(I) hydride. The alkenyl substrates then underwent Cu–H insertion regioselectively, forming a Cu–C bond between the copper atom and the same carbon bearing the Bdan group. The driving force for this observed regioselectivity was attributed to the hyperconjugation between the Cu–C bond and the empty p orbital on boron.²² The generated alkyl cuprates nucleophilically attacked a *N,N*-dialkyl hydroxylamine benzoate to install the amino group on the α carbon. With a SEGPHOS-based chiral bisphosphine ligand to control the stereochemical outcome of the initial hydrocupration process, various α -amino boronates could be synthesized with good to high enantioselectivity (up to 99:1 er). It should be noted that alkenyl Bpin substrates gave no desired products, as they completely decomposed under the standard reaction conditions.

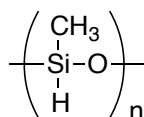


²¹ Nishikawa, D.; Hirano, K.; Miura, M. *J. Am. Chem. Soc.* **2015**, *137*, 15620-15623.

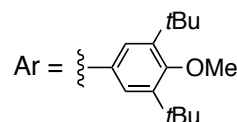
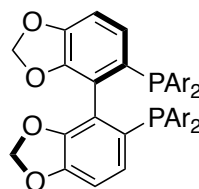
²² For a related computational study, see: Dang, L.; Zhao, H.; Lin, Z. *Organometallics* **2007**, *26*, 2824-2832.



PMHS = polymethylhydrosiloxane



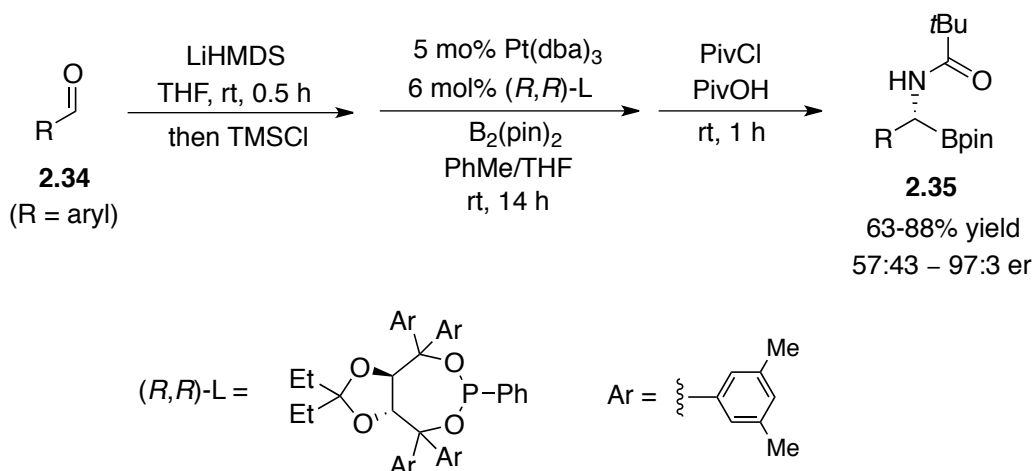
(*R*)-DTBM-SEGPHOS



Equation 2.6 Cu(I)-Catalyzed enantioselective hydroamination of alkenyl Bdan compounds

Morken's group applied a chiral Pt(0)/phosphoramidate complex in asymmetric diboration of aromatic *N*-(trimethylsilyl) aldimines.²³ Employment of this type of substrate brought two advantages: (1) they can be readily prepared by treating aryl aldehydes with LiHMDS; (2) the trimethylsilyl group in the borylated products can be swapped with an acyl group under mild conditions, which makes it convenient to introduce an α -amido boronate fragment into a peptide chain. Hence, they developed a tandem diboration/pivaloylation sequence, and prepared a variety of aryl-substituted α -amidoboronic esters in above 75% overall yields and with high enantioselectivity (up to 97:3 er). Unfortunately, the substrate scope in this strategy is limited to aromatic aldehydes. Aliphatic aldehydes failed to give the desired products with the same method.

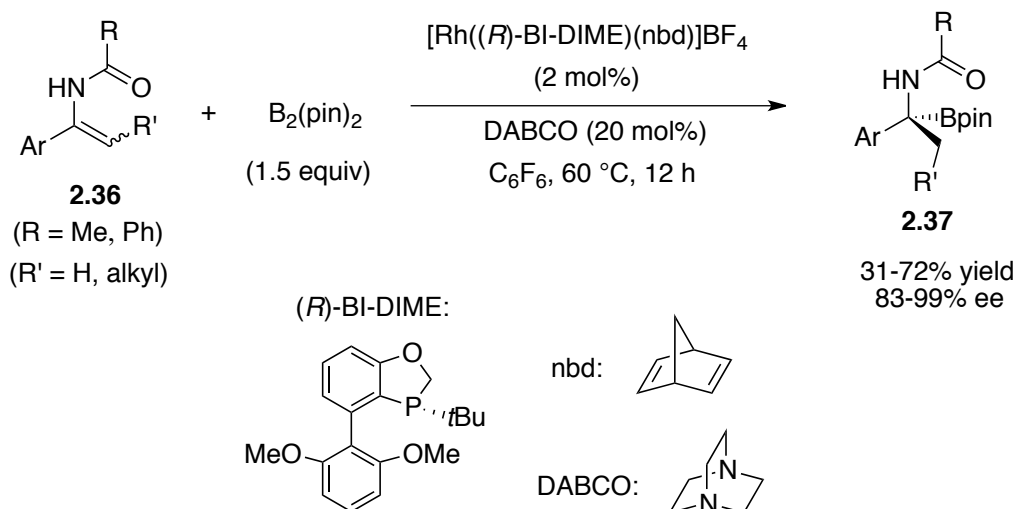
²³ Hong, K., Morken, J. P. *J. Am. Chem. Soc.* **2013**, *135*, 9252-9254.



Scheme 2.4 Tandem diboration/pivaloylation of aromatic *N*-(trimethylsilyl) aldimines

Tang and co-workers reported a Rh(I)-catalyzed enantioselective hydroboration reaction of *N*-acyl enamines to make tertiary α -amidoboronic esters.²⁴ This catalyst-controlled hydroboration proceeded in an anti-Markovnikov fashion, installing the Bpin fragment at the sterically less accessible position. The invented P-chiral monophosphine ligand was critical to the observed reactivity and stereoselectivity. Addition of DABCO further suppressed formation of the other regiomer and other byproducts. Benzylidenebenzamide, an aromatic aldimine, was tested in the same reaction conditions, but the hydroboration product was obtained in 20% yield and with 13% ee. This reactivity difference and the results of further deuterium-labeling experiments they conducted suggested that the active proton in the substrates was involved in the catalytic cycle, which explains generation of hydrogenation products, like compound **2.40**, in absence of any external hydride sources.

²⁴ Hu, N.; Zhao, G.; Zhang, Y.; Liu, X.; Li, G.; Tang, W. *J. Am. Chem. Soc.* **2015**, *137*, 6746-6749.



Equation 2.7 Rh(I)-Catalyzed enantioselective hydroboration of α -aryl-*N*-Acylenamines

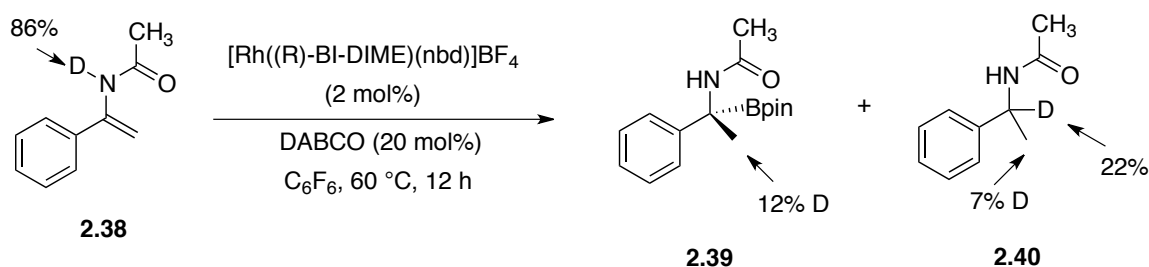


Figure 2.4 The deuterium-labeling experiment in Tang's hydroboration study

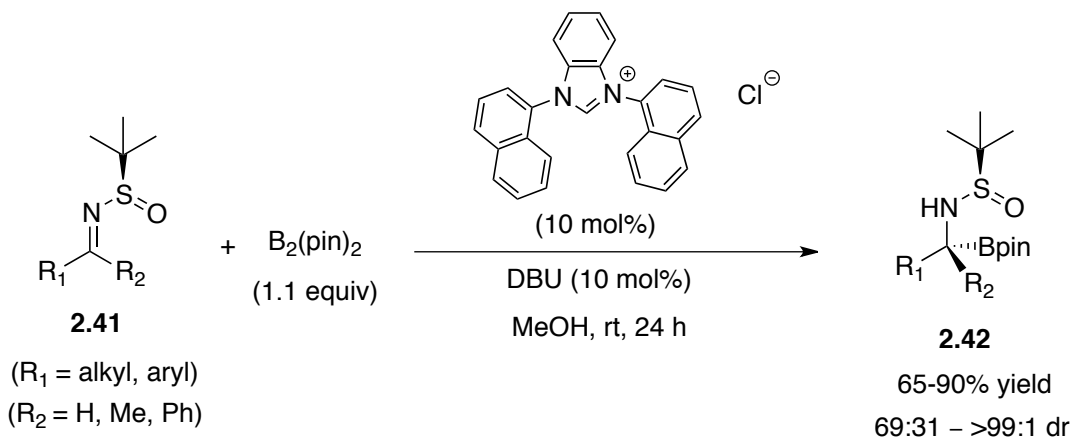
2.2.3 Organocatalytic asymmetric syntheses of α -aminoboronic esters

In absence of transition metals, Lewis bases such as methoxide anion²⁵ or NHCs²⁶ can directly promote nucleophilic addition of pinacolboronyl group to activated or unactivated olefins through forming adducts with $B_2(\text{pin})_2$.

²⁵ For representative examples, see: (a) Bonet, A.; Gulyás, H.; Fernández, E. *Angew. Chem. Int. Ed.* **2010**, *49*, 5130-5134. (b) Bonet, A.; Pubill-Ulldemolins, C.; Bo, C.; Gulyás, H.; Fernández, E. *Angew. Chem. Int. Ed.* **2011**, *50*, 7158-7161. (c) Pubill-Ulldemolins, C.; Bonet, A.; Bo, C.; Gulyás, H.; Fernández, E. *Chem. Eur. J.* **2012**, *18*, 1121-1126.

²⁶ For representative examples, see: (a) Lee, K.-s.; Zhugralin, A. R.; Hoveyda, A. H. *J. Am. Chem. Soc.* **2009**, *131*, 7253-7255. (b) O'Brien, J. M.; Hoveyda, A. H. *J. Am. Chem. Soc.* **2011**, *122*, 7712-7715. (c) Wu, H.; Radomkit, S.; O'Brien, J. M.; Hoveyda, A. H. *J. Am. Chem. Soc.* **2012**, *134*, 8277-8285.

Sun and Fan studied an achiral NHC-catalyzed hydroboration reaction of (*R*)-*N*-*tert*-butanesulfinyl aldimines and imines with B₂(pin)₂ in methanol.²⁷ A combination of a *N,N'*-dinaphthylimidazolium salt (as the NHC precursor) and DBU (as Lewis base) gave the most satisfying yields. In aprotic solvents no desired products were generated. Compared with other protic solvents they tested, methanol turned to be a better proton source. They used ¹¹B-NMR and mass spectrum analysis to try to clarify whether a methoxide/B₂(pin)₂ or NHC/B₂(pin)₂ adduct was responsible for the nucleophilic addition, but the combined information indicated that a complex consisted of NHC, methanol and B₂(pin)₂ may serve as the active intermediate. Notably, α, β-unsaturated substrates (ketones, aldimines and imines) were also evaluated in the established conditions, and 1,4-addition products were obtained as the exclusive products.

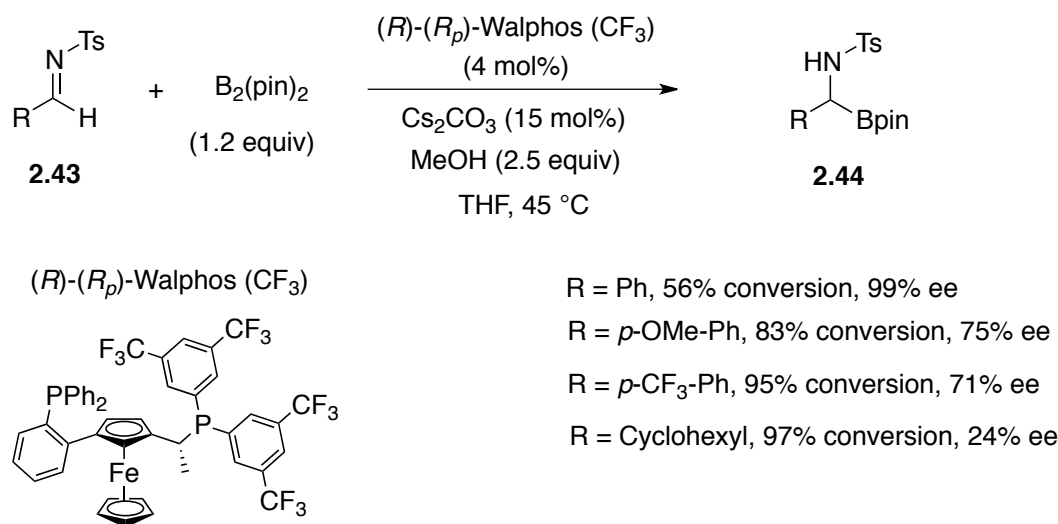


Equation 2.8 NHC-Catalyzed hydroboration of (*R*)-*N*-*tert*-butanesulfinylaldimines and imines

Except strong electron donors, like NHCs, arylphosphines also can be used in organocatalytic borylation reactions. Based on their previous studies,²⁴ Fernández's group examined chiral phosphines in enantioselective hydroboration of *N*-

²⁷ Wen, K.; Chen, J.; Gao, F.; Bhadury, P. S.; Fan, E.; Sun, Z. *Org. Biomol. Chem.* **2013**, *11*, 6350-6356.

tosylaldimines.²⁸ In presence of a Walphos-type chiral bisphosphine or chiral Quinap, aryl-substituted α -sulfonamido boronic acid pinacol esters (three examples) were obtained with moderate to good enantioselectivity, whereas the alkyl substrate gave poor stereoselectivity.



Equation 2.9 Chiral bisphosphines for enantioselective hydroboration of *N*-tosylaldimines

2.3 Proposed catalytic synthesis of α -amido boronates with hemiaminal ethers

Transition metal-catalyzed hydroboration reaction of aldimines or imines provides a straightforward method of synthesizing α -amino boronic esters, but previous catalyst-controlled processes achieved limited success in accessing alkyl-substituted products with reasonable reactivity along with good enantioselectivity.

Our working hypothesis originated from Lin's strategy¹⁹ of *in situ* generation of alkyl-substituted aldimines from corresponding α -amido sulfones. We envisioned that hemiaminal ethers are also potential precursors for aldimines in presence of a strong

²⁸ Solé, C.; Gulyás, H.; Fernández, E. *Chem. Commun.* **2012**, 48, 3769-3771.

Lewis base. Although, thermodynamically, it is unfavorable for deprotonated hemiaminal ethers to release the parent aldimines and alkoxides, forming adducts between $B_2(\text{pin})_2$ and the departed alkoxides may serve as the driving force for the dissociation process.

Based on the following theories, we proposed a catalytic cycle of synthesizing α -amino boronic acid pinacol esters from hemiaminal ethers: (1) catalytic amount of a strong Lewis base deprotonates the substrate, releasing the corresponding aldimine and alkoxide in an equilibrium, (2) the released alkoxide acts as a promoter for forming a Cu-Bpin complex through activation of $B_2(\text{pin})_2$ and the subsequent transmetallation, (3) the copper amide species produced from the borylation step deprotonates one molecule of the substrate to turn over the copper catalyst.

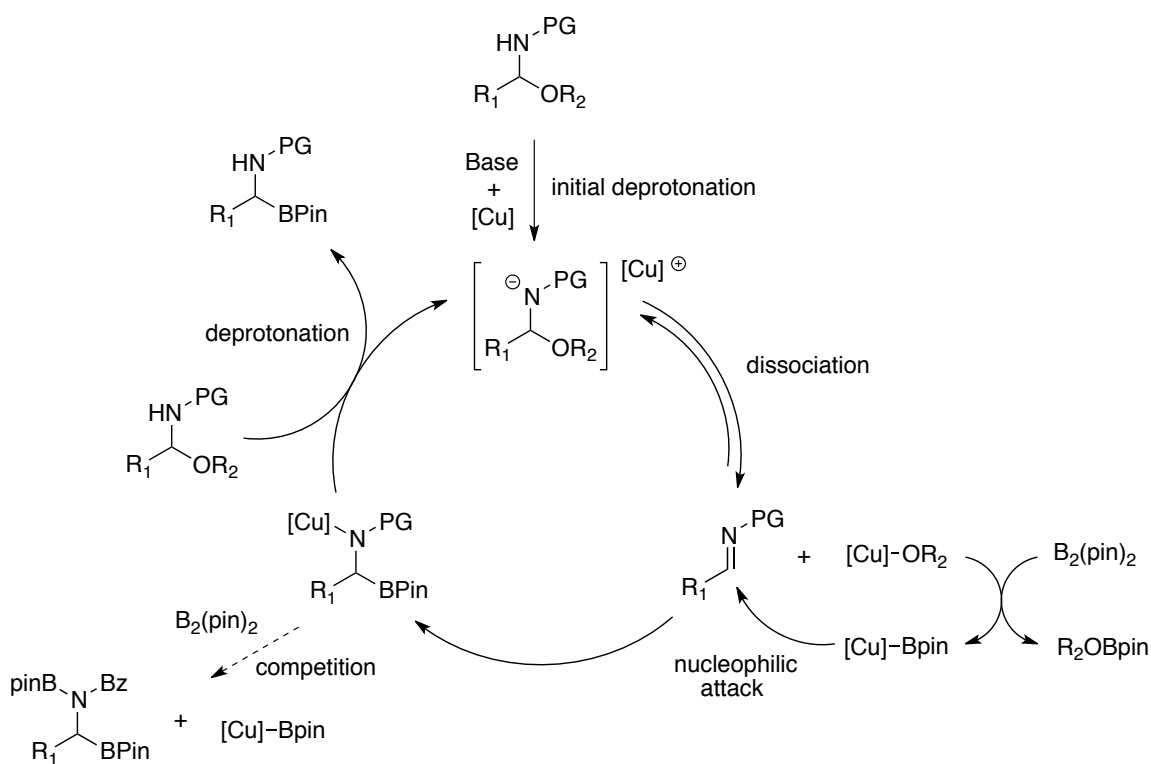
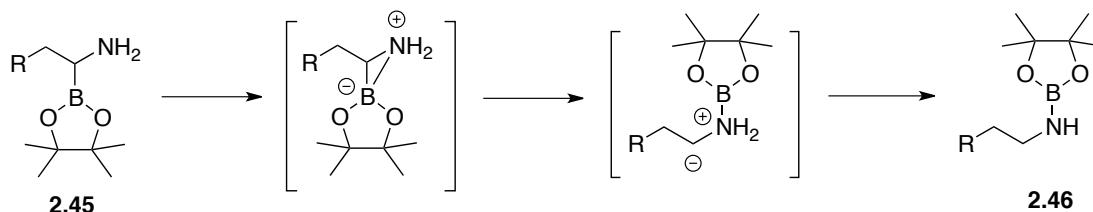


Figure 2.5 Proposed catalytic cycle of borylation of hemiaminal ethers

2.4 Development of copper-catalyzed borylation of hemiaminal ethers

2.4.1 Borylation of the phenyl-substituted hemiaminal methyl ether

Our preliminary exploration started with hemiaminal ether **2.47** as the substrate. The *in situ* generated *N*-benzoyl aldimine has reasonable stability,²⁹ and it is a nonenolizable aldimine. It should be noted that an electron-withdrawing protecting group on the nitrogen, for instance an acyl group, is crucial to the stability of borylated products, because unprotected α -amino boronic acid pinacol esters thermodynamically tend to undergo 1,2-boryl rearrangement.^{1h,5c}



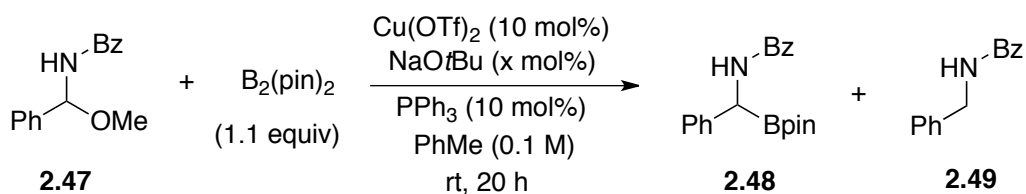
Scheme 2.5 1,2-Boryl rearrangement of unprotected α -amino boronic acid pinacol esters

Considering the added copper precatalyst might function as a Lewis acid and react with the substrate alone to generate an iminium intermediate instead of the desired aldimine, we first studied the influence of base loading on the reaction (Table 2.1). We chose $\text{Cu}(\text{OTf})_2$, which is a relatively strong Lewis acid, as the precatalyst³⁰ and NaOtBu as the Lewis base in the investigation. PPh_3 and toluene were selected as the ligand and solvent, respectively. Since the borylated product **2.48** is a known compound, whose

²⁹ One method of making this aldimine is to heat *N*-(1-methoxy-1-phenylmethyl)benzamide at 120 °C and remove produced methanol via vacuum. For reference, see: (a) Aggarwal, V. K.; Vasse, J.-L. *Org. Lett.* **2003**, 5(21), 3987-3990. (b) Uraguchi, D.; Sorimachi, K.; Terada, M. *J. Am. Chem. Soc.* **2005**, 127, 9360-9361.

³⁰ $\text{Cu}(\text{OTf})_2$ can *in situ* generate CuOTf under a borylation condition. For representative examples, see: (a) Guzman-Martinez, A.; Hoveyda, A. H. *J. Am. Chem. Soc.* **2010**, 132, 10634-10637. (b) Ibrahem, I.; Breistein, P.; Córdova, A. *Angew. Chem. Int. Ed.* **2011**, 50, 12036-12041.

characterization data has been published,^{6b,6c,19} we used 1,3,5-trimethoxybenzene as the internal standard in the ¹H-NMR analysis to accelerate our data collection.



Entry	NaOtBu (mol%)	Conversion (%) ^a	Yield of 2.48 (%) ^a	Yield of 2.49 (%) ^a
1	10	41	17	5
2	20	59	48	10
3	50	78	54	21
4	100	94	25	35

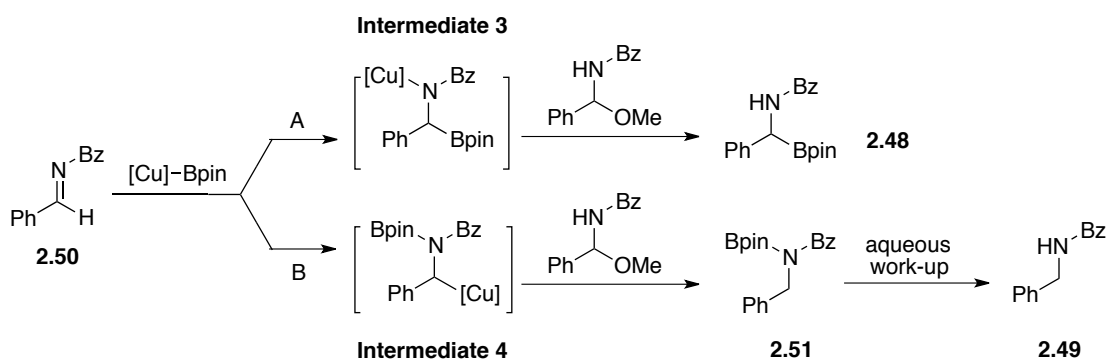
^aDetermined by ¹H-NMR of unpurified products with 1,3,5-trimethoxybenzene as the internal standard. ^bReactions employed 0.1 mmol of **2.47**.

Table 2.1 The influence of base loading^b

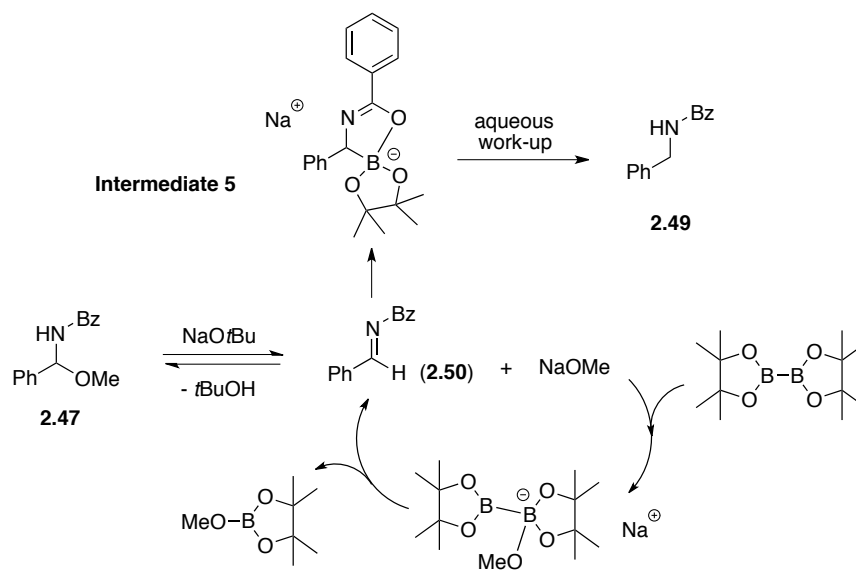
With more NaOtBu being added, both conversion and yield increased (entry 1, 2 and 3, Table 2.1). However, as 1 equivalent of NaOtBu was used, the yield dramatically decreased (entry 4). When the molecular ratio of Cu(OTf)₂ to NaOtBu was 1 to 2, the reaction achieved the optimal conversion and yield (entry 2, Table 2.1).

Meanwhile, upon ¹H-NMR analysis of the crude borylation products, the major byproduct in the reaction was identified to be the “protodeborylation” compound **2.49**. Based on Ellman’s study,¹⁶ we proposed an explanation for generation of this byproduct (Scheme 2.6). *In situ* generated aldimine **2.50** can react with Cu-Bpin complex in two different patterns, in which either Bpin or ligated Cu(I) could be installed at the α-position. Pathway A leads to the desired product, whereas pathway B results in the byproduct. In both cases, one molecule of substrate **2.47** serves as the proton source, and once it gets deprotonated the active copper amide intermediate in the catalytic cycle will

be regenerated. Hence, pathway B does not terminate the catalytic cycle. An argument is that byproduct **2.49** may come from protodeborylation of the borylated product **2.48** during the aqueous work-up. Nonetheless, the yields of this compound from screened conditions were not in a narrow range. For instance, following a consistent work-up procedure, byproduct **2.49** was detected to be 5% from the condition of entry 1 in Table 2.1, but from the condition of entry 4 it was 35%. It is more likely that the byproduct mainly came from different reaction pathways.



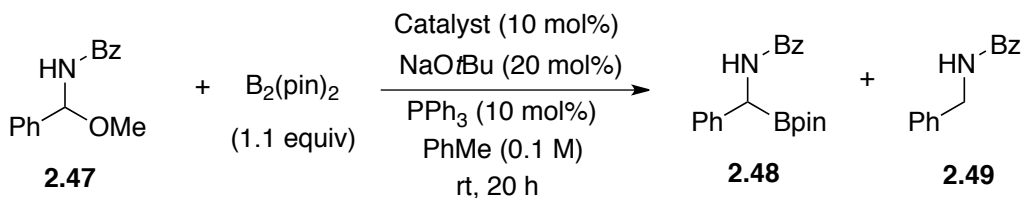
Scheme 2.6 Two possible pathways of the aldimine intermediate undergoing the nucleophilic addition



Scheme 2.7 Proposed NaOMe-mediated borylation of aldimine **2.50**

On the other hand, Fernández's studies^{25,28} of methoxide anion-promoted borylation prompted us to consider another possibility involved in the borylation of substrate **2.47** (Scheme 2.7). NaOMe, generated from deprotonation of the substrate by NaOtBu, can directly form an adduct with B₂(pin)₂ prior to undergoing a salt metathesis with CuCl. Based on Fernández's investigations, this adduct may function as a nucleophile and react with aldimine **2.50** to generate **Intermediate 5**. Stabilization by the phenyl group of the negative charge at the benzylic position may prolong the lifetime of **Intermediate 5** in the reaction solution. Upon aqueous work-up or being quenched by the active proton of substrate **2.47**, **Intermediate 5** can produce byproduct **2.49**. Hence, more NaOMe was generated in the reaction may lead to a higher yield of the byproduct.

We next screened different copper precatalysts in the reaction (Table 2.2), and found that CuBr afforded the most satisfying conversion and yield.

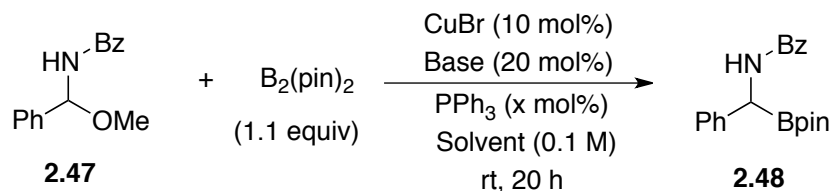


Entry	Catalyst	Conversion (%) ^a	Yield of 2.48 (%) ^a	Yield of 2.49 (%) ^a
1	[CuOTf] ₂ ·C ₆ H ₆ ^b	48	38	8
2	Cu(OTf) ₂	59	48	10
3	CuCl	49	42	6
4	CuCl ₂	12	9	Trace
5	Cu(OAc) ₂	77	64	12
6	Cu(OPiv) ₂	31	17	2
7	CuBr	89	79	16
8	CuBr ₂	77	51	17
9	CuI	90	69	13

^aDetermined by ¹H-NMR of unpurified products with 1,3,5-trimethoxybenzene as the internal standard. ^b5 mol% was used. ^cReaction scale: 0.1 mmol of **2.47**.

Table 2.2 Screening of different copper precatalysts^c

To further improve the reaction, we also studied the influence of different alkaline bases, ligand loadings and solvents on the yield.



Entry	Base	PPh ₃ (mol%)	Solvent	Conversion (%) ^a	Yield (%) ^a
1	NaOtBu	10	PhMe	89	79
2	LiOtBu	10	PhMe	34	22
3	KOtBu	10	PhMe	33	26
4	NaOtBu	20	PhMe	93	79
5	NaOtBu	10	THF	83	43
6	NaOtBu	10	1,4-dioxane	12	Trace
7	NaOtBu	10	CH ₂ Cl ₂	30	12
8	NaOtBu	10	MTBE ^b	96	81
9	NaOtBu	10	Et ₂ O	>98	92 (82) ^c

^aDetermined by ¹H-NMR of unpurified products with 1,3,5-trimethoxybenzene as the internal standard. ^bMTBE: methyl *tert*-butyl ether. ^cThe isolated yield is shown in the parenthesis.

^dReactions employed 0.1 mmol of **2.47**.

Table 2.3 Further studies of other variables in the borylation reactions^d

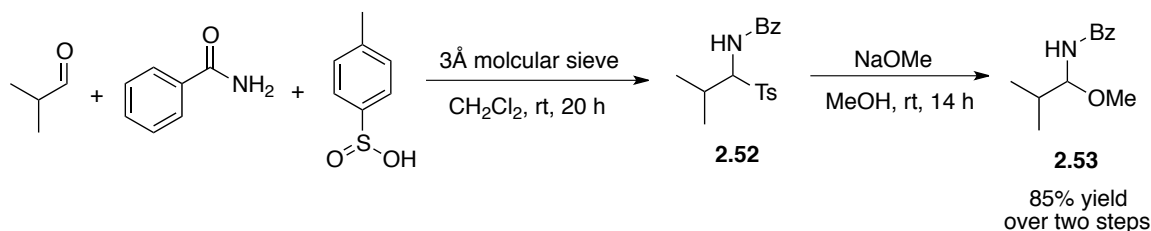
When NaOtBu was replaced with either LiOtBu or KOtBu, the reaction conversion and yield significantly decreased (entry 1, 2 and 3, Table 2.3). The different solubilities of these alkali metal *tert*-butoxides may be responsible for the observed reactivity difference (at room temperature, solubility of NaOtBu in toluene is 7% (w/w), but for LiOtBu and KOtBu it is 4% and 2%, respectively). Solvents with higher coordinating capabilities, like THF or 1,4-dioxane, impeded borylation (entry 4 and 5, Table 2.3). In MTBE and Et₂O the reaction became completely heterogeneous, but better results were achieved (entry 7 and 8, Table 2.3). From the condition of entry 8 we

obtained full conversion and 82% isolated yield. Higher ligand loading marginally enhanced the conversion (entry 4, Table 2.3).

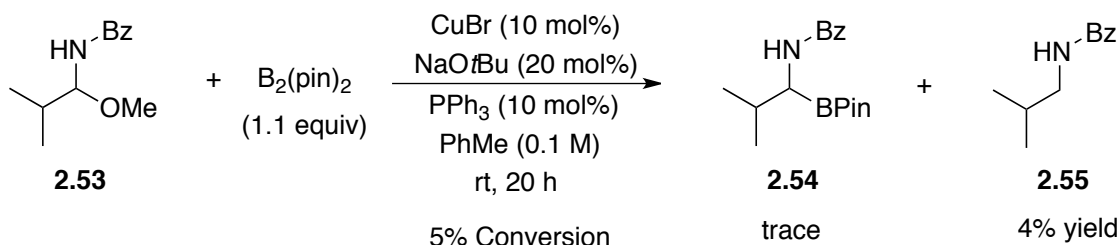
2.4.2 Copper-catalyzed borylation of alkyl-substituted hemiaminal ethers

Alkyl-substituted α -amido boronic esters have broader and more important applications than the aryl-substituted compounds in biological studies. After successfully prepared the borylation product **2.48**, we focused on aliphatic substrates in our method.

Hemiaminal ether **2.53** was selected as the model substrate and tested in the above standard conditions of synthesis of **2.48**, but, unfortunately, only trace amount of desired product was detected by ^1H -NMR study.



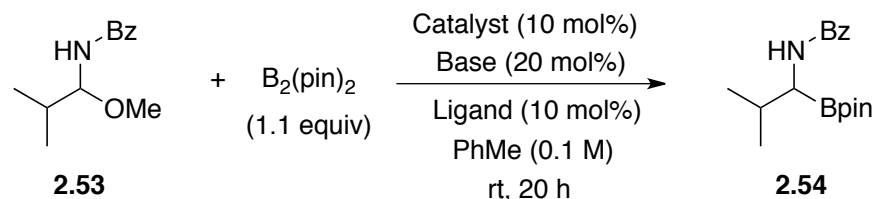
Scheme 2.8 Preparation of an alkyl-substituted hemiaminal ether **2.53**



Equation 2.10 The initial test of the alkyl hemiaminal ether in the borylation conditions

To improve the reactivity, we screened different Cu(I) precatalysts, ligands, alkaline bases and solvents in the reaction conditions (Table 2.4). A combination of CuCl

and NaOtBu turned to be most effective for the borylation, and toluene was a better solvent than Et₂O for the yield. The electron-rich phosphine ligand, PCy₃, gave better results, but a higher loading of this reagent slightly benefited the conversion and yield (entry 14, Table 2.4). Two bidentate phosphine ligands were also evaluated in the reaction (entry 16 and 17), but lower yields were observed.

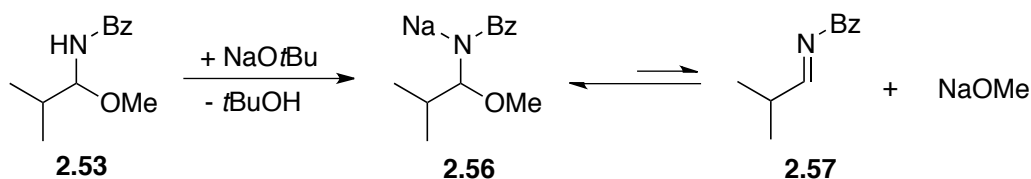


Entry	Catalyst	Base	Ligand	Conversion (%) ^a	Yield (%) ^a
1	CuBr	NaOtBu	PPh ₃	5	trace
2	CuBr	NaOtBu	PCy ₃	24	18
3	CuBr	NaOtBu	P(OiPr) ₃	16	10
4	CuBr	KOtBu	PCy ₃	24	16
5	CuCl	NaOtBu	PCy ₃	45	40
6	[CuOTf] ₂ ·C ₆ H ₆ ^b	NaOtBu	PCy ₃	7	trace
7	Cu(OTf) ₂	NaOtBu	PCy ₃	19	11
8	Cu(OAc) ₂	NaOtBu	PCy ₃	39	26
9	CuI	NaOtBu	PCy ₃	22	4
10	CuCl	NaOtBu	PPh ₃	23	11
11	CuCl	NaOtBu	P(OiPr) ₃	32	21
12	CuCl	LiOtBu	PCy ₃	21	12
13	CuCl	KOtBu	PCy ₃	26	13
14	CuCl	NaOtBu	PCy ₃ ^c	54	44
15	CuCl	NaOtBu ^d	PCy ₃	70	49
16	CuCl	NaOtBu	<i>rac</i> -BINAP	32	16
17	CuCl	NaOtBu	Cy ₂ P-CH ₂ -CH ₂ -PCy ₂	43	18
18 ^d	CuCl	NaOtBu	PCy ₃	49	35

^aDetermined by ¹H-NMR of unpurified products with 1,3,5-trimethoxybenzene as the internal standard. ^b5 mol% was used. ^c20 mol% was used. ^dEt₂O was used as the solvent. ^eReactions employed 0.1 mmol of **2.53**.

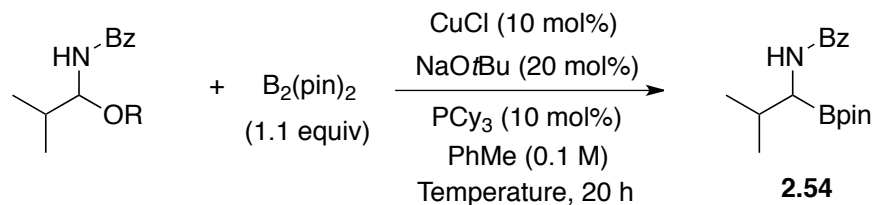
Table 2.4 Optimization of the reaction conditions of synthesis of 2.54^e

The limited success achieved in the above optimization implied that the reaction is kinetically unfavorable. This information drove us to re-evaluate the factors that can facilitate the borylation. Electronically, aliphatic aldimines can be more electrophilic than the aromatic aldimines, because an aryl substituent can donate more electron density to the carbonyl carbon. Therefore, it seems that hemiaminal ether **2.53** would have reacted faster than **2.47**. A rationale for the opposite observation is that the rate of releasing aldimine **2.57** from substrate **2.53** is determined by the dissociation equilibrium (Scheme 2.9). The relatively higher electrophilicity of alkyl-substituted aldimines can make the dissociation direction less favorable, because NaOMe tends to re-attack aldimine **2.57**, shifting the equilibrium to the left.



Scheme 2.9 Proposed dissociation equilibrium of deprotonated substrate **2.53**

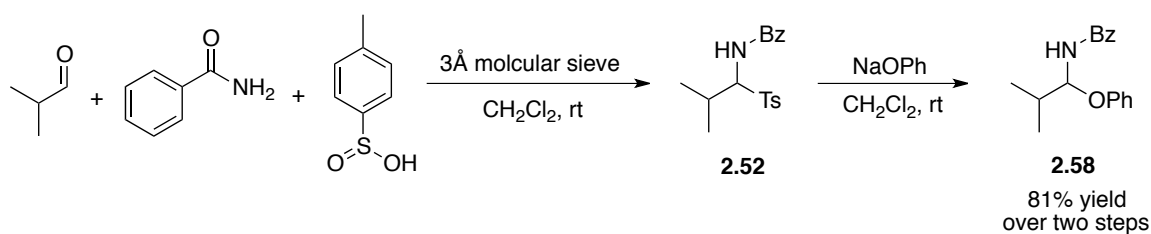
We came up with two separate solutions to accelerate the reaction: (1) increasing reaction temperature; (2) switching the methoxy group in hemiaminal ether **2.53** to an alkoxy group with higher leaving tendency (Table 2.5). As we expected, higher temperature indeed led to higher conversions and yields (entry 2 and 3, Table 2.5). At 50 °C we observed full conversion and 82% NMR yield. As for modification of the substrate, we reasoned that phenoxy group could be a good candidate, as electronically and sterically it is a better leaving group. The substrate **2.58** exhibited superior reactivity (entry 4), which gave product **2.54** in 88% isolated yield at room temperature.



Entry	R	Temperature (°C)	Conversion (%) ^a	Yield (%) ^a
1	Me-	22	45	40
2	Me-	35	68	53
3	Me-	50	>98	82
4	Ph-	22	>98	92 (88) ^b

^aDetermined by ¹H-NMR of unpurified products with 1,3,5-trimethoxybenzene as the internal standard. ^bThe isolated yield is shown in the parenthesis. ^creaction scale: 0.1 mmol.

Table 2.5 Influence of temperature and substrate structure on the reactivity^c

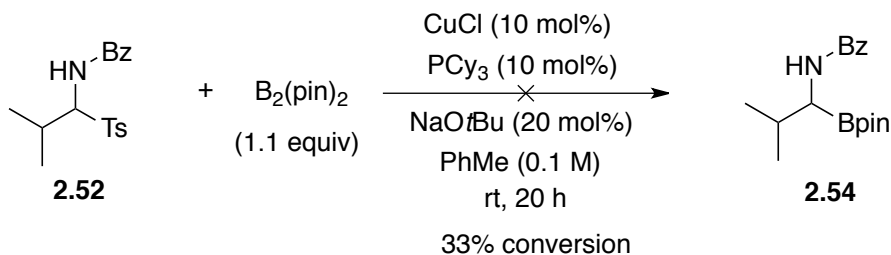


Scheme 2.10 Preparation of hemiaminal ether 2.58

We also evaluated α -amido sulfone **2.52** in the borylation conditions, because α -amido sulfones can be treated as precursors for *N*-acyl imines in presence of a Lewis base.³¹ We observed 33% conversion of the reaction, but no borylation product **2.54** was detected by ¹H-NMR. In addition, 18% benzamide was found in the crude product. One possibility is that either sodium or copper(I) *p*-toluenesulfonate, generated *in situ* from the reaction, stayed as precipitate in the toluene solution and therefore failed to form an

³¹ For reviews, see: (a) Petrini, M. *Chem. Rev.* **2005**, *105*(11), 3949-3977. (b) Yin, B.; Zhang, Y.; Xu, L.-W. *Synthesis* **2010**, *21*, 3583-3595.

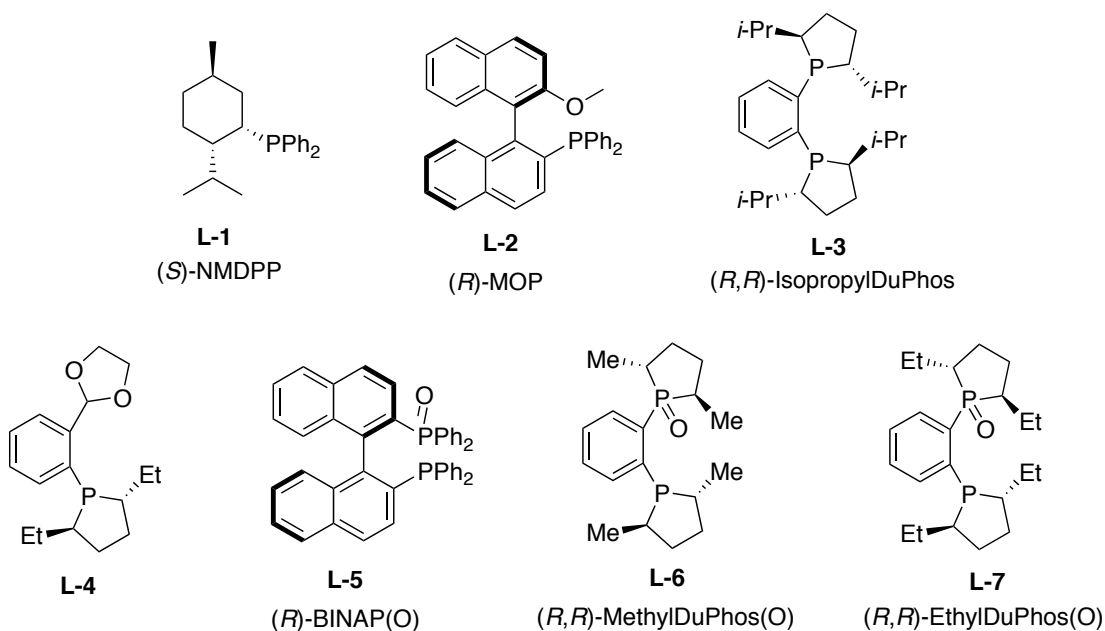
adduct with B₂(pin)₂. Hence, we deduced that the phenoxide released from deprotonation of substrate **2.58** played a role in activation of B₂(pin)₂.

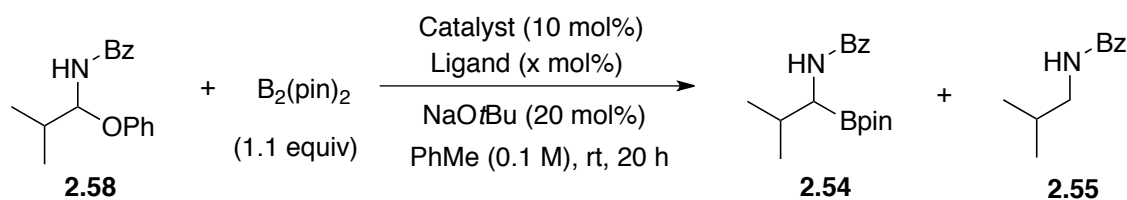


Equation 2.11 The α -amido sulfone as the substrate in the borylation conditions

2.4.3 Development of enantioselective borylation of aliphatic hemiaminal ethers

Synthesis of enantioenriched alkyl-substituted α -amido boronic esters is still a challenge in a catalyst-controlled asymmetric reaction. We envisioned that our borylation strategy could serve as an alternative way to prepare this type of molecule by using a chiral ligand. With the above reactivity issue solved, we screened different chiral ligands in the borylation conditions (Table 2.6).





Entry	Ligand (mol%)	Conversion ^a (%)	Yield of 2.54 (%) ^b	Yield of 2.55 (%) ^a	er ^c
1	—	51	36	2	—
2 ^d	PCy ₃ (10)	39	—	—	—
3	L-1 (20)	93	79	8	53:47
4	L-2 (20)	65	40	<2	67:33
5	L-3 (12)	>98	41	16	48:52
6	L-4 (12)	82	62	<2	51:49
7	L-5 (12)	74	51	3	49:51
8	L-6 (12)	>98	80	<2	87:13
9	L-7 (12)	98	78	8	81:19
10	L-6 (20)	>98	80	<2	89:11

^aDetermined by ¹H-NMR of unpurified products with 1,3,5-trimethoxybenzene as the internal standard. ^bIsolated yield. ^cDetermined by chiral HPLC. ^dCuCl was not added.

Table 2.6 Ligand screening in the enantioselective borylation reaction

The first related information we collected is about the “background” reactions. In our method, the enantioselectivity can be affected by two possible “background” reactions: (1) CuCl can catalyze the borylation in absence of any external ligands, (2) NaOPh, generated *in situ* from the reaction, can mediate the borylation (according to Fernández’s organocatalytic reactions²⁸). The control experiments (entry 1 and 2, Table 2.6) indicated that a copper precatalyst is essential to obtain the borylated product, and that CuCl can appreciably catalyze the reaction without any external ligands. To kinetically suppress the “ligand-free” background reaction, we kept the molecular ratio of phosphine to copper as 2 to 1 in the following ligand screening.

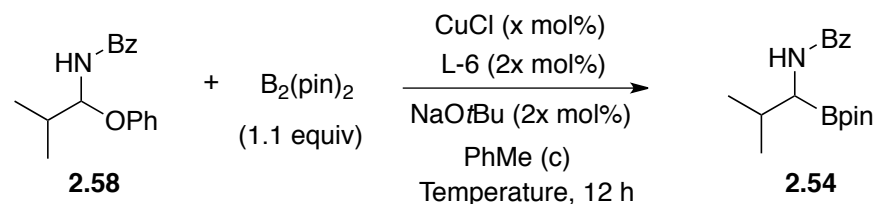
Two monophosphine ligands, **L-1** and **L-2**, were first evaluated (entry 3 and 4, Table 2.6). With ligand **L-1** nearly no enantioselectivity was obtained, but we observed 67:33 er from **L-2**. When (*R,R*)-Isopropyl-DuPhos, **L-3**, was employed, complex mixtures were generated and the isolated desired product turned to be almost racemic (entry 5). While (*R*)-MOP (**L-2**) is well known as a chiral monodentate ligand,³² some studies revealed that the methoxy group in this ligand can serve as a hemilabile coordinating site to a transition metal.³³ In other words, ligand **L-2** might function as a P,O-bidentate ligand in the tested conditions. Following this direction, we examined **L-4** and **L-5**, but, unfortunately, they both gave the racemic product (entry 6 and 7). Switching to the DuPhos-based bisphosphine monoxide ligands (**L-6** and **L-7**), we were pleased to find that they were both effective in enantiocontrol and gave good yields. The reaction employing ligand **L-6** was more enantioselective than that of ligand **L-7** (entry 8 and 9). To further suppress the “background” reaction, the loading of ligand **L-6** was increased to 20 mol%, but the enantioselectivity was slightly improved (entry 10).

We then investigated other variables of the reaction (Table 2.7). Lowering catalyst loading slightly improved the enantioselectivity (entry 3, Table 2.7), but the stereochemical outcome of the reaction was still under good control even at 2.5 mol% catalyst loading (entry 3). On the other hand, the yield of the reaction was improved by using less catalyst (entry 2 and 3). Increasing the reaction concentration accelerated the borylation, which was finished in 15 h, but the yield and enantioselectivity were both slightly diminished (entry 4). While preparing other aliphatic substrates, we found that

³² For a review, see: Hayashi, T. *Acc. Chem. Res.* **2000**, *33*, 354-362.

³³ (a) RajanBabu, T. V.; Nomura, N.; Jin, J.; Radetich, B.; Park, H.; Nandi, M. *Chem. Eur. J.* **1999**, *5*(7), 1963-1968. (b) Nandi, M.; Jin, J.; RajanBabu, T. V. *J. Am. Chem. Soc.* **1999**, *121*, 9899-9900.

several substrates exhibited relatively low solubility in commonly used organic solvents. To avoid low reaction conversions resulting from the solubility issue, we decided to use 0.1 M as the reaction concentration in the following studies. Performing the borylation reaction at 4 °C improved the enantioselectivity at the cost of reaction conversion (54% after 20 h at 4 °C) (entry 5).



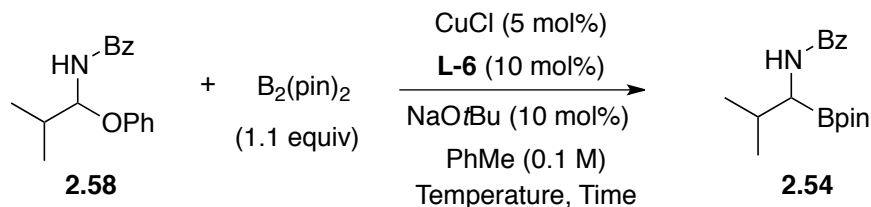
Entry	CuCl (mol%)	c (M)	Temp. (°C)	Conversion (%) ^a	Yield (%) ^b	er ^c
1	10	0.1	22	>98	80	89:11
2	5	0.1	22	>98	90	89:11
3 ^d	2.5	0.1	22	>98	93	90:10
4 ^e	2.5	0.2	22	>98	90	89:11
5 ^f	5	0.1	4	54	43	93:7

^aDetermined by ¹H-NMR of unpurified products with 1,3,5-trimethoxybenzene as the internal standard. ^bIsolated yields. ^cDetermined by chiral HPLC.

^dReaction time: 19 h. ^eReaction time: 15 h. ^fReaction time: 20 h.

Table 2.7 Further optimization of the borylation conditions

In addition, we were curious whether there was a kinetic resolution process involved in our method. Considering the facts that substrate **2.58** contains a stereogenic center and the borylation catalyst is a chiral Cu(I)/phosphine complex, the sterically matched enantiomer of substrate **2.58** will react faster than the mismatched enantiomer. If this were the case, the enantiopurity of product **2.54** would gradually decrease and, meanwhile, the enantiopurity of the unreacted substrate **2.58** would gradually increase, as the conversion increased. To test this hypothesis, we conducted a time study of the above reaction (Table 2.8).



Entry	Temperature (°C)	Time (h)	Conversion (%) ^a	er of 2.54 ^b	er of 2.58 ^b
1 ^c	22	2.5	42	89:11	49.5:50.5
2 ^c	22	8	87	90:10	48:52
3 ^d	22	12	>98	89:11	—
4 ^d	4	20	54	93:7	49:51

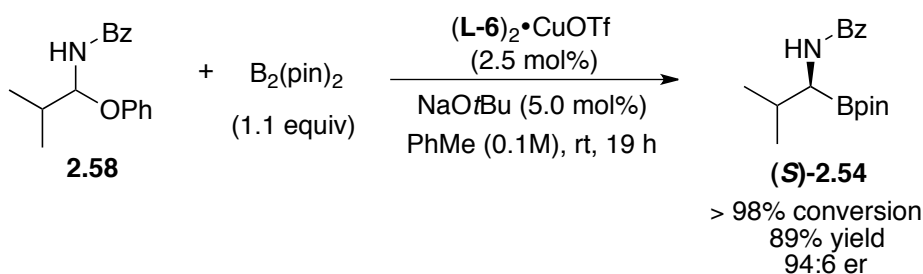
^aDetermined by ¹H-NMR of unpurified products with 1,3,5-trimethoxybenzene as the internal standard. ^bDetermined by chiral HPLC. ^cThe unpurified products were used for the determination. ^dThe purified products were used for the determination.

Table 2.8 A time study of the borylation reaction

The er values of compound **2.54** collected from different reaction time scales indicated that the enantiopurity of the product nearly did not change as the reaction reaching higher conversions (entry 1, 2 and 3, Table 2.8). The unreacted substrate **2.58** became slightly enantioenriched when the reaction proceeded to near completion (entry 2). We also examined the recovered substrate **2.58** from the reaction conducted at 4 °C, and found that it was almost racemic (entry 4). Based on these results, it seems that the racemic substrate **2.58** underwent kinetic resolution during the borylation, but, under the reaction conditions, this compound rapidly racemized or decomposed to the corresponding aldimine, which offset the effect of kinetic resolution.

After made all the above effort, we turned our attention to the copper precatalyst used in the reaction. We noticed that a preformed complex of CuOTf and Methyl-DuPhos monoxide ((**L-6**)₂•CuOTf) is commercially available, and tested this complex in our borylation conditions. To our delight, it produced higher enantioselectivity and a

comparable yield (Equation 2.12). Compared with CuCl, the relatively more Lewis acidic CuOTf may have stronger binding with ligand **L-6** and the *in situ* generated aldimine **2.57**, which can suppress ligand dissociation and make the aldimine adopt a more suitable orientation to avoid close interaction. Additionally, this oxygen-stable³⁴ complex can potentially make the reaction results more reproducible and reliable. It should be noted that the enantiopurity of product **2.54** could be further enhanced to 99:1 through recrystallization from dichloromethane/hexane. The absolute stereochemistry of product **2.54** was assigned to be (*S*)-configuration through the single crystal x-ray structure.



Equation 2.12 The new reaction conditions for borylation of hemiaminal ethers

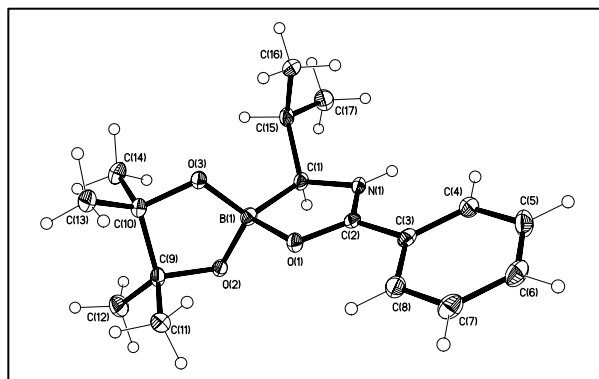


Figure 2.6 The single crystal x-ray structure of enantioenriched compound **2.54**

³⁴ Côté, A.; Charette, A. B. *J. Org. Chem.* **2005**, 70, 10864-10867.

We explored the substrate scope of our enantioselective borylation method with the above new reaction conditions (Figure 2.8).

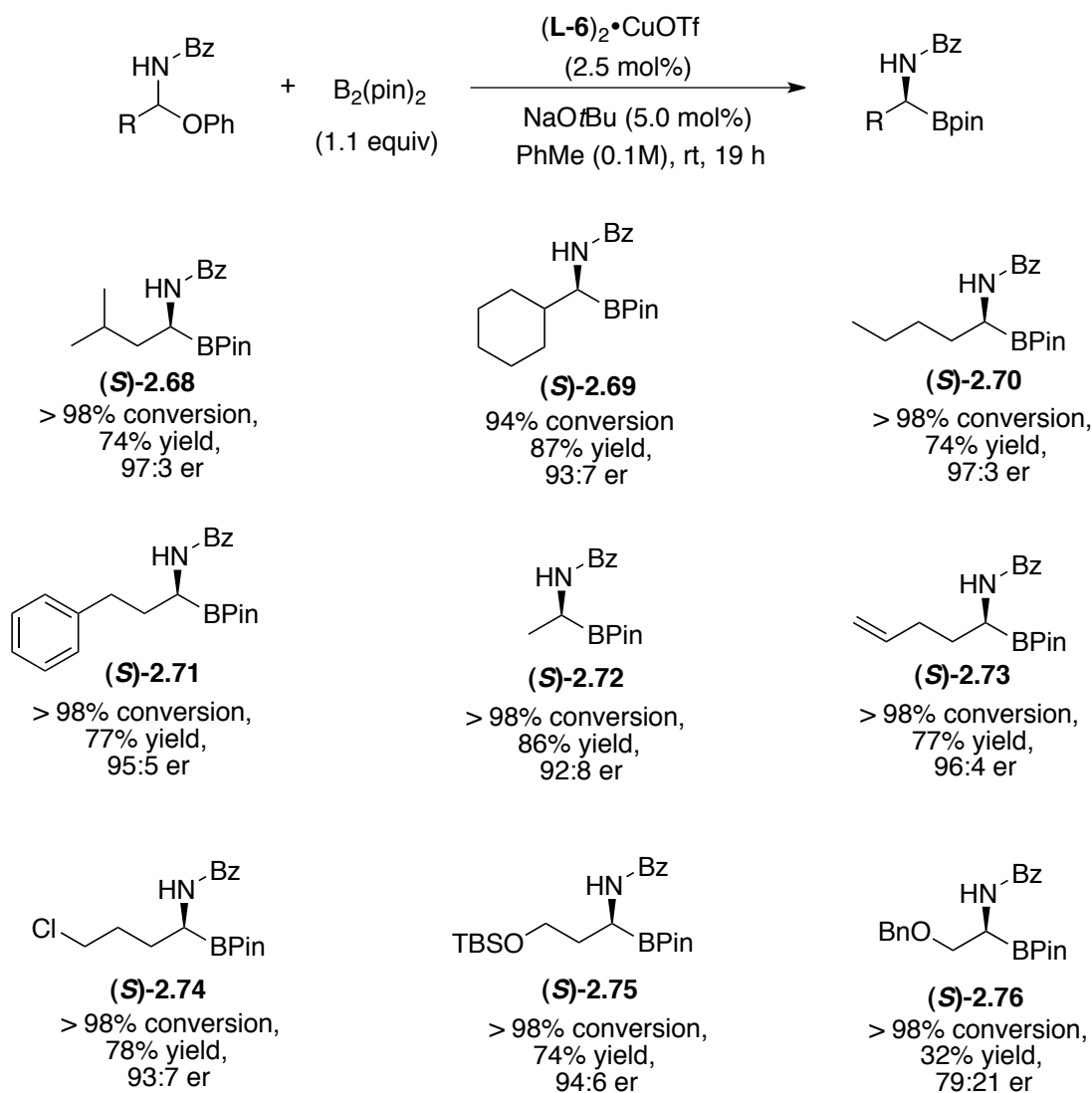


Figure 2.7 Substrate scope of the enantioselective borylation of hemiaminal ethers

When the isopropyl group in substrate **2.58** was replaced with other alkyl groups the reaction proceeded smoothly as well. In most of cases, over 70% isolated yields were achieved. The mass loss mainly came from decomposition of the borylated products during the column purification process, because this type of molecule is sensitive to

commonly used stationary phases³⁵ and tends to stay in the column. The slightly lower conversion observed from synthesis of product **2.69** was attributed to the poor solubility of the substrate in toluene. Substrates containing a longer and more linear side chain gave higher enantioselectivity (**2.68**, **2.70**, **2.71** and **2.73**, Figure 2.8). As for preparation of the methyl-substituted product **2.72**, the small interaction between the substrate and the chiral copper complex may pose difficulty in enantiocontrol, and we indeed observed a lower enantiopurity of **2.72**. In terms of functional group tolerance of our method, we were pleased to find that chlorine, alkenyl or silyl ether were left intact under the borylation conditions. For instance, based on ¹H-NMR of the unpurified product **2.73**, we did not detect olefin hydroboration products. As indicated by the result of product **2.76**, there is a limitation in our substrate scope. We obtained a much lower yield and enantioselectivity from the reaction. Although the major byproduct was isolated, we could not identify its structure. A reasonable explanation for the observed low yield (32%) and low stereoselectivity (79:21 er) of making product **2.76** is that the substrate or the corresponding aldimine *in situ* generated from the reaction replaced the bisphosphine monoxide ligand and chelated with CuOTf, which complicated the borylation reaction and corroded the enantioselectivity.

2.5 Conclusion

We have successfully developed a copper-catalyzed borylation strategy to prepare aromatic and aliphatic α -amido boronic esters. With a chiral bisphosphine monoxide ligand, we also established a protocol of enantioselective synthesis of aliphatic α -amido

³⁵ In our case, Florisil® was used as the stationary phase.

boronic esters. Further evaluation of other substrates containing a readily removable amino protecting group and functionalization of the borylated products are the two future directions of this study.

2.6 Experimental Procedures and Characterization

General Information

Unless otherwise noted, reactions were conducted in oven-dried glassware (160 °C) under dry N₂ atmosphere. Work-up and purification processes were carried out with reagent grade chemicals in air.

Dichloromethane (analytical grade, Aldrich) was purified with a solvent dispensing system (Pure Process Technology) by passing the solvent through two activated neutral alumina columns after being purged with nitrogen, and stored over 3Å molecular sieves in a N₂-filled glovebox. Toluene (PhMe), tetrahydrofuran (THF), diethyl ether (Et₂O), Methyl *tert*-butyl ether (MTBE) are analytical grade products from Fisher, purified by distillation from sodium benzophenone ketyl, and stored over 3Å molecular sieves in a N₂-filled glovebox. Deuterated solvents for NMR studies were purchased from Cambridge Isotope Laboratories, Inc.

Flash column chromatography was conducted on silica gel (SiliaFlash® F60, 230-400 mesh) purchased from Silicycle. Florisil® (200 mesh) used for column chromatography was purchased from Aldrich. Thin-layer chromatography (TLC) was conducted on 250 µm glass-backed silica gel plates. TLC spots were visualized by using ultraviolet light (254 nm), phosphomolybdic acid (PMA), or cerium ammonium molybdate (CAM).

Fourier transform infrared (FTIR) spectra were measured with a Bruker alpha-P spectrophotometer, and transmission peaks are reported in wavenumber (cm^{-1}). ^1H -NMR spectra were measured with a Varian INOVA-600 (600 MHz) spectrometer. Chemical shifts are in ppm with the solvent resonance as the internal standard (CDCl_3 : δ 7.26 ppm, CDCl_2 : 5.32 ppm). Peak data are reported as follows: chemical shift, multiplicity (s = singlet, d = doublet, t = triplet, q = quartet, p = pentet, br = broad, m = multiplet, app = approximate), coupling constants (J , Hz) and integration. ^{13}C -NMR spectra were measured on a Varian INOVA-600 (151 MHz) spectrometer with complete proton decoupling. Chemical shifts are reported in ppm with the solvent resonance as the internal standard (CDCl_3 : δ 77.16 ppm, CDCl_2 : 53.84 ppm). Peak data are reported as follows: chemical shift, multiplicity (singlet unless otherwise noted), and coupling constants (Hz). High-resolution mass spectrometry was performed on a JEOL AccuTOF-DART (positive mode) at the Mass Spectrometry Facility, Boston College. Melting points of solid compounds were determined with a MEL-TEMP II capillary melting point apparatus (Laboratory Devices Inc, USA).

Benzaldehyde, **acetaldehyde**, **pentanal**, **2-methylpropanal**, **3-methylbutanal**, **cyclohexanecarboxaldehyde**, and **3-phenylpropionaldehyde** were purchased from Aldrich and freshly distilled under N_2 before use.

4-pentenal was purchased from Oakwood Chemical and used as received.

Benzyloxyacetaldehyde was purchased from Aldrich and used as received.

4-chloro-1-butanal was prepared according to a published procedure.³⁶

3-(tert-butyldimethylsilyloxy)propanal was prepared according to a published procedure and used without any purification.³⁷

Benzamide was purchased from Aldrich and used as received.

4-Methylbenzenesulfinic acid was freshly prepared according to a published procedure³⁸ and used immediately.

1,2,3-Benzotriazole was purchased from Aldrich and used as received.

Sodium methoxide (NaOMe) was prepared by adding freshly cut sodium metal in anhydrous methanol (HPLC grade, purchased from Fisher Scientific International, Inc.).

Sodium phenoxide (NaOPh) was prepared according to a published procedure³⁹ and stored in a N₂-filled glovebox.

Sodium tert-butoxide (NaOtBu) was purchased from Aldrich and stored in a N₂-filled glovebox.

Bis(pinacolato)diboron (B₂(pin)₂) was purchased from Combi-Blocks Inc. and recrystallized from pentane before use.

Copper(I) chloride (99.99%-Cu) (CuCl) was purchased from Strem Chemicals Inc. and stored in a N₂-filled glovebox.

Copper(I) bromide (99.99%-Cu) (CuBr) was purchased from Aldrich and stored in a N₂-filled glovebox.

³⁶ Smith, S. W.; Fu, G. C. *Angew. Chem. Int. Ed.* **2008**, *47*, 9334-9336.

³⁷ Valot, G.; Regans, C. S.; O'Malley, D. P.; Godineau, E.; Takikawa, H.; Fürstner, A. *Angew. Chem. Int. Ed.* **2013**, *52*, 9534-9538.

³⁸ Münster, N.; Harms, K.; Koert, U. *Chem. Commun.* **2012**, *48*, 1866-1867.

³⁹ Liang, L.-C.; Chien, P.-S.; Lee, P.-Y.; Lin, J.-M.; Huang, Y.-L. *Dalton Trans.* **2008**, 3320-3327.

Tricyclohexylphosphine (PCy₃) was purchased from Strem Chemicals Inc. and stored in a N₂-filled glovebox.

Triphenylphosphine (PPh₃) was purchased from Aldrich, recrystallized from hot benzene, and stored in a N₂-filled glovebox.

L-1, (S)-(+)-Neomenthyldiphenylphosphine, was purchased from Strem Chemicals Inc. and stored in a N₂-filled glovebox.

L-2, (R)-(+)-2-(Diphenylphosphino)-2'-methoxy-1,1'-binaphthyl, was prepared according to a published procedure.⁴⁰

L-3, (+)-1,2-Bis[(2R,5R)-2,5-di-i-propylphospholano]benzene, was purchased from Strem Chemicals Inc. and stored in a N₂-filled glovebox.

L-4, 2-{2-[(2R,5R)-2,5-Diethyl-1-phospholano]phenyl}1,3-dioxolane, was purchased from Strem Chemicals Inc. and stored in a N₂-filled glovebox.

L-5, (R)-2-diphenylphosphino-2'-diphenylphosphinyl-1,1'-binaphthyl, was prepared according to a published procedure.⁴¹

L-6, [1-(2R,5R)-2,5-Dimethylphospholanyl]-[2-(2R,5R)-2,5-dimethylphospholanyl-1-oxide]benzene, was purchased from Strem Chemicals Inc. and stored in a N₂-filled glovebox.

L-7, [1-(2R,5R)-2,5-Diethylphospholanyl]-[2-(2R,5R)-2,5-diethylphospholanyl-1-oxide]benzene, was purchased from Strem Chemicals Inc. and stored in a N₂-filled glovebox.

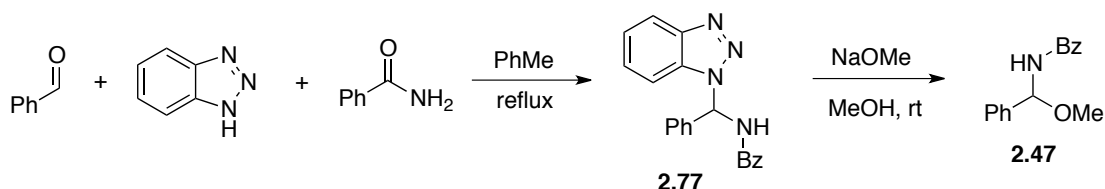
⁴⁰ Uozumi, Y.; Kawatsura, M.; Hayashi, T. *Organic Syntheses* **2002**, 78, 1-13.

⁴¹ (a) Grushin, V. V. *Organometallics* **2001**, 20, 3950-3961. (b) Hu, J.; Hirao, H.; Li, Y.; Zhou, J. *Angew. Chem. Int. Ed.* **2013**, 52, 8676-8680.

(**L-6**)₂•CuOTf, **Bis**{[1-(2*R*,5*R*)-2,5-dimethylphospholanyl]-[2-(2*R*,5*R*)-2,5-dimethylphospholanyl-1-oxide]benzene}Copper(I) trifluoromethanesulfonate was purchased from Alfa Aesar and stored in a N₂-filled glovebox.

Preparation of hemiaminal methyl ethers

N-(methoxyphenylmethyl)benzamide **2.47**



The title compound **2.47** was prepared according to a published procedure⁴² with modification. To a 100 mL round bottom flask containing a stir bar were added benzamide (1.454 g, 12.0 mmol), 1,2,3-benzotriazole (1.429 g, 12.0 mmol), benzaldehyde (1.22 mL, 12.0 mmol), and toluene (20 mL) in sequence. After a condenser and a Dean-Stark trap were installed onto the flask, the apparatus was placed in a 150 °C oil bath. The reaction mixture was stirred under reflux for 30 h, and then allowed to cool down to 22 °C naturally. Diethyl ether (20 mL) was added in the flask, and the resulting mixture was filtered with a Büchner funnel. The off-white solid collected from filtration was further washed with diethyl ether (5×5 mL), air-dried and recrystallized once from toluene (35 mL) to afford *N*-(1-benzotriazolyl-1-phenylmethyl)benzamide **2.77** as white needle-shaped crystals (2.01 g, 51%). This compound was used in the next step without further purification.

⁴² (a) Katritzky, A. R.; Pernak, J.; Fan, W.-Q.; Saczewski, F. *J. Org. Chem.* **1991**, *56*, 4439-4443. (b) Katritzky, A. R.; Fan, W.-Q.; Black, M.; Pernak, J. *J. Org. Chem.* **1992**, *57*, 547-549.

N-(1-benzotriazolyl-1-phenylmethyl)benzamide **2.77** (2.003 g, 6.1 mmol) was added to a stirred solution of sodium methoxide (sodium: 0.281 g, 12.2 mmol, 2.0 equiv) in methanol (24 mL) in one portion. The reaction vessel, a 100 mL round bottom flask containing a stir bar, was fitted with a rubber septum and placed under N₂. The reaction mixture was allowed to stir vigorously at 22 °C for 24 h. The resulted milky white suspension was concentrated *in vacuo*, and the residue was dissolved in a mixture of CH₂Cl₂ (20 mL) and saturated NH₄Cl aqueous solution (30 mL). The obtained biphasic mixture was transferred to a separatory funnel, and the organic layer was isolated. The aqueous layer was extracted with CH₂Cl₂ (2×20 mL). The combined organic layers were washed with H₂O (2×20 mL) and brine (20 mL), dried over Na₂SO₄, filtered and concentrated *in vacuo*. The obtained white solid residue was purified by silica gel column chromatography (dichloromethane: diethyl ether = 80:1) to afford the title compound as a white solid (1.208 g, 82% yield over two steps).

¹H-NMR (600 MHz, CDCl₃) δ 7.82 – 7.80 (m, 2H), 7.54 – 7.50 (m, 3H), 7.46 – 7.44 (m, 2H), 7.41 – 7.38 (m, 1H), 7.36-7.33 (m, 2H), 6.58 (d, *J* = 9.0 Hz, 1H), 6.38 (d, *J* = 9.6 Hz, 1H), 3.55 (s, 3H).

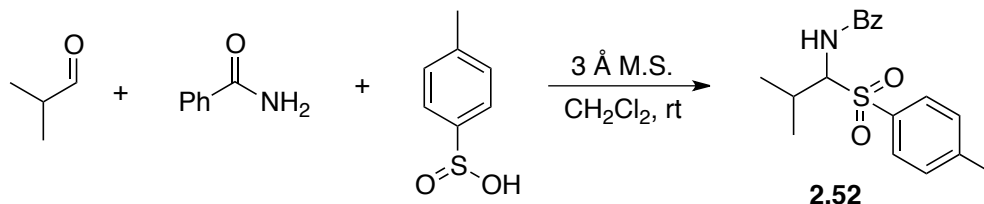
¹³C-NMR (151 MHz, CDCl₃) δ 167.32, 139.33, 133.73, 131.99, 128.66, 128.65, 128.55, 127.10, 125.90, 81.84, 56.21.

FTIR (neat): 3293, 2941, 1649, 1513, 1486, 1446, 1342, 1273, 1088, 1047, 976, 750, 689, 595 cm⁻¹.

HRMS (ESI+) calcd for C₁₅H₁₅NO₂Na ([M+Na]⁺): 264.1000, found: 264.0988.

Melting point: 99-100 °C

***N*-[2-methyl-1-[(4-methylphenyl)sulfonyl]propyl]benzamide 2.52**



To a 50 mL round bottom flask containing a stir bar were added benzamide (0.606 g, 5.0 mmol), 4-methylbenzenesulfonic acid (0.781 g, 5.0 mmol) and 3 Å molecular sieves (0.9 g). The flask was fitted with a rubber septum and placed under N₂, followed by successive addition of CH₂Cl₂ (10.0 mL) and 2-methylpropanal (456 µL, 5.0 mmol) via syringe. The reaction mixture was allowed to stir vigorously at 22 °C for 20 h. The resulted pale yellow cloudy solution was diluted with CH₂Cl₂ (10 mL) and filtered over a pad of celite, and the filter cake was washed with CH₂Cl₂ (2×10 mL). The collected filtrate was concentrated *in vacuo* to afford an off-white solid residue (1.503 g, 91% crude yield). This solid was dried under high vacuum for 3 h, and used in the next step without further purification.

For characterization purpose and reactivity test, a small amount of this compound was purified by silica gel column chromatography (hexanes: dichloromethane: ethyl acetate = 10:10:1) to afford the title compound as a white microcrystalline solid.

¹H-NMR (600 MHz, CDCl₃) δ 7.74 (d, *J* = 8.4 Hz, 2H), 7.63 – 7.62 (m, 2H), 7.55 – 7.52 (m, 1H), 7.44 (t, *J* = 7.8 Hz, 2H), 7.24 (d, *J* = 8.4 Hz, 2H), 6.57 (d, *J* = 10.8 Hz, 1H), 5.32 (dd, *J* = 10.8, 3.6 Hz, 1H), 2.92 – 2.85 (m, 1H), 2.37 (s, 3H), 1.22 (d, *J* = 7.2 Hz, 2H), 1.12 (d, *J* = 7.2 Hz, 2H).

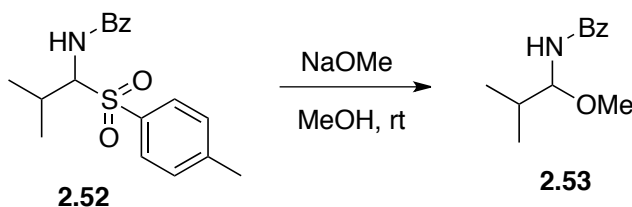
^{13}C -NMR (151 MHz, CDCl_3) δ 166.66, 145.00, 134.83, 133.04, 132.22, 129.78, 128.75, 128.65, 126.90, 72.63, 27.36, 21.66, 20.71, 17.21.

FTIR (neat): 3272, 2975, 2962, 1650, 1592, 1526, 1331, 1298, 1265, 1130, 1077, 802, 698, 618, 591, 565, 526, 422 cm^{-1} .

HRMS (DART+) calcd for $\text{C}_{18}\text{H}_{22}\text{NO}_3\text{S}$ ($[\text{M}+\text{H}]^+$): 332.1320, found: 332.1327.

Melting point: 113-115 $^\circ\text{C}$

N-(1-methoxy-2-methylpropyl)benzamide **2.53**



N-[2-methyl-1-[(4-methylphenyl)sulfonyl]propyl]benzamide **2.52** (1.503 g, 4.54 mmol) was added to a stirred solution of sodium methoxide (sodium: 0.209 g, 9.08 mmol, 2.0 equiv) in methanol (18 mL) in one portion. The reaction vessel, a 100 mL round bottom flask containing a stir bar, was fitted with a rubber septum and placed under N_2 . The reaction mixture was allowed to stir vigorously at 22 $^\circ\text{C}$ for 24 h. The resulted slightly yellow cloudy solution was concentrated *in vacuo*, and the pale yellow semisolid residue was dissolved in a mixture of CH_2Cl_2 (30 mL) and saturated NH_4Cl aqueous solution (30 mL). The obtained biphasic mixture was transferred to a separatory funnel, and the organic layer was isolated. The aqueous layer was extracted with CH_2Cl_2 (2 \times 15 mL). The combined organic layers were dried over Na_2SO_4 , filtered and concentrated *in vacuo*. The obtained pale yellow solid residue was purified by silica gel column

chromatography (hexanes: ethyl acetate = 10:1 to 8:1) to afford the title compound as a white microcrystalline solid (0.757 g, 73% yield over two steps).

^1H -NMR (600 MHz, CDCl_3) δ 7.81–7.79 (m, 2H), 7.55–7.52 (m, 1H), 7.48–7.45 (m, 2H), 6.23 (br d, J = 9.6 Hz, 1H), 5.11 (dd, J = 10.2, 6.0 Hz, 1H), 3.40 (s, 3H), 1.93 (octet, J = 6.6 Hz, 1H), 1.02 (d, J = 6.6 Hz, 3H), 0.99 (d, J = 6.6 Hz, 3H).

^{13}C -NMR (151 MHz, CDCl_3) δ 167.67, 134.14, 131.79, 128.66, 126.92, 85.83, 56.21, 33.28, 17.80, 17.34.

FTIR (neat): 3257, 2962, 2930, 1638, 1532, 1316, 1145, 1086, 1045, 982, 803, 698, 663, 588 cm^{-1} .

HSMS (ESI+) calcd for $\text{C}_{12}\text{H}_{17}\text{NO}_2\text{Na}$ ($[\text{M}+\text{Na}]^+$): 230.1157, found: 230.1157.

Melting point: 94–96 $^\circ\text{C}$

Preparation of hemiaminal phenyl ethers

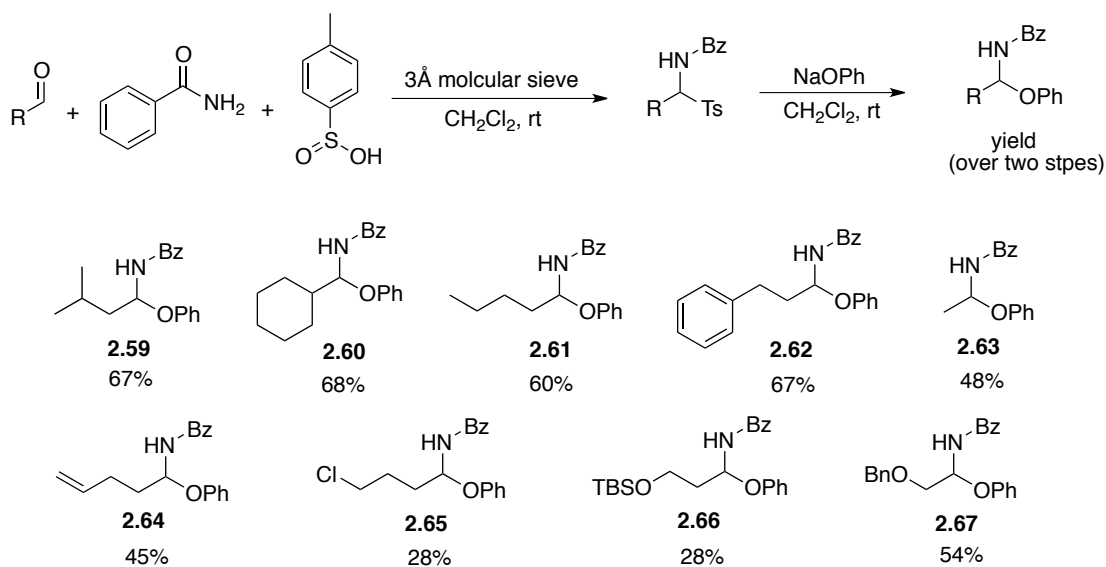
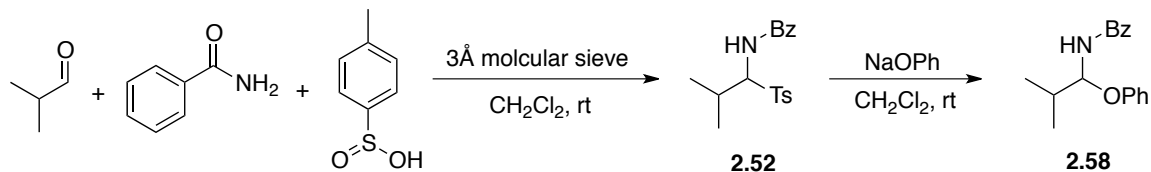


Figure 2.8 Preparation of hemiaminal phenyl ethers

N-(2-methyl-1-phenoxypropyl)benzamide **2.58**



N-[2-methyl-1-[(4-methylphenyl)sulfonyl]propyl]benzamide **2.52** was prepared according to the abovementioned procedure with minor modifications (unreacted benzamide complicates the second step). To a 50 mL round bottom flask containing a stir bar were added benzamide (0.242 g, 2.0 mmol), 4-methylbenzenesulfinic acid (0.406 g, 2.6 mmol, 1.3 equiv) and 3Å molecular sieves (0.36 g). The flask was fitted with a rubber septum and placed under N_2 , followed by sequential addition of CH_2Cl_2 (4.0 mL) and 2-methylpropanal (237 μL , 2.6 mmol, 1.3 equiv) via syringe. The reaction mixture was allowed to stir vigorously at 22 $^\circ\text{C}$ for 20 h. The resulted pale yellow cloudy solution was diluted with a mixture of CH_2Cl_2 (10 mL) and MeOH (5 mL), filtered over a pad of celite. The filter cake was washed with CH_2Cl_2 (2 \times 5 mL). The collected filtrate was concentrated *in vacuo* to afford a pale yellow semisolid that slowly solidifies to an off-white solid (0.755 g, over 100% crude yield). This solid was dried under high vacuum for 3 h and used in the next step without further purification.

In a N_2 -filled glovebox NaOPh (0.302 g, 2.6 mmol, 1.3 equiv) was added to a 100 mL round bottom flask charged with a stir bar and *N*-[2-methyl-1-[(4-methylphenyl)sulfonyl]propyl]benzamide **2.52** (0.755 g, crude form). The vessel was fitted with a rubber septum before it was removed from the glovebox, and placed under N_2 . CH_2Cl_2 (8.0 mL) was added in the flask via syringe, and the reaction mixture was allowed to stir vigorously at 22 $^\circ\text{C}$ for 14 h. The resulted pale yellow thick suspension

was diluted with CH₂Cl₂ (10 mL) and saturated NH₄Cl aqueous solution (15 mL). The resulting biphasic mixture was transferred to a separatory funnel, and the organic layer was isolated. The aqueous layer was extracted with CH₂Cl₂ (2×15 mL). The combined organic layers was washed with saturated Na₂CO₃ aqueous solution (10 mL) and brine (10 mL), dried over Na₂SO₄, filtered and concentrated in vacuo. The obtained white solid residue was triturated with H₂O (4×3 mL) to remove the majority of excess phenol, and then purified by silica gel column chromatography (hexanes: dichloromethane: diethyl ether = 10:10:0.1) to afford the title compound as a white solid (0.441 g, 82% yield over steps).

¹H-NMR (600 MHz, CDCl₃) δ 7.74 – 7.72 (m, 2H), 7.52 – 7.49 (m, 1H), 7.42 (t, *J* = 7.8 Hz, 2H), 7.28 – 7.25 (overlapped with CDCl₃, m, 2H), 7.06 (d, *J* = 7.8 Hz, 2H), 6.95 (t, *J* = 7.2 Hz, 1H), 6.41 (d, *J* = 9.6 Hz, 1H), 6.00 (dd, *J* = 10.2, 6.0 Hz, 1H), 2.17 (octet, *J* = 6.6 Hz 1H), 1.13 (d, *J* = 6.6 Hz, 3H), 1.10 (d, *J* = 6.6 Hz, 3H).

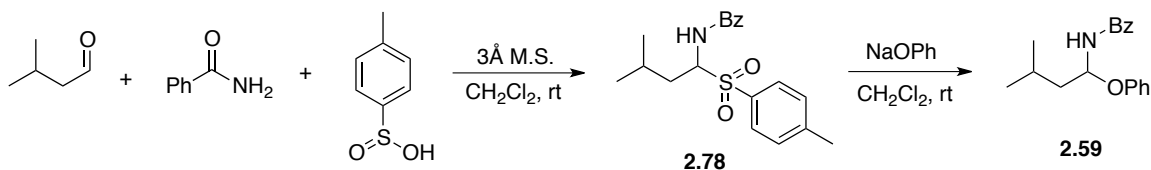
¹³C-NMR (151 MHz, CDCl₃) δ 166.96, 156.66, 133.84, 131.89, 129.62, 128.65, 126.97, 121.57, 115.74, 82.23, 33.84, 17.58, 17.16.

FTIR (neat): 3271, 2960, 1633, 1580, 1536, 1485, 1321, 1225, 1046, 971, 754, 692, 664 cm⁻¹.

HSMS (ESI⁺): calcd for C₁₇H₁₉NO₂Na ([M+Na]⁺): 292.1313, found: 292.1317.

Melting point: 118-121 °C

N-(3-methyl-1-phenoxybutyl)benzamide **2.59**



The title compound was synthesized analogous to compound **2.58** in two steps. 3-Methylbutanal (279 μ L, 2.6 mmol, 1.3 equiv), benzamide (0.242 g, 2.0 mmol), 4-methylbenzenesulfonic acid (0.406 g, 2.6 mmol, 1.3 equiv) and 3 Å molecular sieves (0.36 g) were used to prepare α -amido sulfone **2.78** (0.809 g, crude product). NaOPh (0.302 g, 2.6 mmol, 1.3 equiv) and **2.78** (0.809 g) were used to prepare hemiaminal ether **2.59**. The crude product was purified by silica gel column chromatography (hexanes: dichloromethane: diethyl ether = 10:10:0.1) to afford the title compound as a white solid (0.378 g, 67% over two steps).

¹H-NMR (600 MHz, CDCl₃) δ 7.75 – 7.70 (m, 2H), 7.51 – 7.48 (m, 1H), 7.41 (t, J = 7.8 Hz, 2H), 7.28 – 7.26 (overlapped with CDCl₃, m, 2H), 7.08 (d, J = 8.4 Hz, 2H), 6.96 (t, J = 7.2 Hz, 1H), 6.42 (br d, J = 9.6 Hz, 1H), 6.29 (dt, J = 9.6, 6.0 Hz, 1H), 1.92 (dt, J = 13.2, 6.6 Hz, 2H), 1.87 (dt, J = 13.2, 6.6 Hz, 1 H), 1.73 (dt, J = 13.2, 6.6 Hz, 1H), 1.03 (d, J = 6.6 Hz, 3H), 0.99 (d, J = 6.6 Hz, 2H).

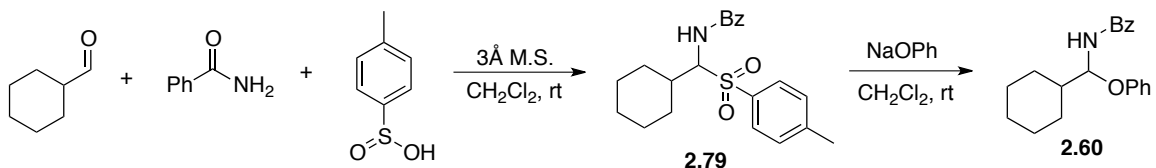
¹³C-NMR (151 MHz, CDCl₃) δ 166.60, 156.45, 133.72, 131.91, 129.64, 128.62, 127.02, 121.65, 115.89, 45.08, 24.60, 22.78, 22.52.

FTIR (neat): 3254, 3069, 2958, 1638, 1538, 1493, 1295, 1226, 1029, 978, 748, 704 cm⁻¹.

HSMS (ESI+) calcd for C₁₈H₂₁NO₂Na ([M+Na]⁺): 306.1470, found: 306.1466.

Melting point: 111-112 °C

N*-(1-cyclohexyl-1-phenoxyethyl)benzamide **2.60*



The title compound was synthesized analogous to **2.58** in two steps. Cyclohexanecarboxaldehyde (315 μL, 2.6 mmol, 1.3 equiv), benzamide (0.242 g, 2.0 mmol), 4-methylbenzenesulfonic acid (0.406 g, 2.6 mmol, 1.3 equiv) and 3 Å molecular sieves (0.36 g) were used to prepare α-amido sulfone **2.79** (0.853 g, crude product). NaOPh (0.302 g, 2.6 mmol, 1.3 equiv) and **2.79** (0.853 g) were used to prepare hemiaminal ether **2.60**. The crude product was purified by silica gel column chromatography (hexanes: dichloromethane: diethyl ether = 10:10:0.1) to afford the title compound as a white solid (0.423 g, 68% over two steps).

¹H-NMR (600 MHz, CDCl₃) δ 7.74 – 7.72 (m, 2H), 7.51 – 7.48 (m, 1H), 7.43 – 7.40 (m, 2H), 7.28 – 7.24 (overlapped with CDCl₃, m, 2H), 7.07 – 7.03 (m, 2H), 6.95 (t, *J* = 7.2 Hz, 1H), 6.42 (br d, *J* = 10.2 Hz, 1H), 5.99 (dd, *J* = 9.6, 6.0 Hz, 1H), 2.02 (br d, *J* = 12.6 Hz, 1H), 1.88 – 1.79 (m, 4H), 1.70 (d, *J* = 12.6 Hz, 1H), 1.33 – 1.17 (m, 5H).

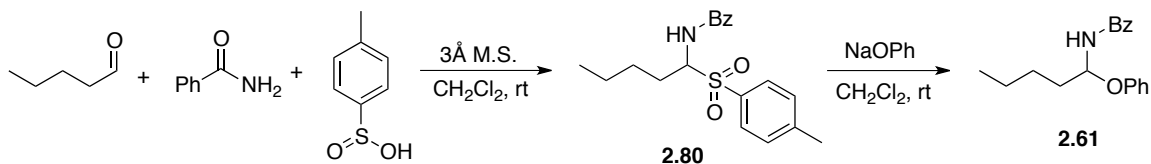
¹³C-NMR (151 MHz, CDCl₃) δ 166.91, 156.76, 133.80, 131.88, 129.61, 128.63, 127.00, 121.53, 115.72, 81.79, 43.36, 28.15, 27.67, 26.26, 25.74, 25.66.

FTIR (neat): 3219, 3062, 2919, 2848, 1635, 1598, 1542, 1485, 1345, 1226, 1027, 1007, 892, 801, 748, 706, 692 cm⁻¹.

HSMS (ESI+) calcd for C₂₀H₂₃NO₂Na ([M+Na]⁺): 332.1626, found: 332.1621.

Melting point: 143-144 °C

N-(1-phenoxypentyl)benzamide **2.61**



The title compound was synthesized analogous to compound **2.58** in two steps. Pentanal (276 μ L, 2.6 mmol, 1.3 equiv), benzamide (0.242 g, 2.0 mmol), 4-methylbenzenesulfonic acid (0.406 g, 2.6 mmol, 1.3 equiv) and 3 Å molecular sieves (0.36 g) were used to prepare α -amido sulfone **2.80** (0.918 g, crude product). NaOPh (0.302 g, 2.6 mmol, 1.3 equiv) and **2.80** (0.918 g) were used to prepare hemiaminal ether **2.61**. The crude product was purified by silica gel column chromatography (hexanes: dichloromethane: diethyl ether = 10:10:0.1) to afford the title compound as a white solid (0.340 g, 60% yield over two steps),

$^1\text{H-NMR}$ (600 MHz, CDCl_3) δ 7.75 – 7.73 (m, 2H), 7.52 – 7.47 (m, 1H), 7.42 – 7.39 (m, 2H), 7.29 – 7.25 (overlapped with CDCl_3 , m, 2H), 7.08 – 7.06 (m, 2H), 6.96 (tt, J = 7.2, 1.2 Hz, 1H), 6.55 (br d, J = 9.6 Hz, 1H), 6.22 (dt, J = 9.6, 6.0 Hz, 1H), 2.04 – 1.98 (m, 1H), 1.90 – 1.84 (m, 1H), 1.57 – 1.36 (m, 4H), 0.93 (t, J = 7.8 Hz, 3H).

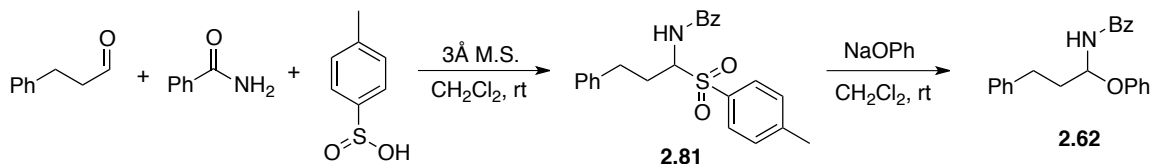
$^{13}\text{C-NMR}$ (151 MHz, CDCl_3) δ 166.69, 156.50, 133.74, 131.90, 129.62, 128.61, 127.02, 121.65, 115.91, 78.74, 35.88, 26.77, 22.39, 13.98.

FTIR (neat): 3273, 2950, 2927, 2866, 1631, 1580, 1534, 1485, 1292, 1217, 1146, 1121, 1078, 1028, 1013, 987, 866, 754, 696, 665 cm^{-1} .

HSMS (ESI+) calcd for $\text{C}_{18}\text{H}_{21}\text{NO}_2\text{Na}$ ($[\text{M}+\text{Na}]^+$): 306.1470, found: 306.1467.

Melting point: 117-119 $^\circ\text{C}$

N-(1-phenoxy-3-phenylpropyl)benzamide **2.62**



The title compound was synthesized analogous to compound **2.58** in two steps. 3-phenylpropionaldehyde (342 μ L, 2.6 mmol, 1.3 equiv), benzamide (0.242 g, 2.0 mmol), 4-methylbenzenesulfonic acid (0.406 g, 2.6 mmol, 1.3 equiv) and 3 Å molecular sieves (0.36 g) were used to prepare α -amido sulfone **2.81** (0.980 g, crude product). NaOPh (0.302 g, 2.6 mmol, 1.3 equiv) and **2.81** (0.980 g) were used to prepare hemiaminal ether **2.62**. The crude product was purified by silica gel column chromatography (hexanes: dichloromethane: diethyl ether = 11:10:0.1) or recrystallization (hexane: ethyl acetate = 5:1) to afford the title compound as a white solid (0.442 g, 67% yield over two steps).

¹H-NMR (600 MHz, CDCl₃) δ 7.63 (d, J = 7.2 Hz, 2H), 7.49 (t, J = 7.2 Hz, 1H), 7.39 (t, J = 7.8 Hz, 2H), 7.31 – 7.23 (overlapped with CDCl₃, m, 5H), 7.21 (t, J = 7.2 Hz, 1H), 7.07 (d, J = 7.8 Hz, 2H), 6.97 (t, J = 7.2 Hz, 1H), 6.44 (d, J = 9.6 Hz, 1H), 6.28 (dt, J = 9.6, 6.0 Hz, 1H), 2.94 (ddd, J = 13.8, 9.6, 6.6 Hz, 1H), 2.84 (ddd, J = 13.8, 9.0, 6.0 Hz, 1H), 2.32 (ddt, J = 13.8, 9.0, 6.6 Hz, 1H), 2.24 (ddt, J = 13.8, 9.0, 6.0 Hz, 1H).

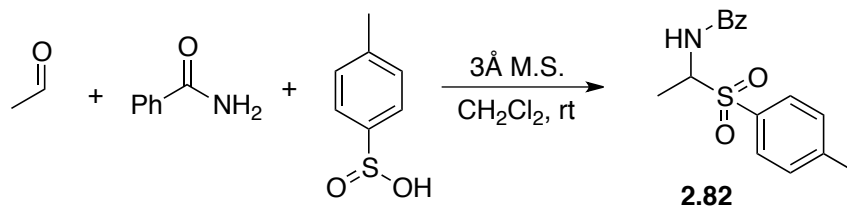
¹³C-NMR (151 MHz, CDCl₃) δ 166.59, 156.34, 140.97, 133.57, 131.94, 129.66, 128.61, 128.58, 128.46, 126.99, 126.16, 121.80, 115.98, 78.25, 37.50, 30.88.

FTIR (neat): 3238, 3062, 3028, 2923, 2856, 1631, 1499, 1542, 1486, 1293, 1224, 1179, 1028, 1010, 989, 751, 696, 502 cm⁻¹.

HSMS (ESI+) calcd for C₂₂H₂₁NO₂Na ([M+Na]⁺): 354.1470, found: 354.1470.

Melting point: 139-140 °C

N*-[1-[(4-methylphenyl)sulfonyl]ethyl]benzamide **2.82*



To a 50 mL round bottom flask containing a stir bar were added benzamide (0.182 g, 1.5 mmol), 4-methylbenzenesulfonic acid (0.305 g, 1.95 mmol, 1.3 mmol) and 3 Å molecular sieves (0.27 g). The flask was fitted with a rubber septum and placed under N₂. CH₂Cl₂ (3.0 mL) and acetaldehyde (420 μL, 7.5 mmol, 5.0 equiv) were sequentially added via syringe, and the reaction mixture was allowed to stir vigorously at 22 °C for 18 h. The resulted yellow viscous cloudy solution was diluted with CH₂Cl₂ (10 mL) and filtered over a pad of celite. The filter cake was washed with CH₂Cl₂ (2×10 mL), and the collected filtrate was concentrated *in vacuo*. The obtained colorless viscous oil residue was purified by silica gel column chromatography (hexanes: dichloromethane: ethyl acetate = 10:10:1) to afford α-amido sulfone **2.82** as a white solid (0.283 g, 62% yield).

¹H-NMR (600 MHz, CDCl₃) δ 7.77 (d, *J* = 8.4 Hz, 2H), 7.63 – 7.58 (m, 2H), 7.52 (t, *J* = 7.2 Hz, 1H), 7.41 (t, *J* = 7.2 Hz, 2H), 7.27 (overlapped with CDCl₃, m, 2H), 6.56 (br d, *J* = 9.6 Hz, 1H), 5.56 (dq, *J* = 10.8, 7.2 Hz, 1H), 2.39 (s, 3H), 1.72 (d, *J* = 7.2 Hz, 3H).

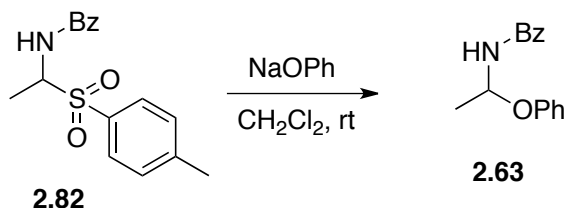
¹³C-NMR (151 MHz, CDCl₃) δ 166.14, 145.24, 133.37, 132.87, 132.18, 129.81, 129.08, 128.65, 127.00, 65.31, 21.69, 13.26.

FTIR (neat): 3260, 3062, 2926, 1645, 1522, 1488, 1310, 1291, 1244, 1139, 1124, 1082, 1020, 812, 714, 694, 670, 641, 570, 534, 520 cm⁻¹.

HSMS (DART+) calcd for C₁₆H₁₈NO₃S ([M+H]⁺): 304.1007, found: 304.0998.

Melting point: 122-125 °C

N*-(1-phenoxyethyl)benzamide **2.63*



In a N_2 -filled glovebox NaOPh (0.0882 g, 0.76 mmol, 0.95 equiv) was added in a 25 mL round bottom flask containing a stir bar. The vessel was fitted with a rubber septum, removed from the glovebox and placed under N_2 . In a 2-dram vial α -amido sulfone **2.82** (0.243 g, 0.8 mmol) was dissolved in CH_2Cl_2 (2.0 mL, plus 2×0.6 mL for rinse), and the obtained solution was added in the reaction flask in one portion. The reaction mixture was allowed to stir vigorously at 22 °C for 14 h. The resulted milky white suspension was diluted with CH_2Cl_2 (5 mL) and H_2O (5 mL), and transferred to a separatory funnel. The organic layer was isolated, and the aqueous layer was extracted with CH_2Cl_2 (2×5 mL). The combined organic layers were washed with brine (10 mL), dried over anhydrous Na_2SO_4 , filtered and concentrated *in vacuo*. The obtained white solid residue was purified by silica gel column chromatography (dichloromethane: hexanes: diethyl ether = 20:10:0.3, plus 0.5% Et_3N) to afford the title compound as a white solid (0.143 g, 78% yield).

^1H -NMR (600 MHz, CDCl_3) δ 7.76 – 7.71 (m, 2H), 7.52 – 7.48 (m, 1H), 7.43 – 7.39 (m, 2H), 7.29 – 7.25 (overlapped with CDCl_3 , m, 2H), 7.08 – 7.03 (m, 2H), 6.97 (tt, $J = 7.2$,

1.2 Hz, 1H), 6.55 (br d, $J = 9.0$ Hz, 1H), 6.37 (dq, $J = 9.0, 5.4$ Hz, 1H), 1.65 (d, $J = 5.4$ Hz, 3H).

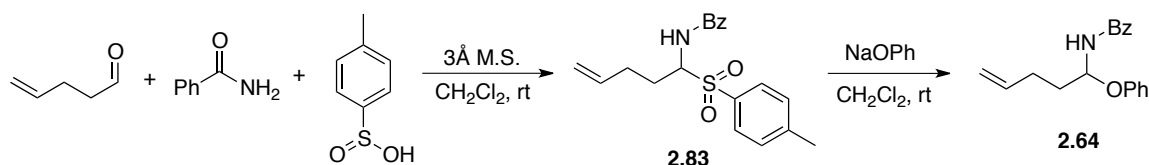
^{13}C -NMR (151 MHz, CDCl_3) δ 166.48, 156.20, 133.67, 131.94, 129.62, 128.62, 127.01, 121.78, 116.07, 75.70, 22.16.

FTIR (neat): 3259, 3067, 2994, 1639, 1592, 1530, 1491, 1291, 1226, 1151, 1105, 1063, 942, 751, 692 cm^{-1} .

HSMS (DART+) calcd for $\text{C}_{15}\text{H}_{15}\text{NO}_2\text{Na}$ ($[\text{M}+\text{Na}]^+$): 264.1000, found: 264.0996.

Melting point: 134-136 $^\circ\text{C}$

N-(4-penten-1-yl-1-phenoxy)benzamide **2.64**



The title compound was synthesized analogous to compound **2.58** in two steps. 4-penten-1-one (257 μL , 2.6 mmol, 1.3 equiv), benzamide (0.242 g, 2.0 mmol), 4-methylbenzenesulfonic acid (0.406 g, 2.6 mmol, 1.3 equiv) and 3 Å molecular sieves (0.36 g) were used to prepare α -amido sulfone **2.83** (0.886 g, crude product). NaOPh (0.302 g, 2.6 mmol, 1.3 equiv) and **2.83** (0.886 g) were used to prepare hemiaminal ether **2.64**. The crude product was purified by silica gel column chromatography (hexanes: dichloromethane: diethyl ether = 10:10:0.1) to afford the title compound as a white solid (0.254 g, 45% yield over two steps).

^1H -NMR (600 MHz, CDCl_3) δ 7.74 – 7.72 (m, 2H), 7.52 – 7.49 (m, 1H), 7.43 – 7.40 (m, 2H), 7.29 – 7.25 (overlapped with CDCl_3 , m, 2H), 7.07 – 7.05 (m, 2H), 6.96 (tt, $J = 7.2$,

1.2 Hz, 1H), 6.50 (br d, $J = 9.0$ Hz, 1H), 6.25 (dt, $J = 9.0, 6.0$ Hz, 1H), 5.88 (ddt, $J = 16.8, 10.2, 6.6$ Hz, 1H), 5.09 (dq, $J = 17.4, 1.8$ Hz, 1H), 5.03 (dq, $J = 10.2, 1.2$ Hz, 1H), 2.38 – 2.24 (m, 2H), 2.10 (ddt, $J = 13.8, 9.0, 6.6$ Hz, 1H), 1.99 (ddt, $J = 13.8, 9.0, 6.0$ Hz, 1H).

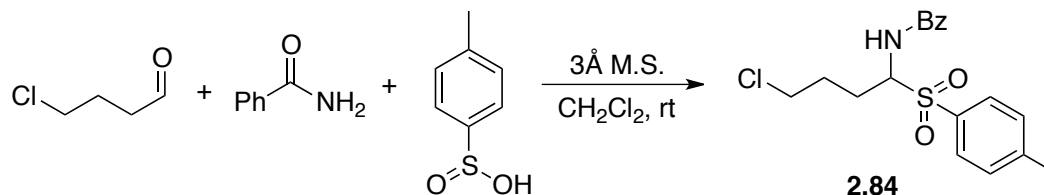
^{13}C -NMR (151 MHz, CDCl_3) δ 166.65, 156.39, 137.20, 133.65, 131.95, 129.63, 128.63, 127.03, 121.76, 115.95, 115.64, 78.32, 35.22, 28.86.

FTIR (neat): 3252, 3067, 1631, 1599, 1532, 1486, 1292, 1222, 1146, 1013, 992, 912, 807, 750, 690 cm^{-1} .

HSMS (DART+) calcd for $\text{C}_{18}\text{H}_{19}\text{NO}_2\text{Na}$ ($[\text{M}+\text{Na}]^+$): 304.1313, found: 304.1312.

Melting point: 87-89 $^\circ\text{C}$

***N*-[4-chloro-1-[(4-methylphenyl)sulfonyl]butyl]benzamide 2.84**



To a 50 mL round bottom flask containing a stir bar were added benzamide (0.303 g, 2.5 mmol, 1.0 equiv), 4-methylbenzenesulfinic acid (0.391 g, 2.5 mmol, 1.0 equiv) and 3 Å molecular sieves (0.45 g). The flask was fitted with a rubber septum and placed under N_2 . CH_2Cl_2 (5.0 mL) and 4-chloro-1-butanal (0.266 g, 2.5 mmol) were sequentially added via syringe. The reaction mixture was allowed to stir vigorously at 22 $^\circ\text{C}$ for 24 h. The resulted yellow cloudy suspension was diluted with a mixture of CH_2Cl_2 (10 mL) and MeOH (5 mL), and filtered over a pad of celite. The filter cake was washed with CH_2Cl_2 (2×5 mL). The collected filtrate was concentrated *in vacuo*. The obtained

colorless gum residue was purified by silica gel column chromatography (hexanes: dichloromethane: ethyl acetate = 10:12:1.2) to afford the α -amido sulfone **2.84** as a white solid (0.279 g, 31% yield).

$^1\text{H-NMR}$ (600 MHz, CDCl_3) δ 7.78 – 7.76 (m, 2H), 7.63 – 7.61 (m, 2H), 7.53 – 7.50 (m, 1H), 7.43 – 7.39 (m, 2H), 7.28 – 7.25 (overlapped with CDCl_3 , m, 2H), 6.73 (d, J = 10.2 Hz, 1H), 5.46 (td, J = 10.8, 3.6 Hz, 1H), 3.61 – 3.54 (m, 2H), 2.55 – 2.49 (m, 1H), 2.39 (s, 3H), 2.14 – 2.07 (m, 1H), 1.93 (dq, J = 9.6, 6.0 Hz, 2H).

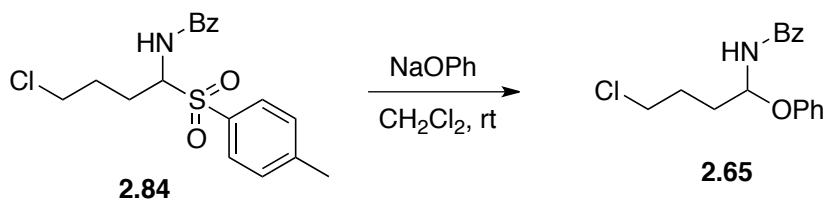
$^{13}\text{C-NMR}$ (151 MHz, CDCl_3) δ 166.59, 145.40, 133.42, 132.61, 132.35, 129.88, 129.01, 128.72, 127.00, 68.51, 43.83, 28.44, 24.47, 21.70.

FTIR (neat): 3214, 3063, 1646, 1524, 1487, 1435, 1329, 1302, 1243, 1142, 1082, 806, 699, 657, 647, 579, 539 cm^{-1} .

HSMS (DART+) calcd for $\text{C}_{18}\text{H}_{21}\text{ClNO}_3\text{S}$ ($[\text{M}+\text{H}]^+$): 366.0931, found: 366.0917.

Melting point: 111-112 $^\circ\text{C}$

***N*-(4-chloro-1-phenoxybutyl)benzamide 2.65**



In a N_2 -filled glovebox sodium phenoxide (0.0838 g, 0.722 mmol, 0.95 equiv) was added in a 25 mL round bottom flask containing a stir bar. The vessel was fitted with a rubber septum, removed from the glovebox and placed under N_2 . In a 2-dram vial α -amido sulfone **2.84** (0.279 g, 0.76 mmol) was dissolved in CH_2Cl_2 (2.0 mL, plus 2 \times 0.5

mL for rinse), and the obtained solution was added in the reaction flask in one portion via a syringe. The reaction mixture was allowed to stir vigorously at 22 °C for 14 h. The resulted milky white suspension was diluted with CH₂Cl₂ (5 mL) and H₂O (5 mL), and transferred to a separatory funnel. The organic layer was isolated, and the aqueous layer was extracted with CH₂Cl₂ (2×5 mL). The combined organic layers were washed with brine (10 mL), dried over anhydrous Na₂SO₄, filtered and concentrated *in vacuo*. The obtained white solid residue was purified by silica gel column chromatography (dichloromethane: hexanes: diethyl ether = 10:5:0.1, plus 5% Et₃N) to afford the title compound as a white solid (0.199 g, 91% yield).

¹H-NMR (600 MHz, CDCl₃) δ 7.76 – 7.69 (m, 2H), 7.53 – 7.48 (m, 1H), 7.42 (t, *J* = 7.8 Hz, 2H), 7.29 – 7.26 (overlapped with CDCl₃, m, 2H), 7.05 (dd, *J* = 8.4, 0.6 Hz, 2H), 6.97 (td, *J* = 7.2, 0.6 Hz, 1H), 6.48 (br d, *J* = 9.6 Hz, 1H), 6.25 (dt, *J* = 9.6, 6.0 Hz, 1H), 3.63 (t, *J* = 6.0 Hz, 2H), 2.20 – 2.13 (m, 1H), 2.10 – 2.03 (m, 2H), 2.02 – 1.95 (m, 1H).

¹³C-NMR (151 MHz, CDCl₃) δ 166.75, 156.19, 133.45, 132.07, 129.70, 128.67, 127.03, 121.91, 115.82, 78.16, 44.48, 33.50, 27.91.

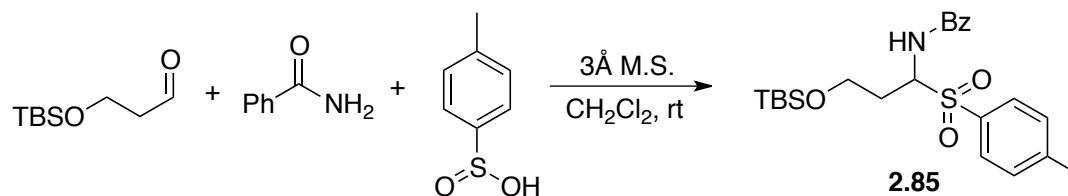
FTIR (neat): 3325, 2954, 1639, 1600, 1583, 1519, 1486, 1447, 1343, 1289, 1229, 1167, 1050, 992, 754, 692, 663, 643 cm⁻¹.

HSMS (DART+) calcd for C₁₇H₁₈ClNO₂Na ([M+Na]⁺): 326.0924, found: 326.0919.

Melting point: 103-104 °C

***N*-[1-[(4-methylphenyl)sulfonyl]-3-(*tert*-butyldimethylsilyloxy)propyl]benzamide**

2.85



To a 50 mL round bottom flask containing a stir bar were added benzamide (0.151 g, 1.25 mmol), 4-methylbenzenesulfonic acid (0.195 g, 1.25 mmol) and 3 Å molecular sieves (0.225 g). The flask was fitted with a rubber septum and placed under N₂. CH₂Cl₂ (1.5 mL) was added in the flask via syringe. In a 1-dram vial 3-(*tert*-butyldimethylsilyloxy)propanal (0.283 g, 1.5 mmol) was dissolved in CH₂Cl₂ (0.5 mL, plus 0.5 mL for rinse), and the obtained solution was added in the reaction flask via syringe. The reaction mixture was allowed to stir vigorously at 22 °C for 20 h. The resulted yellow viscous suspension was diluted with a mixture of CH₂Cl₂ (10 mL) and MeOH (5 mL), and filtered over a pad of celite. The filter cake was washed with CH₂Cl₂ (2×5 mL). The collected filtrate was concentrated in vacuo. The obtained pale yellow gum residue was purified by silica gel column chromatography (hexanes: dichloromethane: ethyl acetate = 10:10:1) to afford the α -amido sulfone **2.85** as a white solid (0.239 g, 45% yield)

¹H-NMR (600 MHz, CDCl₃) δ 7.77 (d, *J* = 8.4 Hz, 2H), 7.60 (dd, *J* = 8.4, 1.2 Hz, 2H), 7.52 – 7.49 (m, 1H), 7.40 (t, *J* = 7.8 Hz, 2H), 7.25 (overlapped with CDCl₃, d, *J* = 7.8 Hz, 2H), 7.02 (d, *J* = 10.2 Hz, 1H), 5.62 (ddd, *J* = 9.6, 9.0, 3.6 Hz, 1H), 4.02 (app ddd, *J* = 10.8, 9.0, 3.6 Hz, 1H), 3.84 (dt, *J* = 10.8, 4.8 Hz, 1H), 2.52-2.46 (m, 1H), 2.38 (s, 3H), 2.27 – 2.21 (m, 1H), 0.83 (s, 9H), 0.027 (s, 3H), -0.008 (s, 3H).

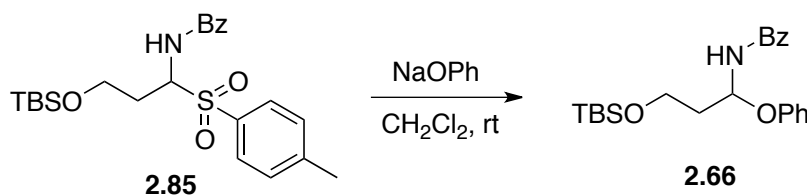
^{13}C -NMR (151 MHz, CDCl_3) δ 166.24, 145.05, 134.03, 133.23, 132.05, 129.74, 129.07, 128.61, 126.96, 67.61, 59.57, 29.80, 25.80, 21.69, 18.23, -5.51, -5.56.

FTIR (neat): 3212, 2954, 2930, 2857, 1646, 1597, 1525, 1486, 1326, 1252, 1143, 1084, 836, 775, 697, 655, 581 cm^{-1} .

HSMS (DART+) calcd for $\text{C}_{23}\text{H}_{34}\text{NO}_4\text{SSi}$ ($[\text{M}+\text{H}]^+$): 448.1978, found: 448.1976.

Melting point: 127-128 $^\circ\text{C}$

N*-[1-phenoxy-3-(*tert*-butyldimethylsilyloxy)propyl]benzamide **2.66*



In a N_2 -filled glovebox NaOPh (0.0573 g, 0.494 mmol, 0.95 equiv) was added in a 25 mL round bottom flask containing a stir bar. The vessel was fitted with a rubber septum, removed from the glovebox and placed under N_2 . In a 2-dram vial α -amido sulfone **2.85** (0.233 g, 0.52 mmol) was dissolved in CH_2Cl_2 (1.1 mL, plus 2×0.5 mL for rinse), and the obtained solution was added in the reaction flask via syringe. The reaction mixture was allowed to stir vigorously at 22 $^\circ\text{C}$ for 14 h. The resulted milky white suspension was diluted with CH_2Cl_2 (5 mL) and H_2O (5 mL), and transferred to a separatory funnel. The organic layer was isolated, and the aqueous layer was extracted with CH_2Cl_2 (2×5 mL). The combined organic layers were washed with brine (10 mL), dried over anhydrous Na_2SO_4 , filtered and concentrated *in vacuo*. The obtained colorless viscous oil residue was purified by silica gel column chromatography (hexanes:

dichloromethane: diethyl ether = 5:2.5:0.1) to afford the title compound as a white solid (0.119 g, 62% yield).

¹H-NMR (600 MHz, CDCl₃) δ 7.76 – 7.72 (m, 2H), 7.66 (br d, *J* = 9.0 Hz, 1H), 7.49 (tt, *J* = 7.2, 1.2 Hz, 1H), 7.42 – 7.37 (m, 2H), 7.29 – 7.26 (overlapped with CDCl₃, m, 2H), 7.16 – 7.12 (m, 2H), 6.96 (tt, *J* = 7.2, 1.2 Hz, 1H), 6.40 (dt, *J* = 9.6, 4.2 Hz, 1H), 4.22 (ddd, *J* = 10.2, 8.4, 4.2 Hz, 1H), 3.87 (dt, *J* = 10.2, 4.8 Hz, 1H), 2.16 – 2.08 (m, 2H), 0.89 (s, 9H), 0.10 (s, 3H), 0.07 (s, 3H).

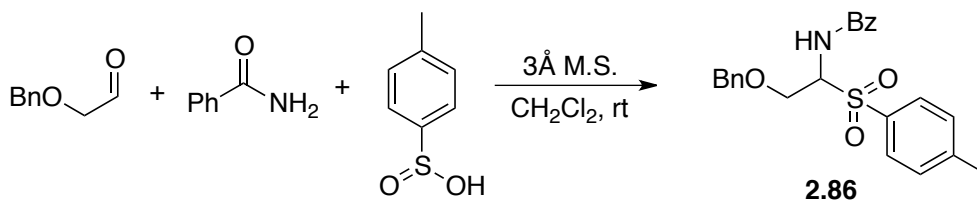
¹³C-NMR (151 MHz, CDCl₃) δ 166.70, 156.54, 134.02, 131.76, 129.54, 128.45, 127.15, 121.70, 116.57, 59.14, 36.60, 25.96, 18.44, -5.36, -5.41.

FTIR (neat): 3293, 2952, 2925, 2853, 1637, 1585, 1532, 1492, 1228, 1107, 1092, 1057, 1027, 1016, 853, 834, 768, 747, 691 cm⁻¹.

HSMS (ESI⁺): calcd for C₂₂H₃₁NO₃SiNa ([M+Na]⁺): 408.1971, found: 408.1964.

Metling point: 71-73 °C

***N*-[1-[(4-methylphenyl)sulfonyl]-2-(phenylmethoxy)ethyl]benzamide 2.86**



To a 50 mL round bottom flask containing a stir bar were added benzamide (0.182 g, 1.5 mmol), 4-methylbenzenesulfinic acid (0.305 g, 1.95 mmol, 1.3 equiv) and 3 Å molecular sieves (0.27 g). The flask was fitted with a rubber septum and placed under N₂. CH₂Cl₂ (1.5 mL) was added in the flask via syringe. In a 1-dram vial benzyloxyacetaldehyde (211 μL, 1.5 mmol) was dissolved in CH₂Cl₂ (1.0 mL, plus 0.5

mL for rinse), and the obtained solution was added in the reaction flask via syringe. The reaction mixture was allowed to stir vigorously at 22 °C for 20 h. The resulted pale yellow viscous suspension was diluted with a mixture of CH₂Cl₂ (10 mL) and MeOH (5 mL), and filtered over a pad of celite. The filter cake was washed with CH₂Cl₂ (2×5 mL). The collected filtrate was concentrated *in vacuo*. The obtained slightly yellow solid residue was purified by silica gel column chromatography (hexanes: dichloromethane: ethyl acetate = 10:5:1 to 10:10:1) to afford the α -amido sulfone **2.86** as a white solid (0.353 g, 57%).

¹H-NMR (600 MHz, CDCl₃) δ 7.79 – 7.75 (m, 2H), 7.65 – 7.64 (m, 2H), 7.53 – 7.50 (m, 1H), 7.42 (t, *J* = 7.8 Hz, 2H), 7.34 – 7.28 (m, 5H), 7.26 (overlapped with CDCl₃, d, *J* = 7.8 Hz, 2H), 7.02 (br d, *J* = 9.6 Hz, 1H) 5.60 (dt, *J* = 9.6, 4.2 Hz, 1H), 4.64 (d, *J* = 12.0 Hz, 1H), 4.59 (d, *J* = 12.0 Hz, 1H) 4.31 (dd, *J* = 10.8, 4.2 Hz, 1H), 3.94 (dd, *J* = 10.8, 4.2 Hz, 1H), 2.39 (s, 3H).

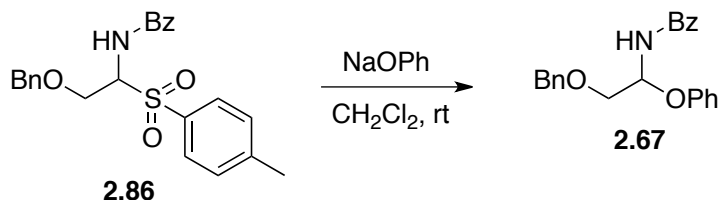
¹³C-NMR (151 MHz, CDCl₃) δ 166.33, 145.24, 136.98, 134.44, 132.89, 132.26, 129.81, 129.00, 128.70, 128.50, 128.02, 127.88, 127.10, 73.66, 68.46, 65.67, 21.70.

FTIR (neat): 3338, 3060, 2999, 1644, 1531, 1490, 1316, 1288, 1145, 1115, 1084, 821, 697, 659, 607, 581, 536 cm⁻¹.

HSMS (DART+) calcd for C₂₃H₂₄NO₄S ([M+H]⁺): 410.1426, found: 410.1411.

Melting point: 128-129 °C

N*-(1-phenoxy-2-(phenylmethoxy)ethyl)benzamide **2.67*



In a N_2 -filled glovebox sodium phenoxide (0.086 g, 0.741 mmol, 0.95 equiv) was added in a 25 mL round bottom flask containing a stir bar. The vessel was fitted with a rubber septum, removed from the glovebox and placed under N_2 . In a 2-dram vial α -amido sulfone **2.86** (0.319 g, 0.78 mmol) was dissolved in CH_2Cl_2 (2.1 mL, plus 2 \times 0.5 mL for rinse), and the obtained solution was added in the reaction flask via syringe. The reaction mixture was allowed to stir vigorously at 22 $^\circ\text{C}$ for 14 h. The resulted milky white suspension was diluted with CH_2Cl_2 (5 mL) and H_2O (5 mL), and transferred to a separatory funnel. The organic layer was isolated, and the aqueous layer was extracted with CH_2Cl_2 (2 \times 5 mL). The combined organic layers were washed with brine (10 mL), dried over anhydrous Na_2SO_4 , filtered and concentrated *in vacuo*. The obtained colorless viscous oil residue was purified by silica gel column chromatography (hexanes: dichloromethane: diethyl ether = 5:5:0.1) to afford the title compound as a white solid (0.244 g, 95% yield).

^1H -NMR (600 MHz, CDCl_3) δ 7.77 – 7.71 (m, 2H), 7.51 (app tt, J = 7.8, 1.2 Hz, 1H), 7.42 (app t, J = 7.8 Hz, 2H), 7.39 – 7.32 (m, 3H), 7.32 – 7.25 (overlapped with CDCl_3 , m, 4H), 7.12 (d, J = 7.8 Hz, 2H), 7.00 – 6.97 (m, 1H), 6.95 (d, J = 9.0 Hz, 1H), 6.36 (dt, J = 9.6, 3.6 Hz, 1H), 4.73 (d, J = 12.0 Hz, 1H), 4.68 (d, J = 12.0 Hz, 1H), 3.90 (dd, J = 10.8, 3.6 Hz, 1H), 3.80 (dd, J = 10.8, 3.6 Hz, 1H).

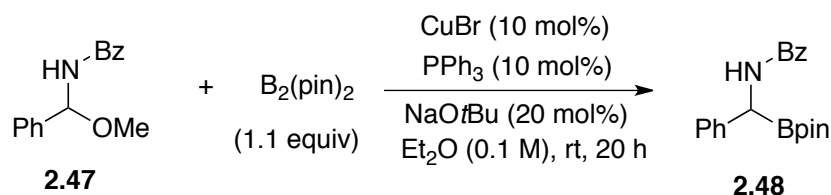
^{13}C -NMR (151 MHz, CDCl_3) δ 166.75, 156.21, 137.57, 133.53, 132.03, 129.62, 128.62, 128.52, 127.95, 127.87, 127.14, 122.01, 116.30, 77.30, 73.79, 70.91.

FTIR (neat): 3272, 3061, 3029, 2872, 1633, 1588, 1538, 1486, 1291, 1226, 1103, 1085, 1042, 1025, 754, 695 cm^{-1} .

HSMS (ESI+) calcd for $\text{C}_{22}\text{H}_{21}\text{O}_3\text{NNa}$ ($[\text{M}+\text{Na}]^+$): 370.1419, found: 370.1424.

Melting point: 117-119 $^\circ\text{C}$

CuBr-catalyzed racemic synthesis of *N*-[phenyl(4,4,5,5-tetramethyl-1,3,2-dioxaborolan-2-yl)methyl]benzamide **2.48 (0.1 mmol scale)**



In a N_2 -filled glovebox *N*-(methoxyphenylmethyl)benzamide **2.47** (0.0241 g, 0.1 mmol), $\text{B}_2(\text{pin})_2$ (0.0279 g, 0.11 mmol, 1.1 equiv), PPh_3 (0.0026 g, 0.01 mmol, 0.1 equiv) and NaOtBu (0.0019 g, 0.02 mmol, 0.2 equiv) were sequentially added in an oven-dried 2-dram vial containing a stir bar. Diethyl ether (1.0 mL) was then added in the vial via syringe. The resulted mixture was stirred vigorously at 22 $^\circ\text{C}$ for 5 min. During the stirring the vial was occasionally tilted to make the NaOtBu solid stuck on the inside wall of the vial dissolved in the solution. CuBr (0.0014 g, 0.01 mmol, 0.1 equiv) was added in the vial in one portion. The vial was sealed with a phenolic screw cap and electrical tape, and removed from the glovebox. The reaction mixture, a milky white suspension, was allowed to stir vigorously at 22 $^\circ\text{C}$ for 20 h before it was diluted with CH_2Cl_2 (10 mL). The obtained solution was transferred into a separatory funnel, and washed with saturated

NH₄Cl aqueous solution (10 mL) and saturated NaHCO₃ aqueous solution (10 mL) in sequence. The two aqueous layers were combined and extracted with CH₂Cl₂ (5 mL). The combined organic layers were washed with brine (10 mL), dried over anhydrous Na₂SO₄, filtered and concentrated to a white solid residue *in vacuo*. The crude product was purified by florisil column chromatography (dichloromethane: hexanes: ethyl acetate = 5:1:0.6 to 5:1:1) to afford the title compound as a white solid (0.0276 g, 82% yield).

¹H-NMR (600 MHz, CDCl₃) δ 8.83 (br s, 1H), 7.90 (d, *J* = 7.8 Hz, 2H), 7.56 (t, *J* = 7.2 Hz, 1H), 7.42 (t, *J* = 7.2 Hz, 2H), 7.29 – 7.22 (overlapped with CDCl₃, m, 2H), 7.19 – 7.12 (m, 3H), 3.94 (s, 1H), 1.04 (s, 6H), 0.96 (s, 6H).

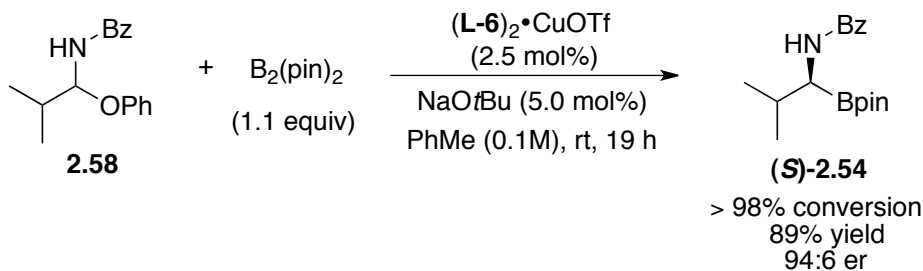
¹³C-NMR (151 MHz, CDCl₃) δ 174.73, 143.59, 136.26, 131.43, 131.14, 130.57, 129.69, 128.87, 128.33, 83.34, 55.60, 27.20, 26.92.

FTIR (neat): 3190, 3066, 2967, 2924, 1602, 1573, 1534, 1522, 1489, 1365, 1193, 1145, 1090, 1000, 932, 753, 696, 642, 589 cm⁻¹.

HSMS (DART+) calcd for C₂₀H₂₅BNO₃ ([M+1]⁺): 338.1928, found: 338.1921.

Enantioselective borylation of alkyl-substituted hemiaminal ethers with a chiral copper(I)/bisphosphine monoxide complex

N-[(1*S*)-2-methyl-1-(4,4,5,5-tetramethyl-1,3,2-dioxaborolan-2-yl)propyl]benzamide (**(S)**-**2.54** (0.25 mmol reaction scale)



In a N₂-filled glovebox *N*-(2-methyl-1-phenoxypropyl)benzamide **2.58** (0.0673 g, 0.25 mmol) and B₂(pin)₂ (0.0698 g, 0.275 mmol, 1.1 equiv) were added in an oven-dried 2-dram vial containing a stir bar. Toluene (2.0 mL) was added in the vial to completely dissolve the two solid materials. Then, NaOtBu (0.0012 g, 0.0125 mmol, 0.05 equiv) was added in the obtained solution, and the resulted mixture was stirred vigorously at 22 °C for 10 min. During the stirring the vial was occasionally tilted to make the NaOtBu solid stuck on the inside wall of the vial dissolved in the solution. (L-6)₂•CuOTf (0.0054 g, 0.00625 mmol, 0.025 equiv) was added in the vial in one portion followed by addition of toluene (0.5 mL) to rinse the inside wall of the vial. The vial was sealed with a phenolic screw cap and electrical tape, and removed from the glovebox. The reaction mixture, a cloudy brown solution, was allowed to stir vigorously at 22 °C for 19 h before it was diluted with CH₂Cl₂ (15 mL). The obtained clear solution was transferred into a separatory funnel, and washed with saturated NH₄Cl aqueous solution (10 mL) and saturated NaHCO₃ aqueous solution (10 mL) in sequence. The two aqueous layers were combined and extracted with CH₂Cl₂ (5 mL). The combined organic layers were washed with brine (10 mL), dried over anhydrous Na₂SO₄, filtered and concentrated to a white solid residue *in vacuo*. The crude product was purified by florisil column chromatography (dichloromethane: hexanes: ethyl acetate = 5:1:0.5 to 5:1:0.7) to afford the title compound as a white solid (0.0675 g, 89% yield, 94:6 er).

¹H-NMR (600 MHz, CD₂Cl₂) δ 7.80 – 7.76 (m, 2H), 7.55 – 7.46 (overlapped with a broad peak, m, 2H), 7.40 (t, *J* = 7.8 Hz, 2H), 2.94-2.92 (m, 1H), 2.06 – 1.99 (m, 1H), 1.263 (s, 6H), 1.258 (s, 6H), 1.03 (d, *J* = 7.2 Hz, 3H), 1.01 (d, *J* = 7.2 Hz, 3H).

^{13}C -NMR (151 MHz, CD_2Cl_2) δ 169.79, 132.68, 131.38, 128.96, 127.99, 82.49, 48.53, 30.50, 25.55, 25.50, 20.76, 20.06.

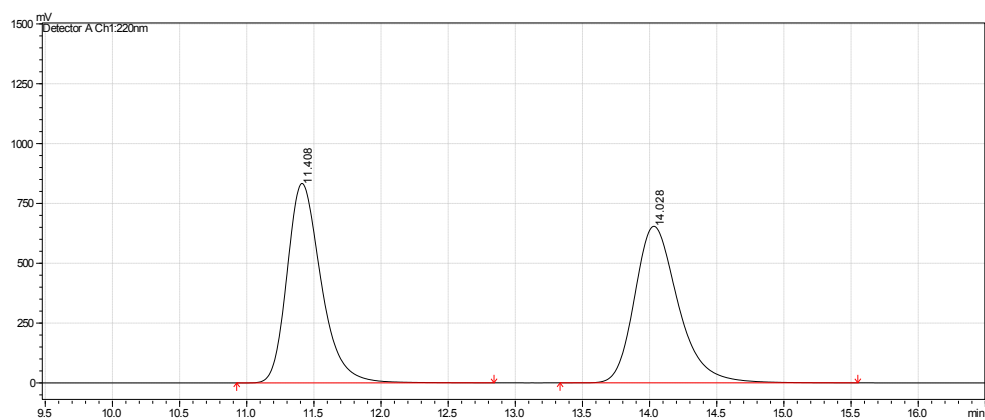
FTIR (neat): 3194, 3072, 2979, 2948, 2927, 1603, 1574, 1526, 1490, 1220, 1185, 1153, 1123, 1107, 1091, 1004, 977, 733, 706, 644 cm^{-1} .

HSMS (DART+) calcd for $\text{C}_{18}\text{H}_{29}\text{BNO}_3$ ($[\text{M}+1]^+$): 318.2241, found: 318.2245.

Melting point: 164-167 $^\circ\text{C}$. $[\alpha]_{\text{D}}^{20} = +31.6$ ($c = 0.46$, THF) for 94:6 er.

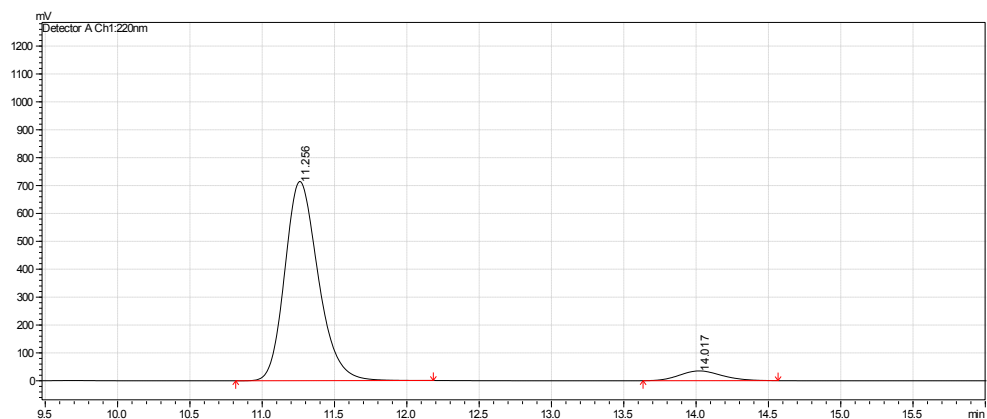
HPLC (Chiralpak® AD-H column, hexanes: isopropanol = 96:4, 0.5 mL/min, 220 nm) t_{R} (Major) = 11.26 min, t_{R} (minor) = 14.02 min. The authentic racemic sample was prepared with CuCl as the catalyst and tricyclohexylphosphine as the ligand.

Authentic racemic product **2.54**



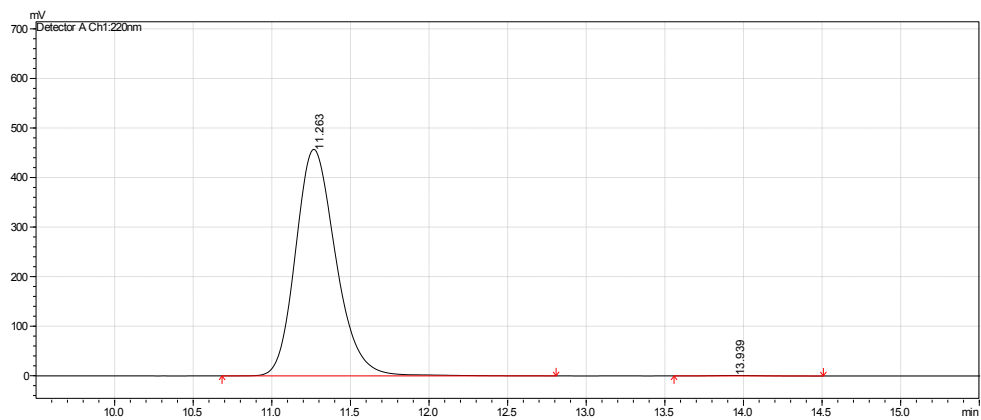
Peak#	Ret. Time (min)	Area (%)
1	11.41	49.95
2	14.03	50.05

Enantioenriched product (*S*)-2.54



Peak#	Ret. Time (min)	Area (%)
1	11.26	94.12
2	14.02	5.88

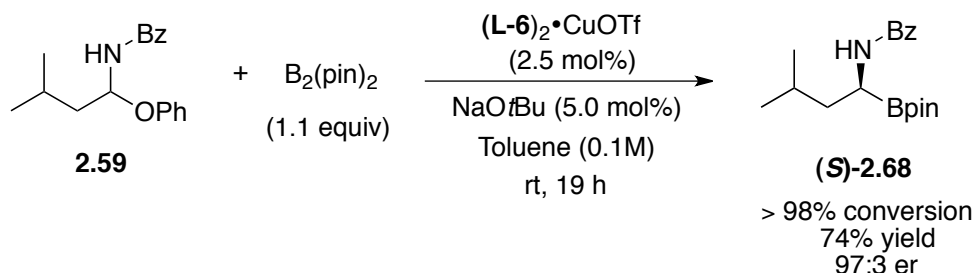
Enantioenriched product (*S*)-2.54 after recrystallization from dichloromethane/hexane



Peak#	Ret. Time (min)	Area (%)
1	11.26	99.77
2	13.94	0.23

***N*-[(1*S*)-3-methyl-1-(4,4,5,5-tetramethyl-1,3,2-dioxaborolan-2-yl)butyl]benzamide**

(*S*)-2.68 (0.4 mmol reaction scale)



In a N_2 -filled glovebox *N*-(3-methyl-1-phenoxybutyl)benzamide **2.59** (0.113 g, 0.4 mmol) and $\text{B}_2(\text{pin})_2$ (0.112 g, 0.44 mmol, 1.1 equiv) were added in an oven-dried 2-dram vial containing a stir bar. Toluene (3.0 mL) was added in the vial to dissolve the two solid materials. Then, NaOtBu (0.0019 g, 0.02 mmol, 0.05 equiv) was added in the obtained solution followed by addition of toluene (0.5 mL) to rinse the inside wall of the vial. The resulted mixture was stirred vigorously at 22 °C for 10 min. During the stirring the vial was occasionally tilted to make the NaOtBu solid stuck on the inside wall of the vial dissolved in the solution. $(\text{L-6})_2 \cdot \text{CuOTf}$ (0.0086 g, 0.01 mmol, 0.025 equiv) was added in the vial in one portion followed by addition of toluene (0.5 mL) to rinse the inside wall of the vial. The vial was sealed with a phenolic screw cap and electrical tape, and removed from the glovebox. The reaction mixture, a cloudy brown solution, was allowed to stir vigorously at 22 °C for 19 h before it was diluted with CH_2Cl_2 (25 mL). The obtained clear solution was transferred into a separatory funnel, and washed with saturated NH_4Cl aqueous solution (15 mL) and saturated NaHCO_3 aqueous solution (15 mL) in sequence. The two aqueous layers were combined and extracted with CH_2Cl_2 (10 mL). The combined organic layers were washed with brine (10 mL), dried over anhydrous Na_2SO_4 , filtered and concentrated to a slightly yellow semi-solid residue *in vacuo*. The crude

product was purified by florisil column chromatography (dichloromethane: hexanes: ethyl acetate = 2:1:0.3 to 2:1:0.5) to afford the title compound as a white solid (0.0946 g, 74% yield, 97:3 er).

$^1\text{H-NMR}$ (600 MHz, CD_2Cl_2) δ 7.79 – 7.73 (m, 2H), 7.57 – 7.52 (m, 1H), 7.48 – 7.36 (overlapped with a broad peak, m, 3H), 3.04 – 2.96 (m, 1H), 1.79 – 1.70 (m, 1H), 1.52 – 1.44 (m, 2H), 1.25 (s, 6H), 1.24 (s, 6H), 0.97 (d, $J = 2.4$ Hz, 3H), 0.96 (d, $J = 2.4$ Hz, 3H).

$^{13}\text{C-NMR}$ (151 MHz, CD_2Cl_2) δ 169.82, 132.57, 129.00, 128.38, 127.75, 81.18, 41.35, 40.64, 25.82, 24.94, 24.90, 23.02, 22.03.

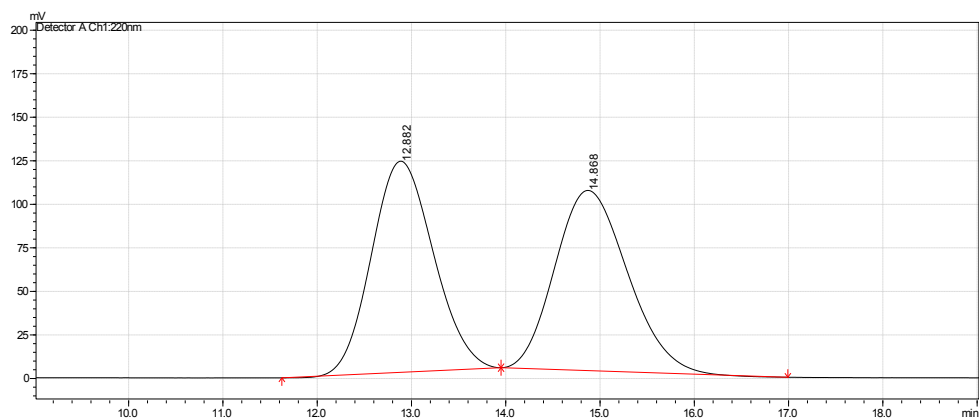
FTIR (neat): 3196, 2960, 2922, 1603, 1574, 1532, 1490, 1200, 1156, 1110, 1100, 1016, 984, 707, 686, 614 cm^{-1} .

HSMS (DART+) calcd for $\text{C}_{18}\text{H}_{29}\text{BNO}_3$ ($[\text{M}+\text{H}]^+$): 318.2241, found: 318.2246.

Melting point: 154-156 $^\circ\text{C}$. $[\alpha]_{\text{D}}^{20} = +22.2$ ($c = 0.325$, THF) for 97:3 er.

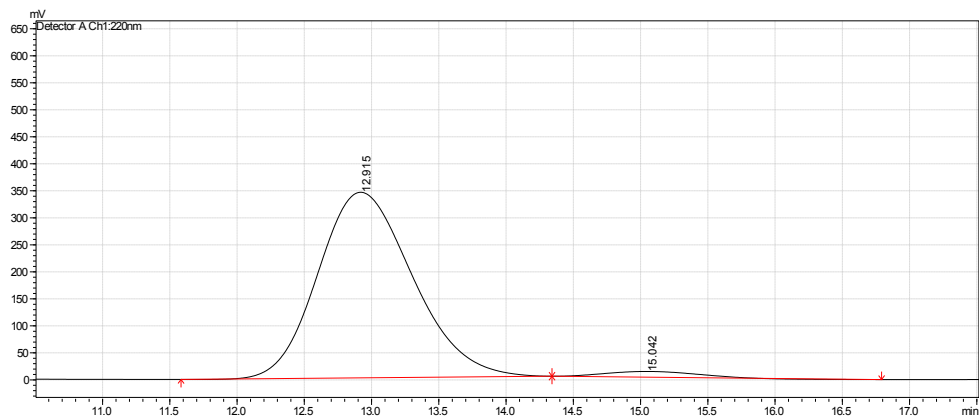
HPLC (Chiralpak® AS-H column, hexanes: isopropanol = 98:2, 0.5 mL/min, 220 nm) t_{R} (Major) = 12.92 min, t_{R} (minor) = 15.04 min. The authentic racemic sample was prepared with CuCl as the catalyst and tricyclohexylphosphine as the ligand.

Authentic racemic product **2.68**

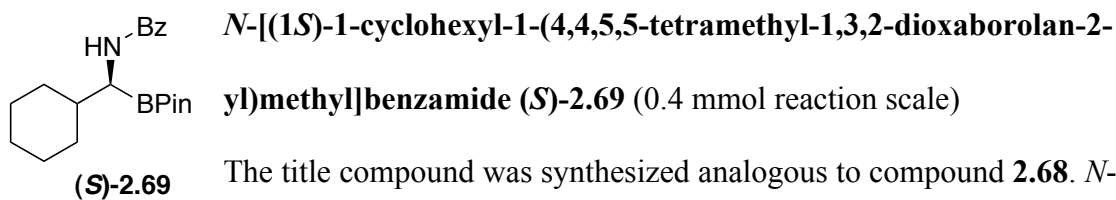


Peak#	Ret. Time (min)	Area (%)
1	12.88	49.99
2	14.87	50.01

Enantioenriched product (*S*)-**2.68**



Peak#	Ret. Time (min)	Area (%)
1	12.92	97.29
2	15.04	2.71



The title compound was synthesized analogous to compound **2.68**. *N*-(1-cyclohexyl-1-phenoxyethyl)benzamide **2.60** (0.124 g, 0.4 mmol) was used in the reaction (Note: **2.60** has very poor solubility in toluene. After 19 h at 22 °C the conversion of **2.60** is 94%). The crude product was purified by florisil column chromatography (dichloromethane: hexanes: ethyl acetate = 2:1:0.3 to 2:1:0.5) to afford the title compound as a white solid (0.119 g, 87%, 93:7 er).

¹H-NMR (600 MHz, CD₂Cl₂) δ 7.81 – 7.77 (m, 2H), 7.57 – 7.52 (m, 1H), 7.47 – 7.42 (m, 2H), 6.97 (s, 1H), 3.06 – 2.99 (m, 1H), 1.85 – 1.77 (m, 2H), 1.77 – 1.70 (m, 2H), 1.70 – 1.63 (m, 2H), 1.32 – 1.21 (overlapped peaks, m, 14H), 1.19 – 1.08 (m, 3H).

¹³C-NMR (151 MHz, CD₂Cl₂) δ 168.60, 132.09, 131.88, 128.48, 127.21, 82.44, 46.11, 39.86, 30.98, 30.18, 26.46, 26.38, 26.36, 24.92, 24.89.

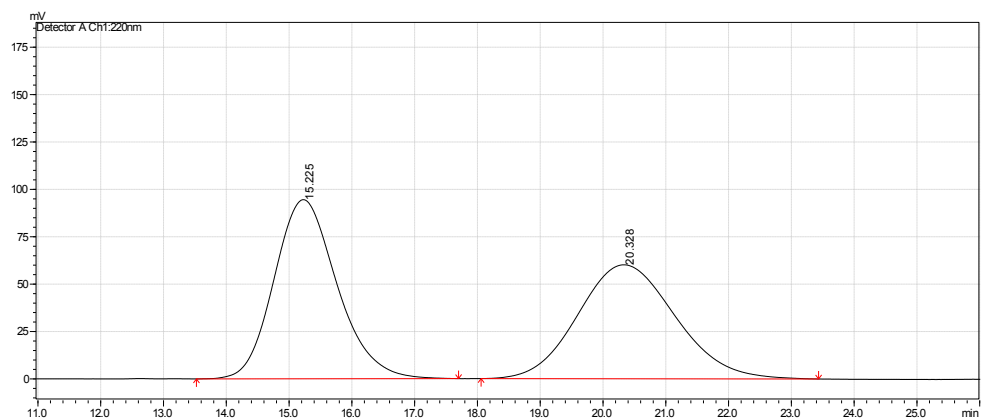
FTIR (neat): 3195, 2970, 2921, 2851, 1604, 1573, 1530, 1487, 1446, 1191, 1155, 1109, 1011, 984, 708, 626 cm⁻¹.

HSMS (DART+) calcd for C₂₀H₃₁BNO₃ ([M+H]⁺): 344.2397, found: 344.2400.

Melting point: 152-153 °C. [α]_D²⁰ = +31.6 (c = 0.38, THF) for 93:7 er.

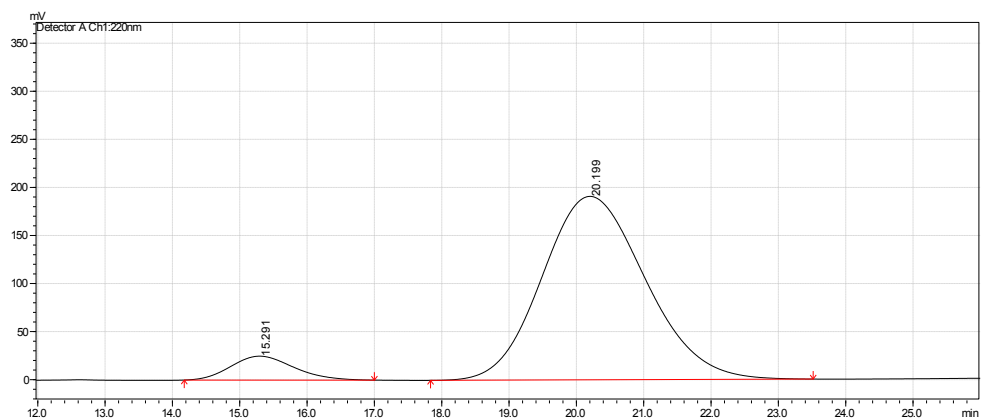
HPLC (Chiralpak® AS-H column, hexanes: isopropanol = 98:2, 0.5 mL/min, 220 nm) t_R (Major) = 20.20 min, t_R (minor) = 15.29 min. The authentic racemic sample was prepared with CuCl as the catalyst and tricyclohexylphosphine as the ligand.

Authentic racemic product **2.69**

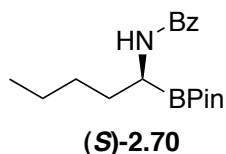


Peak#	Ret. Time (min)	Area (%)
1	15.23	50.35
2	20.33	49.65

Enantioenriched product (*S*)-**2.69**



Peak#	Ret. Time (min)	Area (%)
1	15.29	7.36
2	20.20	92.64



***N*-[*(1S)*-1-(4,4,5,5-tetramethyl-1,3,2-dioxaborolan-2-yl)pentyl]benzamide (*S*)-2.70** (0.4 mmol reaction scale)

The title compound was synthesized analogous to compound **2.68**. *N*-(1-phenoxy)pentylbenzamide **2.61** (0.113 g, 0.4 mmol) was used in the reaction. The crude product was purified by florisil column chromatography (dichloromethane: hexanes: ethyl acetate = 2:1:0.3 to 2:1:0.5) to afford the title compound as a white solid (0.0943 g, 74% yield, 97:3 er).

¹H-NMR (600 MHz, CDCl₃) δ 8.30 (s, 1H), 7.84 – 7.79 (m, 2H), 7.49 – 7.42 (m, 1H), 7.33 (t, *J* = 7.8 Hz, 2H), 2.81 – 2.75 (m, 1H), 1.75 – 1.67 (m, 1H), 1.62 – 1.53 (m, 1H), 1.45 – 1.35 (m, 2H), 1.36 – 1.28 (m, 2H), 1.26 (s, 6H), 1.24 (s, 6H), 0.88 (t, *J* = 7.2 Hz, 3H).

¹³C-NMR (151 MHz, CDCl₃) δ 170.67, 132.86, 128.39, 128.12, 128.03, 80.88, 44.90, 30.87, 30.02, 25.42, 25.08, 22.84, 14.03.

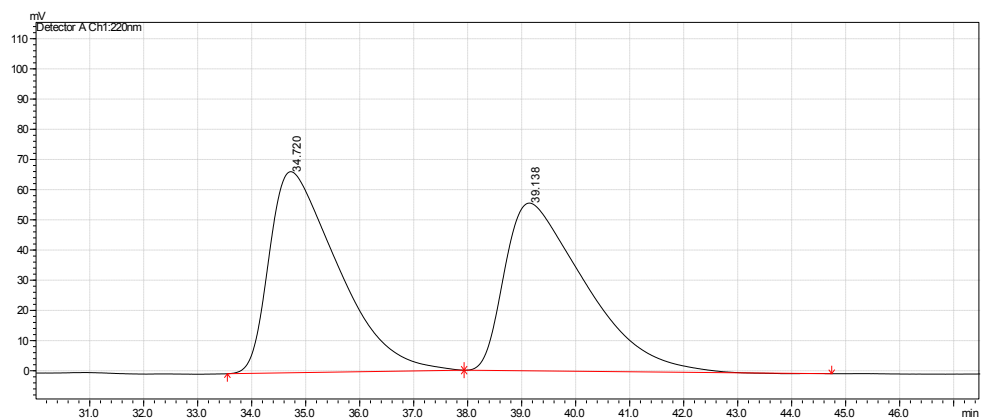
FTIR (neat): 3191, 3073, 2960, 2926, 1601, 1574, 1526, 1488, 1362, 1184, 1155, 1125, 1102, 1016, 874, 707, 684, 569 cm⁻¹.

HSMS (DART+) calcd for C₁₈H₂₉BNO₃ ([M+H]⁺): 318.2241, found: 318.2256.

Melting point: 125-127 °C. [α]_D²⁰ = +36.8 (c = 0.31, THF) for 97:3 er

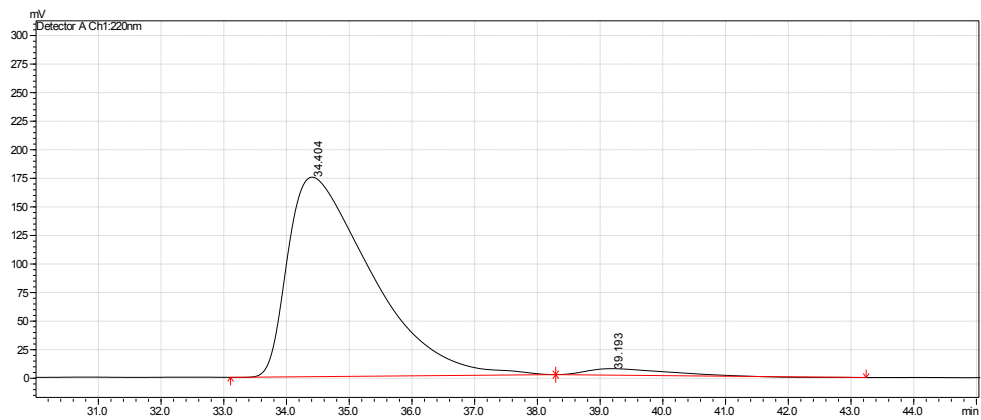
HPLC (Chiralpak® AD-H column, hexanes: isopropanol = 98:2, 0.5 mL/min, 220 nm) t_R (Major) = 34.40 min, t_R (minor) = 39.19 min. The authentic racemic sample was prepared with CuCl as the catalyst and tricyclohexylphosphine as the ligand.

Authentic racemic product **2.70**

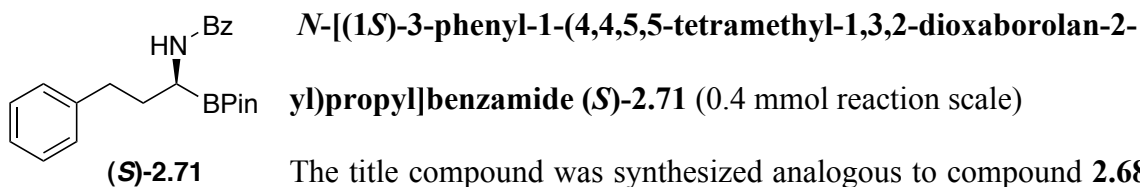


Peak#	Ret. Time (min)	Area (%)
1	34.72	50.53
2	39.14	49.47

Enantioenriched product (*S*)-**2.70**



Peak#	Ret. Time (min)	Area (%)
1	34.40	97.05
2	39.19	2.95



The title compound was synthesized analogous to compound **2.68**.

N-(1-phenoxy-3-phenylpropyl)benzamide **2.62** (0.133 g, 0.4 mmol) was used in the reaction (Note: substrate **2.62** has poor solubility in toluene, but after 19 h at 22 °C it can be completely consumed in the reaction). The crude product was purified by florisil column chromatography (dichloromethane: hexanes: ethyl acetate = 2:1:0.3 to 2:1:0.5) to afford the title compound as a white solid (0.113 g, 77% yield, 95:5 er).

¹H-NMR (600 MHz, CDCl₃) δ 7.55 – 7.51 (m, 2H), 7.51 – 7.48 (m, 1H), 7.38 – 7.34 (m, 2H), 7.34 – 7.30 (m, 2H), 7.28 – 7.25 (m, 2H), 7.25 – 7.22 (m, 1H), 6.92 (s, 1H), 2.93 (ddd, *J* = 13.8, 7.8, 4.8 Hz, 1H), 2.88 (ddd, *J* = 8.4, 4.8, 2.4 Hz, 1H), 2.70 (dt, *J* = 13.8, 8.4 Hz, 1H), 2.12 (ddt, *J* = 14.4, 7.8, 4.8 Hz, 1H), 1.89 (ddd, *J* = 17.4, 14.4, 8.4 Hz, 1H), 1.28 (s, 6H), 1.26 (s, 6H).

¹³C-NMR (151 MHz, CDCl₃) δ 170.48, 142.84, 133.13, 128.73, 128.62, 128.58, 127.74, 127.70, 126.03, 80.81, 45.30, 35.36, 32.77, 25.38, 25.16.

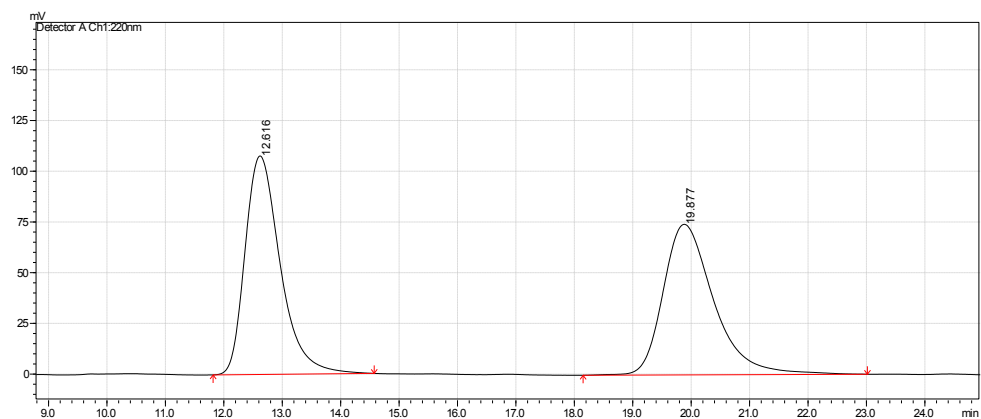
FTIR (neat): 3195, 2967, 2922, 1602, 1572, 1532, 1491, 1383, 1360, 1198, 1152, 1106, 1035, 971, 702, 631, 577 cm⁻¹.

HSMS (DART+) calcd for C₂₂H₂₉BNO₃ ([M+H]⁺): 366.2241, found: 366.2235.

Melting point: 135-137 °C. [α]_D²⁰ = +39.5 (c = 0.41, THF) for 95:5 er.

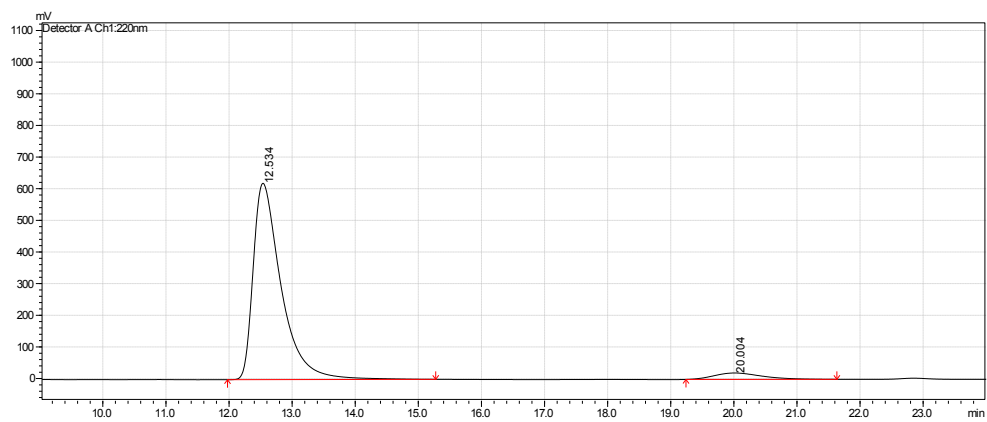
HPLC (Chiralpak® OD-H column, hexanes: isopropanol = 96:4, 0.5 mL/min, 220 nm) t_R (Major) = 12.53 min, t_R (minor) = 20.00 min. The authentic racemic sample was prepared with CuCl as the catalyst and tricyclohexylphosphine as the ligand.

Authentic racemic product **2.71**

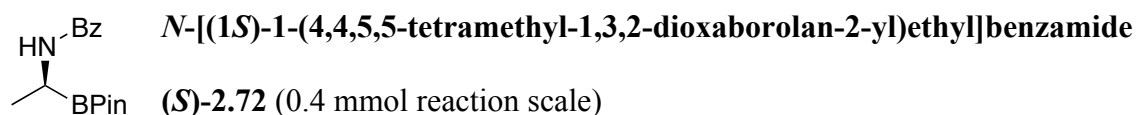


Peak#	Ret. Time (min)	Area (%)
1	12.62	50.20
2	19.88	49.80

Enantioenriched product (*S*)-**2.71**



Peak#	Ret. Time (min)	Area (%)
1	12.53	94.72
2	20.00	5.28



(*S*)-2.72 The title compound was synthesized analogous to compound **2.68**. *N*-(1-phenoxyethyl)benzamide **2.63** (0.0965 g, 0.4 mmol) was used in the reaction. The crude product was purified by florisil column chromatography (dichloromethane: hexanes: ethyl acetate = 2:1:0.3 to 2:1:1.2) to afford the title compound as a colorless gum (0.0946, 86%, 92:8 er).

¹H-NMR (600 MHz, CDCl₃) δ 9.60 (br s, 1H), 7.80 (d, *J* = 7.2 Hz, 2H), 7.40 – 7.35 (m, 1H), 7.28 – 7.22 (overlapped with CDCl₃, m, 2H), 2.77 (q, *J* = 7.2 Hz, 1H), 1.25 (overlapped peak, s, 6H), 1.24 (overlapped peak, d, *J* = 7.2 Hz, 3H), 1.22 (overlapped peak, s, 6H).

¹³C-NMR (151 MHz, CDCl₃) δ 170.95, 132.99, 128.35, 128.25, 126.85, 80.47, 41.04, 25.23, 24.79, 16.17.

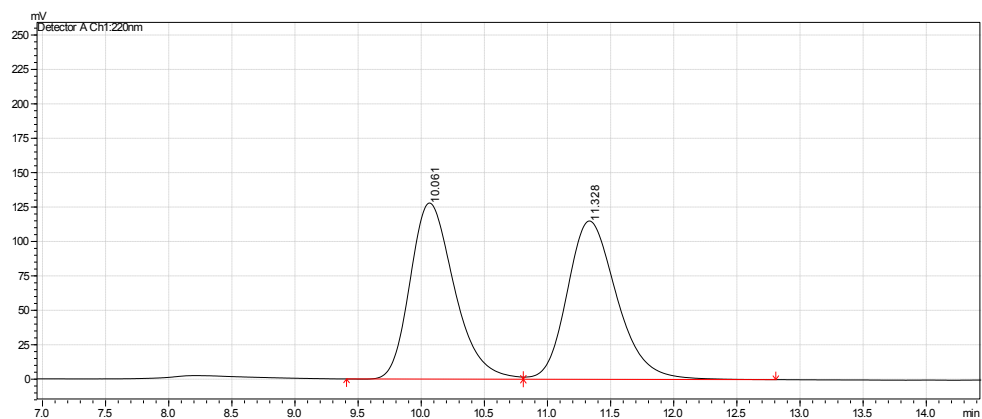
FTIR (neat): 3195, 3066, 2969, 2926, 1610, 1577, 1528, 1489, 1363, 1240, 1186, 1159, 1124, 967, 945, 709, 608 cm⁻¹.

HSMS (DART+) calcd for C₁₅H₂₃BNO₃ ([M+H]⁺): 276.1771, found: 276.1774.

[α]_D²⁰ = +28.2 (c = 0.425, THF) for 92:8 er.

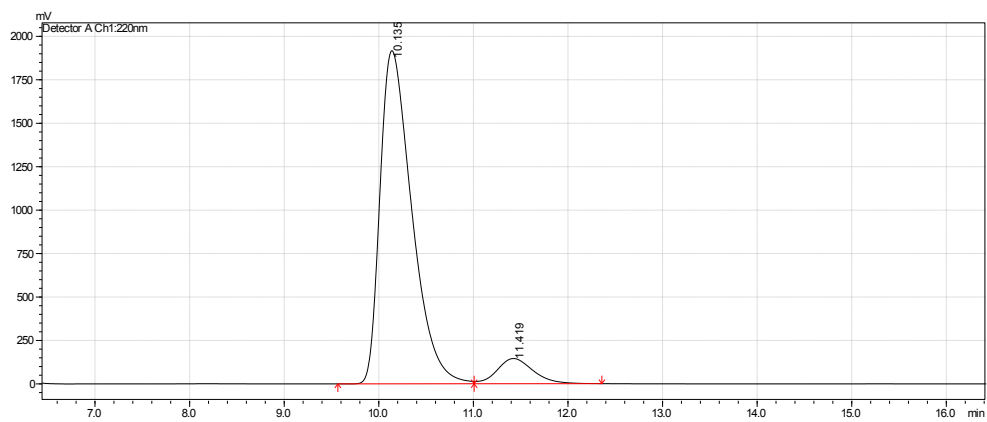
HPLC (Chiralpak® AS-H column, hexanes: isopropanol = 96:4, 0.5 mL/min, 220 nm) t_R (Major) = 10.14 min, t_R (minor) = 11.42 min. The authentic racemic sample was prepared with CuCl as the catalyst and tricyclohexylphosphine as the ligand.

Authentic racemic product **2.72**

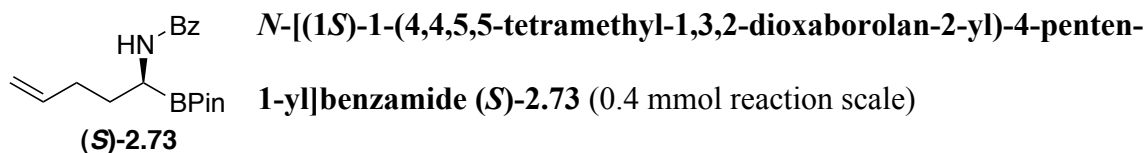


Peak#	Ret. Time (min)	Area (%)
1	10.06	49.77
2	11.33	50.23

Enantioenriched product (*S*)-**2.72**



Peak#	Ret. Time (min)	Area (%)
1	10.14	92.10
2	11.42	7.90



The title compound was synthesized analogous to compound **2.68**. *N*-(4-penten-1-yl-1-phenoxy)benzamide **2.64** (0.113, 0.4 mmol) was used in the reaction. The crude product was purified by florisil column chromatography (dichloromethane: hexanes: ethyl acetate = 2:1:0.3 to 2:1:0.5) to afford the title compound as a white solid (0.097 g, 77% yield, 96:4 er).

¹H-NMR (600 MHz, CDCl₃) δ 7.93 (s, 1H), 7.81 – 7.75 (m, 2H), 7.53 – 7.49 (m, 1H), 7.39 (t, *J* = 7.8 Hz, 2H), 5.87 (ddt, *J* = 17.4, 10.2, 6.6 Hz, 1H), 5.08 (dq, *J* = 17.4, 1.2 Hz, 1H), 5.01 – 4.96 (m, 1H), 2.88 – 2.81 (m, 1H), 2.27 – 2.20 (m, 2H), 1.88 – 1.79 (m, 1H), 1.72 – 1.64 (m, 1H), 1.27 (s, 6H), 1.25 (s, 6H).

¹³C-NMR (151 MHz, CDCl₃) δ 170.70, 139.34, 133.07, 128.60, 128.08, 127.90, 114.78, 80.95, 44.56, 32.57, 30.28, 25.35, 25.08.

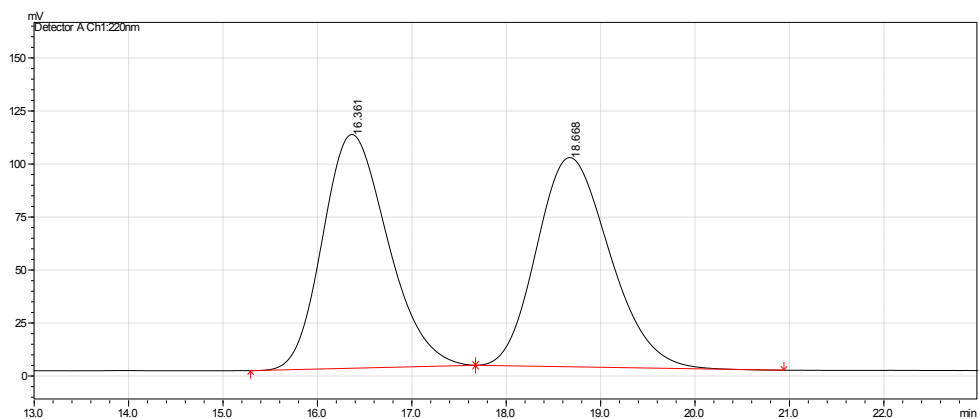
FTIR (neat): 3192, 3073, 2968, 2923, 1601, 1574, 1526, 1488, 1362, 1199, 1150, 1106, 1020, 708, 684, 627, 562 cm⁻¹.

HSMS (DART+) calcd for C₁₈H₂₇BNO₃ ([M+H]⁺): 316.2084, found: 316.2094.

Melting point: 141-142 °C. [α]_D²⁰ = +35.2 (c = 0.335, THF) for 96:4 er.

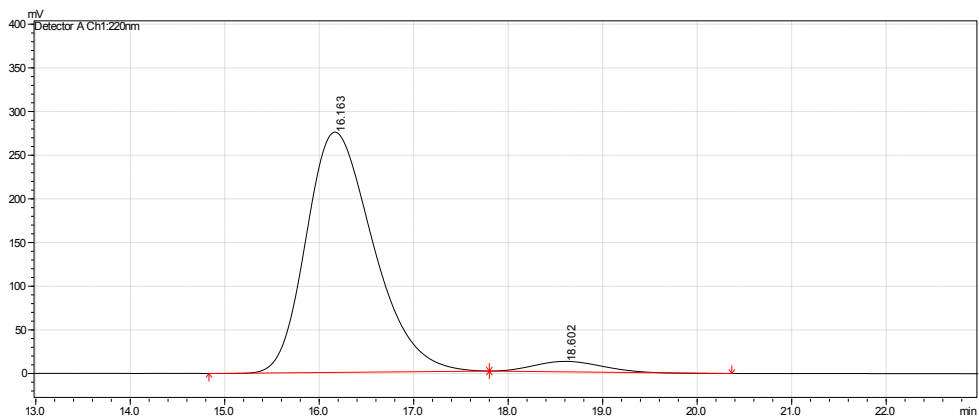
HPLC (Chiralpak® AS-H column, hexanes: isopropanol = 98:2, 0.5 mL/min, 220 nm) t_R (Major) = 16.16 min, t_R (minor) = 18.60 min. The authentic racemic sample was prepared with CuCl as the catalyst and tricyclohexylphosphine as the ligand.

Authentic racemic product **2.73**

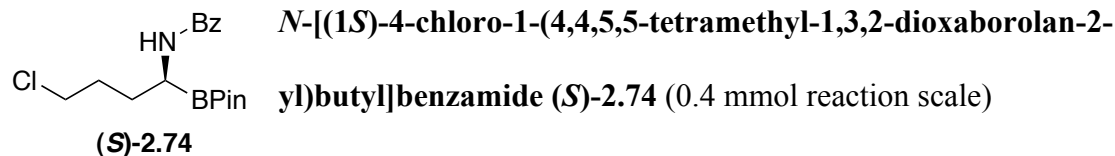


Peak#	Ret. Time (min)	Area (%)
1	16.36	49.91
2	18.67	50.09

Enantioenriched product (*S*)-**2.73**



Peak#	Ret. Time (min)	Area (%)
1	16.16	95.86
2	18.60	4.14



The title compound was synthesized analogous to compound **2.68**.

N-(4-chloro-1-phenoxybutyl)benzamide **2.65** (0.122 g, 0.4 mmol) was used in the reaction. The crude product was purified by florisil column chromatography (dichloromethane: hexanes: ethyl acetate = 2:1:0.3 to 2:1:0.9) to afford the title compound as a white solid (0.105 g, 78%, 93:7 er).

¹H-NMR (600 MHz, CDCl₃) δ 8.87 (s, 1H), 7.85 – 7.79 (m, 2H), 7.47 – 7.42 (m, 1H), 7.32 (t, *J* = 7.8 Hz, 2H), 3.57 – 3.46 (m, 2H), 2.76 – 2.69 (m, 1H), 1.96 – 1.86 (m, 2H), 1.86 – 1.69 (m, 2H), 1.26 (s, 6H), 1.24 (s, 6H).

¹³C-NMR (151 MHz, CDCl₃) δ 171.09, 133.22, 128.48, 128.22, 127.29, 80.97, 45.16, 44.42, 30.55, 28.72, 25.49, 25.15.

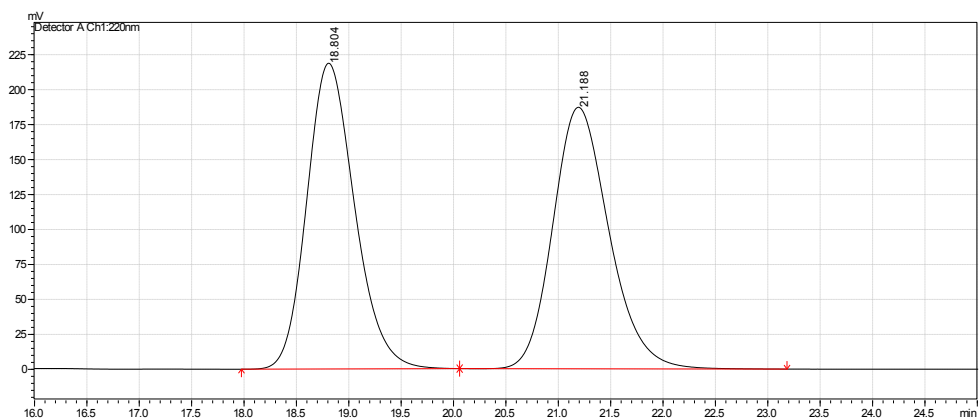
FTIR (neat): 3186, 3076, 2966, 2921, 1603, 1569, 1531, 1487, 1362, 1186, 1138, 1013, 970, 948, 807, 733, 712, 686, 623, 612, 578 cm⁻¹.

HSMS (DART+) calcd for C₁₇H₂₆BClNO₃ ([M+H]⁺): 338.1694, found: 338.1705.

Melting point: 158-160 °C. [α]_D²⁰ = +46.7 (c = 0.445, THF) for 93:7 er.

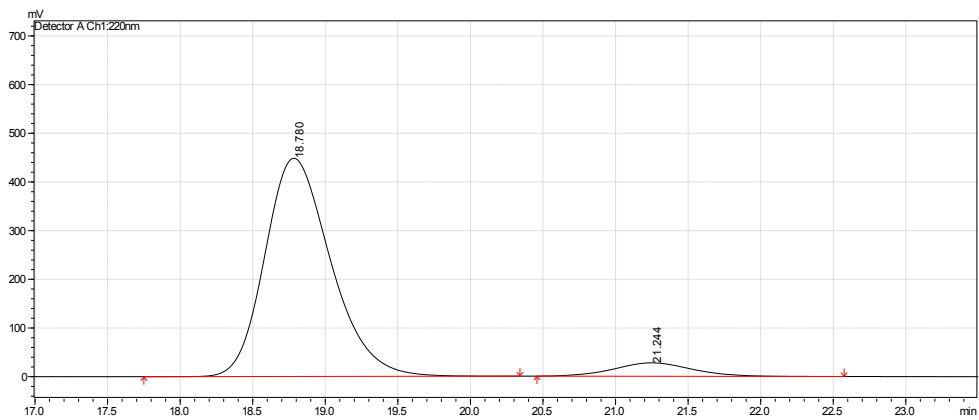
HPLC (Chiralpak® AD-H column, hexanes: isopropanol = 96:4, 0.5 mL/min, 220 nm) t_R (Major) = 18.78 min, t_R (minor) = 21.24 min. The authentic racemic sample was prepared with CuCl as the catalyst and tricyclohexylphosphine as the ligand.

Authentic racemic product **2.74**

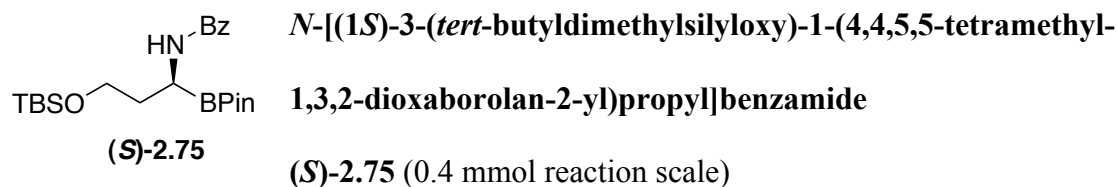


Peak#	Ret. Time (min)	Area (%)
1	18.80	49.94
2	21.19	50.06

Enantioenriched product (*S*)-**2.74**



Peak#	Ret. Time (min)	Area (%)
1	18.78	93.20
2	21.24	6.80



The title compound was synthesized analogous to compound **2.68**. *N*-[1-phenoxy-3-(*tert*-butyldimethylsilyloxy)propyl]benzamide **2.66** (0.154 g, 0.4 mmol) was used in the reaction. The crude product was purified by florisil column chromatography (dichloromethane: hexanes: ethyl acetate = 2:1:0.3 to 2:1:0.5) to afford the title compound as a white solid (0.124 g, 74%, 94:6 er).

^1H -NMR (600 MHz, CDCl_3) δ 8.33 (s, 1H), 7.77 (app d, $J = 7.8$ Hz, 2H), 7.57 (app td, $J = 7.2, 0.6$ Hz, 1H), 7.44 (t, $J = 7.8$ Hz, 2H), 3.99 (dt, $J = 9.6, 3.6$ Hz, 1H), 3.87 – 3.78 (m, 1H), 2.92 – 2.84 (m, 1H), 1.83 – 1.76 (m, 2H), 1.254 (s, 6H), 1.246 (s, 6H), 0.90 (s, 9H), 0.11 (s, 3H), 0.07 (s, 3H).

^{13}C -NMR (151 MHz, CDCl_3) δ 173.26, 136.01, 131.35, 130.51, 129.92, 82.86, 69.13, 49.73, 35.37, 28.66, 27.99, 27.72, 20.98, -2.64, -2.72.

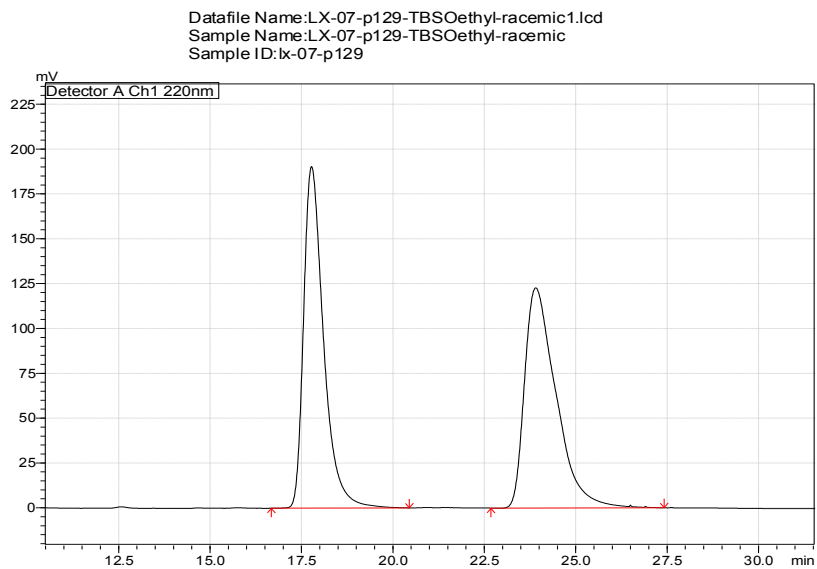
FTIR (neat): 3192, 3072, 2955, 2928, 2856, 1609, 1576, 1527, 1489, 1362, 1250, 1154, 1092, 1074, 1026, 833, 772, 706, 634, 579 cm^{-1} .

HSMS (DART+) calcd for $\text{C}_{22}\text{H}_{39}\text{BNO}_4\text{Si}$ ($[\text{M}+\text{H}]^+$): 420.2741, found: 420.2742.

Melting point: 104-106 $^\circ\text{C}$. $[\alpha]_{\text{D}}^{20} = +30.9$ ($c = 0.46$, THF) for 94:6 er.

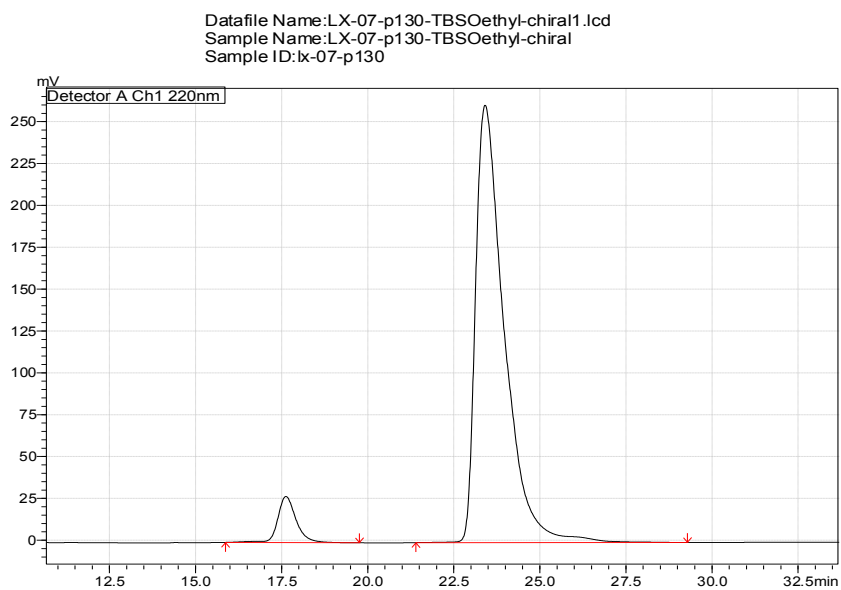
HPLC (Chiralpak® AZ-H column, hexanes: isopropanol = 99:1, 0.5 mL/min, 220 nm) t_{R} (Major) = 23.41 min, t_{R} (minor) = 17.63 min. The authentic racemic sample was prepared with CuCl as the catalyst and tricyclohexylphosphine as the ligand.

Authentic racemic product **2.75**

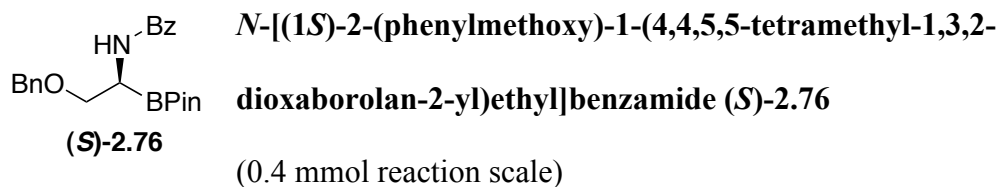


Peak#	Ret. Time (min)	Area (%)
1	17.78	49.62
2	23.91	50.38

Enantioenriched product (*S*)-**2.75**



Peak#	Ret. Time (min)	Area (%)
1	17.63	6.38
2	23.41	93.62



The title compound was synthesized analogous to compound **2.68**. *N*-(1-phenoxy-2-(phenylmethoxy)ethyl]benzamide **2.67** (0.139 g, 0.4 mmol) was used in the reaction. The crude product was purified by florisil column chromatography (dichloromethane: hexanes: ethyl acetate = 2.5:1:0.5 to 2.5:1:0.8) to afford the title compound as a white solid (0.0487 g, 32% yield, 79:21 er).

¹H-NMR (600 MHz, CDCl₃) δ 7.81 – 7.77 (m, 2H), 7.62 – 7.56 (overlapped peaks, m, 2H), 7.48 – 7.44 (m, 2H), 7.37 – 7.26 (m, 5H), 4.57 (d, *J* = 11.4 Hz, 1H), 4.49 (d, *J* = 11.4 Hz, 1H), 3.77 (dd, *J* = 10.2, 3.6 Hz, 1H), 3.63 – 3.60 (m, 1H), 3.17 – 3.11 (m, 1H), 1.24 (s, 12H).

¹³C-NMR (151 MHz, CDCl₃) δ 171.82, 138.37, 133.76, 128.83, 128.46, 128.04, 127.85, 127.72, 126.74, 80.32, 73.06, 72.38, 46.07, 25.26, 24.93.

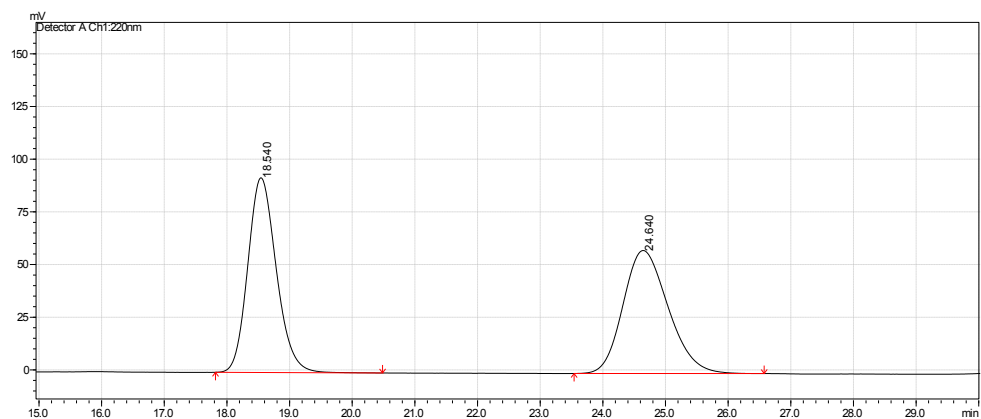
FTIR (neat): 3387, 3057, 2962, 2923, 1600, 1573, 1523, 1488, 1361, 1191, 1156, 1108, 1066, 1017, 755, 710, 688, 628, 582, 460 cm⁻¹.

HSMS (DART+) calcd for C₂₂H₂₉BNO₄ ([M+H]⁺): 382.2190, found: 382.2171.

Melting point: >180 °C (start decomposing). [α]_D²⁰ = +26.7 (c = 0.33, THF) for 79:21 er.

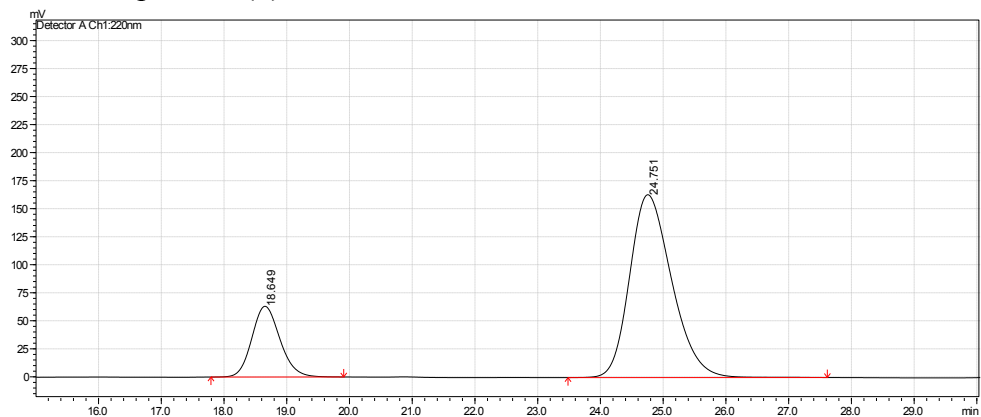
HPLC (Chiralpak® AD-H column, hexanes: isopropanol = 96:4, 0.5 mL/min, 220 nm) t_R (Major) = 24.75 min, t_R (minor) = 18.65 min. The authentic racemic sample was prepared with CuCl as the catalyst and tricyclohexylphosphine as the ligand.

Authentic racemic product **2.76**



Peak#	Ret. Time (min)	Area (%)
1	18.54	50.01
2	24.64	49.99

Enantioenriched product (*S*)-**2.76**



Peak#	Ret. Time (min)	Area (%)
1	18.65	20.58
2	24.75	79.42

Single crystal x-ray data of enantioenriched (*S*)-2.54

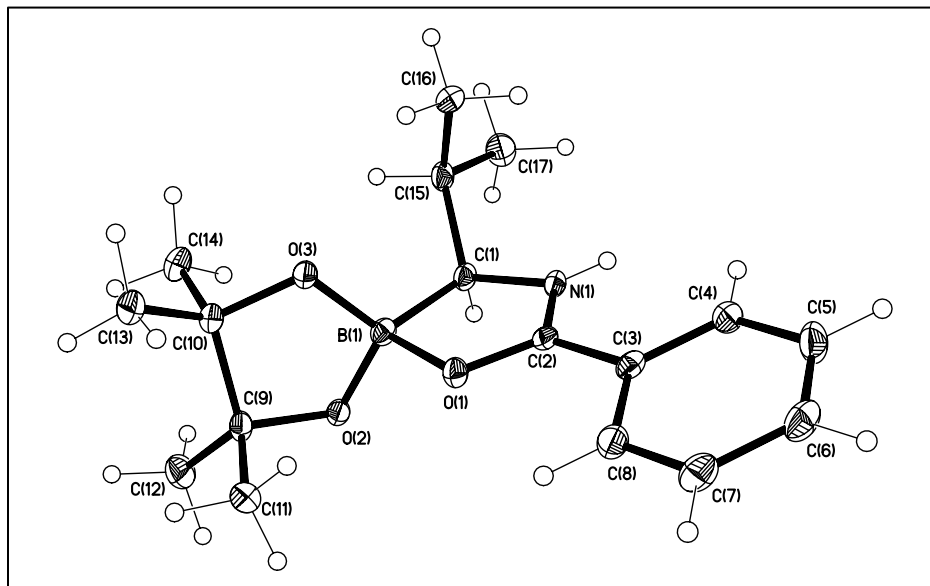


Table 1. Crystal data and structure refinement for $C_{17}H_{26}BNO_3 \cdot CH_2Cl_2$.

Identification code	$C_{17}H_{26}BNO_3 \cdot CH_2Cl_2$	
Empirical formula	$C_{18}H_{28}BCl_2NO_3$	
Formula weight	388.12	
Temperature	100(2) K	
Wavelength	1.54178 \approx	
Crystal system	Orthorhombic	
Space group	$P2_12_12_1$	
Unit cell dimensions	$a = 9.3865(7) \approx$	$a = 90^\circ$.
	$b = 10.8411(8) \approx$	$b = 90^\circ$.
	$c = 20.0415(14) \approx$	$c = 90^\circ$.
Volume	$2039.4(3) \approx^3$	

Z	4
Density (calculated)	1.264 Mg/m ³
Absorption coefficient	2.990 mm ⁻¹
F(000)	824
Crystal size	0.600 x 0.400 x 0.250 mm ³
Theta range for data collection	6.461 to 66.755°.
Index ranges	-10 ≤ h ≤ 11, -12 ≤ k ≤ 12, -23 ≤ l ≤ 23
Reflections collected	16822
Independent reflections	3549 [R(int) = 0.0307]
Completeness to theta = 66.750°	99.5 %
Absorption correction	Semi-empirical from equivalents
Max. and min. transmission	0.7528 and 0.4816
Refinement method	Full-matrix least-squares on F ²
Data / restraints / parameters	3549 / 3 / 243
Goodness-of-fit on F ²	1.071
Final R indices [I > 2σ(I)]	R1 = 0.0245, wR2 = 0.0629
R indices (all data)	R1 = 0.0246, wR2 = 0.0630
Absolute structure parameter	0.045(3)
Extinction coefficient	na
Largest diff. peak and hole	0.230 and -0.183 e.Å ⁻³

Table 2. Atomic coordinates (× 10⁴) and equivalent isotropic displacement parameters (≈ × 10³) for C₁₇H₂₆BNO₃•CH₂Cl₂. U(eq) is defined as one third of the trace of the orthogonalized U^{ij} tensor.

	x	y	z	U(eq)
O(1)	4562(1)	4639(1)	5008(1)	14(1)
O(2)	2657(1)	3846(1)	4251(1)	14(1)
O(3)	4702(1)	4694(1)	3792(1)	15(1)
N(1)	5715(2)	2879(1)	5130(1)	13(1)
B(1)	4186(2)	3932(2)	4325(1)	14(1)
C(1)	4990(2)	2618(2)	4489(1)	14(1)
C(2)	5388(2)	3974(2)	5367(1)	13(1)
C(3)	5899(2)	4476(2)	6010(1)	14(1)
C(4)	6952(2)	3889(2)	6375(1)	18(1)
C(5)	7435(2)	4422(2)	6965(1)	24(1)
C(6)	6862(2)	5526(2)	7187(1)	23(1)
C(7)	5801(2)	6099(2)	6825(1)	22(1)
C(8)	5319(2)	5580(2)	6234(1)	18(1)
C(9)	2218(2)	4869(2)	3832(1)	16(1)
C(10)	3532(2)	5019(2)	3363(1)	17(1)
C(11)	1983(2)	5998(2)	4273(1)	19(1)
C(12)	835(2)	4527(2)	3484(1)	23(1)
C(13)	3748(2)	6325(2)	3101(1)	23(1)
C(14)	3514(2)	4111(2)	2780(1)	23(1)
C(15)	6002(2)	2113(2)	3951(1)	17(1)

C(16)	7378(2)	2854(2)	3901(1)	22(1)
C(17)	6325(2)	736(2)	4046(1)	23(1)
C(1S)	6856(3)	6711(2)	4378(1)	28(1)
Cl(1S)	8143(1)	6042(1)	4908(1)	32(1)
Cl(2S)	7638(1)	7018(2)	3584(1)	45(1)
Cl(2Y)	7204(7)	7513(6)	3709(3)	34(2)

Table 3. Bond lengths [\approx] and angles [∞] for $C_{17}H_{26}BNO_3 \cdot CH_2Cl_2$.

O(1)-C(2)	1.281(2)
O(1)-B(1)	1.607(2)
O(2)-B(1)	1.446(2)
O(2)-C(9)	1.451(2)
O(3)-B(1)	1.435(2)
O(3)-C(10)	1.440(2)
N(1)-C(2)	1.315(3)
N(1)-C(1)	1.483(2)
N(1)-H(1N)	0.826(19)
B(1)-C(1)	1.645(3)
C(1)-C(15)	1.537(2)
C(1)-H(1)	0.976(19)
C(2)-C(3)	1.478(2)
C(3)-C(4)	1.386(3)

C(3)-C(8)	1.389(3)
C(4)-C(5)	1.391(3)
C(4)-H(4)	0.9500
C(5)-C(6)	1.385(3)
C(5)-H(5)	0.9500
C(6)-C(7)	1.380(3)
C(6)-H(6)	0.9500
C(7)-C(8)	1.388(3)
C(7)-H(7)	0.9500
C(8)-H(8)	0.9500
C(9)-C(12)	1.520(3)
C(9)-C(11)	1.525(3)
C(9)-C(10)	1.559(3)
C(10)-C(13)	1.524(3)
C(10)-C(14)	1.528(3)
C(11)-H(11A)	0.9800
C(11)-H(11B)	0.9800
C(11)-H(11C)	0.9800
C(12)-H(12A)	0.9800
C(12)-H(12B)	0.9800
C(12)-H(12C)	0.9800
C(13)-H(13A)	0.9800
C(13)-H(13B)	0.9800

C(13)-H(13C)	0.9800
C(14)-H(14A)	0.9800
C(14)-H(14B)	0.9800
C(14)-H(14C)	0.9800
C(15)-C(16)	1.524(3)
C(15)-C(17)	1.536(3)
C(15)-H(15)	1.0000
C(16)-H(16A)	0.9800
C(16)-H(16B)	0.9800
C(16)-H(16C)	0.9800
C(17)-H(17A)	0.9800
C(17)-H(17B)	0.9800
C(17)-H(17C)	0.9800
C(1S)-Cl(2Y)	1.631(5)
C(1S)-Cl(1S)	1.765(2)
C(1S)-Cl(2S)	1.785(2)
C(1S)-H(1S1)	0.9900
C(1S)-H(1S2)	0.9900
C(2)-O(1)-B(1)	110.06(14)
B(1)-O(2)-C(9)	106.96(14)
B(1)-O(3)-C(10)	109.14(14)
C(2)-N(1)-C(1)	112.22(15)

C(2)-N(1)-H(1N)	123.7(16)
C(1)-N(1)-H(1N)	124.0(16)
O(3)-B(1)-O(2)	107.21(15)
O(3)-B(1)-O(1)	106.52(14)
O(2)-B(1)-O(1)	109.66(14)
O(3)-B(1)-C(1)	119.45(15)
O(2)-B(1)-C(1)	114.82(16)
O(1)-B(1)-C(1)	98.25(13)
N(1)-C(1)-C(15)	113.08(14)
N(1)-C(1)-B(1)	102.59(14)
C(15)-C(1)-B(1)	116.92(14)
N(1)-C(1)-H(1)	108.2(13)
C(15)-C(1)-H(1)	107.1(13)
B(1)-C(1)-H(1)	108.6(13)
O(1)-C(2)-N(1)	116.51(15)
O(1)-C(2)-C(3)	118.64(17)
N(1)-C(2)-C(3)	124.84(16)
C(4)-C(3)-C(8)	120.30(17)
C(4)-C(3)-C(2)	121.52(17)
C(8)-C(3)-C(2)	118.16(17)
C(3)-C(4)-C(5)	119.36(18)
C(3)-C(4)-H(4)	120.3
C(5)-C(4)-H(4)	120.3

C(6)-C(5)-C(4)	120.37(19)
C(6)-C(5)-H(5)	119.8
C(4)-C(5)-H(5)	119.8
C(7)-C(6)-C(5)	120.04(18)
C(7)-C(6)-H(6)	120.0
C(5)-C(6)-H(6)	120.0
C(6)-C(7)-C(8)	120.05(18)
C(6)-C(7)-H(7)	120.0
C(8)-C(7)-H(7)	120.0
C(7)-C(8)-C(3)	119.87(18)
C(7)-C(8)-H(8)	120.1
C(3)-C(8)-H(8)	120.1
O(2)-C(9)-C(12)	108.75(15)
O(2)-C(9)-C(11)	108.61(14)
C(12)-C(9)-C(11)	109.75(16)
O(2)-C(9)-C(10)	101.77(14)
C(12)-C(9)-C(10)	115.08(15)
C(11)-C(9)-C(10)	112.38(16)
O(3)-C(10)-C(13)	109.33(16)
O(3)-C(10)-C(14)	107.94(15)
C(13)-C(10)-C(14)	109.68(15)
O(3)-C(10)-C(9)	102.59(14)
C(13)-C(10)-C(9)	114.18(16)

C(14)-C(10)-C(9)	112.70(16)
C(9)-C(11)-H(11A)	109.5
C(9)-C(11)-H(11B)	109.5
H(11A)-C(11)-H(11B)	109.5
C(9)-C(11)-H(11C)	109.5
H(11A)-C(11)-H(11C)	109.5
H(11B)-C(11)-H(11C)	109.5
C(9)-C(12)-H(12A)	109.5
C(9)-C(12)-H(12B)	109.5
H(12A)-C(12)-H(12B)	109.5
C(9)-C(12)-H(12C)	109.5
H(12A)-C(12)-H(12C)	109.5
H(12B)-C(12)-H(12C)	109.5
C(10)-C(13)-H(13A)	109.5
C(10)-C(13)-H(13B)	109.5
H(13A)-C(13)-H(13B)	109.5
C(10)-C(13)-H(13C)	109.5
H(13A)-C(13)-H(13C)	109.5
H(13B)-C(13)-H(13C)	109.5
C(10)-C(14)-H(14A)	109.5
C(10)-C(14)-H(14B)	109.5
H(14A)-C(14)-H(14B)	109.5
C(10)-C(14)-H(14C)	109.5

H(14A)-C(14)-H(14C)	109.5
H(14B)-C(14)-H(14C)	109.5
C(16)-C(15)-C(17)	110.70(16)
C(16)-C(15)-C(1)	112.45(15)
C(17)-C(15)-C(1)	112.39(16)
C(16)-C(15)-H(15)	107.0
C(17)-C(15)-H(15)	107.0
C(1)-C(15)-H(15)	107.0
C(15)-C(16)-H(16A)	109.5
C(15)-C(16)-H(16B)	109.5
H(16A)-C(16)-H(16B)	109.5
C(15)-C(16)-H(16C)	109.5
H(16A)-C(16)-H(16C)	109.5
H(16B)-C(16)-H(16C)	109.5
C(15)-C(17)-H(17A)	109.5
C(15)-C(17)-H(17B)	109.5
H(17A)-C(17)-H(17B)	109.5
C(15)-C(17)-H(17C)	109.5
H(17A)-C(17)-H(17C)	109.5
H(17B)-C(17)-H(17C)	109.5
Cl(2Y)-C(1S)-Cl(1S)	125.2(3)
Cl(1S)-C(1S)-Cl(2S)	109.37(14)
Cl(1S)-C(1S)-H(1S1)	109.8

Cl(2S)-C(1S)-H(1S1)	109.8
Cl(1S)-C(1S)-H(1S2)	109.8
Cl(2S)-C(1S)-H(1S2)	109.8
H(1S1)-C(1S)-H(1S2)	108.2

Symmetry transformations used to generate equivalent atoms:

Table 4. Anisotropic displacement parameters ($\approx^2 \times 10^3$) for $C_{17}H_{26}BNO_3 \bullet CH_2Cl_2$. The anisotropic displacement factor exponent takes the form: $-2p^2 [h^2 a^{*2} U^{11} + \dots + 2 h k a^* b^* U^{12}]$

	U^{11}	U^{22}	U^{33}	U^{23}	U^{13}	U^{12}
O(1)	16(1)	15(1)	12(1)	0(1)	-2(1)	0(1)
O(2)	14(1)	16(1)	12(1)	2(1)	0(1)	-1(1)
O(3)	13(1)	21(1)	13(1)	4(1)	-1(1)	0(1)
N(1)	15(1)	16(1)	9(1)	1(1)	-1(1)	2(1)
B(1)	15(1)	15(1)	11(1)	-2(1)	-1(1)	-1(1)
C(1)	15(1)	17(1)	10(1)	0(1)	-2(1)	-1(1)
C(2)	11(1)	17(1)	11(1)	2(1)	2(1)	-1(1)
C(3)	15(1)	16(1)	11(1)	0(1)	2(1)	-4(1)
C(4)	19(1)	21(1)	14(1)	-3(1)	-1(1)	3(1)
C(5)	26(1)	29(1)	16(1)	-2(1)	-8(1)	5(1)

C(6)	28(1)	27(1)	14(1)	-5(1)	-1(1)	-5(1)
C(7)	29(1)	19(1)	17(1)	-4(1)	2(1)	-1(1)
C(8)	20(1)	19(1)	15(1)	1(1)	0(1)	1(1)
C(9)	17(1)	18(1)	14(1)	5(1)	-2(1)	1(1)
C(10)	17(1)	22(1)	12(1)	3(1)	-1(1)	2(1)
C(11)	18(1)	20(1)	19(1)	2(1)	1(1)	4(1)
C(12)	17(1)	30(1)	23(1)	3(1)	-5(1)	1(1)
C(13)	22(1)	26(1)	21(1)	10(1)	2(1)	2(1)
C(14)	27(1)	30(1)	12(1)	2(1)	-1(1)	1(1)
C(15)	20(1)	22(1)	10(1)	-1(1)	-3(1)	5(1)
C(16)	20(1)	31(1)	14(1)	3(1)	4(1)	6(1)
C(17)	28(1)	23(1)	19(1)	-5(1)	-2(1)	8(1)
C(1S)	31(1)	28(1)	26(1)	-4(1)	0(1)	-4(1)
Cl(1S)	26(1)	39(1)	31(1)	3(1)	3(1)	1(1)
Cl(2S)	43(1)	66(1)	26(1)	12(1)	-1(1)	-28(1)

Table 5. Hydrogen coordinates ($\times 10^4$) and isotropic displacement parameters ($\approx \times 10^{-3}$) for $C_{17}H_{26}BNO_3 \cdot CH_2Cl_2$.

	x	y	z	U(eq)
H(1N)	6230(20)	2379(19)	5328(10)	16
H(1)	4270(20)	1988(19)	4568(11)	17

H(4)	7341	3129	6225	22
H(5)	8162	4027	7216	28
H(6)	7199	5887	7589	27
H(7)	5399	6850	6981	26
H(8)	4595	5979	5982	22
H(11A)	1275	5804	4617	28
H(11B)	1638	6685	4000	28
H(11C)	2883	6230	4486	28
H(12A)	950	3733	3257	35
H(12B)	594	5165	3156	35
H(12C)	69	4464	3814	35
H(13A)	3867	6893	3478	34
H(13B)	2916	6573	2838	34
H(13C)	4601	6351	2819	34
H(14A)	4441	4123	2555	34
H(14B)	2768	4349	2463	34
H(14C)	3322	3278	2947	34
H(15)	5502	2198	3513	20
H(16A)	7151	3722	3816	32
H(16B)	7961	2531	3535	32
H(16C)	7908	2785	4321	32
H(17A)	6913	441	3675	35
H(17B)	5429	271	4057	35

H(17C)	6838	615	4467	35
H(1S1)	6500	7489	4577	34
H(1S2)	6039	6142	4325	34

Table 6. Torsion angles [$^{\circ}$] for $C_{17}H_{26}BNO_3 \cdot CH_2Cl_2$.

C(10)-O(3)-B(1)-O(2)	-3.65(19)
C(10)-O(3)-B(1)-O(1)	-120.99(15)
C(10)-O(3)-B(1)-C(1)	129.16(16)
C(9)-O(2)-B(1)-O(3)	-19.44(18)
C(9)-O(2)-B(1)-O(1)	95.82(15)
C(9)-O(2)-B(1)-C(1)	-154.71(14)
C(2)-O(1)-B(1)-O(3)	-119.32(16)
C(2)-O(1)-B(1)-O(2)	124.98(16)
C(2)-O(1)-B(1)-C(1)	4.83(17)
C(2)-N(1)-C(1)-C(15)	132.08(16)
C(2)-N(1)-C(1)-B(1)	5.25(18)
O(3)-B(1)-C(1)-N(1)	108.78(17)
O(2)-B(1)-C(1)-N(1)	-121.75(15)
O(1)-B(1)-C(1)-N(1)	-5.55(15)
O(3)-B(1)-C(1)-C(15)	-15.5(2)
O(2)-B(1)-C(1)-C(15)	113.92(17)

O(1)-B(1)-C(1)-C(15)	-129.87(15)
B(1)-O(1)-C(2)-N(1)	-2.0(2)
B(1)-O(1)-C(2)-C(3)	178.10(15)
C(1)-N(1)-C(2)-O(1)	-2.3(2)
C(1)-N(1)-C(2)-C(3)	177.54(16)
O(1)-C(2)-C(3)-C(4)	-170.41(16)
N(1)-C(2)-C(3)-C(4)	9.8(3)
O(1)-C(2)-C(3)-C(8)	7.9(2)
N(1)-C(2)-C(3)-C(8)	-171.90(17)
C(8)-C(3)-C(4)-C(5)	-0.7(3)
C(2)-C(3)-C(4)-C(5)	177.59(18)
C(3)-C(4)-C(5)-C(6)	0.5(3)
C(4)-C(5)-C(6)-C(7)	0.3(3)
C(5)-C(6)-C(7)-C(8)	-0.9(3)
C(6)-C(7)-C(8)-C(3)	0.6(3)
C(4)-C(3)-C(8)-C(7)	0.2(3)
C(2)-C(3)-C(8)-C(7)	-178.18(17)
B(1)-O(2)-C(9)-C(12)	154.45(15)
B(1)-O(2)-C(9)-C(11)	-86.14(17)
B(1)-O(2)-C(9)-C(10)	32.58(17)
B(1)-O(3)-C(10)-C(13)	144.75(16)
B(1)-O(3)-C(10)-C(14)	-95.99(17)
B(1)-O(3)-C(10)-C(9)	23.21(18)

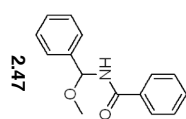
O(2)-C(9)-C(10)-O(3)	-33.82(17)
C(12)-C(9)-C(10)-O(3)	-151.22(16)
C(11)-C(9)-C(10)-O(3)	82.18(17)
O(2)-C(9)-C(10)-C(13)	-151.99(16)
C(12)-C(9)-C(10)-C(13)	90.6(2)
C(11)-C(9)-C(10)-C(13)	-36.0(2)
O(2)-C(9)-C(10)-C(14)	82.00(18)
C(12)-C(9)-C(10)-C(14)	-35.4(2)
C(11)-C(9)-C(10)-C(14)	-162.00(16)
N(1)-C(1)-C(15)-C(16)	-46.7(2)
B(1)-C(1)-C(15)-C(16)	72.1(2)
N(1)-C(1)-C(15)-C(17)	79.0(2)
B(1)-C(1)-C(15)-C(17)	-162.19(16)

Symmetry transformations used to generate equivalent atoms:

Table 7. Hydrogen bonds for C₁₇H₂₆BNO₃•CH₂Cl₂ [\approx and ∞].

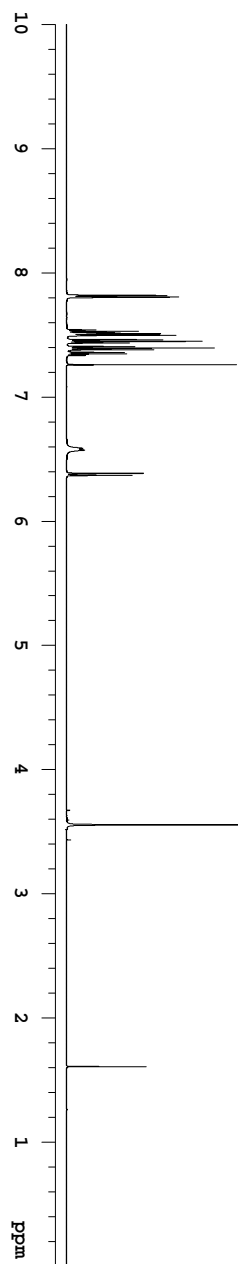
D-H...A	d(D-H)	d(H...A)	d(D...A)	<(DHA)
N(1)-H(1N)...O(2)#1	0.826(19)	2.07(2)	2.890(2)	174(2)

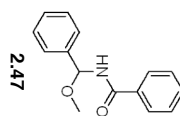
Symmetry transformations used to generate equivalent atoms: #1 x+1/2,-y+1/2,-z+1



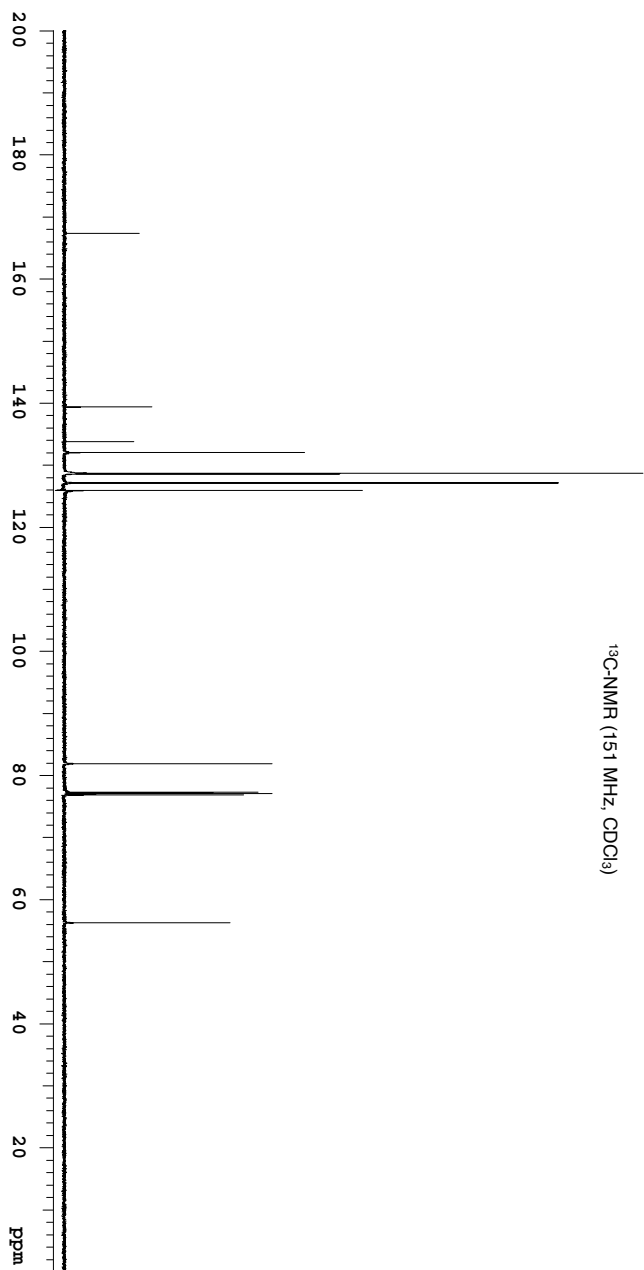
2.47

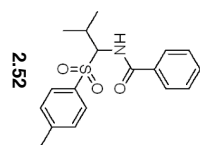
$^1\text{H-NMR}$ (600 MHz, CDCl_3)



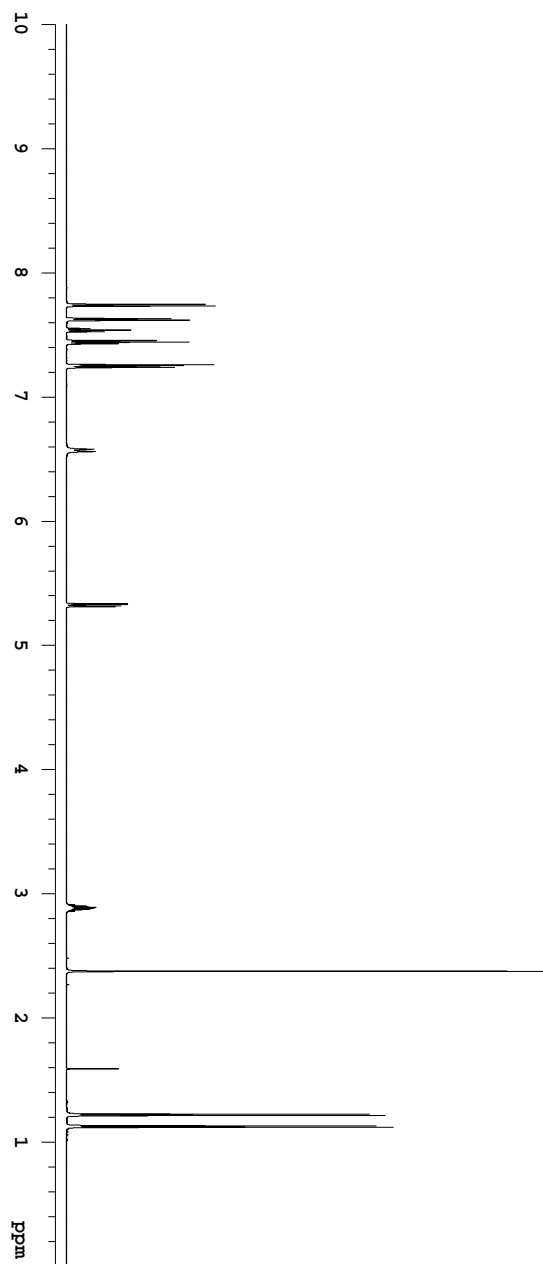


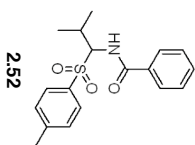
¹³C-NMR (151 MHz, CDCl₃)



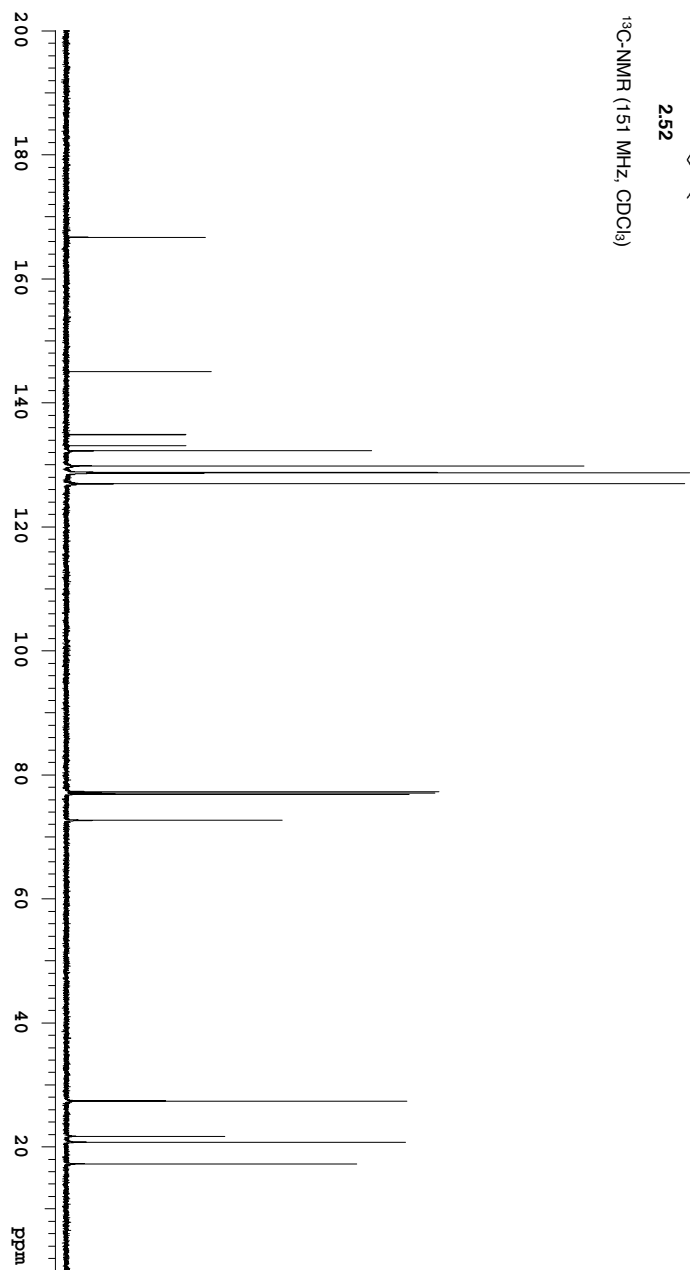


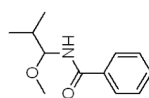
¹H-NMR (600 MHz, CDCl₃)





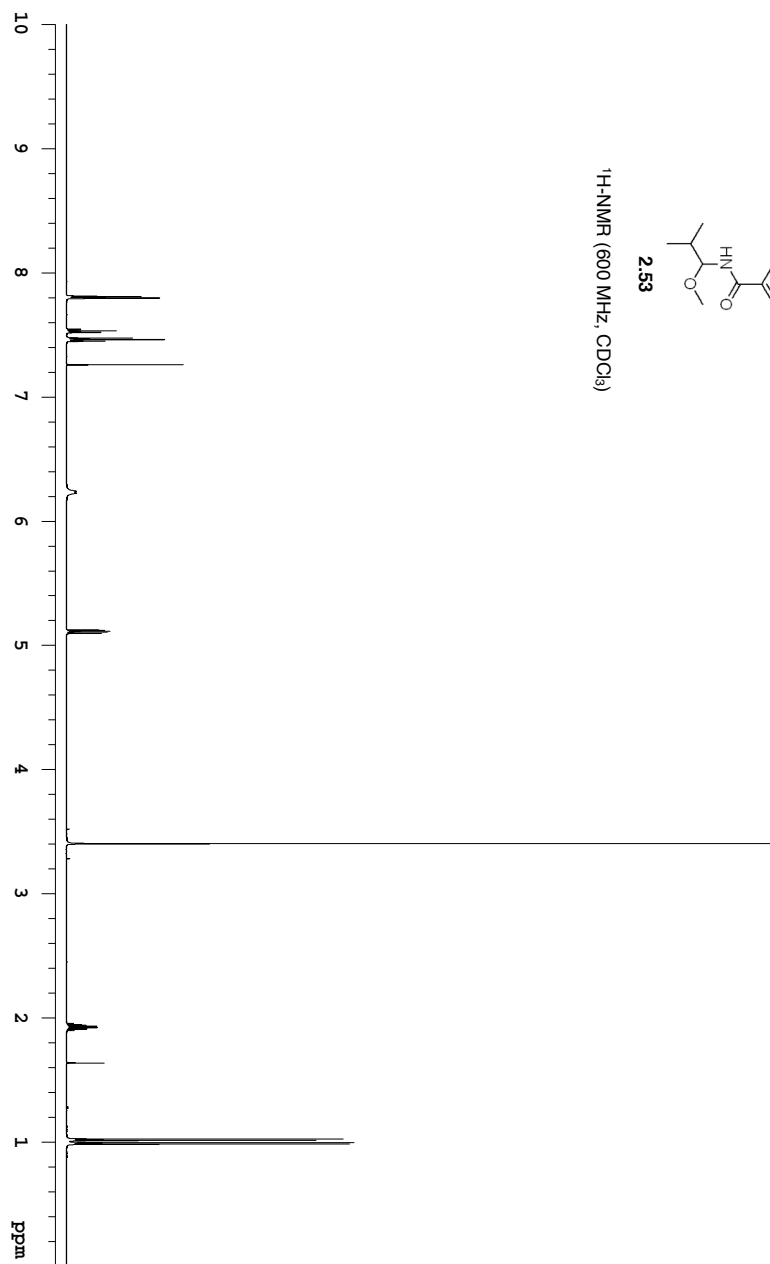
^{13}C -NMR (151 MHz, CDCl_3)

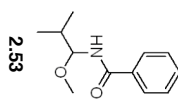




2.53

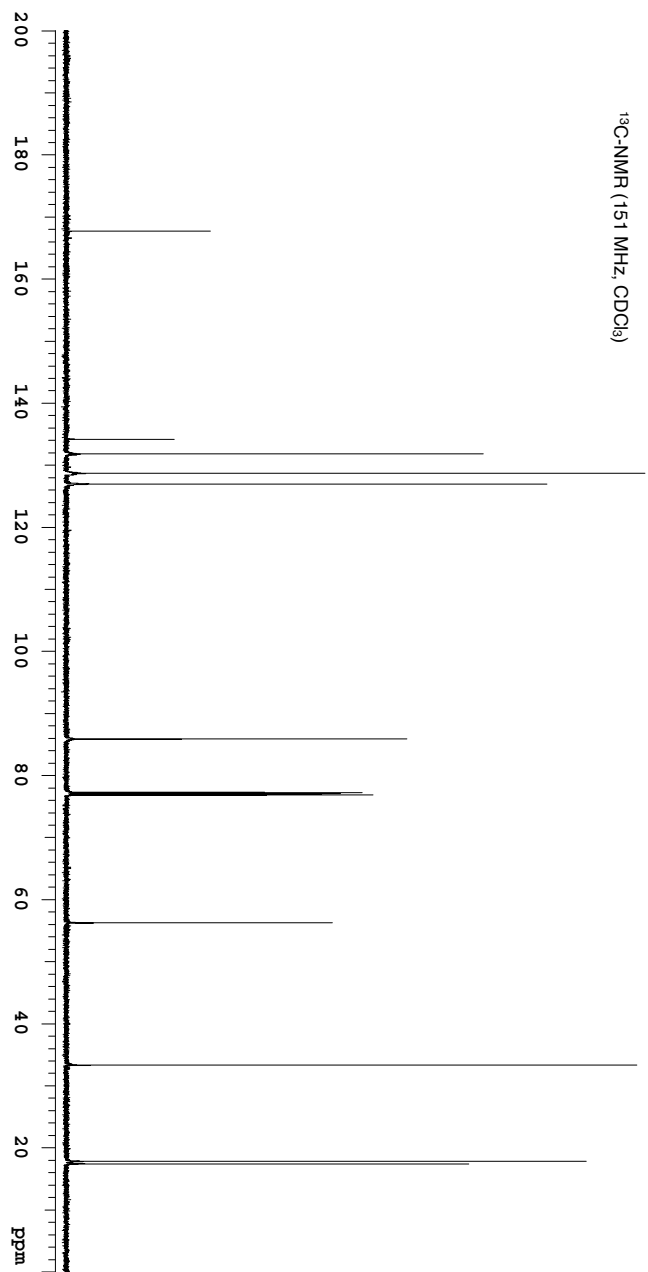
$^1\text{H-NMR}$ (600 MHz, CDCl_3)

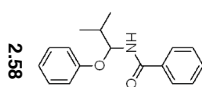




2.53

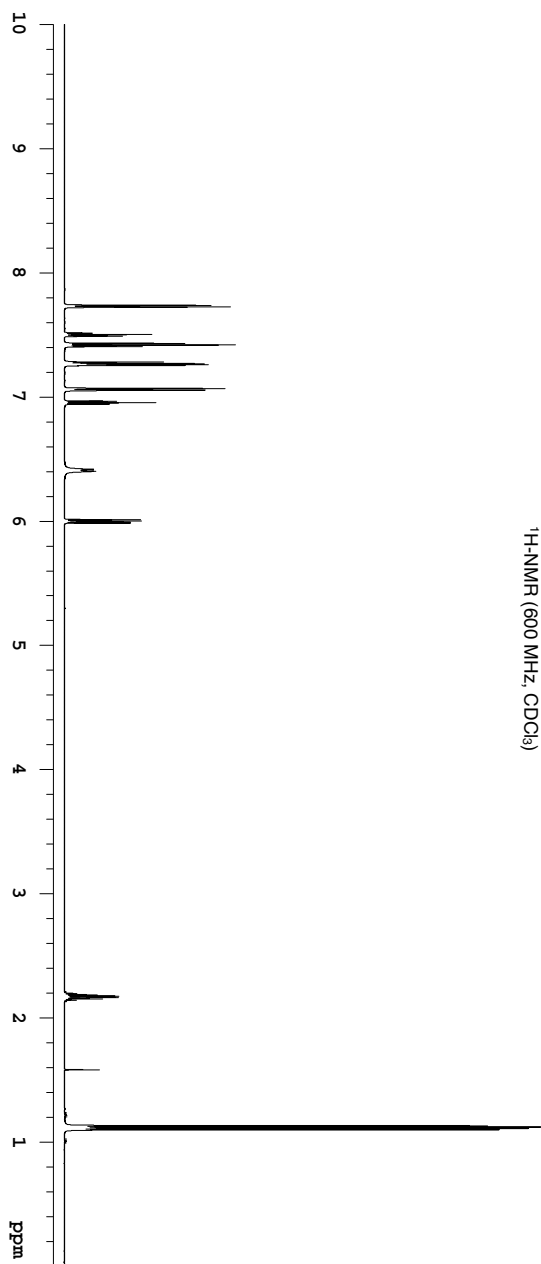
^{13}C -NMR (151 MHz, CDCl_3)

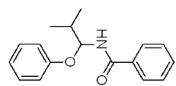




2.58

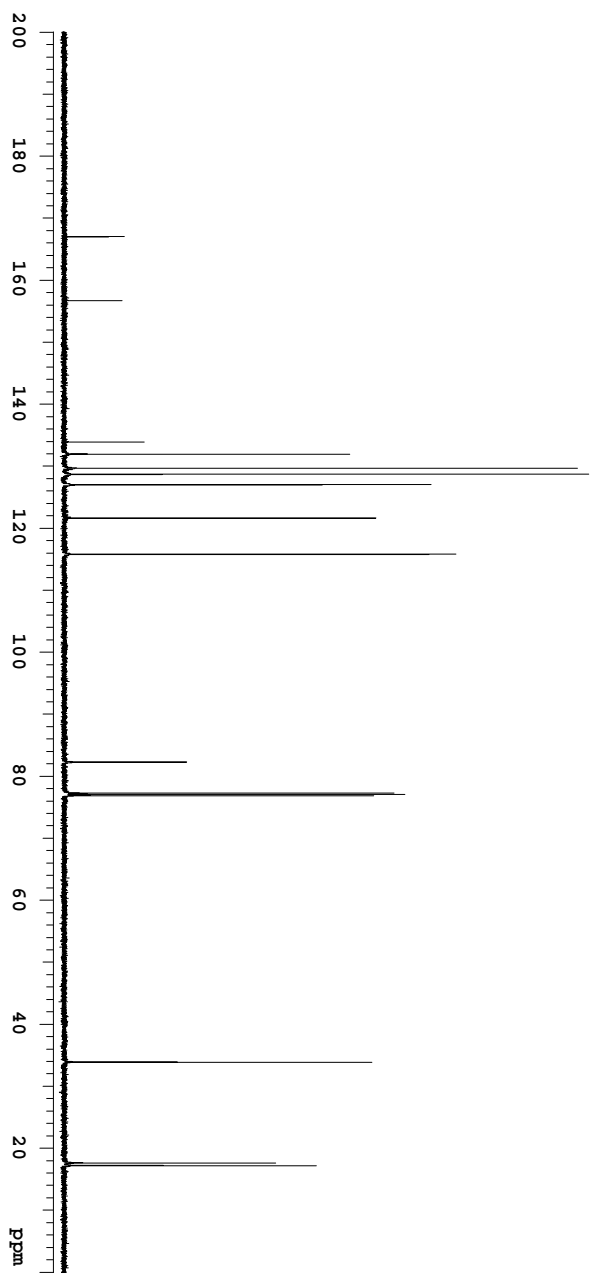
¹H-NMR (600 MHz, CDCl₃)



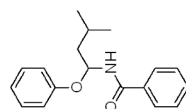


2.58

^{13}C -NMR (151 MHz, CDCl_3)

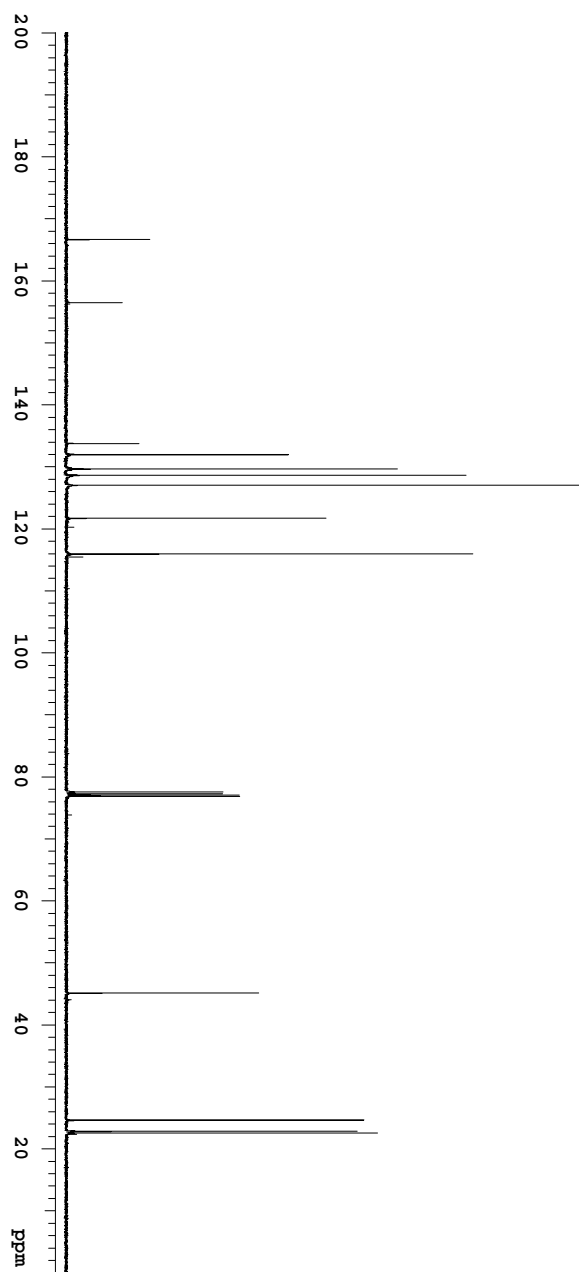


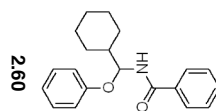




2.59

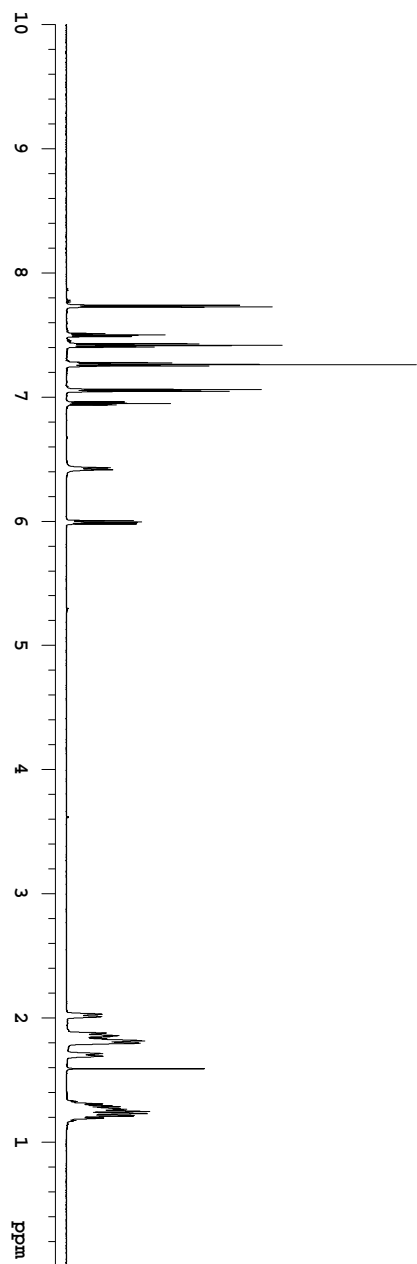
^{13}C -NMR (151 MHz, CDCl_3)

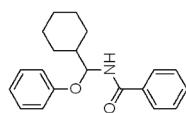




2.60

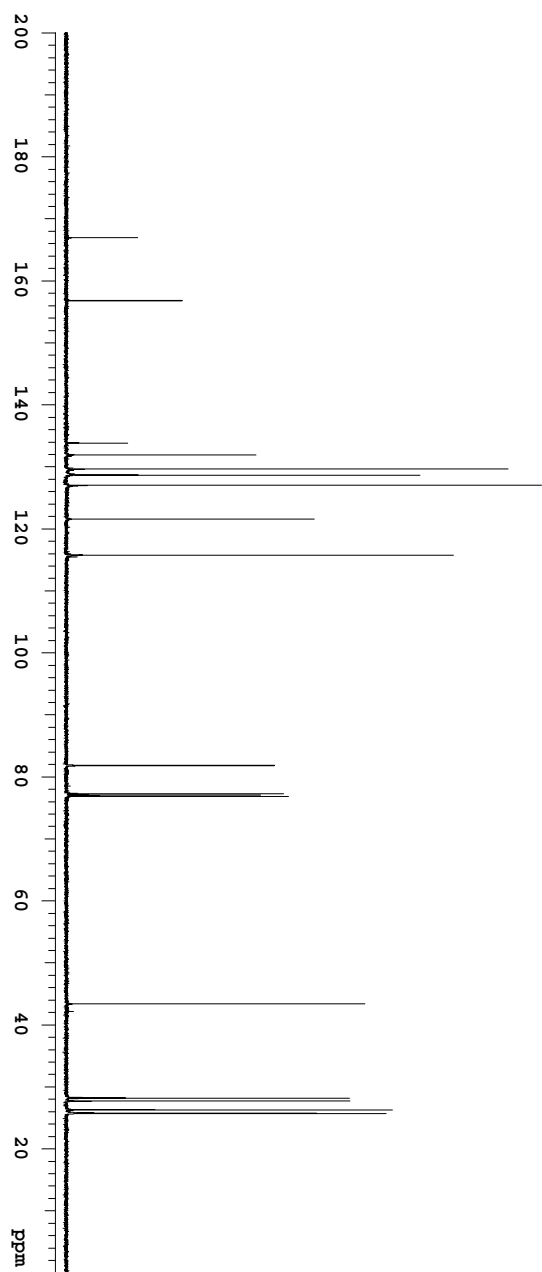
¹H-NMR (600 MHz, CDCl₃)

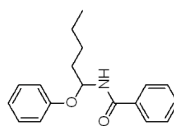




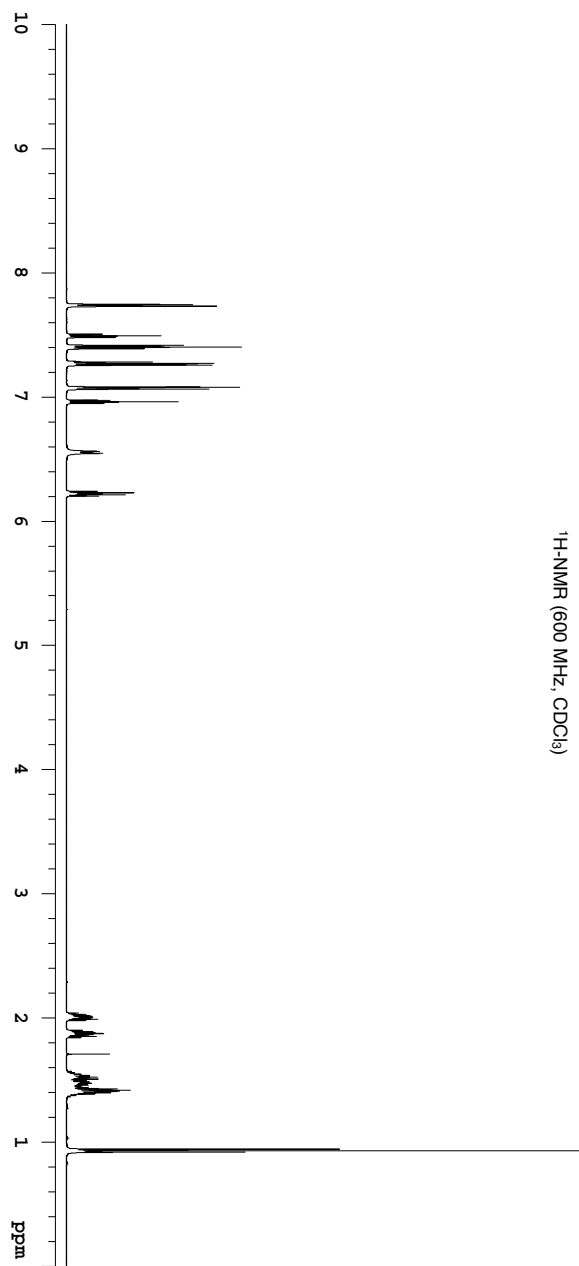
2.60

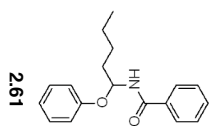
¹³C-NMR (151 MHz, CDCl₃)



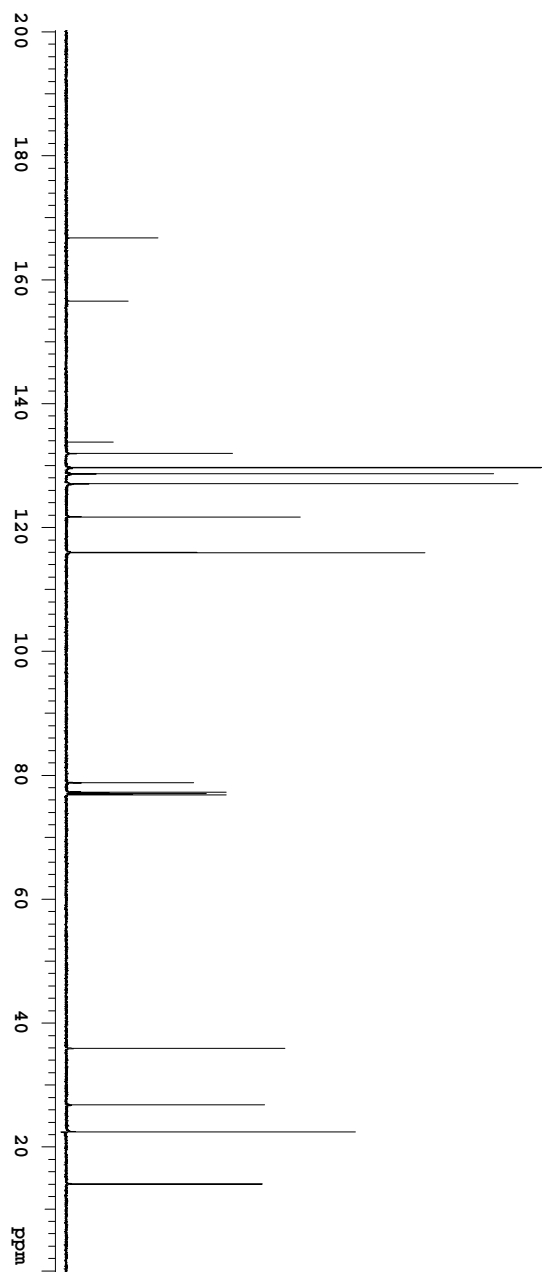


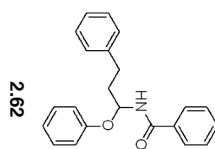
2.61

¹H-NMR (600 MHz, CDCl₃)

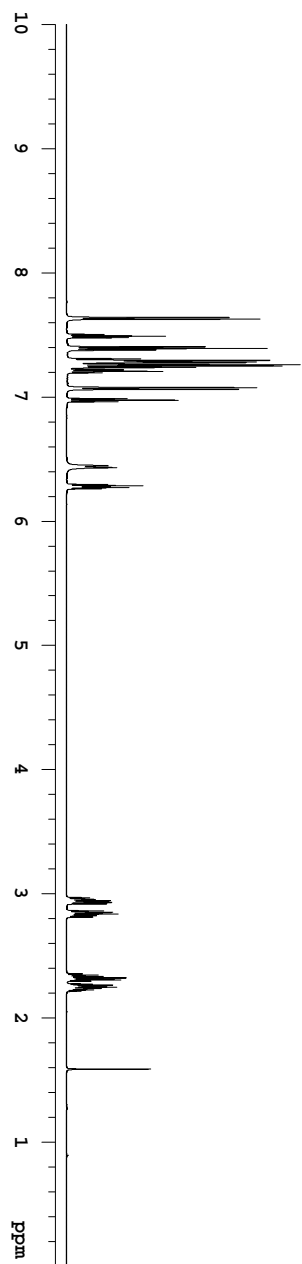


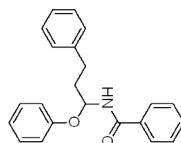
^{13}C -NMR (151 MHz, CDCl_3)





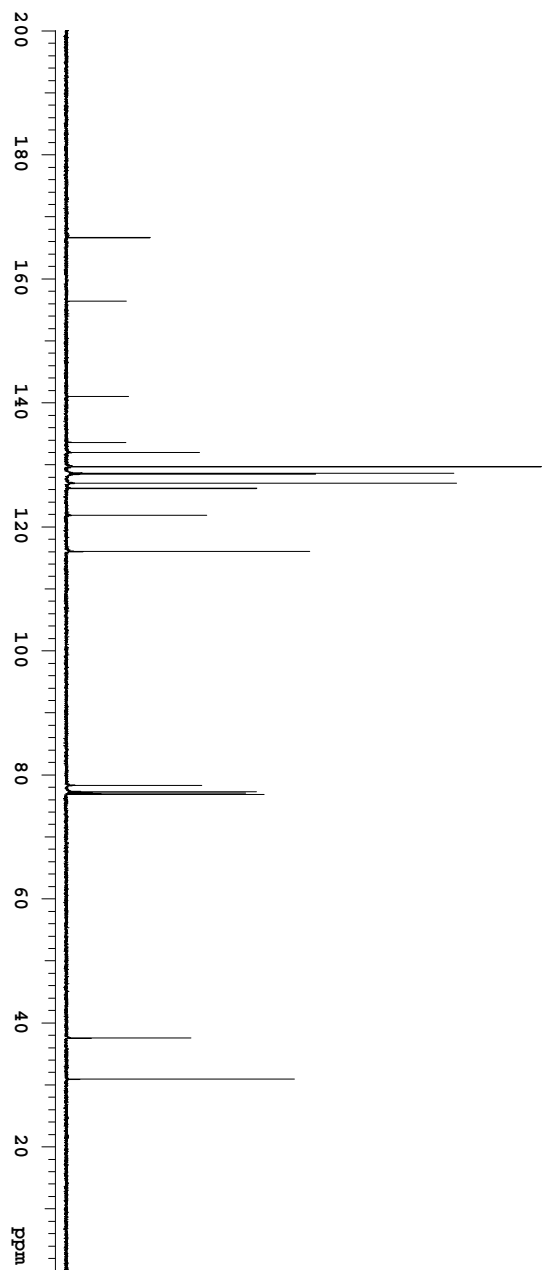
2.62

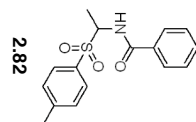
¹H-NMR (600 MHz, CDCl₃)



2.62

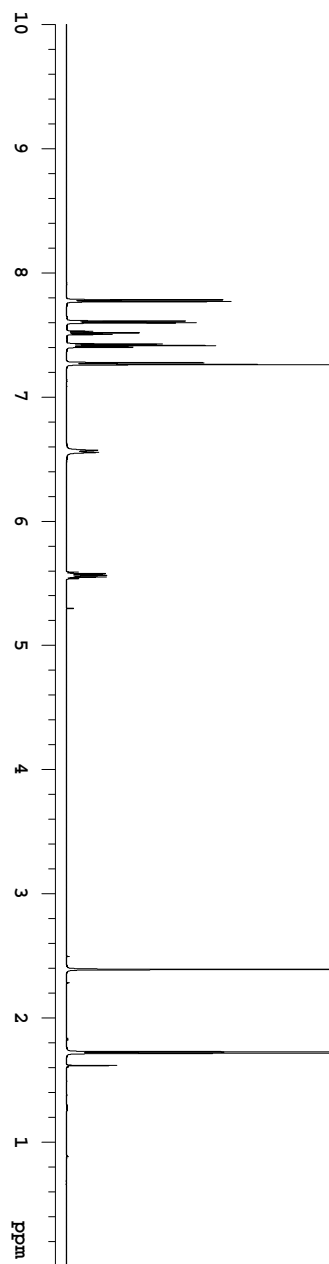
^{13}C -NMR (151 MHz, CDCl_3)

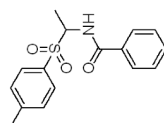




2.82

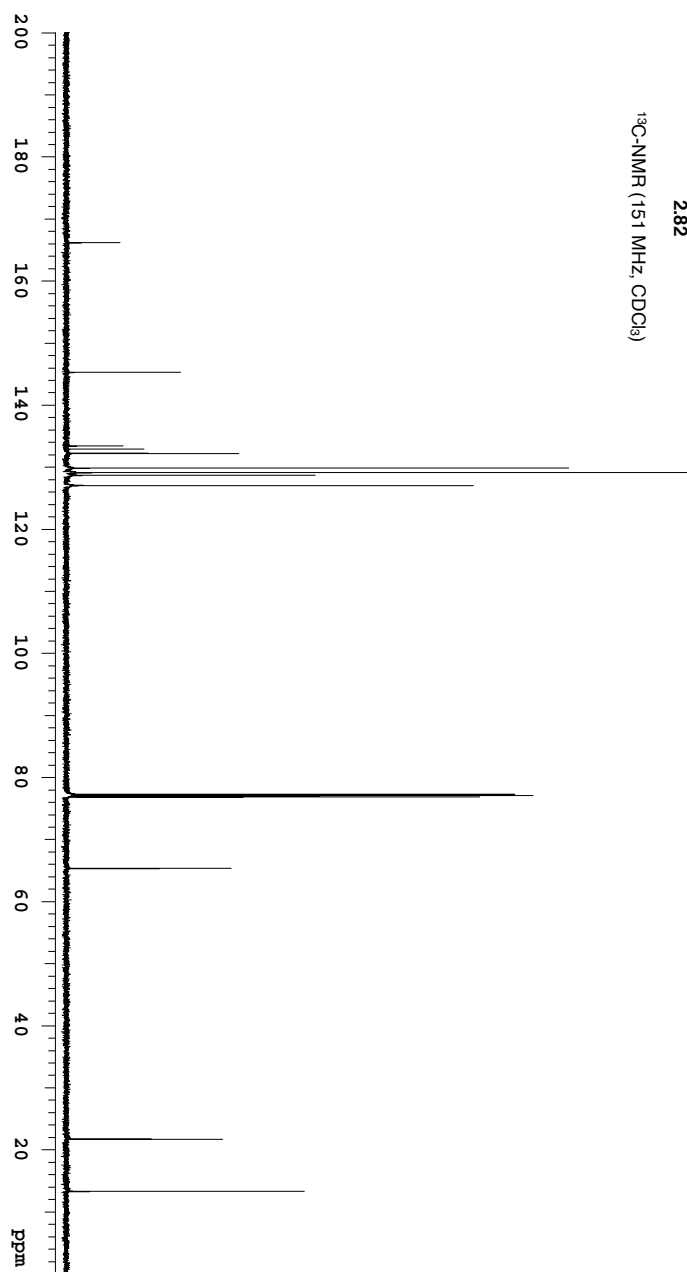
$^1\text{H-NMR}$ (600 MHz, CDCl_3)

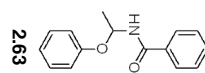




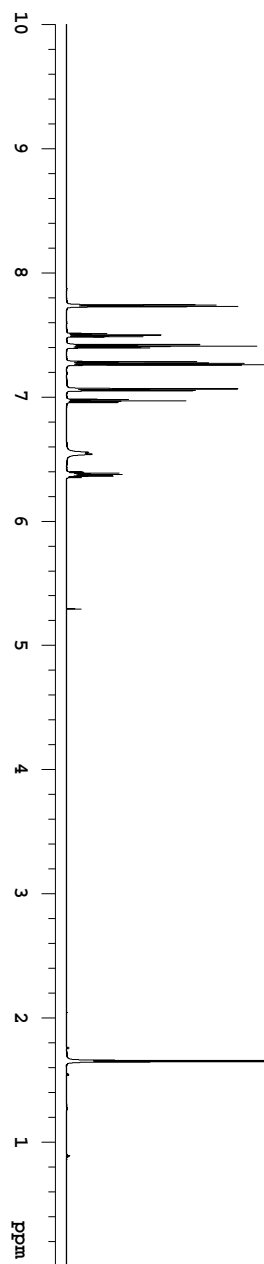
2.82

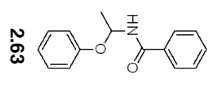
^{13}C -NMR (151 MHz, CDCl_3)



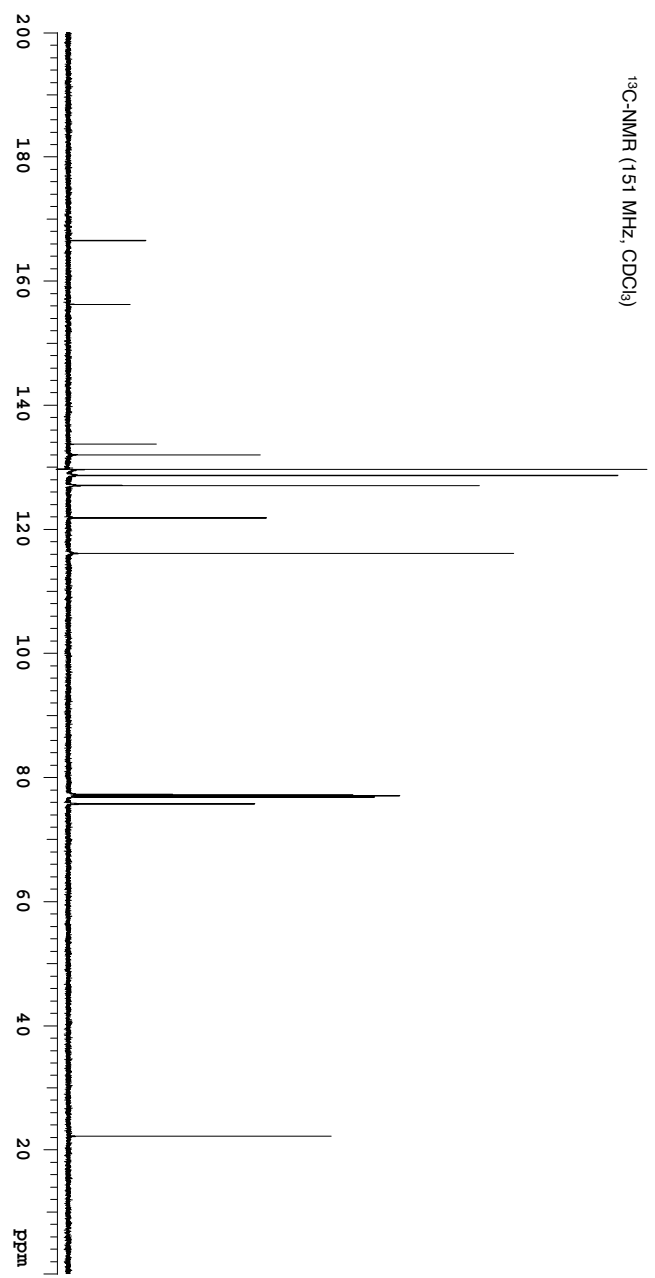


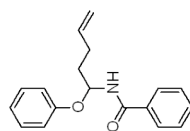
2.63

¹H-NMR (600 MHz, CDCl₃)



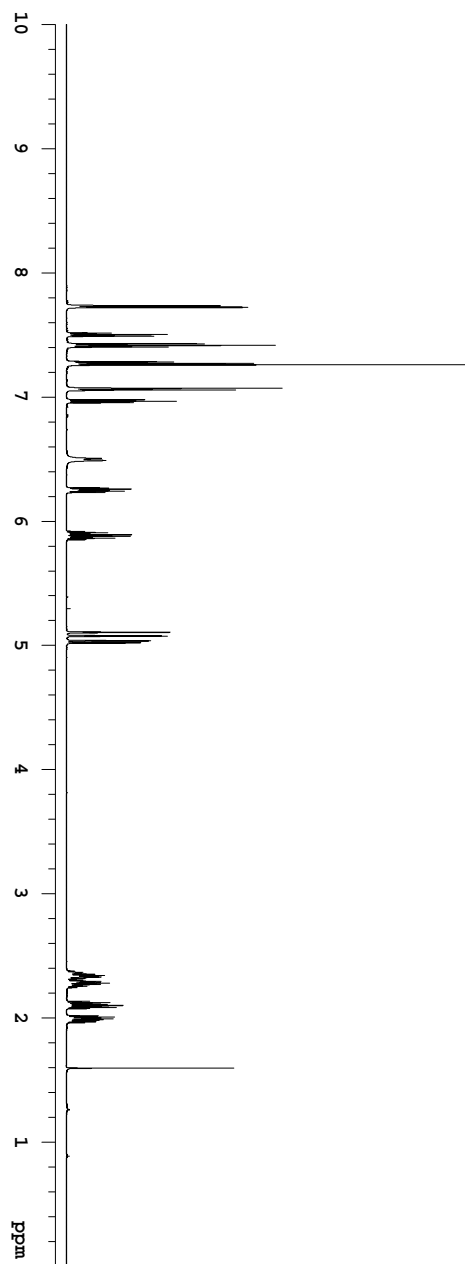
¹³C-NMR (151 MHz, CDCl₃)

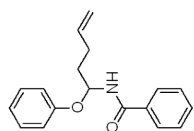




2.64

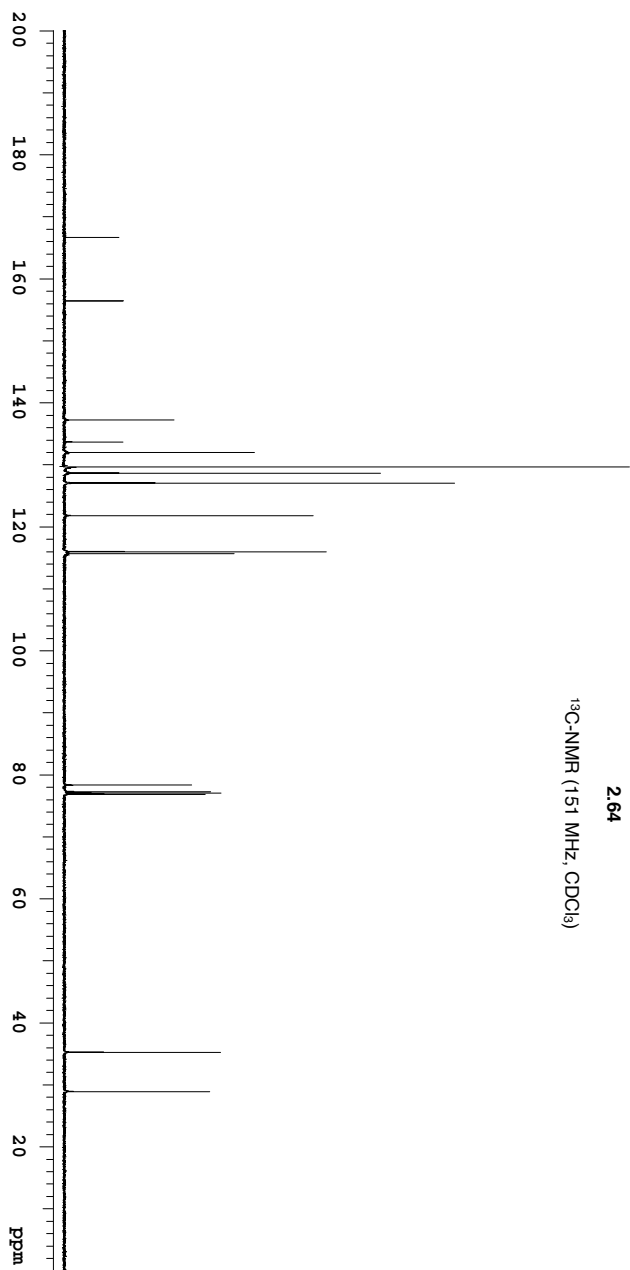
¹H-NMR (600 MHz, CDCl₃)

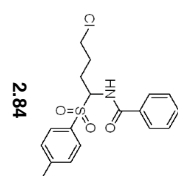




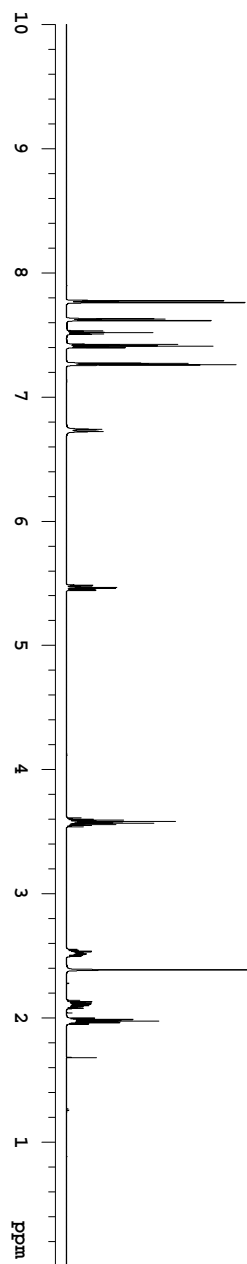
2.64

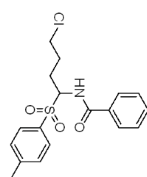
^{13}C -NMR (151 MHz, CDCl_3)





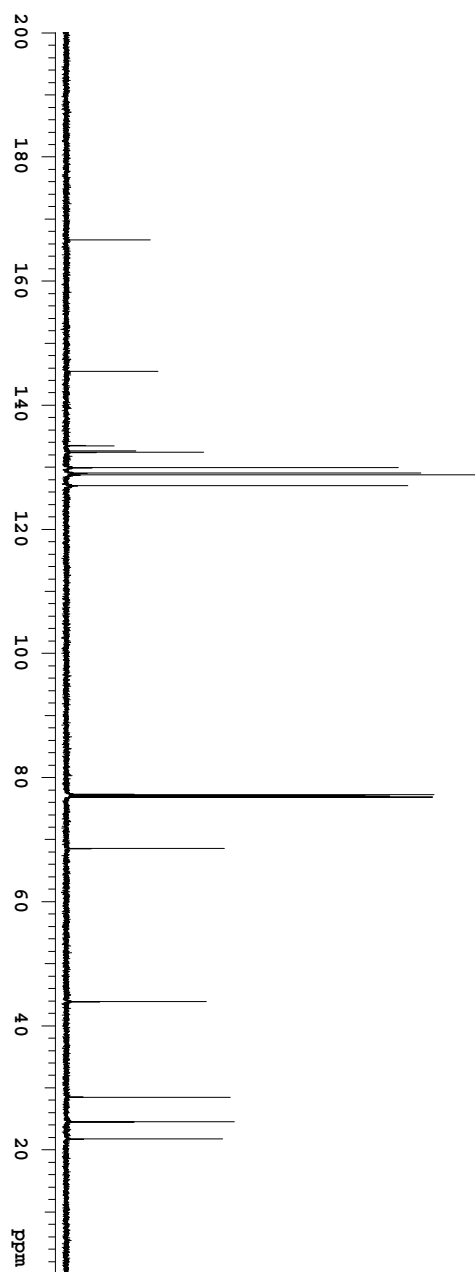
¹H-NMR (600 MHz, CDCl₃)

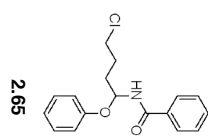




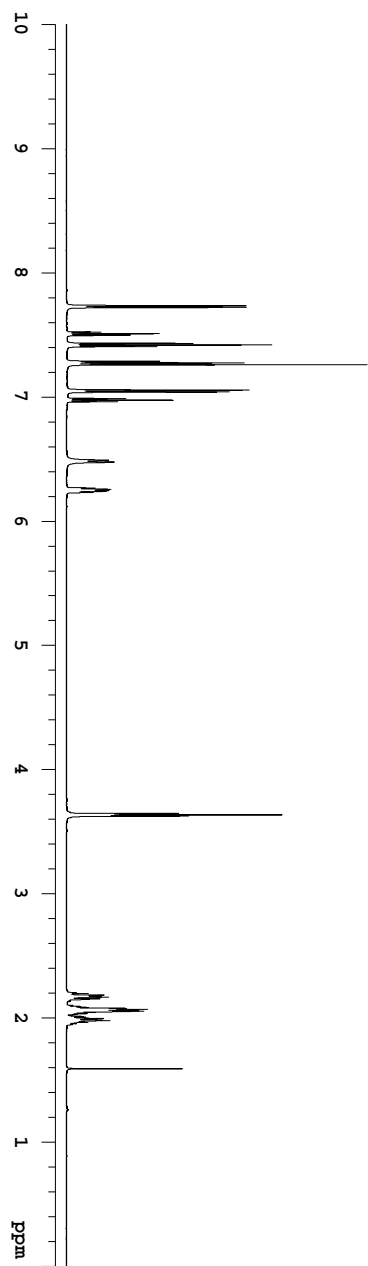
2.84

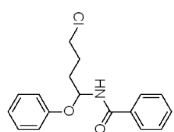
¹³C-NMR (151 MHz, CDCl₃)





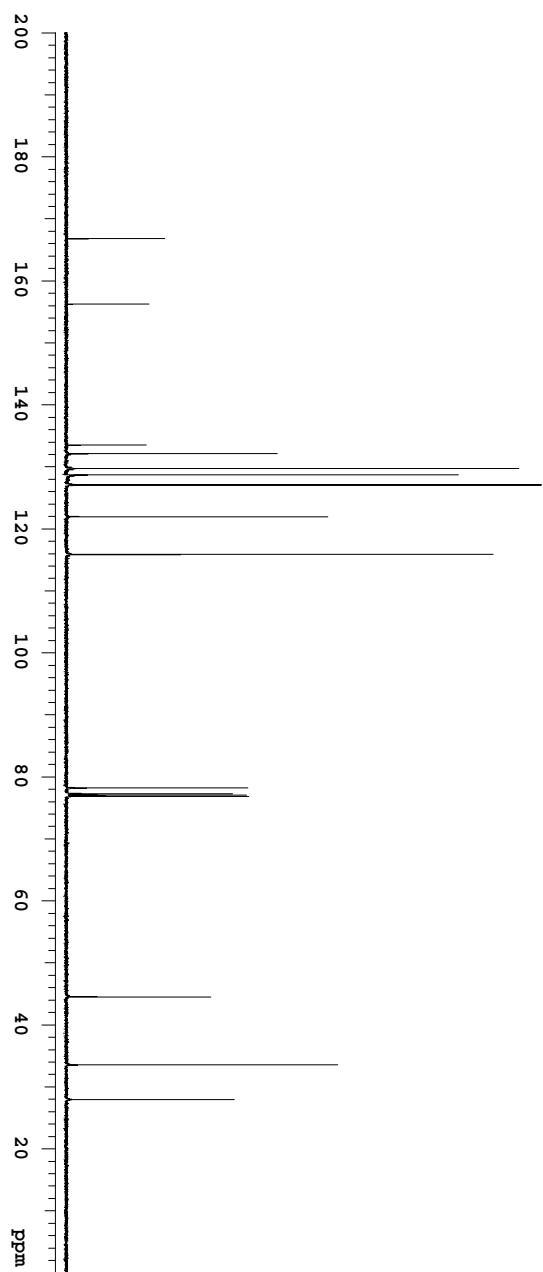
¹H-NMR (600 MHz, CDCl₃)

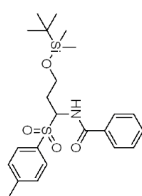




2.65

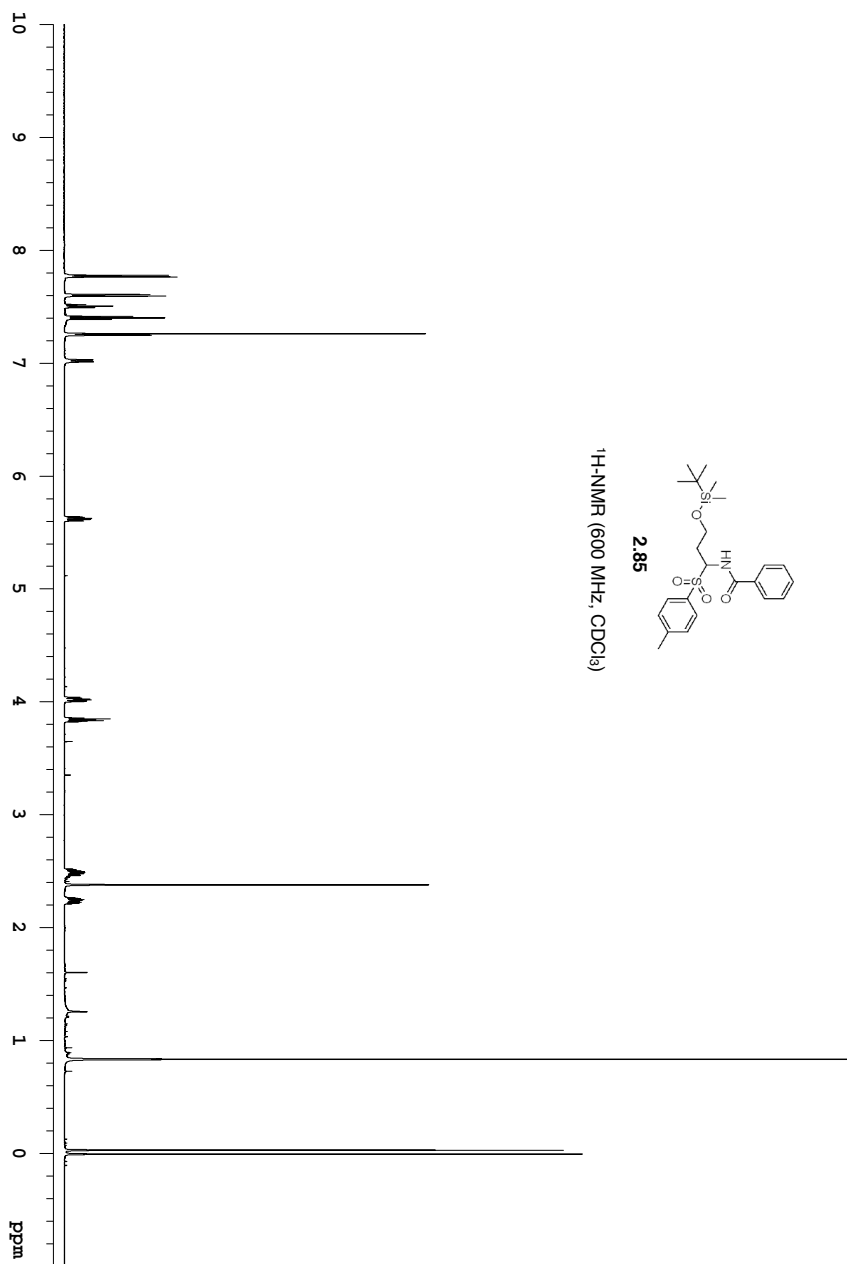
^{13}C -NMR (151 MHz, CDCl_3)

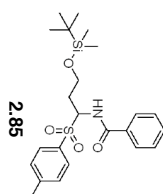




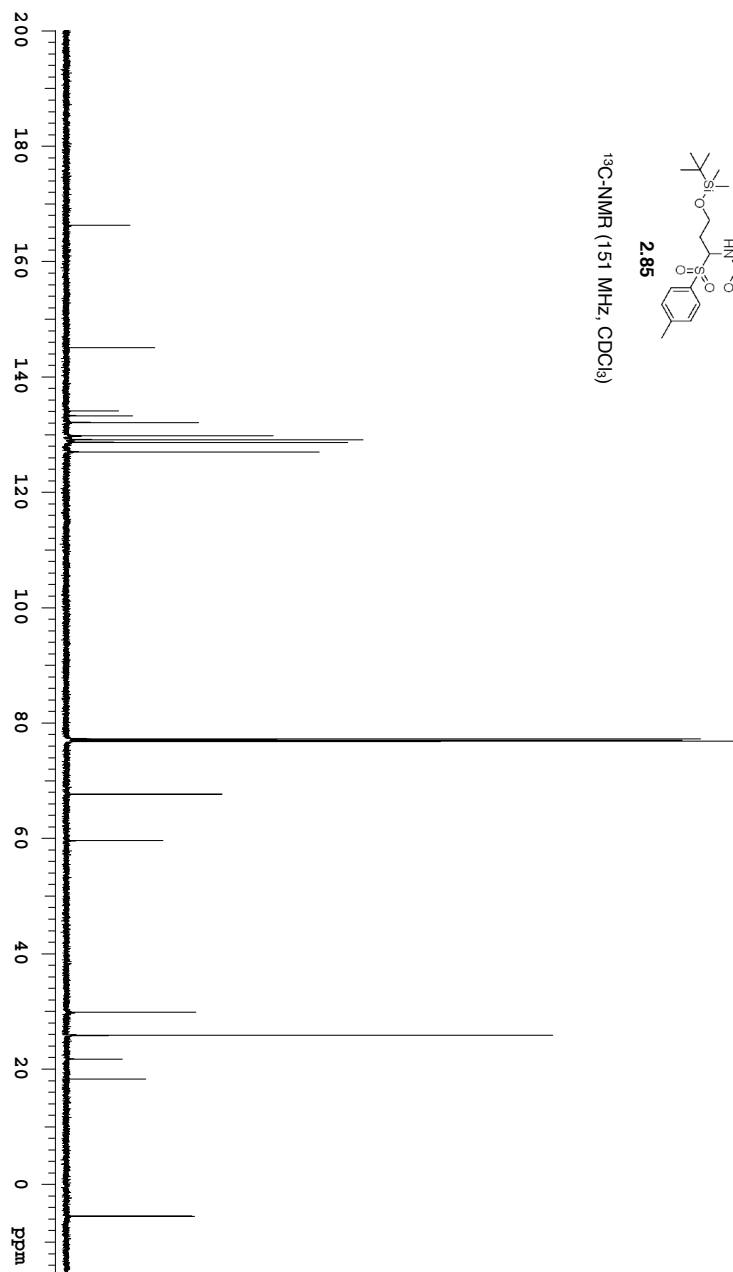
2.85

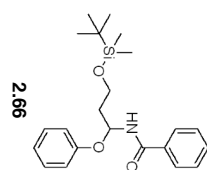
¹H-NMR (600 MHz, CDCl₃)





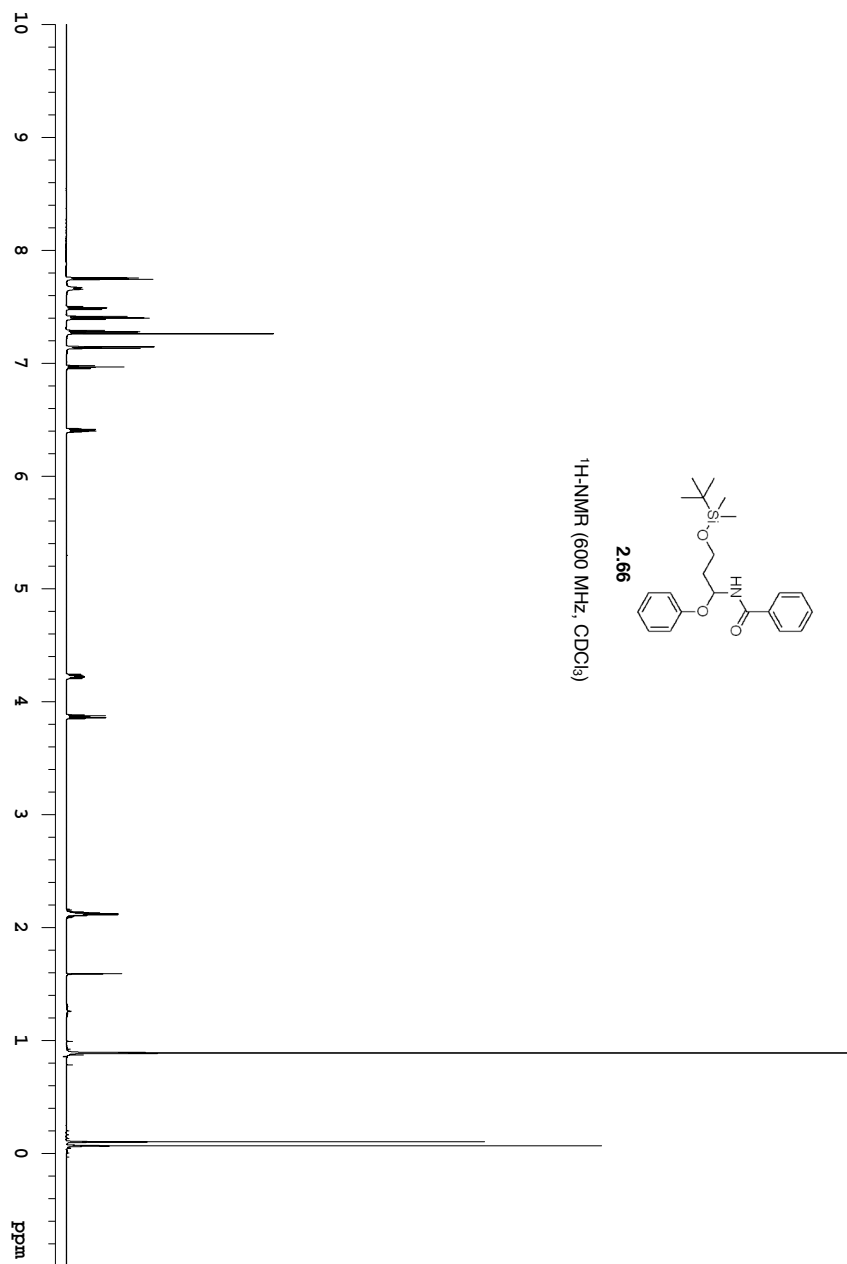
^{13}C -NMR (151 MHz, CDCl_3)

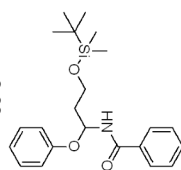




2.66

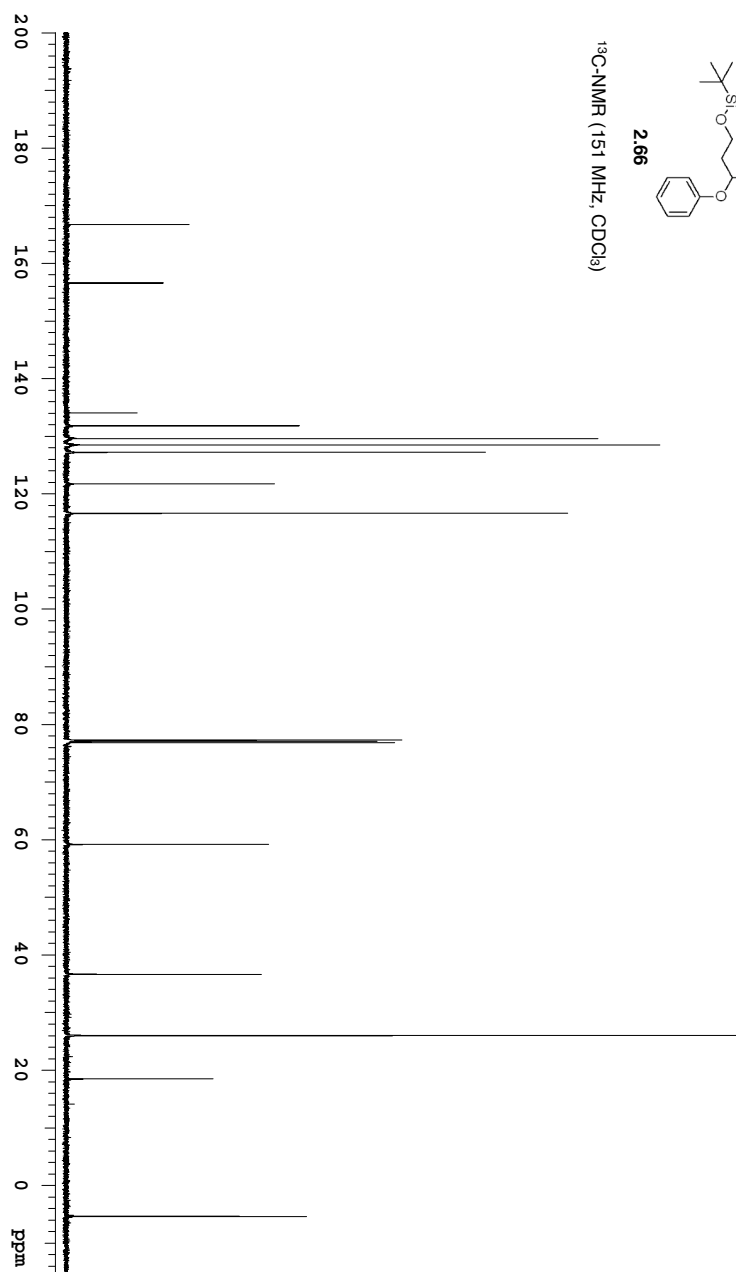
¹H-NMR (600 MHz, CDCl₃)

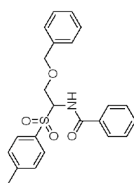




2.66

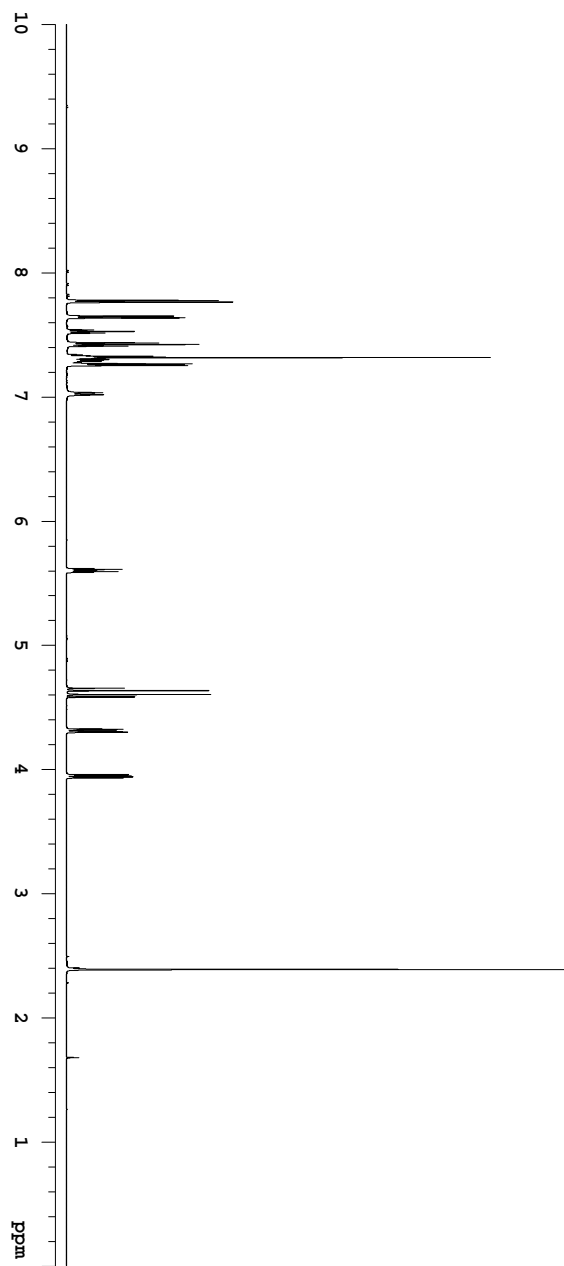
^{13}C -NMR (151 MHz, CDCl_3)

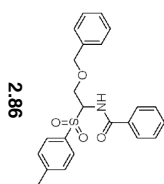




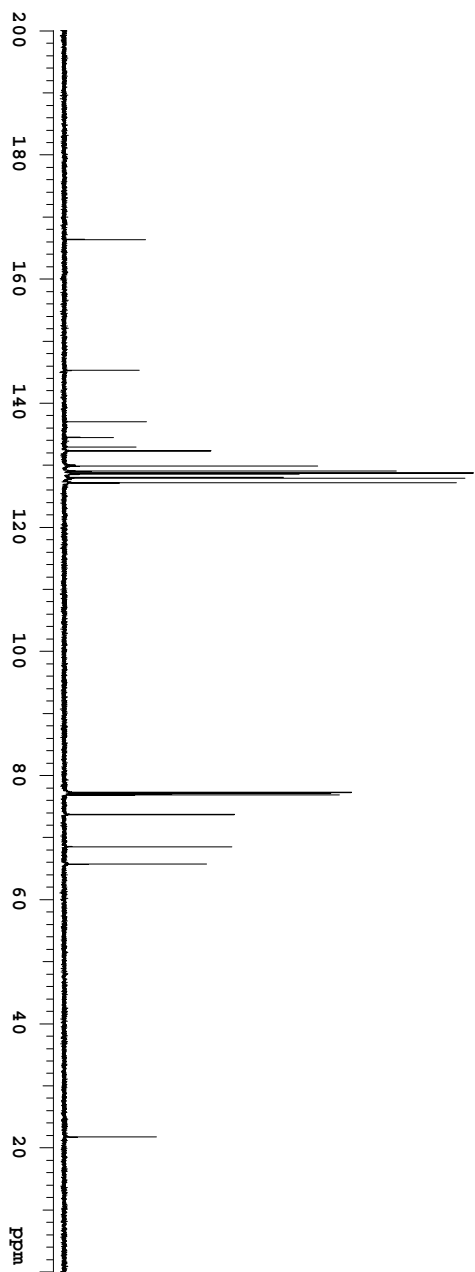
2.86

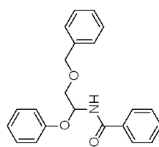
¹H-NMR (600 MHz, CDCl₃)





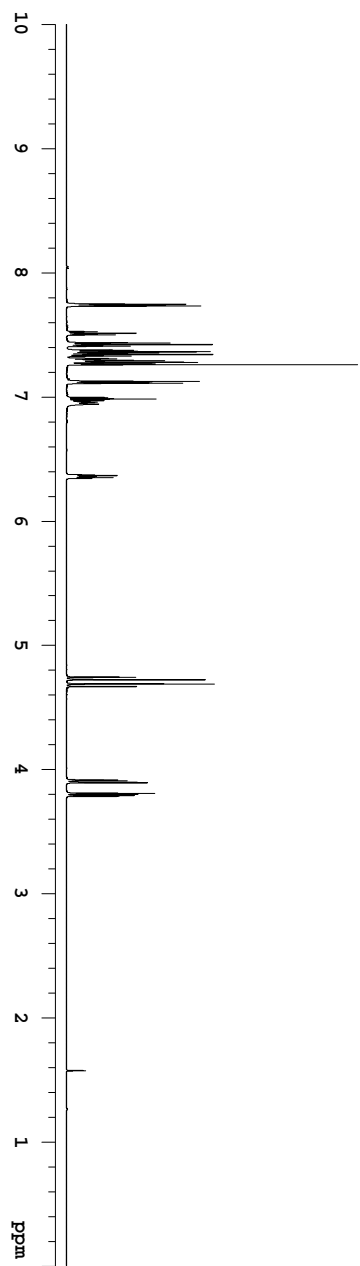
¹³C-NMR (151 MHz, CDCl₃)

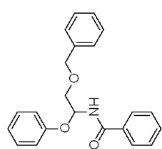




2.67

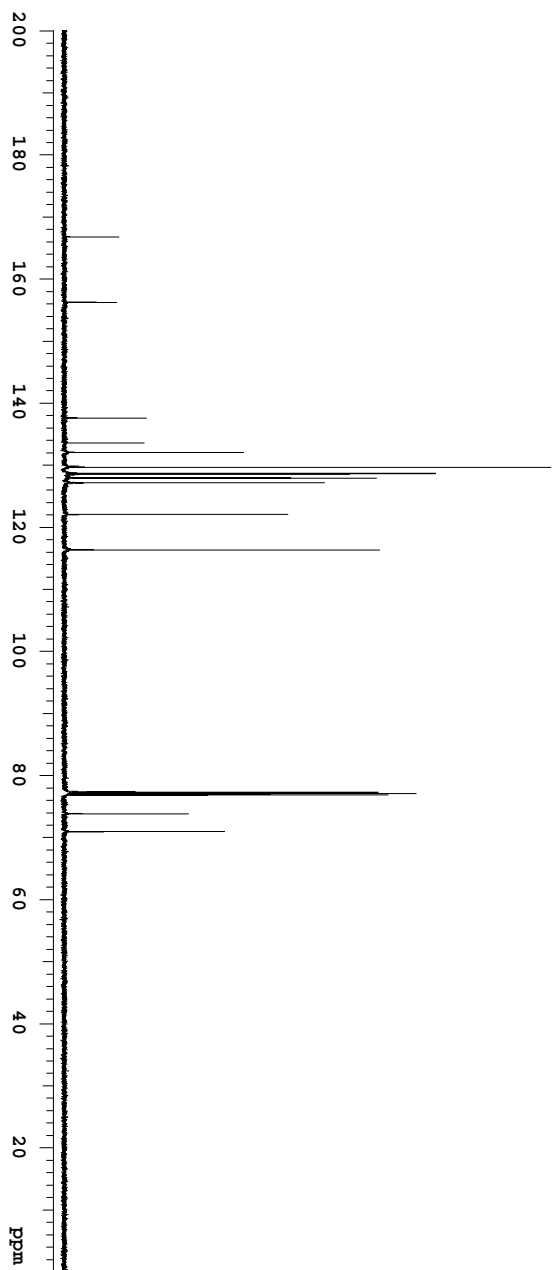
¹H-NMR (600 MHz, CDCl₃)

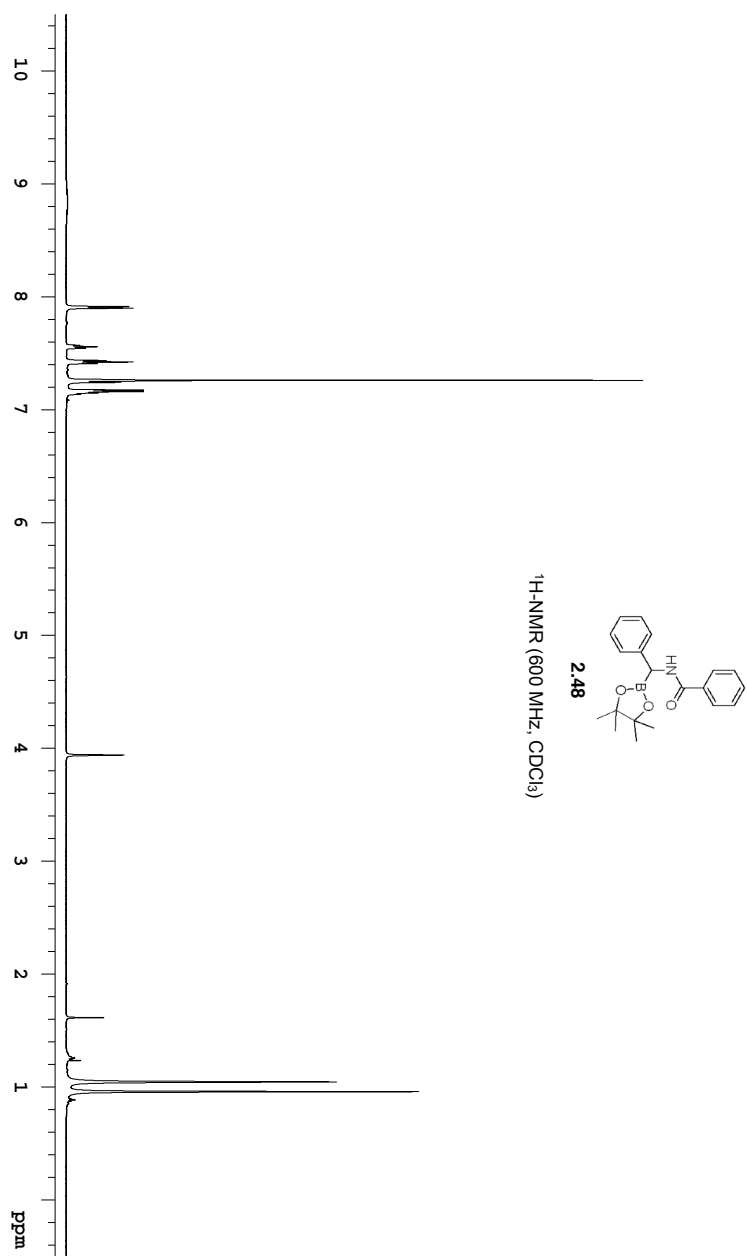


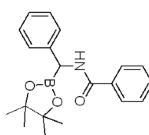


2.67

^{13}C -NMR (151 MHz, CDCl_3)

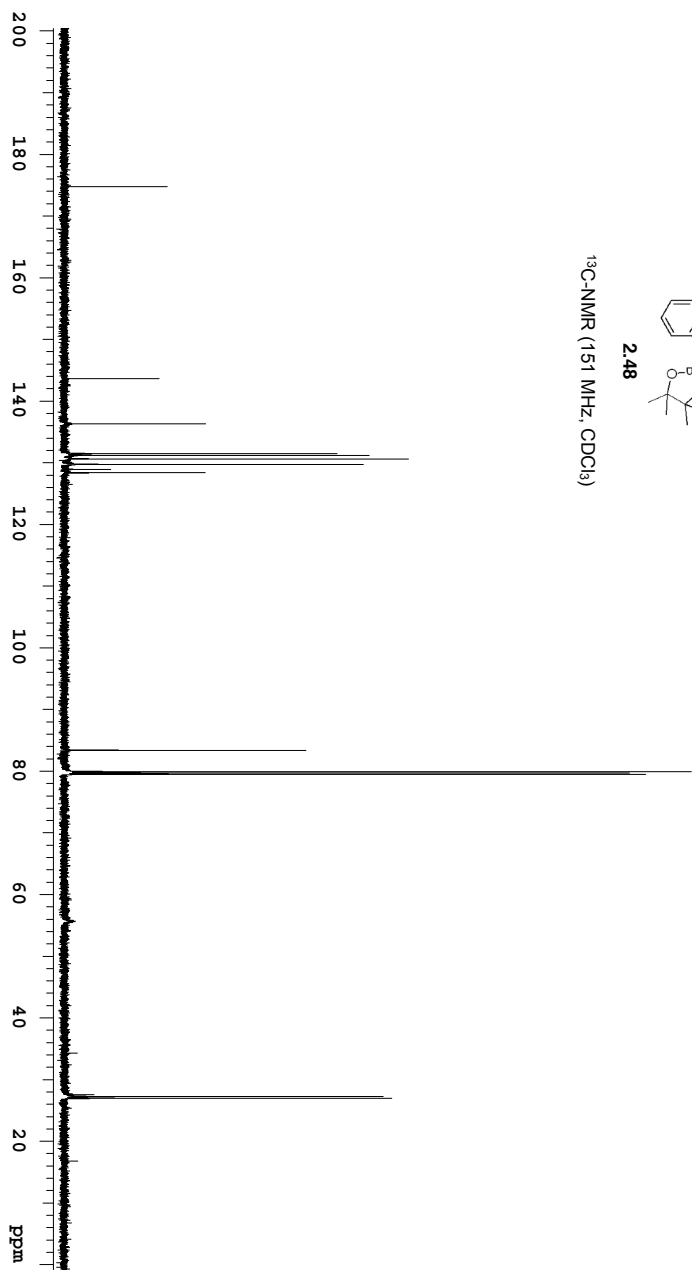


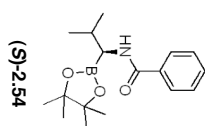




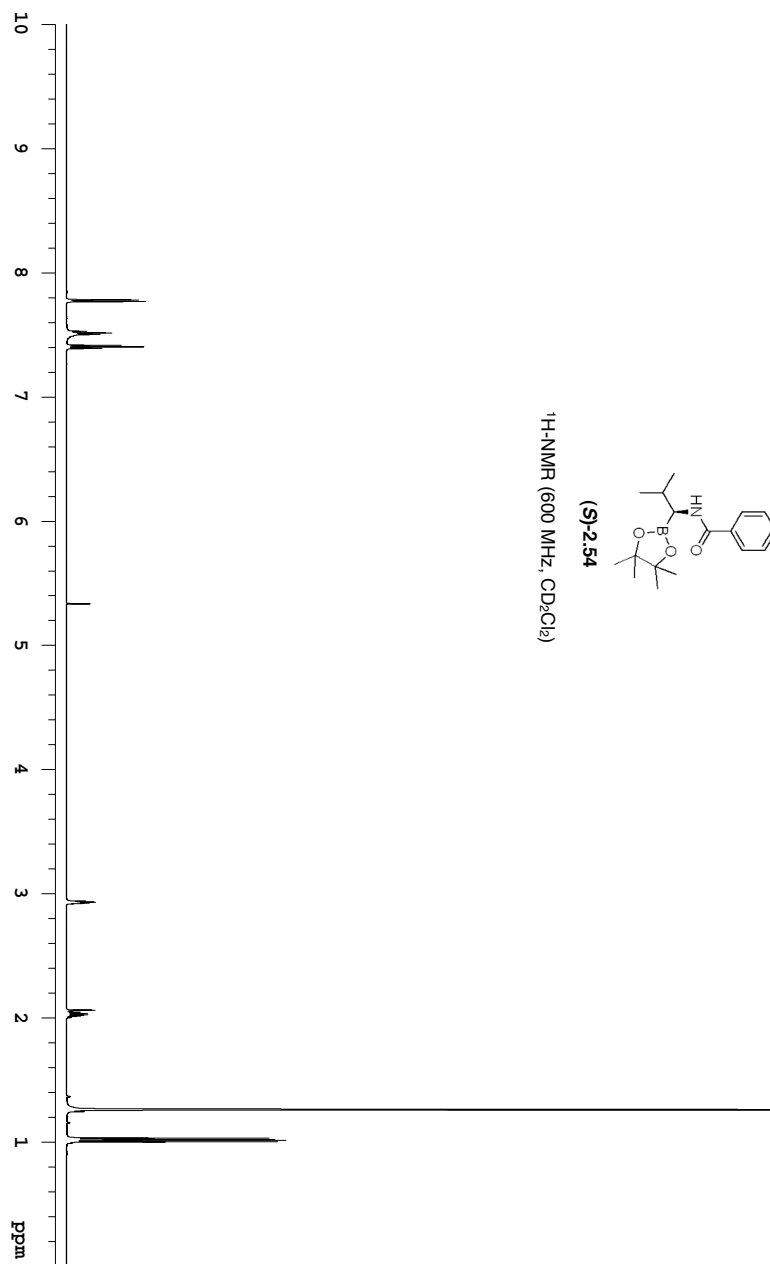
2.48

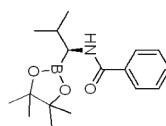
^{13}C -NMR (151 MHz, CDCl_3)





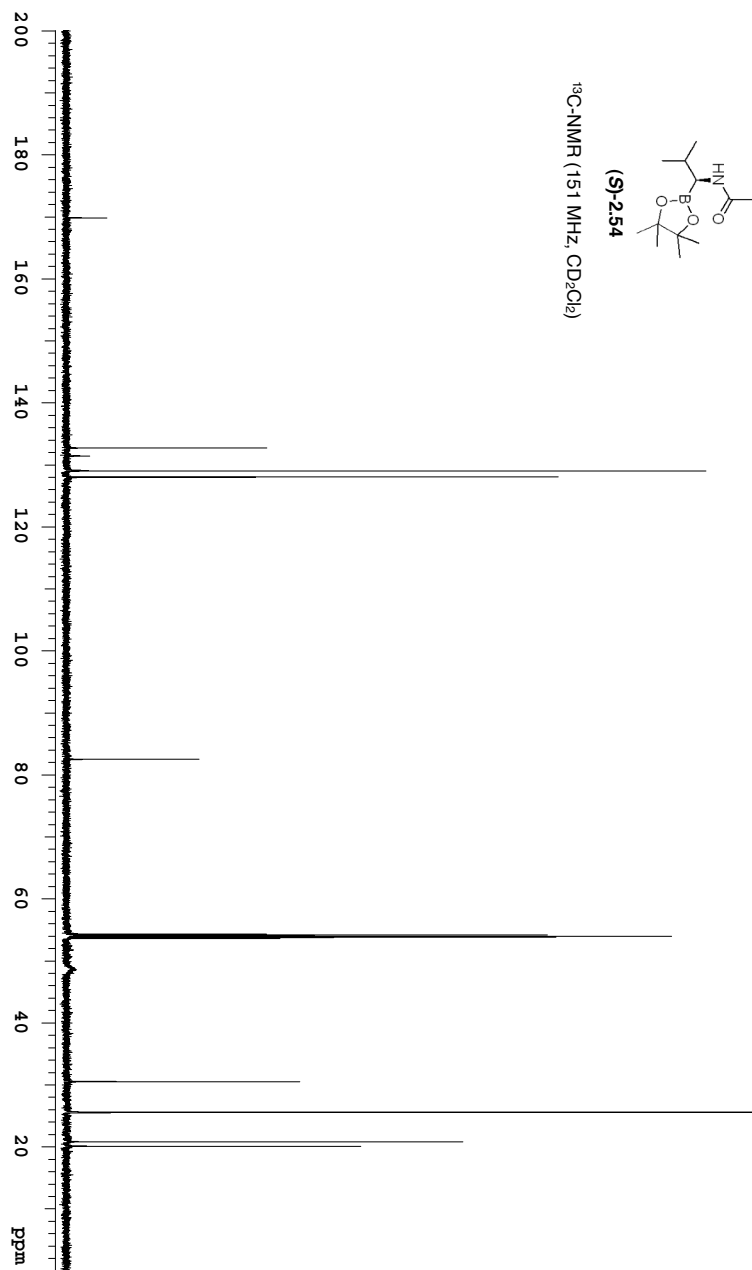
¹H-NMR (600 MHz, CD₂Cl₂)

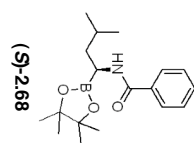




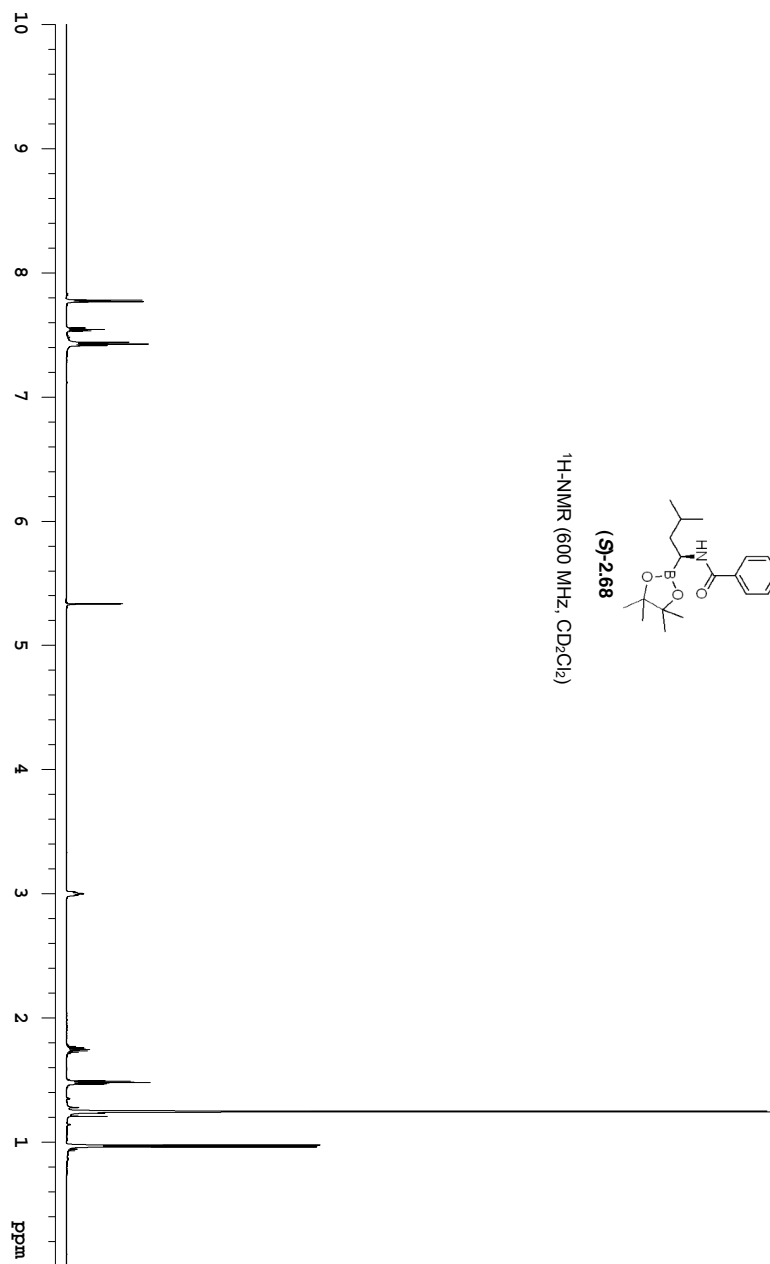
(S)-2.54

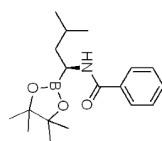
^{13}C -NMR (151 MHz, CD_2Cl_2)





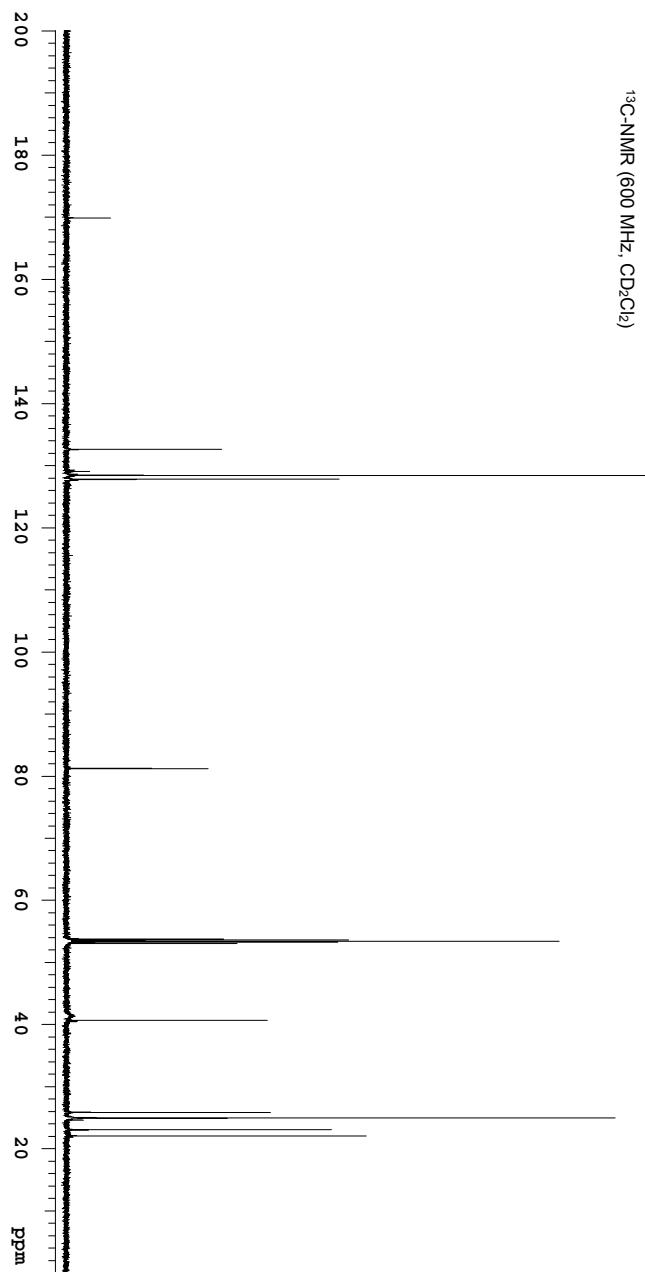
¹H-NMR (600 MHz, CD₂Cl₂)

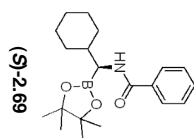




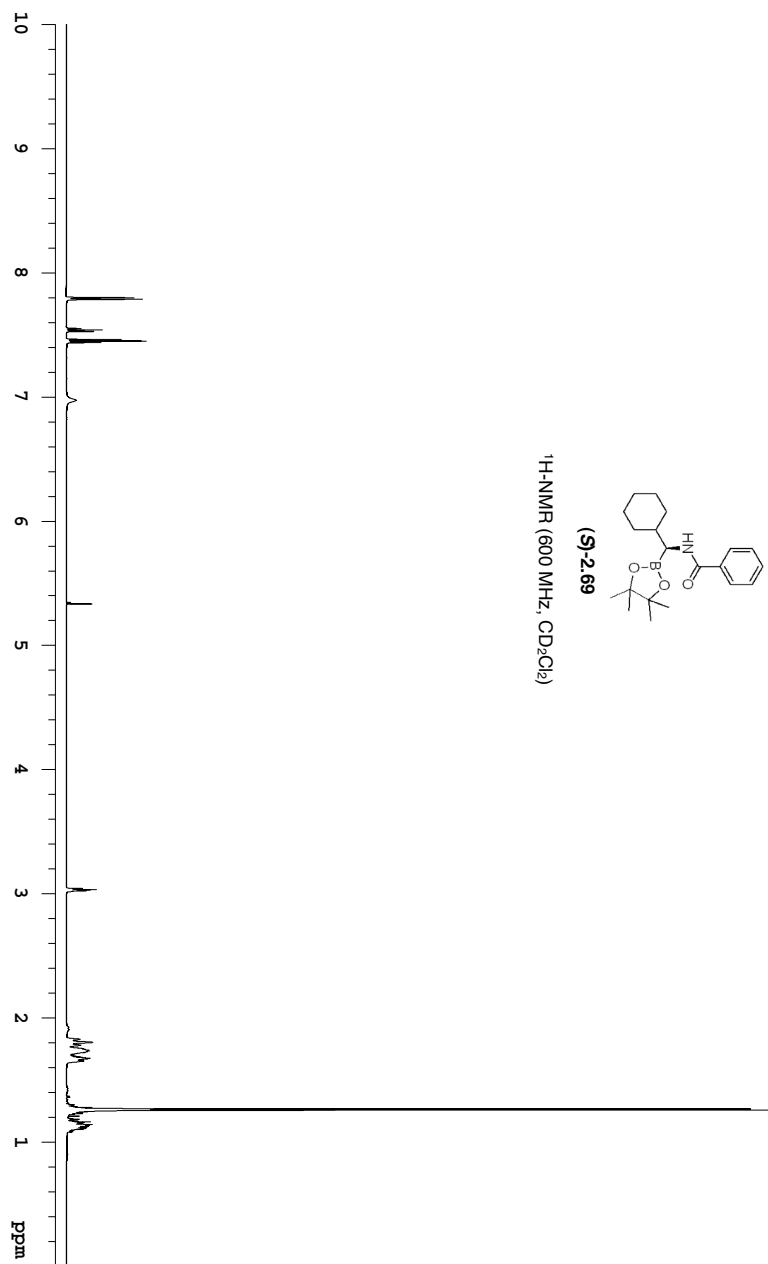
(S)-2.68

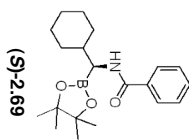
^{13}C -NMR (600 MHz, CD_2Cl_2)



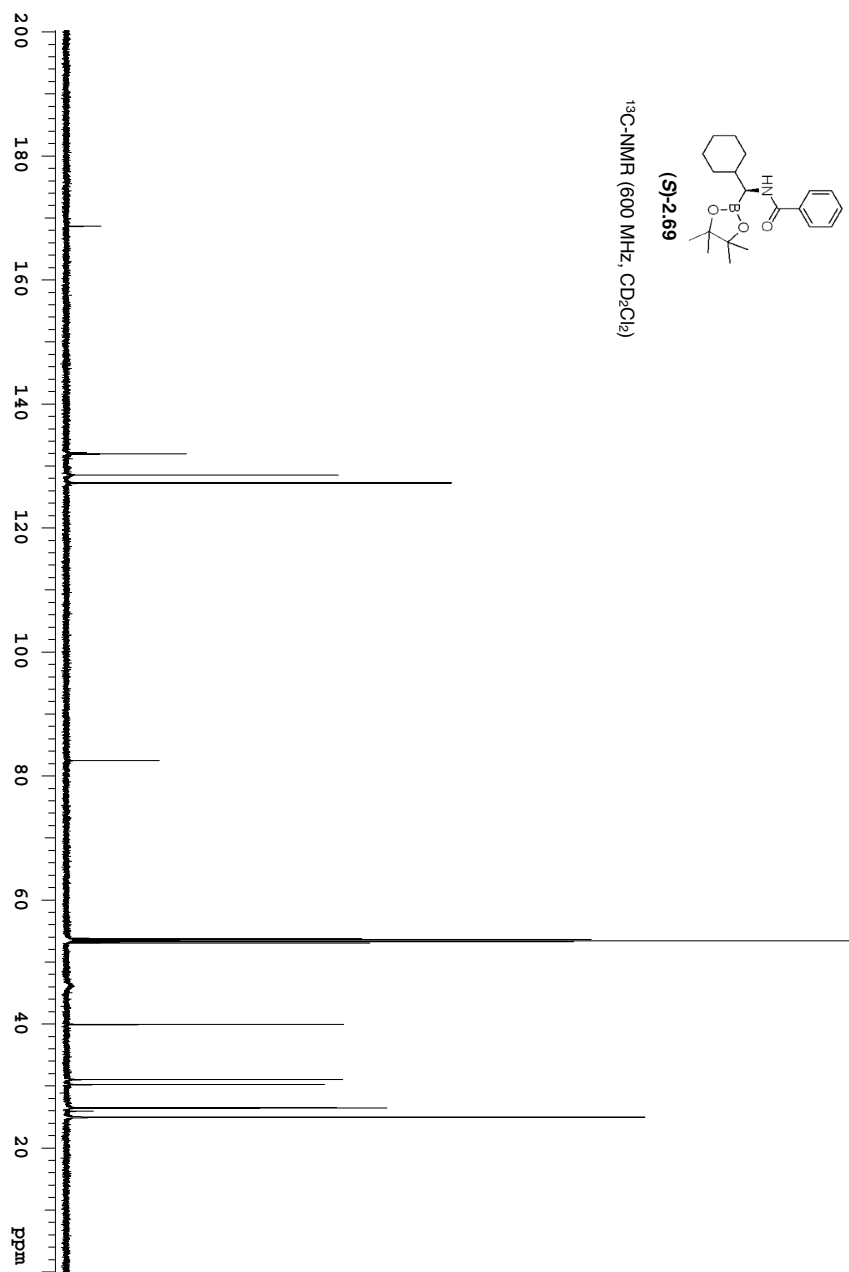


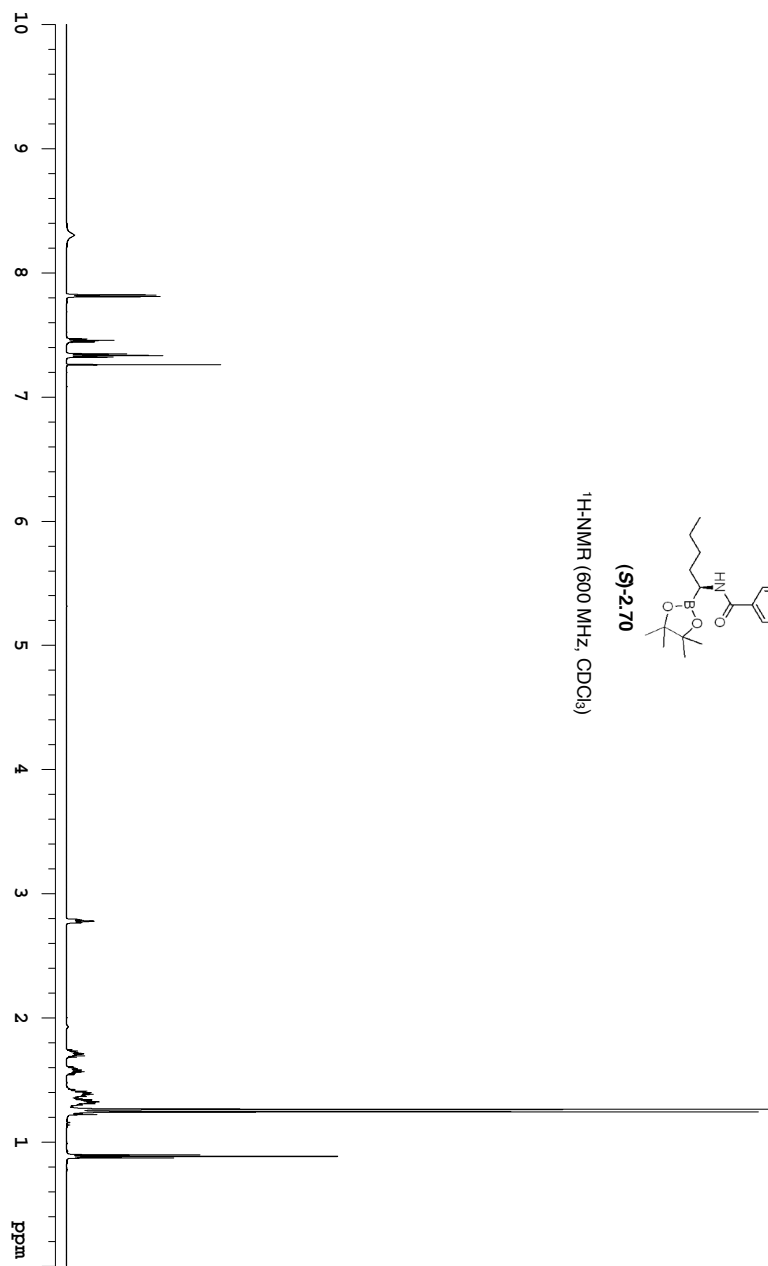
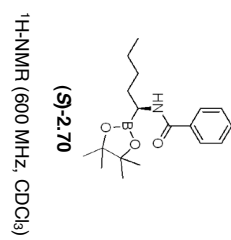
¹H-NMR (600 MHz, CD₂Cl₂)

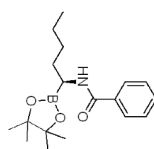




^{13}C -NMR (600 MHz, CD_2Cl_2)

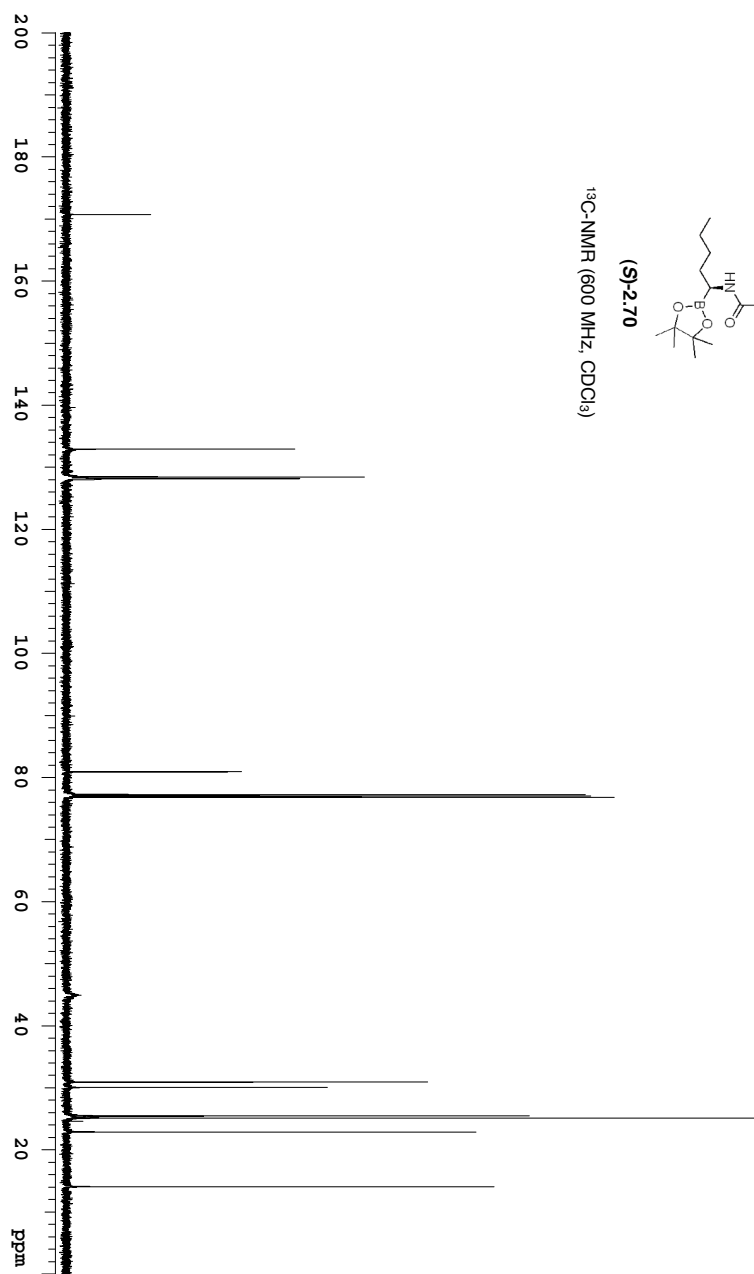


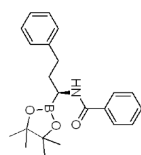




(S)-2.70

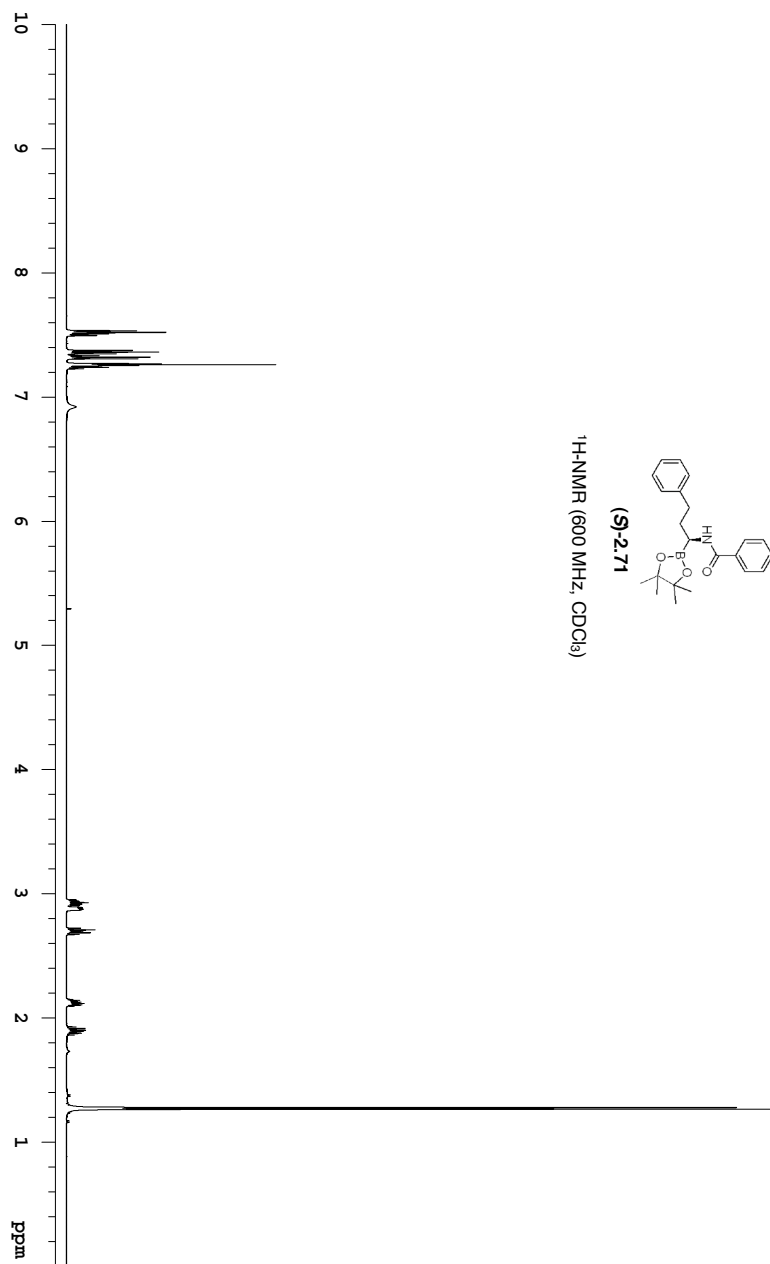
¹³C-NMR (600 MHz, CDCl₃)

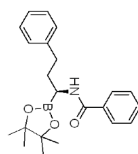




(S)-2.71

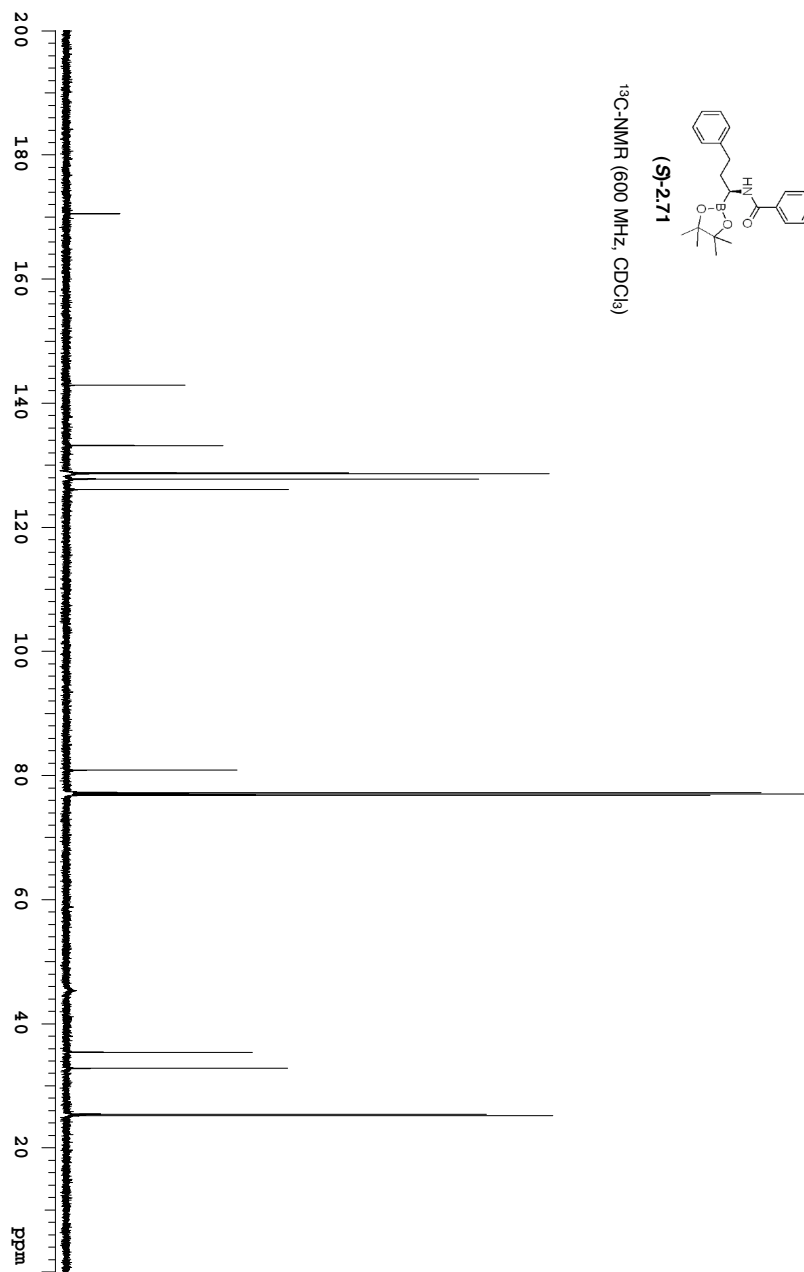
¹H-NMR (600 MHz, CDCl₃)

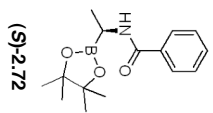




(S)-2.71

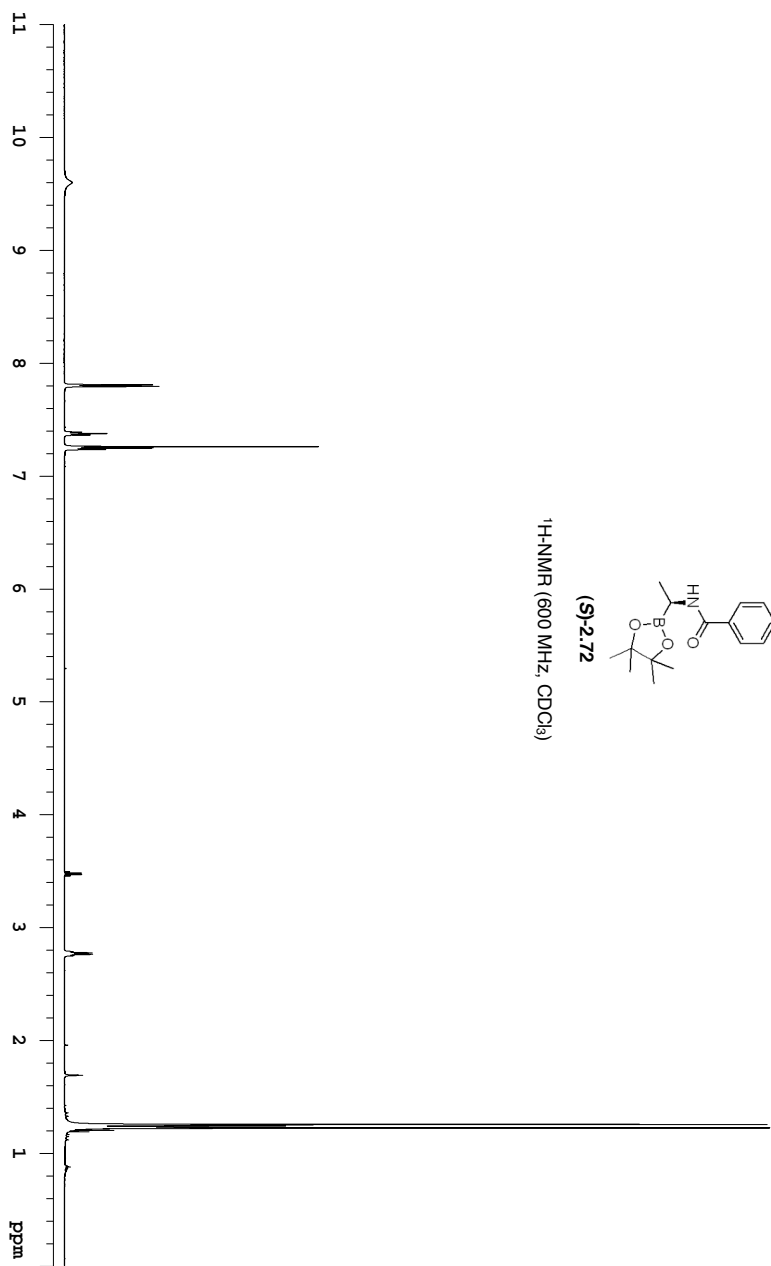
^{13}C -NMR (600 MHz, CDCl_3)

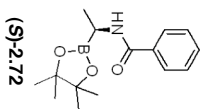




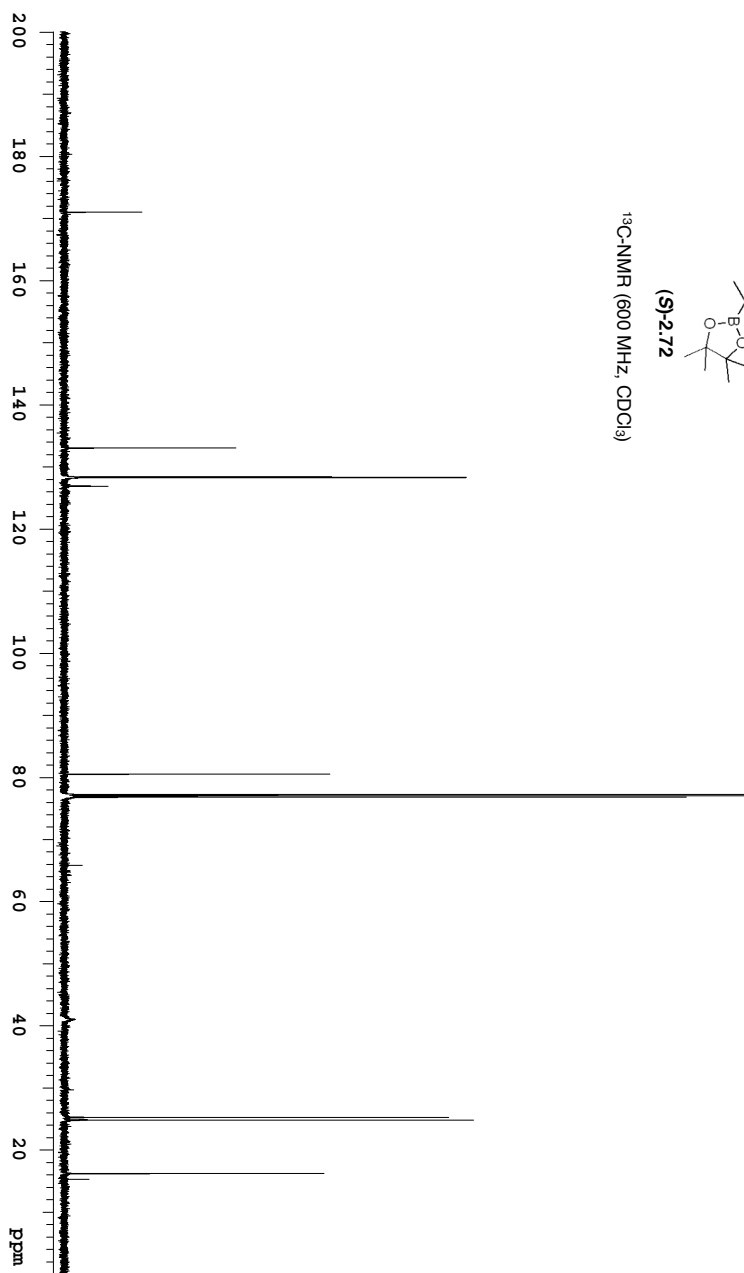
(S)-2.72

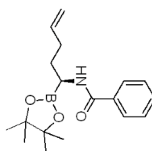
¹H-NMR (600 MHz, CDCl₃)



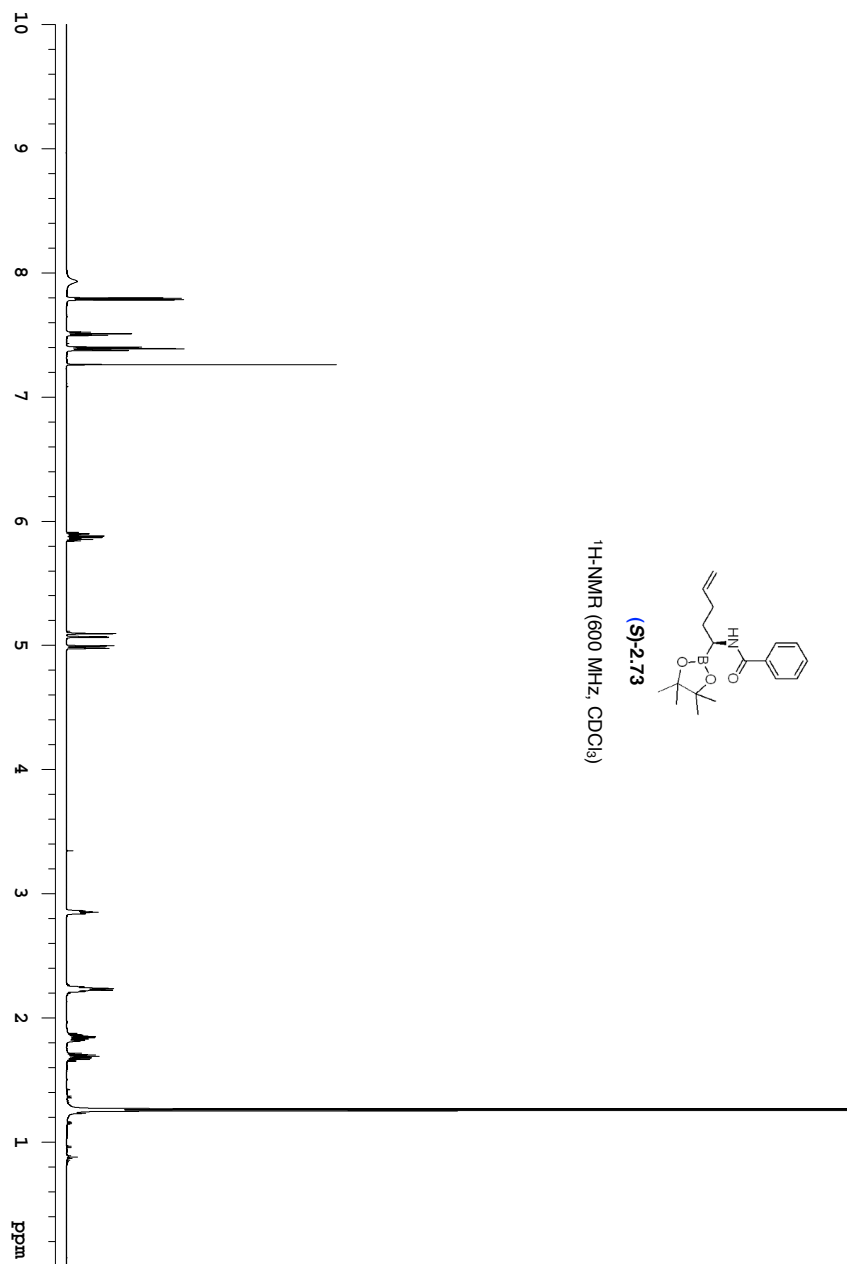


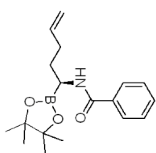
^{13}C -NMR (600 MHz, CDCl_3)





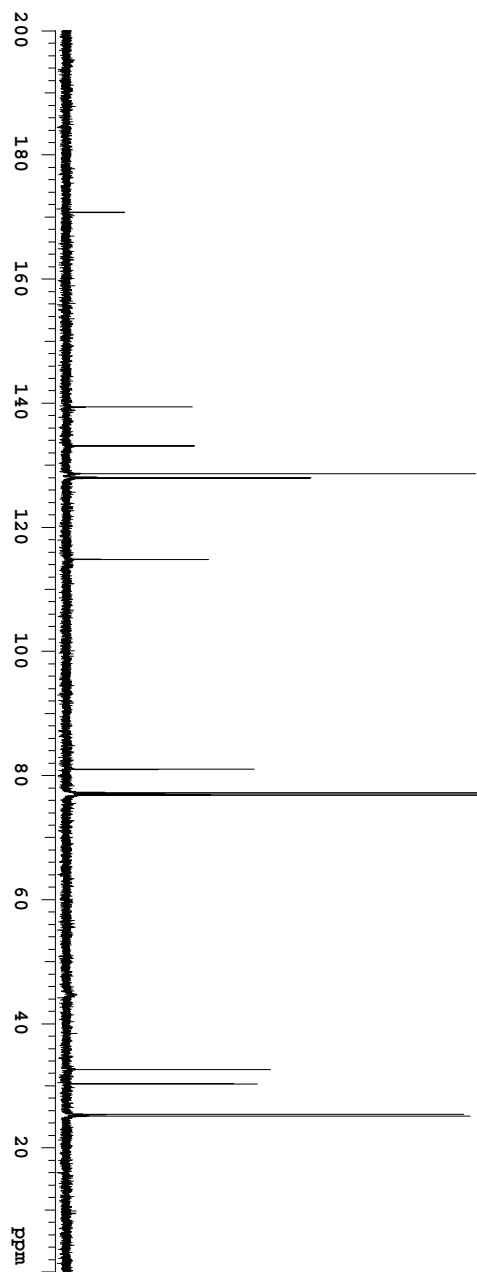
¹H-NMR (600 MHz, CDCl₃)

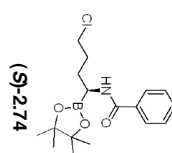




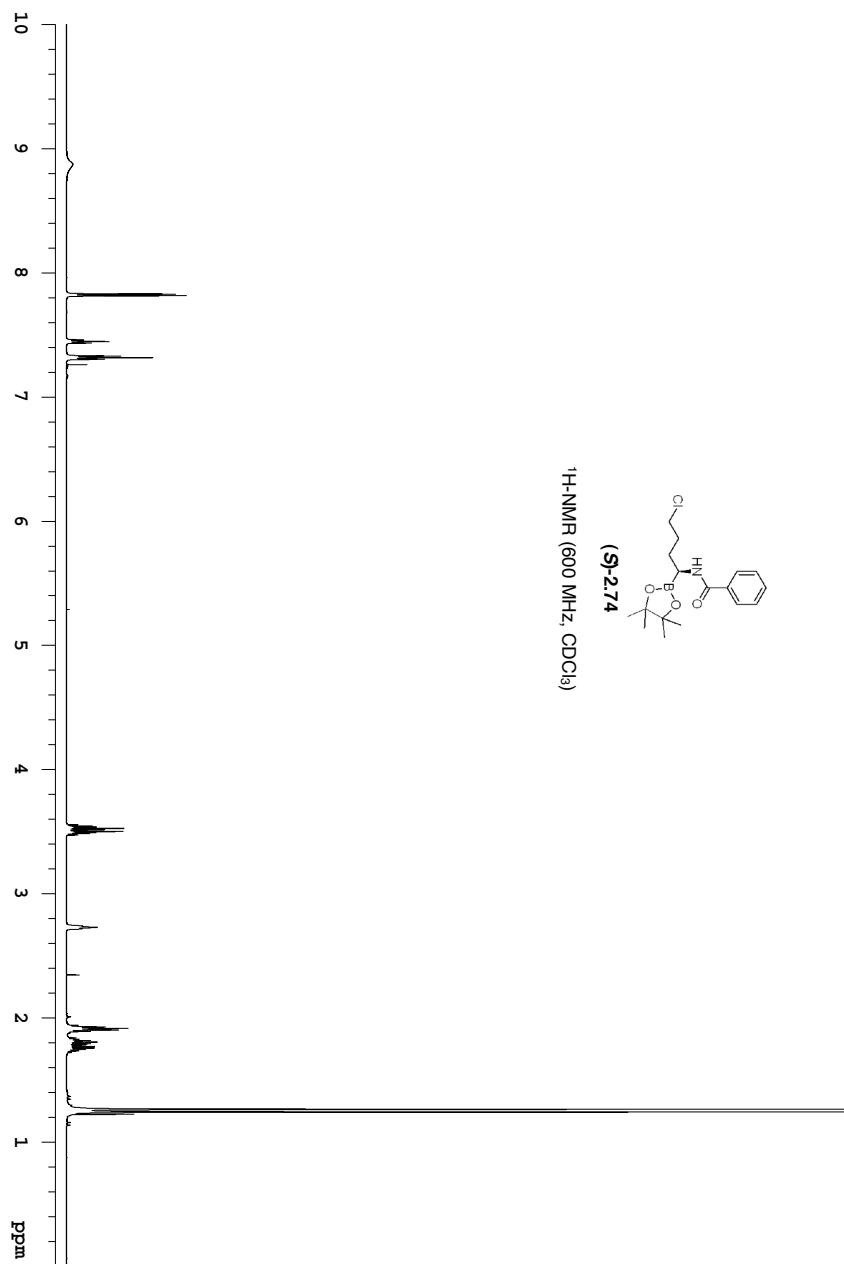
(S)-2.73

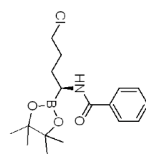
^{13}C -NMR (600 MHz, CDCl_3)





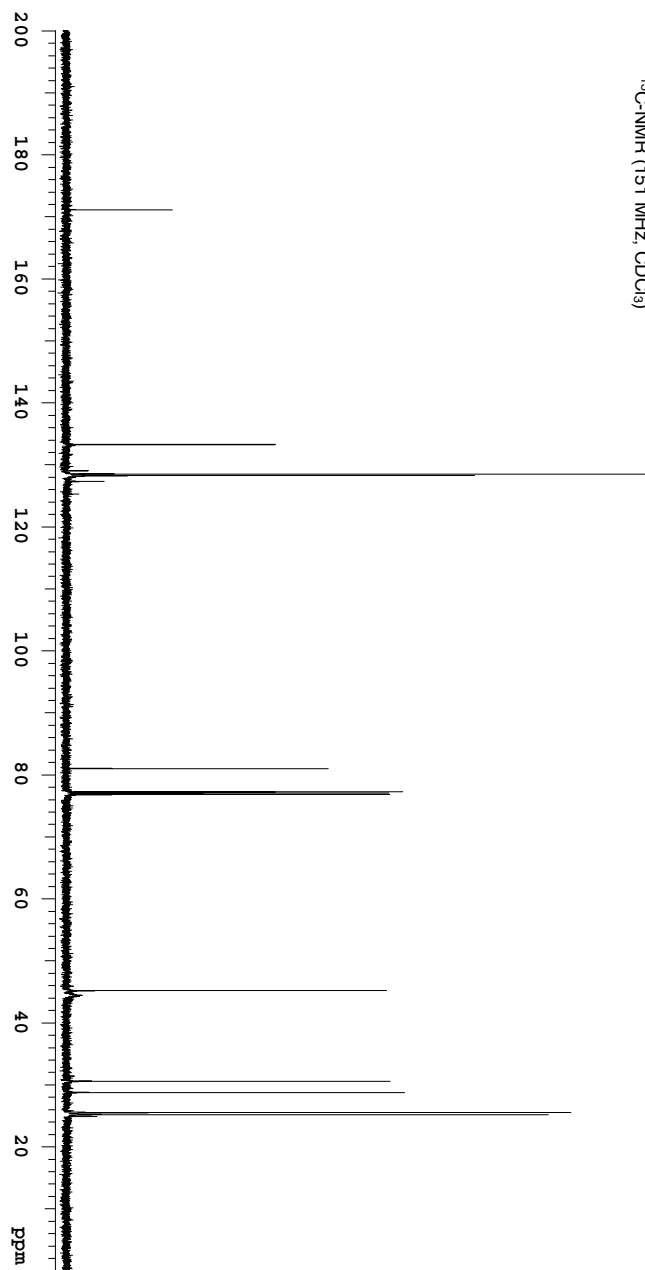
¹H-NMR (600 MHz, CDCl₃)

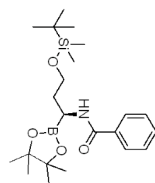
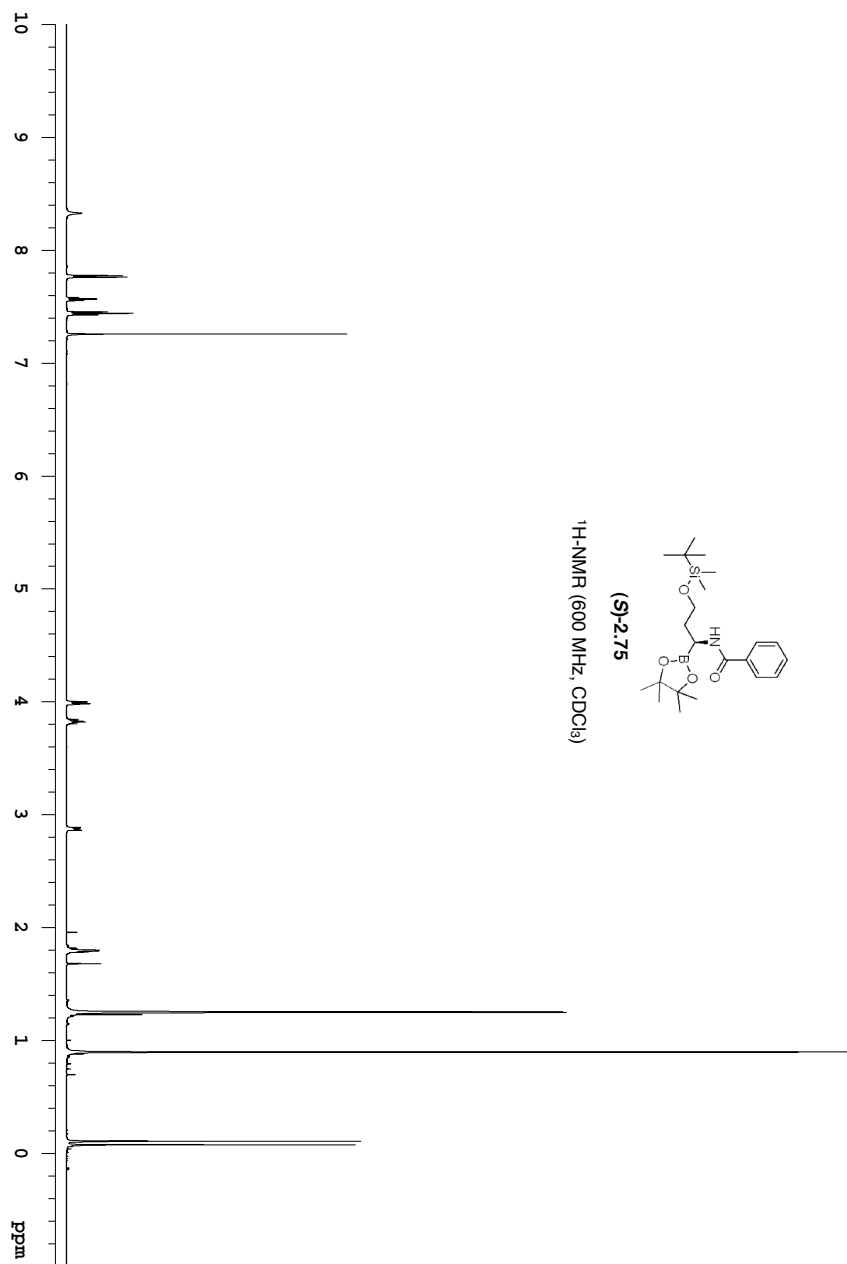


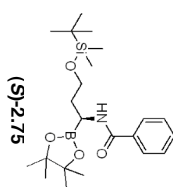


(S)-2.74

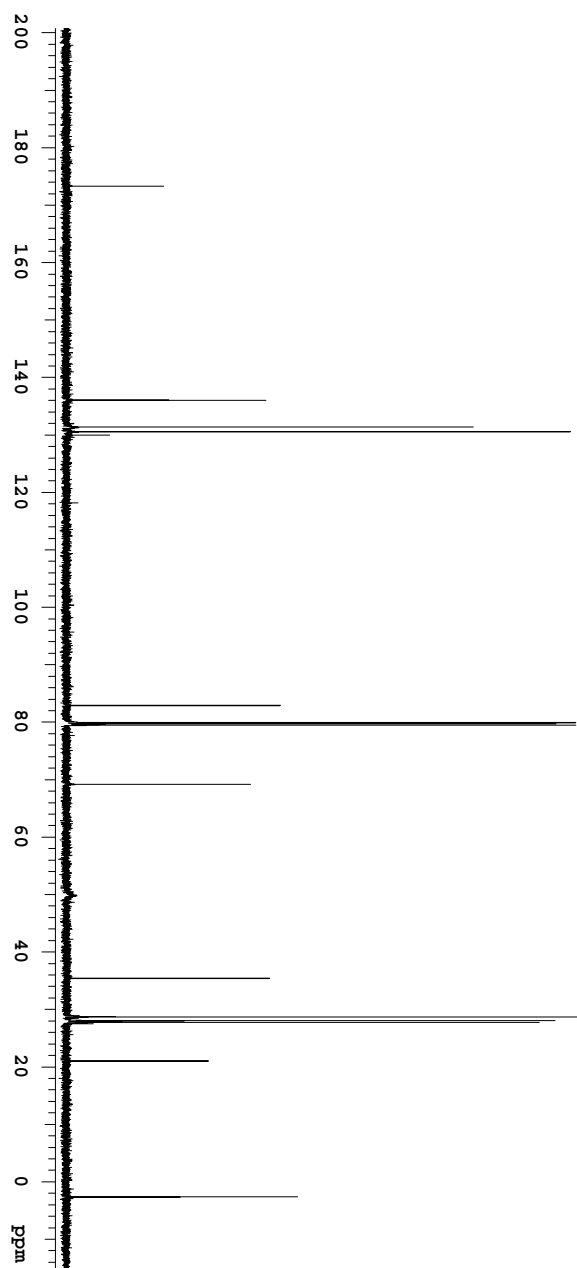
^{13}C -NMR (151 MHz, CDCl_3)

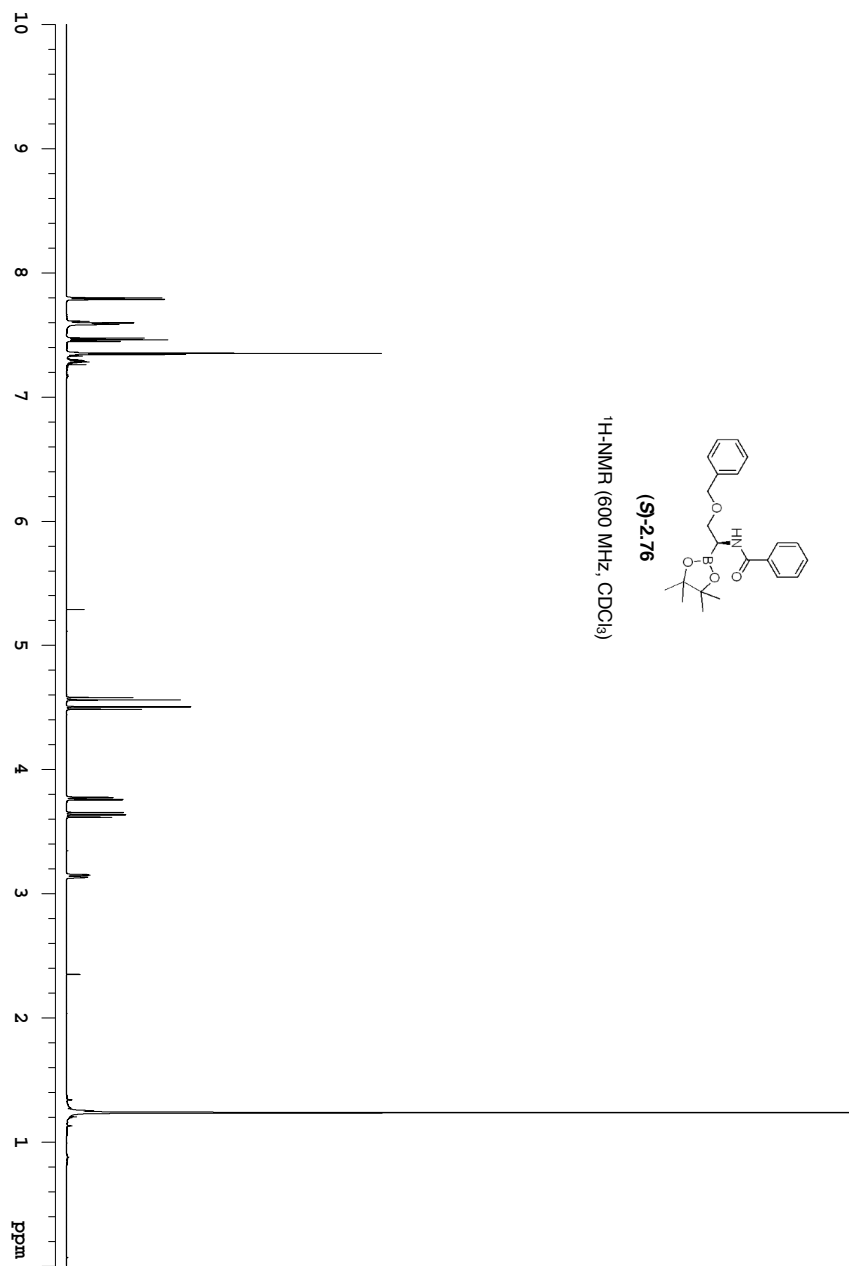
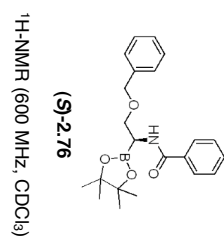


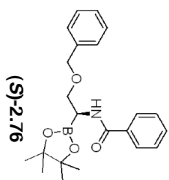
**(S)-2.75**¹H-NMR (600 MHz, CDCl₃)



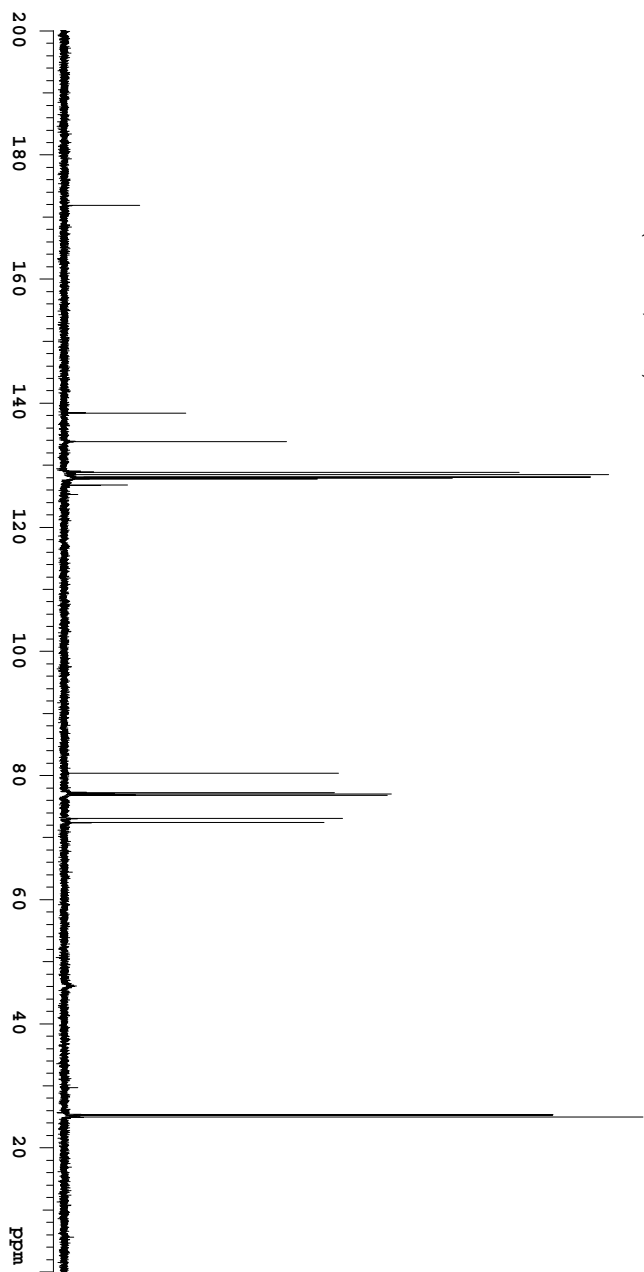
¹³C-NMR (600 MHz, CDCl₃)







^{13}C -NMR (600 MHz, CDCl_3)



Chapter 3

Ruthenium-Catalyzed Tandem Reactions for Constructing *N*-Protected 2,3-Dihydroxypyrrolidines and 2,3-Dihydroxypiperidines

3.1 General Introduction

The application of degenerate pathways of Grubbs' catalysts in non-metathesis reactions¹ has become an active branch in the field of tandem catalysis.² Many examples have demonstrated that tandem metathesis reactions are useful synthetic tools to perform sequential transformations of alkenyl groups in a more economic and efficient fashion, such as tandem olefin metathesis-hydrogenation,³ oxidation,⁴ cyclopropanation⁵ and hydroarylation.⁶

¹ For a review, see: Alcaide, B.; Almendros, P.; Luna A. *Chem. Rev.* **2009**, *109*, 3817-3858.

² For general reviews, see: (a) Fogg, D. E.; dos santos, E. N. *Coord. Chem. Rev.* **2004**, *248*, 2365-2379. (b) Ajamian, A.; Gleason, J. L. *Angew. Chem. Int. Ed.* **2004**, *43*, 3754-3760. (c) Wasilke, J.-C.; Obrey, S.; Baker, R. T.; Bazan, G. C. *Chem. Rev.* **2005**, *105*, 1001-1020. (d) Shindoh, N.; Takemoto, Y.; Takasu, K. *Chem.-Eur. J.* **2009**, *15*, 12168-12179. For a review of tandem catalysis in enantioselective reactions, see: (d) Chapman, C.; Frost, C. *Synthesis* **2007**, 1-21.

³ (a) Louie, J.; Bielawski, C. W.; Grubbs, R. H. *J. Am. Chem. Soc.* **2001**, *123*, 11312-11313. (b) Camm, K. D.; Castro, N. M.; Liu, Y.; Czechura, P.; Snelgrove, J. L.; Fogg, D. E., *J. Am. Chem. Soc.* **2007**, *129*, 4168.

⁴ (a) Beligny, S.; Eibauer, S.; Maechling, S.; Blechert, S. *Angew. Chem. Int. Ed.* **2006**, *45*, 1900-1903. (b) Scholte A. A.; An, M. H.; Snapper, M. L. *Org. Lett.* **2006**, *8*, 4759-4762. (c) Schmidt B.; Krehl S.; Hauk, S. *J. Org. Chem.* **2013**, *78*, 5427-5435.

⁵ Kim, B. G.; Snapper, M. L. *J. Am. Chem. Soc.* **2006**, *128*, 52-53.

⁶ Chen, J.-R.; Li, C.-F.; An, X.-L.; Zhang, J.-J.; Zhu, X.-Y.; Xiao, W.-J. *Angew. Chem. Int. Ed.* **2008**, *47*, 2489-2492.

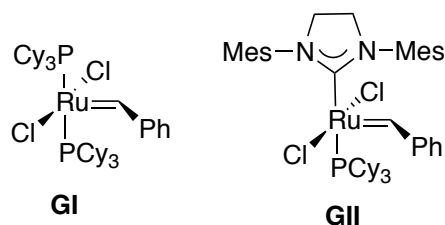
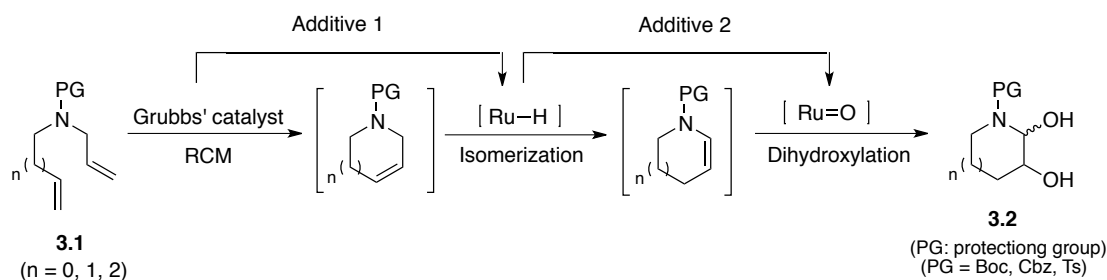


Figure 3.1 Commercially available Grubbs' catalysts

Herein we aim to develop a three-step tandem sequence, which includes ring-closing metathesis (RCM), olefin isomerization and olefin dihydroxylation, to make *N*-protected 2,3-dihydropyrrolidines and 2,3-dihydropiperidines from readily available nitrogen-tethered dienes **3.1** (Scheme 3.1). The Grubbs' catalyst added in the first step will serve as the metal source in the subsequent two transformations. Olefin isomerization would normally be catalyzed by ruthenium hydride while olefin dihydroxylation would be catalyzed by ruthenium oxide. A suitable additive will function as the promoter to modify the different catalyst precursor between steps.



Scheme 3.1 Proposed tandem RCM/olefin isomerization/dihydroxylation sequence

The anticipated challenges are (1) minimizing side effects of additives on the following reaction and (2) the limited number of electron-rich olefins shown to participate in Ru-catalyzed dihydroxylations. Ruthenium tetroxide is known to be a

robust catalyst for olefin dihydroxylation under specific conditions.⁷ However, in a recently reported study of tandem Z-selective cross metathesis/olefin dihydroxylation by Robert Grubbs, it was noted that unfunctionalized electron-rich olefins inhibited the Ru-catalyzed dihydroxylation.⁸ In addition, the variation of oxidation states of ruthenium through the proposed tandem sequence is ambiguous to us, which makes the dihydroxylation step more challenging.

N-Protected 2,3-dihydroxypyrrolidines and 2,3-dihydroxypiperidines are versatile building blocks in synthesis. The hemiaminal motif can be treated as a masked aminoaldehyde and used as a reactant in Wittig reactions;⁹ the acid-labile hydroxyl group or the derived acetate at 2-position makes these compounds good precursors for the corresponding iminium ions.¹⁰ The iminium intermediates can react with a nucleophile to introduce a new substituent onto the heterocyclic rings.

In 2005 Takeuchi and Harayama reported a racemic synthesis of Febrifugine, a potent antimalarial alkaloid.^{9a} 2,3-Dihydroxy-*N*-(benzyloxycarbonyl)piperidine **3.4** was used in a Wittig reaction to access the key intermediate (*E*)- ω -amidoenone **3.5**, which

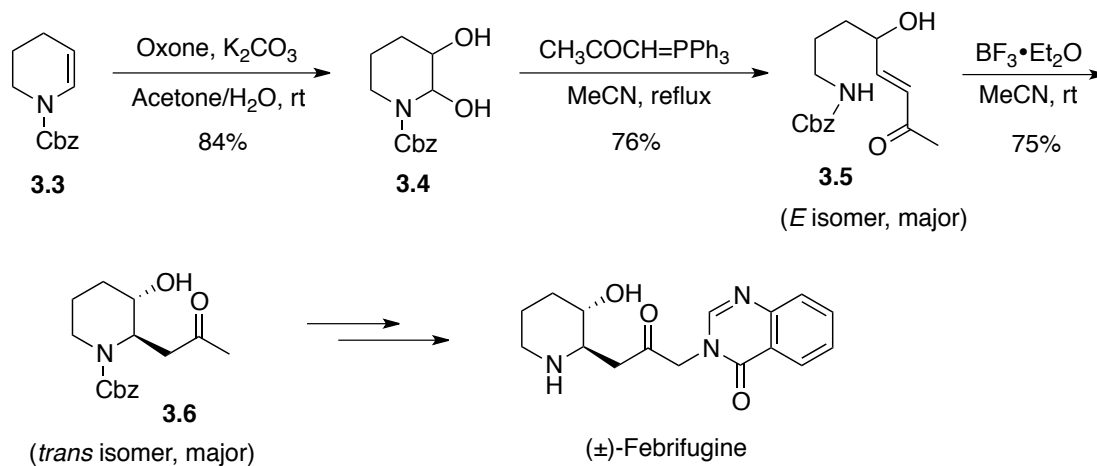
⁷ For reviews of RuO₄ in oxidations, see: (a) Plietker, B.; Niggemann, M. *Org. Biomol. Chem.* **2004**, *2*, 2403-2407. (b) Plietker, B. *Synthesis* **2005**, *15*, 2453-2472.

⁸ Dornan, P. K.; Wickens, Z. K.; Grubbs, R. H. *Angew. Chem. Int. Ed.* **2015**, *54*, 7134-7138.

⁹ (a) Takeuchi, Y.; Oshige, M.; Azuma, K.; Abe, H.; Harayama, T. *Chem. Pharm. Bull.* **2005**, *53*(7), 868-869. (b) Sukemoto, S.; Oshige, M.; Sato, M.; Mimura, K.-i.; Nishioka, H.; Abe, H.; Harayama, T.; Takeuchi, Y. *Synthesis* **2008**, 3081-3087. (c) McLaughlin, N. P.; Evans, P. *J. Org. Chem.* **2010**, *75*, 518-521.

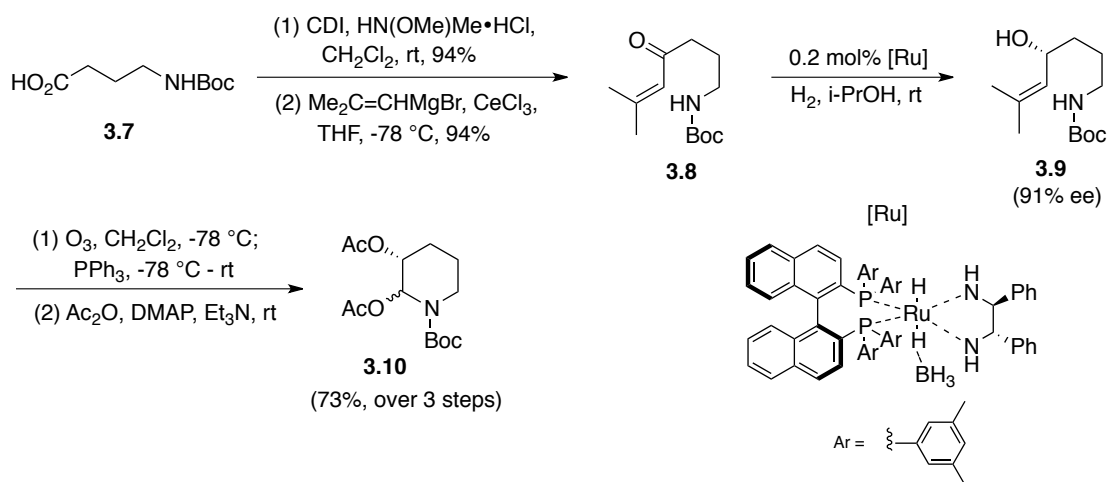
¹⁰ For reviews of chemistry of acyliminium ion, see: (a) Speckamp, W. N.; Moolenaar, M. J. *Tetrahedron* **2000**, *56*, 3817-3856. (b) Maryanoff, B. E.; Zhang, H.-C.; Cohen, J. H.; Turchi, I. J.; Maryanoff, C. A. *Chem. Rev.* **2004**, *104*, 1431-1628. (c) Yazici, A.; Pyne, S. G. *Synthesis* **2009**, *3*, 339-368. (d) Yazici, A.; Pyne, S. G. *Synthesis* **2009**, *4*, 513-541. For representative examples of *N*-protected 2,3-dihydroxypyrrolidines and 2,3-dihydroxypiperidine as precursors to iminium ions, see: (e) Macdonald, S. J. F.; Spooner, J. E.; Dowle, M. D. *Synlett* **1998**, 1375-1377. (f) Batey, R. A.; Mackay, D. B. *Tetrahedron Lett.* **2000**, *41*, 9935-9938. (g) Okitsu, O.; Suzuki, R.; Kobayashi, S. *J. Org. Chem.* **2001**, *66*, 809-823. (h) Martin, C. L.; Overman, L. E.; Rohde, J. M. *J. Am. Chem. Soc.* **2010**, *132*, 4894-4906. (i) Miller, K. E.; Wright, A. J.; Olesen, M. K.; Hovey, M. T.; Scheerer, J. R. *J. Org. Chem.* **2015**, *80*, 1569-1576.

underwent a Lewis-acid catalyzed diastereoselective Michael addition to construct the 2,3-disubstituted piperidine fragment in the target molecule (Scheme 3.2).

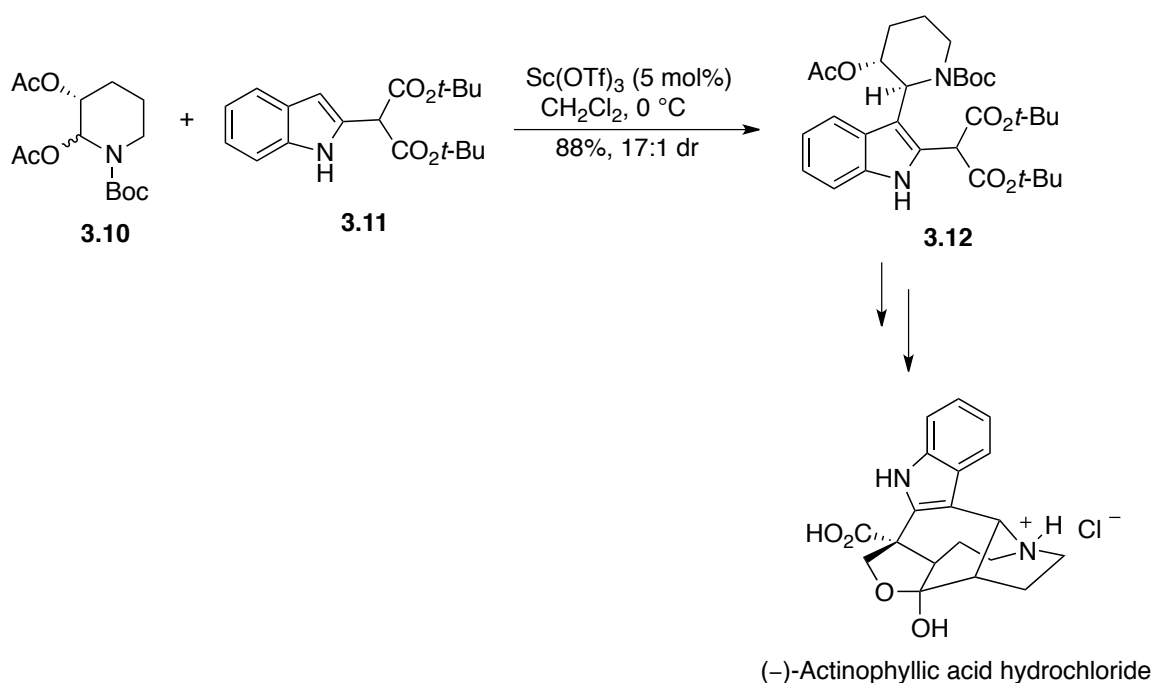


Scheme 3.2 Racemic 2,3-dihydropiperidine in Wittig reaction

Overman's group developed a synthetic route to access enantioenriched (*3R*)-2,3-diacetoxy-*N*-(tert-butoxycarbonyl)piperidine **3.10**, and used this compound in the total synthesis of (-)-actinophyllic acid (Scheme 3.4).^{9h} In presence of catalytic amount of $\text{Sc}(\text{OTf})_3$, **3.10** reacts with the substituted indole in a highly diastereoselective way.



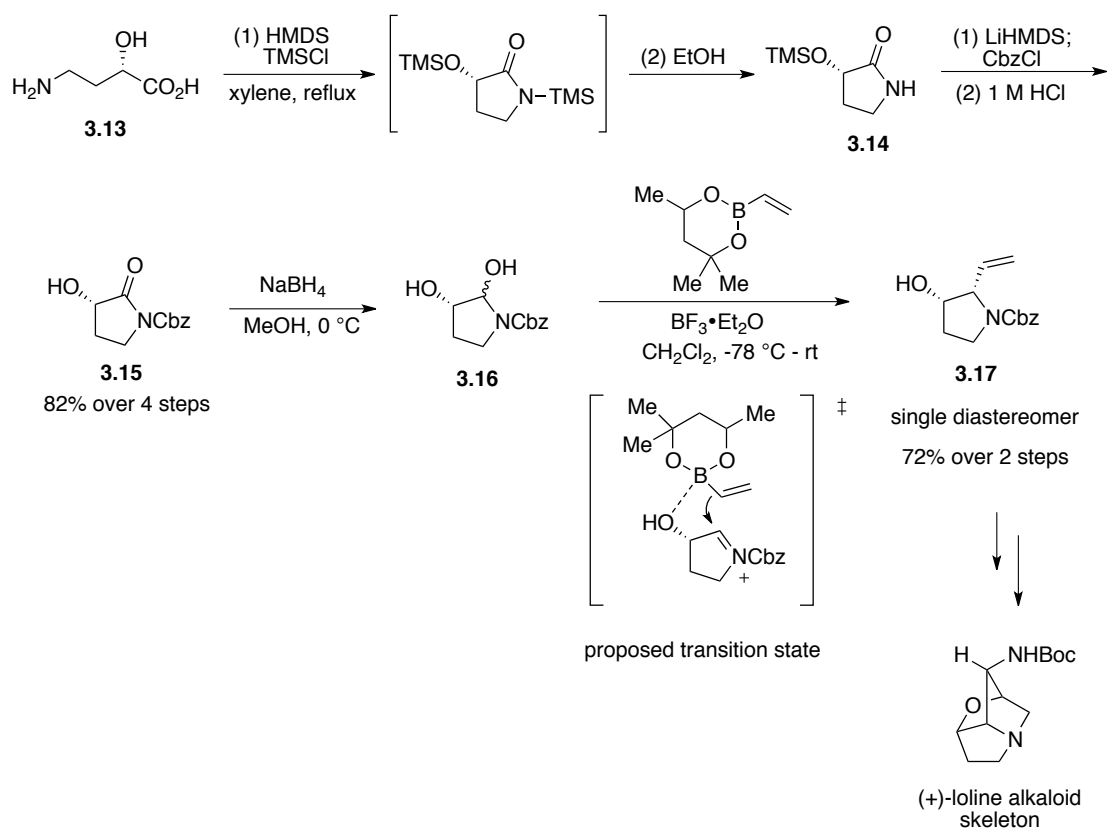
Scheme 3.3 Enantioselective synthesis of 2,3-dihydropiperidine diacetate



Scheme 3.4 2,3-Dihydroxypiperidine diacetate as an acyliminium ion precursor

Scheerer and coworkers applied Petasis borono-Mannich addition developed by Batey¹¹ in their recent synthesis of (+)-loline alkaloid skeleton (Scheme 3.5).⁹ⁱ Enantioenriched (3*S*)-2,3-dihydroxy-*N*-(benzyloxycarbonyl)pyrrolidine **3.16** was prepared from commercially available (*S*)-4-amino-2-hydroxybutanoic acid **3.13**, and used as a *N*-acyliminium ion precursor directly. The hydroxyl group at 3-position may coordinate with the vinyl boronate reagent and hence function as a directing group in the highly diastereoselective nucleophilic addition.

¹¹ Batey, R. A.; Mackay, D. B.; Santhakumar, V. *J. Am. Chem. Soc.* **1999**, *121*, 5075-5076.



Scheme 3.5 2,3-Dihydroxypyrrolidine in Petasis borono-Mannich addition

Our proposed tandem sequence can provide an alternative method of synthesizing 2,3-dihydroxypyrrolidines and 2,3-dihydroxy piperidines, and demonstrate the synthetic utility of a carefully designed tandem reaction in building up molecular complexity in a rapid fashion.

3.2 Background

3.2.1 Tandem RCM/olefin isomerization process

Ruthenium hydride complexes were well-known catalysts for olefin isomerization of allyl alcohols, allyl ethers and allyl amides in 1970s and 1980s.¹² The driving force for this type of transformation is that the carbon-carbon double bond migrates to a thermodynamically more favorable position after undergoing a series of reversible hydrometallation/ β -hydride elimination.¹³ If the ruthenium alkylidene species in the post-metathesis phase could be efficiently converted to a ruthenium hydride complex, an olefin isomerization reaction can be coupled to olefin metathesis reactions. Based on employing different hydride sources, several tandem RCM/olefin isomerization strategies have been developed.

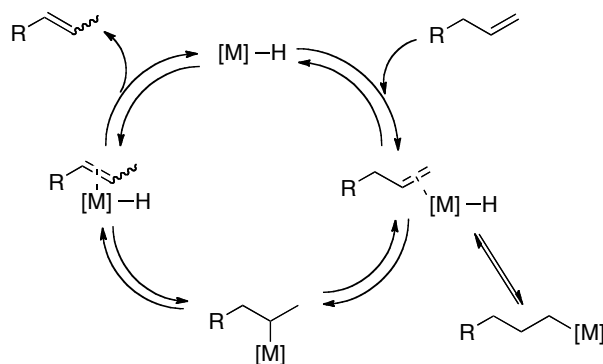


Figure 3.2 A general mechanism of transition metal hydride-catalyzed olefin isomerization

¹² (a) Sasson, Y.; Rempel, G. L.; *Tetrahedron Lett.* **1974**, 47, 4133-4136. (b) Suzuki, H.; Koyama, Y.; Moro-oka, Y.; Ikawa, T. *Tetrahedron Lett.* **1979**, 16, 1415-1418. (c) Suzuki, H.; Yashima, H.; Hirose, T.; Takahashi, M.; Moro-oka, Y.; Ikawa, T. *Tetrahedron Lett.* **1980**, 21, 4927-4930. (d) Stille, J. K.; Becker, Y. *J. Org. Chem.* **1980**, 45, 2139-2145.

¹³ For discussion of the general mechanisms, see: McGrath, D. V.; Grubbs, R. H. *Organometallics* **1994**, 13, 224-235.

Grubbs' group successfully isolated a new ruthenium hydride complex **3.18** from thermal decomposition of **GII**,¹⁴ and proved that it is an active olefin isomerization catalyst.^{13a,b} This finding not only rationalizes observed isomerization of some terminal olefins in a slow olefin metathesis reaction,¹⁵ but also sheds some light on developing a tandem RCM/olefin isomerization method. Fustero and coworkers reported an additive-free protocol¹⁶ for this type of tandem sequence (Figure 3.3). The ruthenium hydride species *in situ* generated through thermal decomposition of **GII** was believed to be the catalyst in olefin isomerization step.

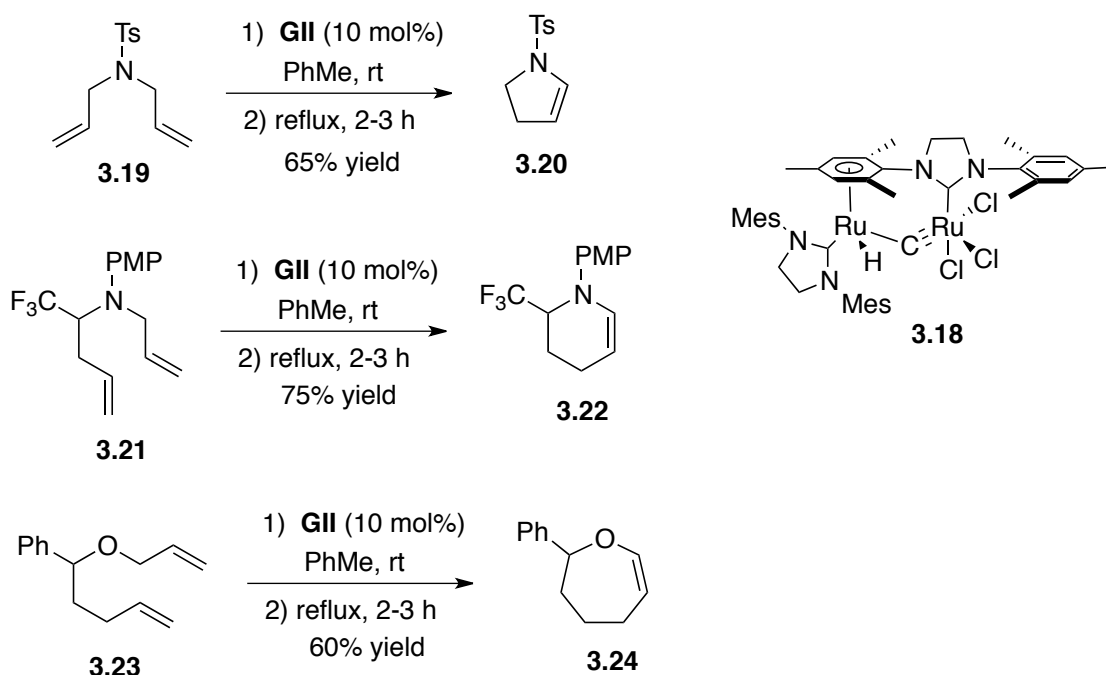


Figure 3.3 An additive-free strategy for tandem RCM/olefin isomerization

¹⁴ (a) Hong, S. H.; Day, M. W.; Grubbs, R. H. *J. Am. Chem. Soc.* **2004**, *126*, 7414-7415. (b) Hong, S. H.; Sanders, D. P.; Lee, C. W.; Grubbs, R. H., *J. Am. Chem. Soc.* **2005**, *127*, 17160-17161. (c) Hong, S. H.; Wenzel, A. G.; Salguero, T. T.; Day, M. W.; Grubbs, R. H. *J. Am. Chem. Soc.* **2007**, *129*, 7961-7968.

¹⁵ Some representative examples, see: (a) Formentín, P.; Gimeno, N.; Steinke, J. H.; Vilar, R. *J. Org. Chem.* **2005**, *70*, 8235-8238. (b) Michalak, M.; Wicha, J. *Synlett* **2005**, *15*, 2277-2280. (c) Hekking, K. F. W.; Waalboer, D. C. J.; Moelands, M. A. H.; van Delf F. L.; Rutjes, F. P. J. T. *Adv. Synth. Catal.* **2008**, *350*, 95-106.

¹⁶ Fustero, S.; Sánchez-Roselló, M.; Jiménez, D.; Sanz-Cervera, J. F.; del Pozo, C.; Aceña, J. L. *J. Org. Chem.* **2006**, *71*, 2706-2714.

Schmidt used substoichiometric amount of NaBH₄ or NaH (ca. 50 mol%) to generate ruthenium hydrides from **GI** (Figure 3.4).¹⁷ The nucleophilic replacement between sodium or boron hydride bond and ruthenium chloride bond might account for generation of ruthenium hydrides.^{17c} Nonetheless, functional groups tolerance is the limitation to this method, in which free hydroxy groups can be deprotonated and ester groups can be slowly reduced under the reaction conditions.

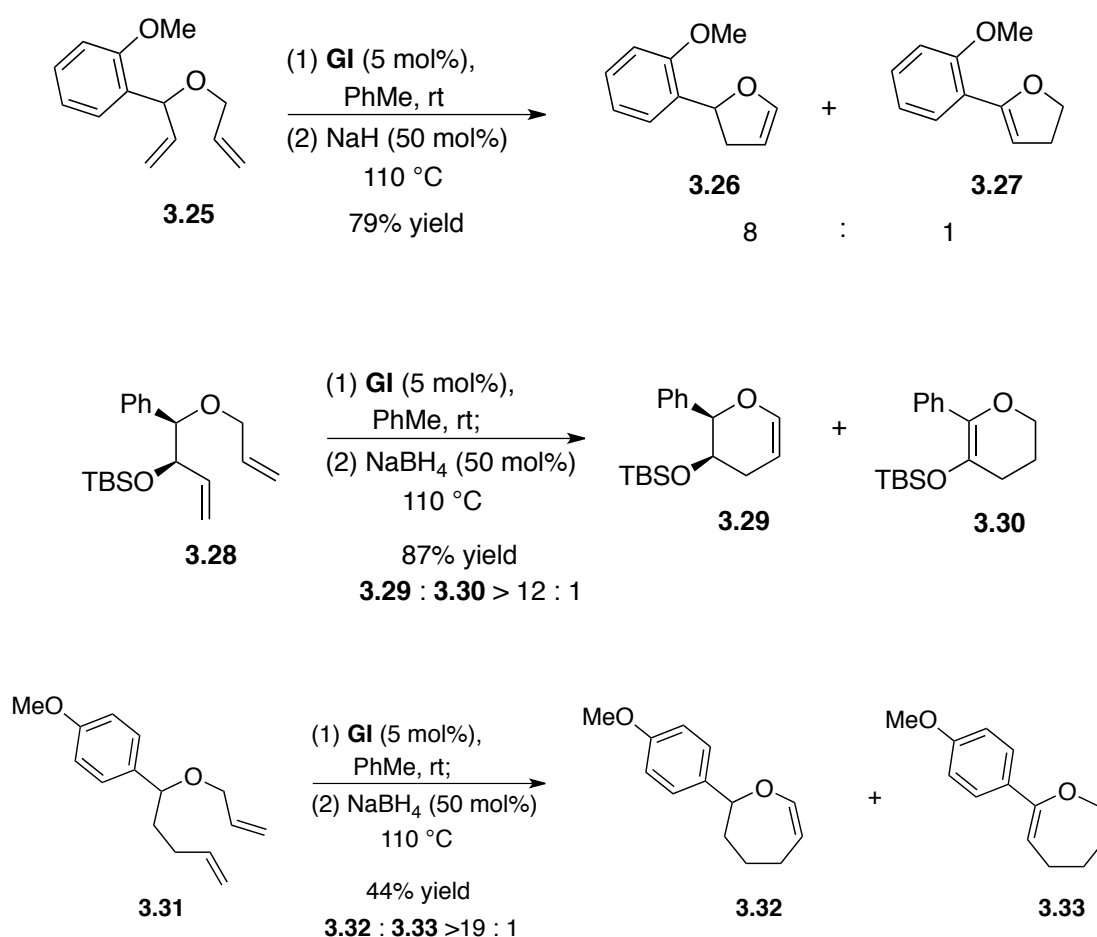


Figure 3.4 Use of NaH or NaBH₄ as the hydride source in tandem RCM/olefin isomerization

¹⁷ (a) Schmidt, B. *Eur. J. Org. Chem.* **2003**, 816-819. (b) Schmidt, B. *J. Org. Chem.* **2004**, 69, 7672-7687. (c) Schmidt, B. *J. Mol. Catal. A.* **2006**, 254, 53-57.

Schmidt also found that triethylsilane can function as a hydride source for modification of **GI**, despite longer reaction time was usually needed for good conversions in olefin isomerization step (Figure 3.5).^{17b,c} While it was not disclosed by Schmidt whether substoichiometric amount of triethylsilane would be insufficient, Cossy and coworkers observed that with excess of triethylsilane a tandem RCM/hydrogenation reaction could occur.¹⁸ It should be mentioned that for the substrates containing primary alcohols a faster dehydrogenative silylation could take place prior to the olefin migration (Figure 3.5).¹⁹

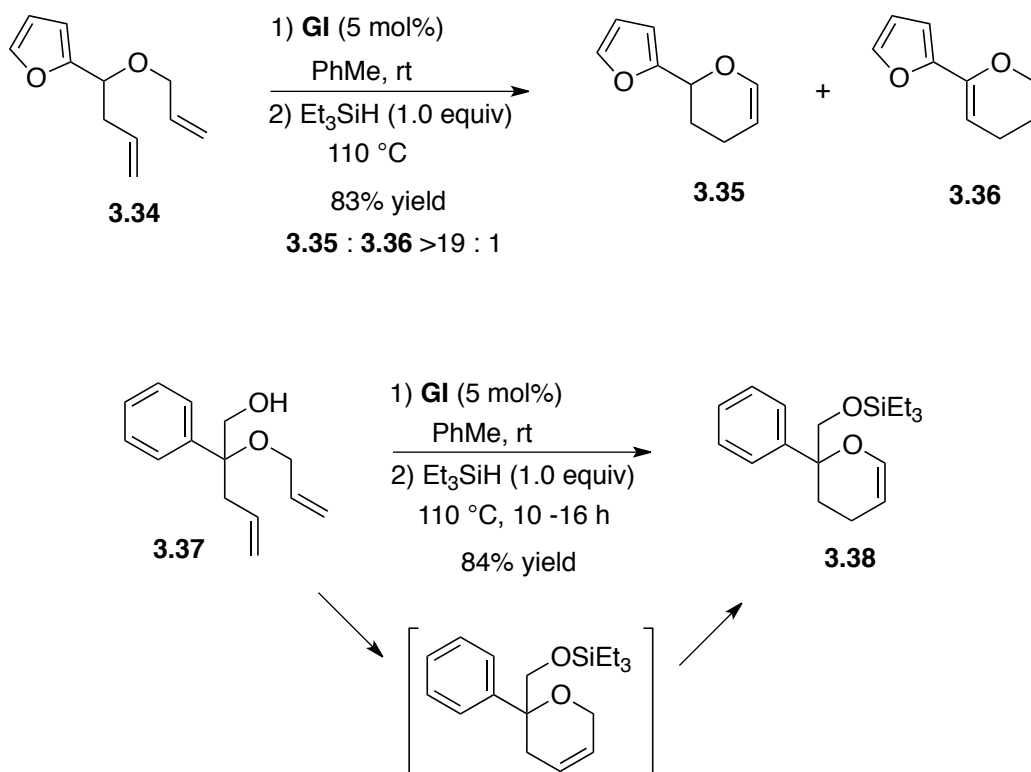


Figure 3.5 Use of triethylsilane as the hydride source in tandem RCM/olefin isomerization

¹⁸ Menozzi, C.; Dalko, P. I.; Cossy, J. *Synlett* **2005**, 16, 2449-2452.

¹⁹ Maifeld, S. V.; Miller, R. L.; Lee, D. *Tetrahedron Lett.* **2002**, 43, 6363-6366.

Inspired by Mol's study of **GI** reacting with primary alcohols in presence of inorganic or organic bases,²⁰ Schmidt discovered that *i*PrOH/NaOH is a more effective additive (Figure 3.6).^{17b} Presumably, the higher nucleophilicity of *in situ* generated isopropoxide benefits formation of ruthenium alkoxide species, which undergo β -hydride elimination to produce ruthenium hydrides. This protocol did not give satisfactory results for making five-membered rings, because isomerized products were further hydrogenated under the reaction conditions. However, this side reaction is relatively slow to the six-membered rings in the same reaction time scale.

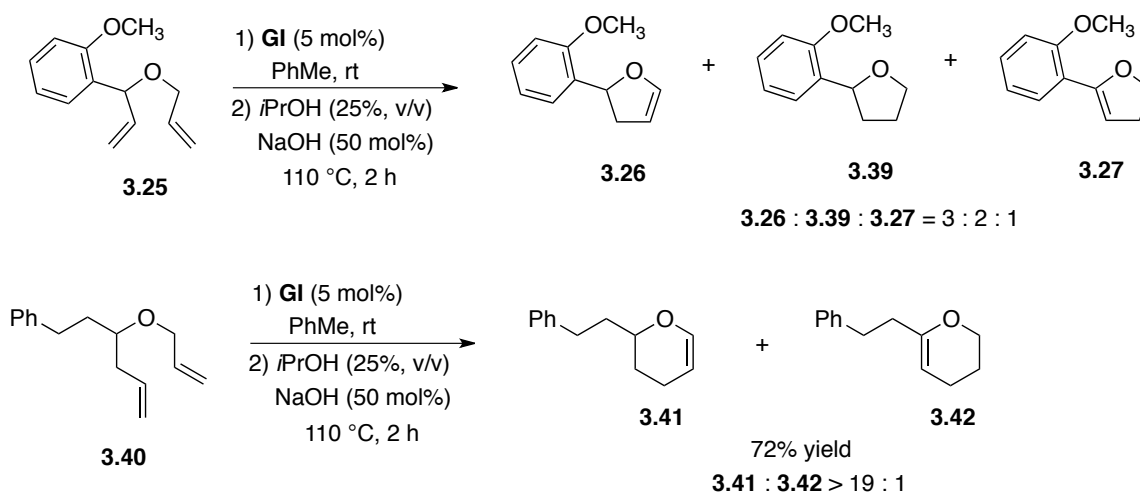


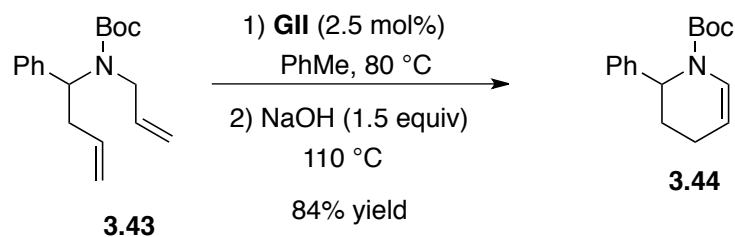
Figure 3.6 Use of *i*PrOH/NaOH as the additives in tandem RCM/olefin isomerization

More recently, Schmidt discovered that NaOH alone could be an effective additive in a tandem RCM/olefin isomerization reaction to make *N*-protected cyclic enamines (Equation 3.1).²¹ With 2.5 mol% **GII** as the ruthenium source a variety of substituted *N*-Boc-1,2,3,4-tetrahydropyridines were successfully prepared. It was not disclosed what role NaOH played in promoting the olefin isomerization step. It might

²⁰ Dinger, M. B.; Mol, J. C. *Organometallics* **2003**, 22, 1089-1095.

²¹ Schmidt, B.; Hauke, S.; Mühlenberg, N. *Synthesis* **2014**, 46, 1648-1658.

facilitate formation of ruthenium hydride **3.18**, according to a mechanism proposed by Grubbs in his study of thermal decomposition of **GII**.^{14c}



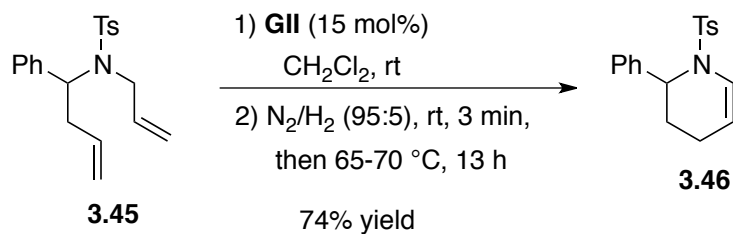
Equation 3.1 Use of NaOH as an additive in tandem RCM/olefin isomerization

Hydrogen gas is a more straightforward, cleaner and cheaper hydride source. Based on Fogg's studies of hydrogenolysis of Grubbs' catalysts under hydrogen atmosphere,²² The Snapper group found a mild condition to conduct tandem RCM/olefin isomerization (Equation 3.2 and Table 3.1).²³ After the metathesis step a gas mixture of N₂/H₂ (95:5), which is commercially available, was bubbled into the reaction solution for minutes, and then the reaction vessel was sealed and heated at 70 °C. With the highly diluted hydrogen source, olefin hydrogenation products were suppressed to less than 10%. In addition to cyclic enol ethers, they also reported the first example of making a *N*-protected cyclic enamine via a tandem RCM/olefin isomerization strategy. Immediate NMR studies of the reaction solutions sparged with N₂/H₂ mixture did not detect formation of a ruthenium hydride or other new ruthenium complexes.²³ To clarify whether this short gas-introducing process is necessary, they conducted a control

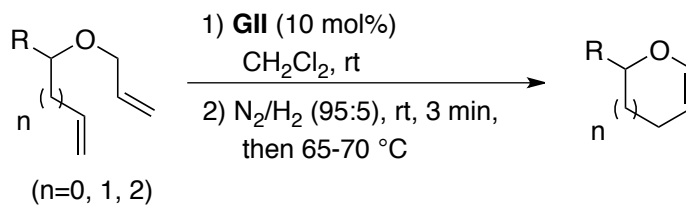
²² (a) Smanantha, D. D.; Yap, G. P. A.; Fogg, D. E. *Inorg. Chem.* **2000**, *39*, 5412-5414. (b) Drouin, S. D.; Zamanian, F.; Fogg, D. E. *Organometallics* **2001**, *20*, 5495-5497. (c) Beach, N. J.; Camm, K. D.; Fogg, D. E. *Organometallics* **2010**, *29*, 5450-5455.

²³ Sutton, A. E.; Seigel, B. A.; Finnegan, D. F.; Snapper, M. L. *J. Am. Chem. Soc.* **2002**, *124*, 13390-13391.

experiment and proved that the thermal decomposition of **GII** did not lead to an appreciable olefin isomerization under the same conditions.



Equation 3.2 Use of N_2/H_2 as the hydride source in tandem RCM/olefin isomerization



Entry	Substrate	Product	Yield (%)
1	<p>3.47</p>	<p>3.48</p>	46
2	<p>3.49</p>	<p>3.50</p>	58
3	<p>3.51</p>	<p>3.52</p>	54

Table 3.1 Use of N_2/H_2 mixture as the hydride source in tandem RCM/olefin isomerization

3.2.2 Ruthenium tetroxide-catalyzed dihydroxylation of olefins

As an analog of OsO_4 , RuO_4 can catalyze olefin dihydroxylation as well. However, carbonyl compounds, such as two molecules of aldehydes, are frequently observed as the major over-oxidation products from RuO_4 -catalyzed olefin dihydroxylation reactions. A general explanation for this oxidative cleavage of olefins is that RuO_4 , more electron-deficient than OsO_4 , tends to gain more electrons from double bonds and be reduced to low-valent ruthenium oxide species.²⁴ Frenking et al. established a computational model to explain different oxidative behaviors of RuO_4 and OsO_4 with olefins (Figure 3.7).²⁴ Due to the lower energy barrier (2.5 kcal/mol), the key Ru (VIII) intermediate in dihydroxylation can readily adopt the double-bond scission pathway. It is worth mentioning that this undesired reaction pathway is also synthetically useful, because it can serve as an alternative method to olefin ozonolysis.²⁵

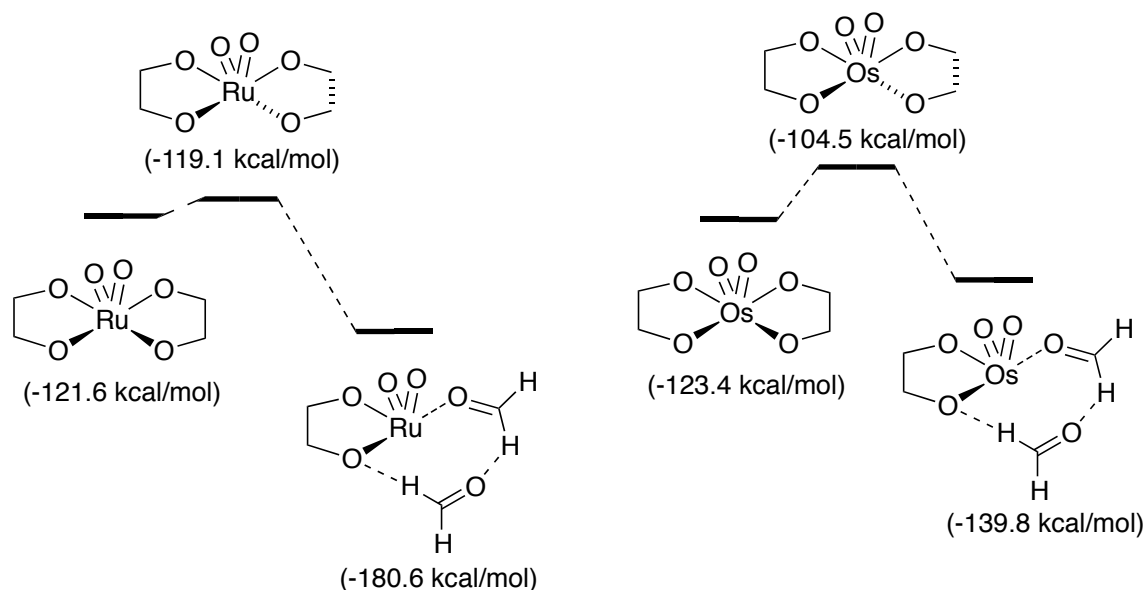
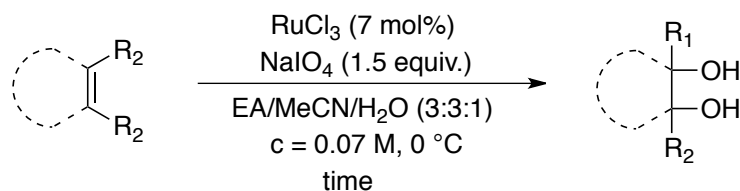


Figure 3.7 Energy diagram of oxidative olefin cleavage via RuO_4 and OsO_4

²⁴ Frunzke, J.; Loschen, C.; Frenking, G. *J. Am. Chem. Soc.* **2004**, *126*, 3642-3652.

²⁵ Yang, D.; Zhang, C. *J. Org. Chem.* **2001**, *66*, 4814-4818.

The breakthrough in RuO₄-catalyzed olefin dihydroxylation was achieved in the 1990's. A solvent mixture, EtOAc/MeCN/H₂O (3:3:1), provided a good solution to tune the reactivity of RuO₄ to the desired pathway (Table 3.2).²⁶



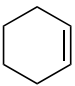
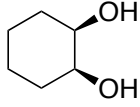
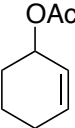
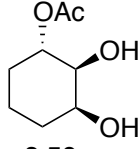
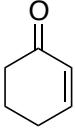
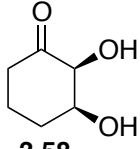
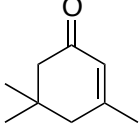
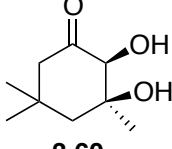
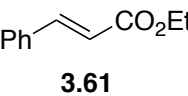
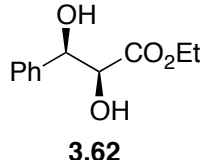
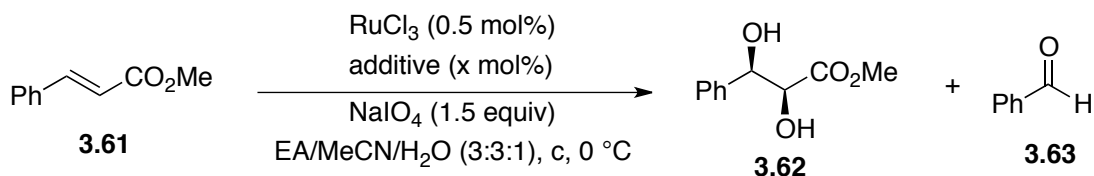
Entry	Substrate	Time (min)	Product	Yield (%)
1	 3.53	0.5	 3.54	58
2	 3.55	3	 3.56	72
3	 3.57	0.5	 3.58	36
4	 3.59	3	 3.60	81
5	 3.61	3	 3.62	77

Table 3.2 RuO₄-catalyzed olefin dihydroxylation in a solvent mixture

²⁶ (a) Shing, J. K. M.; Tai, V. W.-F.; Tam, E. K. W. *Angew. Chemie. Int. Ed.* **1994**, *33*, 2312-2313. (b) Shing, J. K. M.; Tam, E. K. W.; Tai, V. W.-F.; Chung, I. H. F.; Jiang Q. *Eur. Chem. J.* **1996**, *2*, 50-57. (c) Shing, T. K. M.; Tam, E. K. W. *Tetrahedron Lett.* **1999**, *40*, 2179-2180.

Due to the short reaction time, from half minute up to three minutes, this oxidation method was also called as “flash dihydroxylation”.^{26a} *Electron-deficient or sterically hindered olefins, which are conventionally difficult substrates in OsO₄-catalyzed olefin dihydroxylations, gave more satisfying yields in this method.*

Considering diols and aldehydes are generated from the same ruthenate intermediate through two competing routes, Plietker and Niggemann proposed that addition of a proton source would benefit generation of diols by facilitating the hydrolysis process (Table 3.3).²⁷ Through screening, sulfuric acid (2M aqueous solution) turned to be most effective, and the accelerated turnover of RuO₄ allowed a much lower catalyst loading (0.5 mol%) to be used. In order to improve tolerance of functional groups, the same group subsequently investigated the influence of Lewis acids on dihydroxylation, and discovered that CeCl₃ gave the best chemoselectivity along with good conversions among the screened metal chlorides (Table 3.3).^{28,29}



Entry	Additive (x mol%)	c (M)	3.62:3.63 ^a	Yield (%)
1	—	0.07	2.8:1	47
2	aq. H ₂ SO ₄ (5)	0.07	3.8:1	71
3	—	0.28	2:1	61 ^b
4	CeCl ₃ •7H ₂ O (10)	0.28	21:1	82

^aDetermined by GC. ^bConversion, determined by GC.

Table 3.3 Influence of different additives on selectivity and yields of olefin dihydroxylation

²⁷ Plietker, B.; Niggemann, M. *Org. Lett.* **2003**, 5, 3353-3356.

²⁸ Plietker, B.; Niggemann, M. *J. Org. Chem.* **2005**, 70, 2402-2405.

²⁹ Metal bromides and iodides will be oxidized under the same reaction conditions.

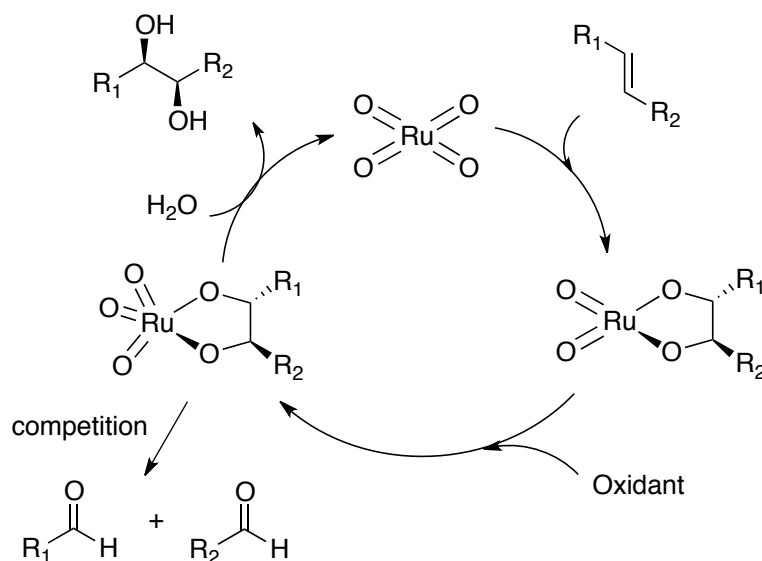


Figure 3.8 Proposed catalytic cycle of RuO_4 -catalyzed olefin dihydroxylation

Although the specific mechanism of CeCl_3 in Plietker's dihydroxylation strategy is still unclear, Plietker assessed the possible role of this reagent: (1) decreasing pH value of the reaction solutions, similar to the effect of sulfuric acid; (2) *in situ* reacting with NaIO_4 to form a Ce(IV) -periodato complex, which possesses higher redox potential.

Reoxidant	pH value	Redox potential (V)	3.62:3.63
NaIO_4	2.8	1.020	1:1
$\text{CeCl}_3/\text{NaIO}_4$	1.94	1.075	10.2:1
$\text{H}[\text{Ce}(\text{IO}_6)]/\text{NaIO}_4$	2.61	1.071	4.6:1

Table 3.4 Influence of CeCl_3 as an additive on pH and redox potential

An argument about generation of aldehydes or ketones in the above mentioned catalytic system is that they may come from a rapid glycol cleavage of *cis*-diol products by NaIO_4 , instead of oxidative cleavage of corresponding olefins by RuO_4 . To gain some insight on the relative rate of these two possible pathways, Plietker treated hydrobenzoin (1,2-diphenyl-1,2-ethanediol) with NaIO_4 and set up a dihydroxylation reaction of *trans*-

stilbene at the same time.²⁷ When the dihydroxylation reaction reached almost full conversion, the glycol cleavage of hydrobenzoin was still in initiation phase. This implies that if the RuO₄-catalyzed dihydroxylation was quenched in timely fashion, one should not observe any glycol cleavage of generated 1,2-diols by NaIO₄.

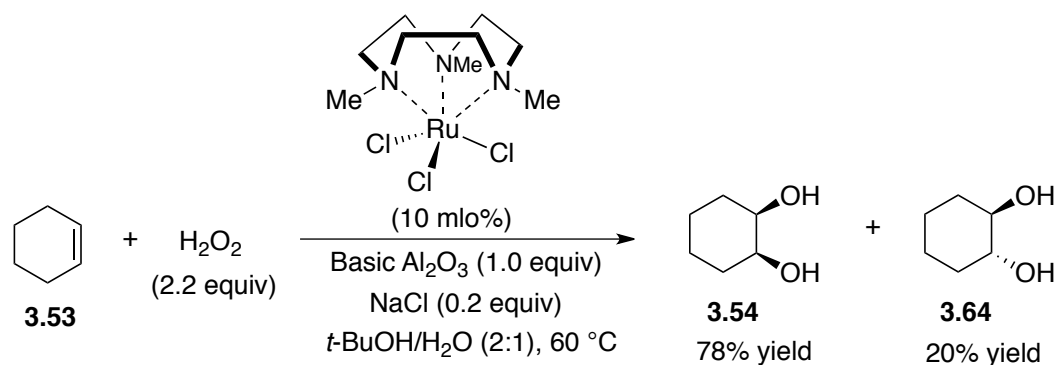
3.2.3 Low-valent Ruthenium oxide-catalyzed dihydroxylation of olefins

Low-valent ruthenium oxide species can also be used in dihydroxylation of olefins, but only few examples have been published. Che's group first studied the stoichiometric *cis*-dihydroxylation of unfunctionalized olefins with a Ru(VI) complex,³⁰ and then developed a ruthenium (III)-based catalytic system for synthesizing *cis*-diols from olefins with hydrogen peroxide as the oxidant.³¹ In the latter case, basic alumina and NaCl were employed as additives to improve the selectivity toward *cis*-products, but the mechanism of them in the reaction was unclear. With the Ru(III)/H₂O₂ system most simple olefins gave good yields and high selectivities, but electron-deficient olefins reacted tardily in the same condition. When **3.61** was used as the substrate no reaction occurred. Che and co-workers also investigated a Ru(IV)/porphyrin complex-catalyzed dihydroxylation of styrenes.³² Diols products were generated through *in situ* ring-opening hydrolysis of corresponding epoxide intermediates.

³⁰ Yip, W.-P.; Yu, W.-Y.; Zhu, N.; Che, C.-M. *J. Am. Chem. Soc.* **2005**, *127*, 14239-14249.

³¹ Yip, W.-P.; Ho, C.-M.; Zhu, N.; Lau, T.-C.; Che, C.-M. *Chem. Asian J.* **2008**, *3*, 70-77.

³² Hu, W.-X.; Li, P.-R.; Jiang, G.; Che, C.-M.; Chen, J. *Adv. Synth. Catal.* **2010**, *352*, 3190-3194.



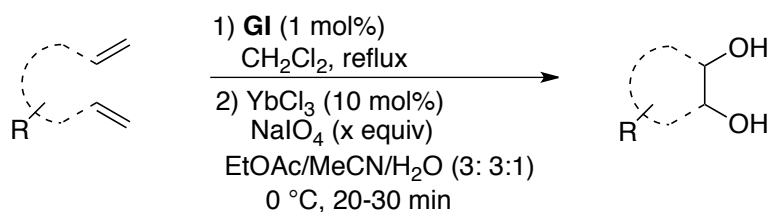
Equation 3.3 Low-valent Ru-catalyzed olefin dihydroxylation

3.2.4 Tandem RCM/olefin dihydroxylation reactions³³

Blechert's group reported the first tandem RCM/olefin dihydroxylation sequence (Table 3.5).³⁴ Through control experiments with different Grubbs' catalysts, they found NHC-ligated ruthenium catalysts exhibited a relatively lower activity in oxidation. The strong affinity between NHC and ruthenium presumably restrained generation of the active ruthenium oxide smoothly.³⁴ Electron-deficient alkenes produced in the RCM step gave higher yields of the diol products. To achieve better yields in dihydroxylation step, dichloromethane, the solvent used in metathesis step, needs to be fully removed. Small amount of this solvent residing in metathesis products caused low yields in oxidation. In addition, they used YbCl_3 , instead of CeCl_3 , as an additive in the dihydroxylation step.

³³ For tandem cross metathesis/olefin dihydroxylation, see reference 8, 34 and 35.

³⁴ Beligny, S.; Eibauer, S.; Maechling, S.; Blechert, S. *Angew. Chemie. Int. Ed.* **2006**, 45, 1900-1903.



Entry	NaIO_4 (equiv)	Substrate	Product	Yield (%)
1	1.6	 3.65	 3.66	33
2	1.6	 3.67	 3.68	63
3	1.4	 3.69	 3.70	88 (0.8:1 dr)
4	1.4	 3.71	 3.72	49 (24:1 dr)

Table 3.5 Representative examples of Blechert's tandem RCM/olefin dihydroxylation

Shortly after Blechert's publication, the Snapper group also reported a tandem RCM/olefin dihydroxylation protocol (Table 3.6),³⁵ in which ethyl acetate was used as the solvent in the metathesis step to avoid an extra solvent-swapping operation in

³⁵ Scholte, A. A.; An, M. Y.; Snapper, M. L. *Org. Lett.* **2006**, 8, 4759-4762.

Blechert's method. The typically used solvent composition, EtOAc/MeCN/H₂O = 3:3:1, in RuO₄-catalyzed olefin dihydroxylation was modified to EtOAc/MeCN/H₂O = 6:6:1.

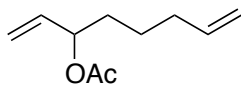
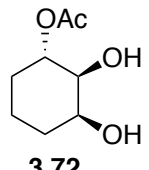
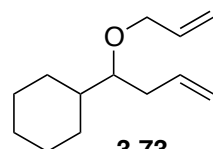
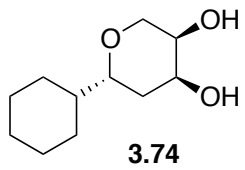
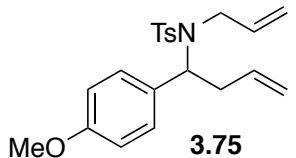
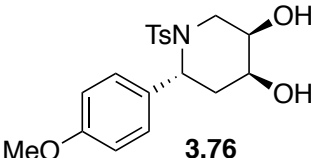
$ \begin{array}{c} \text{1) GII (5 mol\%)} \\ \text{EtOAc, rt} \\ \text{2) CeCl}_3 \cdot 7\text{H}_2\text{O (10 mol\%)} \\ \text{NaIO}_4 \text{ (1.5 equiv)} \\ \text{EtOAc/MeCN/H}_2\text{O (6:6:1), 0 }^\circ\text{C} \end{array} $			
Entry	Substrate	Product	Yield (%)
1	 3.71	 3.72	60 (22:1 dr)
2	 3.73	 3.74	69 (1.5:1 dr)
3	 3.75	 3.76	77 (7:1 dr)

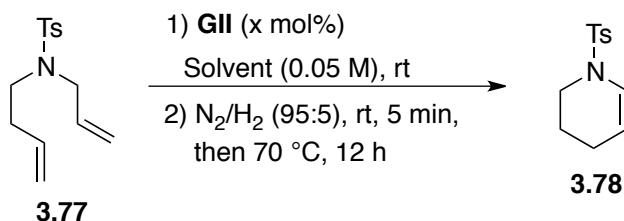
Table 3.6 Representative examples of Snapper's tandem RCM/olefin dihydroxylation

We envisioned that the tandem RCM/olefin isomerization strategy developed by the Snapper group is more compatible with our proposed three-step tandem sequence. The N₂/H₂ (95:5) mixture used as the additive in the olefin isomerization step will leave the least “contamination” to the following dihydroxylation reaction. On the other hand, the ene-carbamates and ene-sulfonamides generated from the olefin isomerization step are electron-rich olefins, which may not be applicable in RuO₄-catalyzed olefin dihydroxylation. Hence, we started to explore specific reaction conditions for each step in our proposed three-step tandem sequence.

3.3 Modification of previously established RCM/olefin isomerization condition

In order to simplify the procedure for the olefin dihydroxylation step, we decided to modify the established RCM/olefin isomerization condition developed by our group. RuO₄-catalyzed olefin dihydroxylation requires a specific solvent mixture (EtOAc/MeCN/H₂O, 3:3:1) to achieve good yields, but our tandem RCM/olefin isomerization strategy employs CH₂Cl₂ in the sequential two steps. To avoid a solvent swapping operation (from CH₂Cl₂ to EtOAc/MeCN/H₂O), it would be more practical to use EtOAc as the initial solvent. More importantly, Blechert's study revealed that small amount of CH₂Cl₂ was detrimental to Ru-catalyzed olefin dihydroxylation.³⁴

Control experiments were first conducted to test the solvent effect (Table 3.7). Diene **3.77** was chosen as the model substrate, because an analog of this compound (**3.45**) was successfully applied in a tandem RCM/olefin isomerization reaction.²³



Entry	GII (mol%)	Solvent	Yield (%)
1	15	CH ₂ Cl ₂	98
2	10	CH ₂ Cl ₂	98
3	10	EtOAc	24 ^a

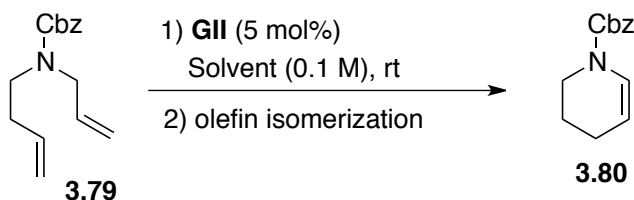
^a73% RCM product was isolated.

Table 3.7 Solvent effect on tandem RCM/olefin isomerization reaction

At the same catalyst loading ene-sulfonamide **3.78** was generated in a high yield in CH₂Cl₂ but in a much lower yield in EtOAc (entry 2 and 3). 73% RCM product was recovered from the reaction of entry 3 in Table 3.7, which indicated that the low yield of

the tandem reaction was not due to an unsuccessful RCM reaction but to an unsuccessful olefin isomerization. Presumably, EtOAc competed with the ring-closing metathesis product to coordinate with the active ruthenium complex, and hence made olefin isomerization sluggish.

In case that diene **3.77** is not a good substrate in the new condition, a *N*-Cbz diene **3.79** was examined for optimization of the olefin isomerization condition (Table 3.8).



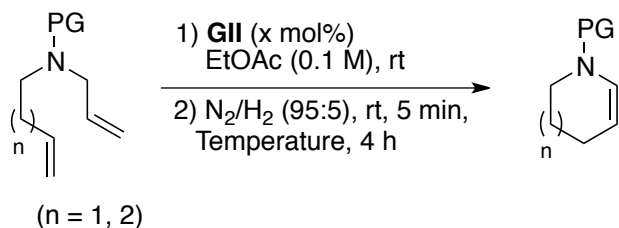
Entry	Solvent	Hydride Source	Temp. (°C)	Time (h)	Yield (%)
1	CH ₂ Cl ₂	N ₂ /H ₂ (95:5), rt, 5 min	70	12	76
2	EtOAc	N ₂ /H ₂ (95:5), rt, 5 min	70	12	19
3	EtOAc	N ₂ /H ₂ (95:5), rt, 10 min	70	12	14
4	EtOAc	N ₂ /H ₂ (95:5), rt, 5 min	100	12	96
5	EtOAc	N ₂ /H ₂ (95:5), rt, 5 min	100	4	90
6	EtOAc	—	100	4	11

Table 3.8 Optimization of the olefin isomerization step

Switching the solvent from CH₂Cl₂ to EtOAc also led to a low yield (entry 1 and 2, Table 3.8). Prolonging the time of bubbling the gas mixture (N₂/H₂, 95:5) into the reaction solution did not solve this problem (entry 3), although it was expected that more ruthenium hydride could be generated through exposing **GII** to H₂ atmosphere. Finally, we found that increasing temperature of the isomerization step was an effective and direct way to regain the reactivity (96% yield, entry 4), and the reaction time could be reduced to 4 h with slight drop in yield (entry 5). Since there is a precedent that showed the Ru-H complex generated from thermal decomposition of **GII** were effective enough for olefin

isomerization,¹⁶ someone would argue that our method might rely on a similar mechanism and the aid of an external hydride source is unnecessary. To resolve this confusion, we did a blank experiment (entry 6) to demonstrate that introduction of highly diluted H₂ is imperative for a good yield.

Next, we evaluated other diene substrates in the new tandem RCM/olefin isomerization conditions (Table 3.9 and Table 3.10).



Entry	Substrate	Product	GII (mol%)	Temp. (°C)	Yield (%)
1	<p>3.81</p>	<p>3.82</p>	5	100	71
			10	100	34
2	<p>3.77</p>	<p>3.78</p>	5	100	14
			10	100	34
			10	120	89
3	<p>3.83</p>	<p>3.84</p>	5	100	51
			10	100	68

Table 3.9 Optimization of the olefin isomerization step

N-Boc diene **3.81** reacted smoothly under the optimal condition used for **3.79**, but diene **3.77** still showed a much lower reactivity (entry 1 and 2, Table 3.9). While increasing catalyst loading did improve the yield of ene-sulfonamide **3.78**, higher temperature was found to be more effective. At 120 °C after 4 h ene-sulfonamide **3.78** was obtained in 89% isolated yield (entry 2). For preparation of the seven-membered ring product **3.84**, the reaction also went sluggishly, and we observed another olefin regiomers from ¹H-NMR of the unpurified product. By increasing catalyst loading to 10 mol%, we improved the yield of cyclic ene-carbamate **3.84** to 68% (entry 3), which is synthetically useful for the dihydroxylation step.

Entry	Substrate	Product	Time (h)	Yield (%)
1	 3.85	 3.86	4	81
			2	84
2	 3.87	 3.88	2	67
3	 3.89	 3.90	2	86

Table 3.10 Optimization of olefin isomerization step

The reaction time for making five-membered rings can be further reduced to 2 h while achieving a comparable yield (entry 1 and 2, Table 3.10). A possible explanation for this observation is that in the course of β -hydride elimination the heterocyclic rings needs to adopt a suitable conformation to reach good orbital alignment of the C-Ru bond and the adjacent C-H bond, and the energy barrier between the envelope conformation and the half-chair conformation of a five-membered ring is relatively lower (for cyclopentane, it is less than 3 kcal/mol). For the six-membered rings, the energy barrier between a chair and a half-chair conformation is relatively higher (for cyclohexane, it is about 10 kcal/mol). Thus, olefin isomerization of five-membered heterocyclic rings is faster than that of the six-membered rings.

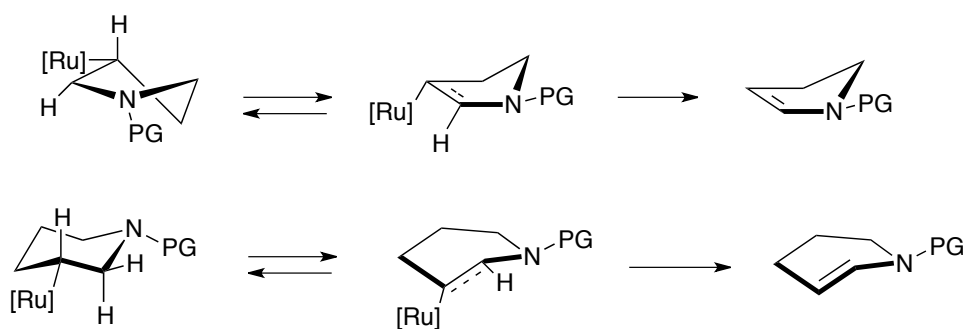
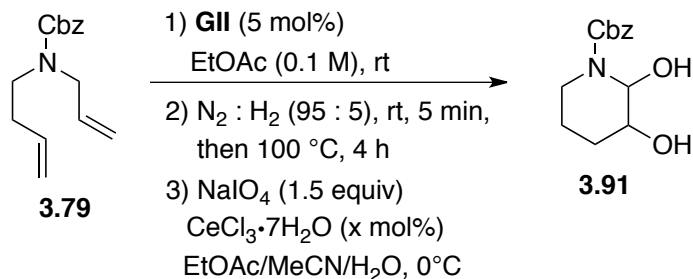


Figure 3.9 Proposed transition states of β -hydride elimination

3.4 Development of tandem RCM/olefin isomerization/olefin dihydroxylation sequence

As the new condition for tandem RCM/olefin isomerization was established, we started to investigate the olefin dihydroxylation step. The basis of this exploration is the previously reported $\text{RuCl}_3/\text{NaIO}_4/\text{CeCl}_3 \cdot 7\text{H}_2\text{O}$ catalytic system for olefin dihydroxylation.

Diene **3.79** was selected as the model substrate in the three-step tandem reaction, as the OsO₄-catalyzed dihydroxylation of ene-carbamate **3.80** to make diol **3.91** had been reported before.^{9b,10g} Through adjusting additive loading and specific solvent composition, we assessed the effect of these two factors on the reaction yield and the ratio of *cis/trans* diastereomers.



Entry	CeCl ₃ ·7H ₂ O (mol%)	EtOAc/MeCN/H ₂ O	Time (min)	Yield ^a (%)	dr ^b (<i>cis:trans</i>)
1	10	3:3:1	35	41(33) ^c	1.2:1
2	25	3:3:1	45	53	1.4:1
3	25	6:6:1	60	60(46) ^c	1.5:1
4	25	4:6:1	60	52	1.6:1
5	25	4:6:3	50	35	2.3:1
6	—	3:3:1	15	38(<24) ^c	2.0:1

^aDetermined by ¹H-NMR of the unpurified product with 1,3,5-trimethoxybenzene as the internal standard. ^bDetermined by integrations of ¹H-NMR of the unpurified products. ^cThe isolated yield is shown in the parenthesis.

Table 3.11 Exploration of key factors in the olefin dihydroxylation step

With the same dihydroxylation condition reported by Plietker, only 33% diol **3.91** was obtained (entry 1). The major byproduct was also isolated, but we could not identify its specific structure. Through comparison of the ¹H-NMR and high-resolution mass spectra of the desired product and the byproduct, we tentatively assigned the byproduct to be a dimer of diol **3.91** (two molecules **3.91** condensed with each other by losing one molecule H₂O). In absence of CeCl₃·7H₂O the ene-carbamate **3.80** was completely

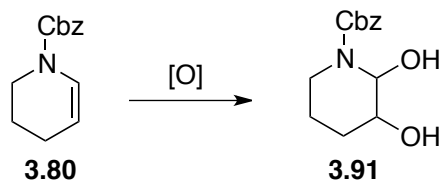
consumed in the oxidation step in 15 min, and the byproduct was the major product (> 39% isolated yield, entry 6). It should be noted that separation of the desired product and the byproduct is quite difficult, due to their close R_f values (with a hexanes/ethyl acetate mixture as the developing solvent, they show as the same spot in TLC; with a mixture of dichloromethane, hexanes and ethanol, the R_f difference of them is 0.08 after being developed twice on the TLC plate). The result of entry 6 suggested that addition of a Lewis acid suppressed formation of the byproduct, and it ruled out the theory that CeCl₃ caused formation of the byproduct. We also tried other oxidants, for instance, N-Methylmorpholin N-oxide (NMO), (NH₄)₂S₂O₈ or KBrO₃, to replace NaIO₄, but they either gave no reaction or produced very low conversion in the dihydroxylation step.

We assumed that lowering the concentration of IO₄ anion in the solution could be an effective way to improve the yield. The inspiration for this assumption is that CeCl₃ can *in situ* react with NaIO₄ to generate a water-insoluble Ce(IV)-periodato complex,³⁶ which might serve as the actual oxidant in the Ru-catalyzed dihydroxylation, and addition of 10 mol% CeCl₃•7H₂O indeed prolonged the reaction time needed for full conversion of ene-carbamate **3.80** in the dihydroxylation step and resulted in a higher yield (entry 1 and entry 6, Table 3.11). When the additive loading was increased to 25 mol% we observed a further improved yield (entry 2, Table 3.11). Another way to “manipulate” the concentration of IO₄ anion is changing the composition of reaction solvent. NaIO₄ is soluble in MeCN and H₂O but insoluble in EtOAc. When less H₂O is added, less NaIO₄ will be dissolved in the organic phase, whereas decreasing EtOAc added in the solvent

³⁶ Levason, W.; Oldroyd, R. D. *Polyhedron* **1998**, *15*(3), 409-13.

will lead to more NaIO₄ being dissolved. Results of entry 2, 3, 4 and 5 in Table 3.11 indicated that reducing the content of H₂O in the solvent benefitted the yield.

The diastereoselectivity in the above dihydroxylation reaction is more complicated than we thought. Although, according to the mechanism of OsO₄-catalyzed olefin dihydroxylation, someone would expect the *cis*-isomer as the absolute product, it is known that dihydroxylation of ene-carbamate **3.80** can also produce a *trans*-diol.^{9b,10g} Shū Kobayashi found that the diastereomeric ratio was sensitive to specific dihydroxylation conditions (Table 3.12).



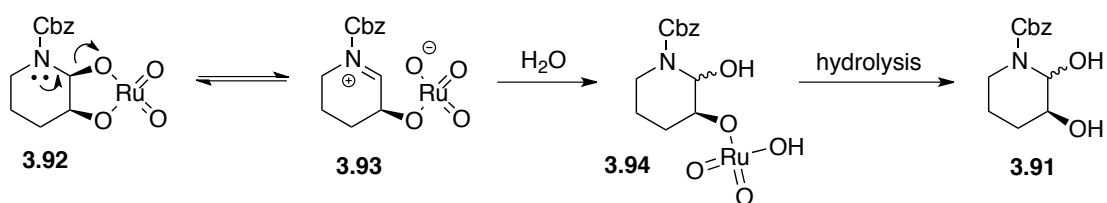
Entry	Dihydroxylation condition	Yield	dr ^a (<i>cis:trans</i>)
1	MC ^b OsO ₄ (5 mol%)	79	100:0
	NMO (1.5 equiv)		
	Acetone/MeCN/H ₂ O (1:1:1)		
2	K ₂ OsO ₄ •2H ₂ O (1.7 mol%)	73	4:1
	K ₃ Fe(CN) ₆ (3.0 equiv)		
	CH ₃ SO ₂ NH ₂ (0.08 equiv)		
	K ₂ CO ₃ (3.0 equiv)		
	<i>t</i> -BuOH/H ₂ O (1:1)		

^aDetermined by ¹H-NMR. ^bMC: Microencapsulated.

Table 3.12 Kobayashi's study of dihydroxylation of ene-carbamate 3.80

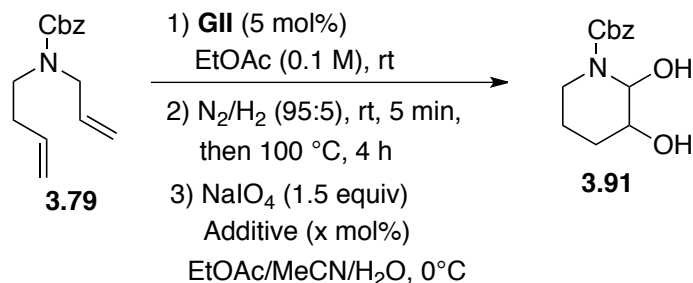
If the *cis*- and *trans*-isomers were not thermally interconvertible under the dihydroxylation condition, an iminium intermediate **3.93** could be used to explain observed epimerization at C-2 position. Ru(VIII) is more Lewis acid than Os(VIII). If RuO₄ were the catalyst in the dihydroxylation step, it would be highly possible that the

cyclic ruthenate fragment acted as a leaving group to generate **3.93**, which could be further trapped by H₂O in a less stereoselective fashion. In addition, Ce(IV) or the active proton generated from CeCl₃ and NaIO₄ in the aqueous phase can coordinate with one Ru-O double bond, making the ruthenium more Lewis acidic and a better leaving group. On the other hand, if *cis* and *trans*-isomers were interconverting to each other under the reaction condition, the diastereomeric ratio would be eventually under thermodynamic control after the *cis* and *trans*-diols reached equilibrium. For the condition of entry 1 in Table 3.11, if the reaction was quenched at 15 min before it proceeded to completion, we observed 1.1:1 ratio of the *cis*-diol to *trans*-diol. Based on the results in Table 3.11, it is more likely that the diastereomeric ratio of product **3.91** is eventually thermodynamically controlled under the reaction conditions.



Scheme 3.6 The proposed pathway of epimerization of the hydroxyl group at C-2 position

After some insight was gained of how additive loading and solvent composition can affect the yield, we continued to optimize the dihydroxylation step (Table 3.13).



Entry	Additive (mol%)	EtOAc/MeCN/H ₂ O	Time (min)	Yield ^a (%)	dr ^b (<i>cis:trans</i>)
1	CeCl ₃ •7H ₂ O (25)	8:8:1	90	49	1.4:1
2	CeCl ₃ •7H ₂ O (25)	10:10:1	120	43	1.4:1
3	CeCl ₃ •7H ₂ O (10)	10:10:1	165	52	1.5:1
4	LaCl ₃ •7H ₂ O (25)	10:10:1	180	56	1.5:1
5	LaCl ₃ •7H ₂ O (25)	8:8:1	135	50	1.3:1
6 ^c	LaCl ₃ •7H ₂ O (25)	10:10:1	210	50	1.5:1

^aIsolated yields after column chromatography. ^bDetermined by integrations of ¹H-NMR of the unpurified products. ^c1.25 equiv NaIO₄ was used.

Table 3.13 Further optimization of the olefin dihydroxylation step

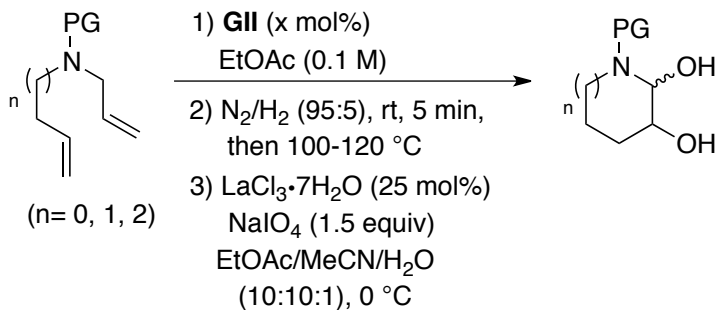
A concern we had was that the hydroxyl group at C-2 position in the product is acid-labile. A high Lewis acidic environment can cause decomposition of diol **3.91**. On the other hand, NaIO₃, the main reduced product of NaIO₄, is a weak Lewis base (pK_a of HIO₃ is 0.75) and may buffer the acidity introduced by addition of CeCl₃•7H₂O. Furthermore, as the reaction time was prolonged the oxidative cleavage of diol **3.91** by NaIO₄ might become more appreciable. Hence, a carefully balanced condition is important to the dihydroxylation step.

At 25 mol% loading of CeCl₃•7H₂O further reduction of H₂O content in the reaction solvent decreased the yield (entry 1 and 2, Table 3.13). Lowering CeCl₃•7H₂O to 10 mol% while maintaining the solvent composition enhanced the yield (entry 2 and 3). We think this variation reflected the acidity of the reaction environment where the stability of diol **3.91** also should be taken into account. Considering CeCl₃•7H₂O or

$\text{YbCl}_3 \cdot 6\text{H}_2\text{O}$ is effective in promoting RuO_4 -catalyzed olefin dihydroxylation, it is reasonable to select a less Lewis acidic lanthanide trichloride as the additive to relieve the potential stability issue with diol **3.91**. Imamoto and coworkers already demonstrated that La^{3+} is less Lewis acidic than Ce^{3+} under their evaluating conditions.³⁷ When 25 mol% $\text{LaCl}_3 \cdot 7\text{H}_2\text{O}$ was used to replace $\text{CeCl}_3 \cdot 7\text{H}_2\text{O}$, a higher yield was achieved (entry 4). 1.25 equiv of NaIO_4 was also tried in the reaction, but the yield was slightly diminished (entry 6). When 1.0 equiv NaIO_4 was used the dihydroxylation could not proceed to completion even after 9 h at 0 °C. Thus, the condition of entry 6 in Table 3.13 was found to be the optimal condition for the last step.

With all the optimal conditions for the designed tandem sequence established, we evaluated other diene substrates in our method.

³⁷ Tsuruta, H.; Yamaguchi, K.; Imamoto, T. *Tetrahedron* **2003**, *59*, 10419-10438.



Entry	Substrate	GII (mol%)	Product	Yield ^a (%)	dr ^b
1	3.85	5	3.95	16	2:1
2	3.89	5	3.96	36	1.5:1
3	3.81	5	3.97	40	2:1 (<i>cis:trans</i>)
4	3.79	5	3.91	61	1.5:1 (<i>cis:trans</i>)
5	3.77	10	3.98	74	6.1:1
6	3.83	10	3.99	29	1.7:1

^aIsolated yields. ^bDetermined by integrations of ¹H-NMR of the purified products.

Table 3.14 Substrate scope of tandem RCM/olefin isomerization/olefin dihydroxylation

The yields of obtained 1,2-diol products, which contain different protecting groups and ring sizes, manifested the influence of electronic effect and ring strain on the Ru-catalyzed olefin dihydroxylation. Substrates bearing a more electron-withdrawing protecting group produced higher yields. Compared with Boc and Cbz group, tosyl group is more electron-withdrawing and the protected nitrogen atom donates less electron density to the alkenyl moiety in the corresponding ene-sulfonamides. Previously reported studies concluded that electron-deficient olefins are more suitable in RuO₄-catalyzed dihydroxylations. The results we obtained confirmed this conclusion. For instance, the yields of six-membered ring products increased from diol **3.97**, **3.91** to **3.98** (entry 3, 4 and 5), which matches the distinctive electron-withdrawing capabilities of Boc, Cbz and Ts groups. Notably, the isolated yields of ene-carbamate **3.80** (90%, entry 5, Table 3.8) and ene-sulfonamide **3.78** (89%, entry 2, Table 3.9) are very close to each other, hence the overall yields of the tandem reactions reflect their reactivity difference in the dihydroxylation step. This trend was also observed by comparing the yield of diol **3.96** and **3.95** (entry 1 and 2).

Additionally, the significant difference of the yields obtained from different ring systems drove us to think that ring strain may pose impact on their reactivities. From the ¹H-NMR of the unpurified products we did observe aldehyde signals, which presumably come from the oxidative cleavage products of either cyclic enamine intermediates or the 1,2-diols. Based on the integrations of ¹H-NMR of the crude products, the ratio of diol **3.98** to the corresponding aldehyde byproduct is 27.5:1, but for diol **3.96** this ratio is about 1:1. A possible explanation is that five and seven-membered heterocyclic rings contain higher ring strain, compared with that of six-membered rings, hence the ruthenate

intermediates in the dihydroxylation step tend to undergo an electrocyclic ring opening to generate aldehydes to release the ring strain.^{7a}

It should be noted that purification of the final products, especially, for diol **3.95** and **3.96**, is quite challenging, due to generation of multiple products (from the crude product of **3.95** or **3.96**, we observed over ten spots on the TLC plate), and we could not identify the isolated byproducts. Furthermore, in case that the complexity of TLC analysis of the crude products arose from different diastereomers and conformational isomers, we used two-dimensional TLC technique to examine the column-purified diol **3.95**, **3.97**, **3.91** and **3.99**, but we did not find any visible off-diagonal spots on the TLC plate.

3.5 Conclusion

We have developed a three-step tandem reaction sequence to prepare N-protected 2,3-dihydroxypyrrolidines and 2,3-dihydroxypiperidines from nitrogen-tethered dienes. By optimizing the Ru-catalyzed olefin dihydroxylation step, we discovered the conditions that could be applied to the electronically challenging olefins. The future aim of this research is submitting additional substituted substrates to our method.

3.6 Experimental Procedures and Characterizations

General information

Unless otherwise noted, reactions were conducted in oven-dried glassware (160 °C) under dry N₂ atmosphere. Work-up and purification processes were carried out with reagent grade chemicals in air. Pressure tubes (#15 Ace-Thred) and PTFE plugs

equipped with PTFE[®] O-rings used for tandem reactions were purchased from Ace Glass Incorporated.

Dichloromethane, tetrahydrofuran (THF), and acetonitrile (MeCN) used for reactions are analytical grade products purchased from Aldrich, and purified with a solvent dispensing system (Pure Process Technology) by passing the solvent through two activated neutral alumina columns after being purged with nitrogen. N,N-dimethylformamide used for reactions was purchased from Aldrich (anhydrous form, sure sealed bottle) and used without further purification. Ethyl acetate used for reactions was purchased from Fisher Scientific International Inc. (ACS grade), distilled over anhydrous CaSO₄ and stored over activated 3Å molecular sieves. Deuterated solvents for NMR studies were purchased from Cambridge Isotope Laboratories, Inc. The mixture of N₂/H₂ (N₂:H₂ = 95:5) was purchased from Airgas.

Flash column chromatography was conducted on silica gel (SiliaFlash[®] F60, 230-400 mesh) purchased from Silicycle. High performance flash chromatography (HPFC) for preparative purpose was carried out with pre-packed silica gel columns (Biotage Si) on a Biotage Horizon HPFC system. Thin-layer chromatography (TLC) was conducted on 250 µm glass-backed silica gel plates. TLC spots were visualized by using ultraviolet light (254 nm), iodine chamber, or phosphomolybdic acid (PMA).

Fourier transform infrared (FTIR) spectra were measured with a Bruker alpha-P spectrophotometer, and transmission peaks are reported in wavenumber (cm⁻¹). ¹H NMR spectra were measured with a Varian INOVA-500 (500 MHz) or INOVA-600 (600 MHz) spectrometer. Chemical shifts are in ppm with the residual solvent resonance as the internal standard (CDCl₃: δ 7.26 ppm; acetone-*d*₆: δ 2.05 ppm). Peak data are reported as

follows: chemical shift, multiplicity (s = singlet, d = doublet, t = triplet, q = quartet, p = pentet, br = broad, m = multiplet, app = approximate), coupling constants (J , Hz) and integration. ^{13}C NMR spectra were measured on a Varian INOVA-500 (126 MHz) or INOVA-600 (151 MHz) spectrometer with complete proton decoupling. Chemical shifts are reported in ppm with the residual solvent resonance as the internal standard (CDCl_3 : δ 77.16 ppm; acetone- d_6 : δ 206.68 ppm and 29.92 ppm). High-resolution mass spectrometry was performed on a JEOL AccuTOF-DART (positive mode) at the Mass Spectrometry Facility, Boston College.

Allylamine was purchased from Acros and used as received.

3-Butenylamine Hydrochloride was purchased from Aldrich and used as received.

Di-*tert*-butyl Dicarboxylate was purchased from Advanced ChemTech and used as received.

Benzyl Chloroformate was purchased from Acros and used as received.

***p*-Toluenesulfonyl Chloride** was purchased from Aldrich and used as received.

Triethylamine was purchased from Aldrich and distilled under N_2 before use.

Allylbromide was purchased from Aldrich and distilled under N_2 before use.

5-Bromo-1-pentene was purchased from TCI and used as received.

Sodium Hydride (NaH , 95%, dry) was purchased from Aldrich and stored in a N_2 -filled glovebox.

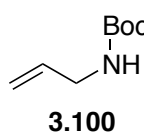
Sodium Periodate (NaIO_4) was purchased from Aldrich and used as received.

Cerium(III) Chloride Heptahydrate ($\text{CeCl}_3 \cdot 7\text{H}_2\text{O}$) was purchased from Aldrich and stored in a desiccator filled with anhydrous calcium sulfate.

Lanthanum(III) Chloride Heptahydrate ($\text{LaCl}_3 \cdot 7\text{H}_2\text{O}$) was purchased from Alfa Aesar and stored in a desiccator filled with anhydrous calcium sulfate.

[1,3-Bis(2,4,6-trimethylphenyl)-2-imidazolidinylidene]dichloro(phenylmethylene)-(tricyclohexylphosphine)ruthenium (Grubbs' second generation catalyst, **GII**) was donated by Materia and purified on a short silica gel column (hexane: diethyl ether = 2:1) before use.

Preparation of substrates



tert*-Butyl *N*-allylcarbamate **3.100*

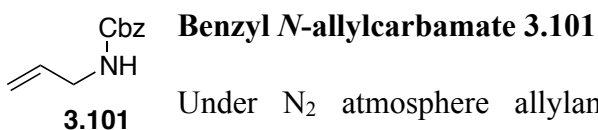
To a 50 mL round bottom flask containing a stir bar were added allylamine (0.571 g, 748 μL , 10.0 mmol) and CH_2Cl_2 (20 mL). The flask was cooled with an ice bath followed by addition of di-*tert*-butyl dicarbonate (2.62 g, 12 mmol, 1.2 equiv) in one portion. After 10 min the ice bath was removed. The reaction mixture was allowed to stir vigorously at 22 °C for 4 h before H_2O (20 mL) was added. The resulting biphasic mixture was transferred to a separatory funnel. The organic layer was isolated, and the aqueous layer was extracted with CH_2Cl_2 (2 \times 10 mL). The combined organic layers were dried over anhydrous Na_2SO_4 , filtered and concentrated *in vacuo*. The obtained pale yellow oil residue was purified by silica gel column chromatography (hexanes: ethyl acetate = 20:1) to afford the title compound as a colorless microcrystalline solid (1.243 g, 79%).

^1H -NMR (600 MHz, CDCl_3) δ 5.84 (ddt, J = 17.1, 10.8, 5.4 Hz, 1H), 5.18 (dq, J = 17.1, 1.8 Hz, 1H), 5.11 (dq, J = 10.2, 1.2 Hz, 1H), 4.60 (br s, 1H), 3.75 (br s, 2H), 1.45 (s, 9H).

^{13}C -NMR (151 MHz, CDCl_3) δ 155.73, 134.89, 115.63, 79.29, 43.04, 28.36.

FTIR (neat): 3338, 2979, 1676, 1523, 1363, 1269, 1250, 1159, 1134, 1019, 951, 926, 862, 665, 641 cm^{-1} .

HSMS (DART+) calcd for $\text{C}_8\text{H}_{16}\text{NO}_2$ ($[\text{M}+\text{H}]^+$): 158.1181, found: 158.1189.



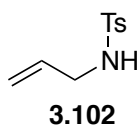
Under N_2 atmosphere allylamine (0.571 g, 748 μL , 10.0 mmol), triethylamine (1.67 mL, 12.0 mmol, 1.2 equiv) and CH_2Cl_2 (20 mL) were added to a 2-neck round bottom flask containing a stir bar via syringe. The flask was cooled to 0 $^\circ\text{C}$ with an ice bath. Benzyl chloroformate (2.05 g, 1.71 mL, 12.0 mmol, 1.2 equiv) was then added dropwise via syringe. Upon complete addition (ca. 3 min) the ice bath was removed. The milky white cloudy solution was stirred vigorously at 22 $^\circ\text{C}$ for 6 h before H_2O (15 mL) was added. The resulting biphasic mixture was transferred to a separatory funnel. The organic layer was isolated, and the aqueous phase was extracted with CH_2Cl_2 (2 \times 15 mL). The combined organic layers were washed with brine (25 mL), dried over anhydrous Na_2SO_4 , filtered and concentrated *in vacuo*. The obtained yellow oil residue was purified by silica gel column chromatography (hexanes: ethyl acetate = 8:1) to afford the title compound as colorless oil (1.82 g, 95%).

^1H -NMR (600 MHz, CDCl_3) δ 7.38 – 7.29 (m, 5H), 5.85 (ddt, J = 16.8, 10.2, 5.4 Hz, 1H), 5.19 (dq, J = 17.4, 1.2 Hz, 1H), 5.15 – 5.10 (overlapped peaks, m, 3H), 4.86 (br s, 1H), 3.90 – 3.73 (br t, J = 4.8 Hz, 2H)

^{13}C -NMR (151 MHz, CDCl_3) δ 156.23, 136.51, 134.43, 128.51, 128.12, 116.06, 66.76, 43.49.

FTIR (neat): 3330, 3065, 3033, 2949, 1695, 1645, 1516, 1453, 1420, 1340, 1239, 1132, 1062, 1026, 987, 916, 775, 735, 695 cm^{-1} .

HSMS (DART+) calcd for $\text{C}_{11}\text{H}_{14}\text{NO}_2$ ($[\text{M}+\text{H}]^+$): 192.1025, found: 192.1026.



***N*-allyl-4-methylbenzenesulfonamide 3.102**

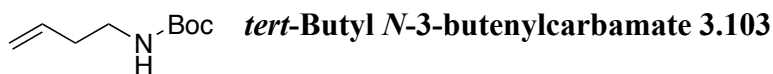
Allyl amine (0.571 g, 748 μL , 10.0 mmol), triethylamine (1.67 mL, 12 mmol, 1.2 equiv) and CH_2Cl_2 (30 mL) were added in a 50 mL round bottom flask containing a stir bar. The vessel was cooled to 0 $^\circ\text{C}$ with an ice bath followed by addition of 4-methylbenzenesulfonyl chloride (2.29 g, 12 mmol, 1.2 equiv) in one portion. The reaction mixture was stirred at 0 $^\circ\text{C}$ for 10 min then at 22 $^\circ\text{C}$ for 5 h before H_2O (30 mL) was added. The resulting biphasic mixture was transferred to a separatory funnel. The organic layer was isolated, and the aqueous layer was extracted with CH_2Cl_2 (2 \times 10 mL). The combined organic layers were washed with brine (40 mL), dried over anhydrous Na_2SO_4 , filtered and concentrated *in vacuo*. The obtained pale yellow oil residue was purified by silica gel column chromatography (hexanes: ethyl acetate = 4:1) to afford the title compound as a white solid (2.10 g, 99%).

^1H -NMR (600 MHz, CDCl_3) δ 7.75 (d, J = 8.4 Hz, 2H), 7.31 (d, J = 8.4 Hz, 2 H), 5.72 (ddt, J = 17.4, 10.2, 5.4, 1 H), 5.16 (dq, J = 17.4 Hz, 1.2 Hz, 1H), 5.09 (dq, J = 10.2, 1.2 Hz, 1H), 4.48 (br t, J = 4.8 Hz, 1H), 3.58 (tt, J = 6.0, 1.2 Hz, 2H), 2.43 (s, 3H).

^{13}C -NMR (151 MHz, CDCl_3) δ 143.49, 136.89, 132.96, 129.76, 127.13, 117.67, 45.75, 21.58.

FTIR (neat): 3245, 2926, 2858, 1594, 1421, 1316, 1287, 1155, 1092, 1061, 934, 873, 809, 663, 568, 546, 483 cm^{-1} .

HSMS (DART+) calcd for C₁₀H₁₄NO₂S ([M+H]⁺): 212.0745, found: 212.0742.



3.103 To a 50 mL round bottom flask containing a stir bar were added 3-butenylamine hydrochloride (0.538 g, 5.0 mmol), CH₂Cl₂ (20 mL) and triethylamine (0.84 mL, 6.0 mmol, 1.2 equiv) in sequence. After a clear solution was obtained di-*tert*-butyl dicarbonate (1.31 g, 6 mmol, 1.2 equiv) was added in one portion. The reaction mixture was stirred at 22 °C for 4.5 h before saturated NaHCO₃ aqueous solution (20 mL) was added. The resulting biphasic mixture was transferred to a separatory funnel. The organic layer was isolated, and the aqueous layer was extracted with CH₂Cl₂ (20 mL). The combined organic layers were washed with brine (20 mL), dried over anhydrous Na₂SO₄, filtered and concentrated *in vacuo*. The obtained yellow oil residue was purified by silica gel column chromatography (hexanes: ethyl acetate = 20:1) to afford the title compound as colorless oil (0.811 g, 95%).

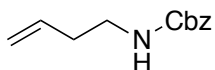
¹H-NMR (600 MHz, CDCl₃) δ 5.75 (ddt, *J* = 17.4, 10.2, 7.2 Hz, 1H), 5.11 – 5.05 (m, 2 H), 4.55 (s, 1H), 3.19 (br q, *J* = 6.6 Hz, 2H), 2.23 (q, *J* = 6.6 Hz, 2H), 1.43 (s, 9H).

¹³C-NMR (151 MHz, CDCl₃) δ 155.86, 135.32, 117.01, 79.09, 39.61, 34.18, 28.39.

FTIR (neat): 3347, 2977, 2931, 1688, 1641, 1512, 1452, 1391, 1365, 1274, 1248, 1166, 1039, 1015, 913, 865, 780, 632 cm⁻¹.

HSMS (DART+) calcd for C₉H₁₈NO₂ ([M+H]⁺): 172.1338, found: 172.1341.

Benzyl *N*-3-butenylcarbamate 3.104



3.104

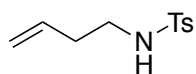
To a 50 mL 2-neck round bottom flask containing a stir bar was added 3-butenylamine hydrochloride (0.538 g, 5.0 mmol). The flask was then sealed with a rubber septum and placed under N₂ atmosphere. CH₂Cl₂ (20 mL) and triethylamine (1.74 mL, 12.5 mmol, 2.5 equiv) were added in sequence via syringe. After a clear solution was obtained the vessel was cooled to 0 °C with an ice bath. Benzyl chloroformate (0.86 mL, 6.0 mmol, 1.2 equiv) was added dropwise via syringe. Upon complete addition (ca. 3 min), the resulting milky white cloudy solution was stirred at 0 °C for 15 min then at 22 °C for 5 h before H₂O (15 mL) was added. The resulting biphasic mixture was transferred to a separatory funnel. The organic layer was isolated, and the aqueous layer was extracted with CH₂Cl₂ (2×15 mL). The combined organic layers were washed with brine (25 mL), dried over Na₂SO₄, filtered and concentrated *in vacuo*. The obtained yellow oil residue was purified by silica gel column chromatography (hexanes: ethyl acetate = 10:1) to afford the title compound as colorless oil (0.921 g, 90%).

¹H-NMR (600 MHz, CDCl₃) δ 7.38 – 7.28 (m, 5H), 5.75 (ddt, *J* = 17.4, 10.2, 7.2 Hz, 1H), 5.13 – 5.05 (m, 4H), 4.79 (br s, 1H), 3.28 (q, *J* = 6.6 Hz, 2H), 2.26 (q, *J* = 6.6 Hz, 2H)

¹³C-NMR (151 MHz, CDCl₃) δ 156.28, 136.58, 135.04, 128.49, 128.10, 128.08, 117.32, 66.62, 40.06, 34.10.

FTIR (neat): 3331, 3066, 2938, 1694, 1520, 1453, 1245, 1216, 1131, 1023, 914, 735, 695, 640. 603 cm⁻¹.

HSMS (DART+) calcd for C₁₂H₁₆NO₂ ([M+H]⁺): 206.1181, found: 206.1192.



3.105

***N*-3-butenyl-4-methylbenzenesulfonamide 3.105**

To a 50 mL round bottom flask containing a stir bar were added 3-butenylamine hydrochloride (0.538 g, 5.0 mmol), triethylamine (1.74 mL, 12.5 mmol, 2.5 equiv) and CH₂Cl₂ (20 mL). After a clear solution was obtained the vessel was cooled to 0 °C with an ice bath followed by addition of 4-methylbenzenesulfonyl chloride (1.14 g, 6.0 mmol, 1.2 equiv) in one portion. The reaction mixture was stirred vigorously at 0 °C for 20 min then at 22 °C for 6 h before H₂O (20 mL) was added. The resulting biphasic mixture was transferred to a separatory funnel. The organic layer was isolated, and the aqueous layer was extracted with CH₂Cl₂ (2×15 mL). The combined organic layers were washed with brine (25 mL), dried over anhydrous Na₂SO₄, filtered and concentrated *in vacuo*. The obtained pale yellow oil residue was purified by silica gel column chromatography (hexanes: ethyl acetate = 4:1) to afford the title compound as colorless oil (1.103 g, 98%).

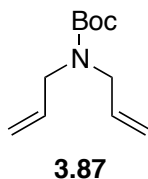
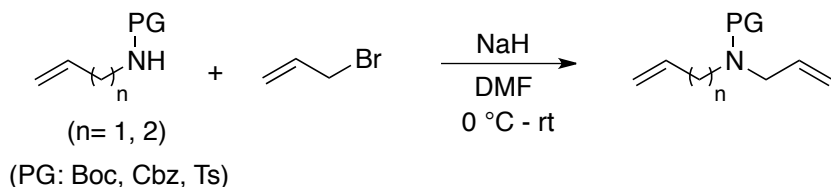
¹H-NMR (600 MHz, CDCl₃) δ 7.74 (d, *J* = 8.4 Hz, 2 H), 7.30 (d, *J* = 8.4 Hz, 2 H), 5.62 (ddt, *J* = 16.8, 10.2, 7.2 Hz, 1H), 5.06 (partially overlapped dq, *J* = 10.2, 1.2 Hz 2H), 5.03 (partially overlapped, dq, *J* = 17.4 Hz, 1.8 Hz), 4.59 (br s, 1 H), 3.01 (q, *J* = 6.6 Hz, 2H), 2.42 (s, 3H), 2.19 (tq, *J* = 6.6, 1.2 Hz, 2H).

¹³C-NMR (151 MHz, CDCl₃) δ 143.54, 137.08, 134.29, 129.83, 127.24, 118.23, 42.21, 33.73, 21.64.

FTIR (neat): 3275, 2927, 1641, 1597, 1424, 1320, 1154, 1091, 1073, 915, 813, 660, 566, 548 cm⁻¹.

HSMS (DART+) calcd for C₁₁H₁₆NO₂S ([M+H]⁺): 226.0902, found: 226.0913.

The representative procedure of alkylation of monosubstituted amines



tert-Butyl *N,N*-diallylcarbamate **3.87**

In a N_2 -filled glovebox NaH (0.288 g, 12.0 mmol, 3.0 equiv) was added in a 25 mL round bottom flask containing a stir bar. The flask was sealed with a rubber septum before removed from the glovebox, and placed under N_2 atmosphere. DMF (3.0 mL) was added in the flask via syringe, and then the vessel was cooled to 0 °C with an ice bath. In a separate 5 mL pear-shaped flask *tert*-Butyl *N*-allylcarbamate **3.100** (0.628 g, 4.0 mmol) was dissolved in DMF (1.0 mL, plus 2×0.5 mL for rinse), and the obtained solution was added in the cooled flask dropwise via syringe. Upon complete addition (ca. 3 min) the ice bath was removed. The milky white cloudy solution was stirred vigorously at 22 °C for 20 min. The flask was cooled to 0 °C with an ice bath before allyl bromide (1.04 mL, 12.0 mmol, 3.0 equiv) was added in one portion via syringe. The ice bath was removed, and the reaction mixture was allowed to stir vigorously at 22 °C for 3 h until TLC analysis indicated complete consumption of the monosubstituted amine. Saturated NH_4Cl aqueous solution (5.0 mL) was added to quench the reaction. The resulting mixture was diluted with H_2O (30 mL) and CH_2Cl_2 (15 mL), and transferred to a separatory funnel. The organic phase was isolated, and the aqueous phase was extracted with CH_2Cl_2 (15 mL). The combined organic layers were washed with H_2O (2×15 mL) and brine (30 mL), dried over anhydrous Na_2SO_4 , filtered and

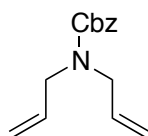
concentrated *in vacuo*. The obtained yellow oil residue was purified by silica gel column chromatography (hexanes: ethyl acetate = 30:1) to afford the title compound as colorless oil (0.532 g, 67% yield).

^1H -NMR (600 MHz, CDCl_3) of two carbamate rotamers (peaks become broad, due to slow rotation of $\text{N-C}(\text{sp}^2)$ bond): δ 5.81 – 5.69 (m, 2H), 5.168 – 5.04 (m, 4H), 3.95 – 3.63 (overlapped broad peaks, m, 4H), 1.44 (s, 9H).

^{13}C -NMR (151 MHz, CDCl_3) of two carbamate rotamers: δ 155.38, 133.98, 116.54, 116.12, 79.55, 48.69, 28.36.

FTIR (neat): 2977, 2929, 1691, 1643, 1454, 1402, 1365, 1291, 1245, 1171, 1149, 993, 917, 870, 770 cm^{-1} .

HSMS (DART+) calcd for $\text{C}_{11}\text{H}_{20}\text{NO}_2$ ($[\text{M}+\text{H}]^+$): 198.1494, found: 198.1499.



Benzyl *N,N*-diallylcarbamate 3.85

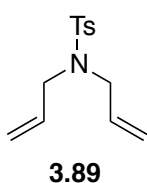
Following the representative alkylation procedure, Benzyl *N*-allylcarbamate **3.85** (0.764 g, 4.0 mmol), NaH (0.228 g, 12.0 mmol, 3.0 equiv) and allyl-bromide (1.04 mL, 12.0 mmol, 3.0 equiv) were used in the reaction. The crude product was purified by silica gel column chromatography (hexanes: ethyl acetate = 25:1) to afford the title compound as slightly yellow oil (0.818 g, 88%).

^1H -NMR (600 MHz, CDCl_3) of two carbamate rotamers (peaks become broad, due to slow rotation of $\text{N-C}(\text{sp}^2)$ bond): δ 7.38 – 7.27 (m, 5H), 5.77 (br s, 2H), 5.26 – 5.05 (overlapped peaks, m, 6H), 3.97 – 3.81 (overlapped broad peaks, m, 4H).

^{13}C -NMR (151 MHz, CDCl_3) two carbamate rotamers: δ 155.99, 136.79, 133.48, 128.41, 127.88, 127.74, 117.15, 116.68, 67.14, 49.12, 48.49.

FTIR (neat): 3067, 3033, 2981, 1696, 1497, 1455, 1235, 1150, 1091, 1054, 991, 920, 767, 734, 696 cm^{-1} .

HSMS (DART+) calcd for $\text{C}_{14}\text{H}_{18}\text{NO}_2$ ($[\text{M}+\text{H}]^+$): 232.1338, found: 232.1344.



***N,N*-diallyl-4-methylbenzenesulfonamide 3.89**

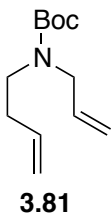
Following the representative alkylation procedure, *N*-allyl-4-methylbenzenesulfonamide **3.102** (0.844 g, 4.0 mmol), NaH (0.228 g, 12.0 mmol, 3.0 equiv) and allyl bromide (1.04 mL, 12.0 mmol, 3.0 equiv) were used in the reaction. The crude product was purified by silica gel column chromatography (hexanes: ethyl acetate = 13:1) to afford the title compound as slightly yellow oil (0.977 g, 97%).

^1H -NMR (600 MHz, CDCl_3) δ 7.69 (d, J = 7.8 Hz, 2H), 7.29 (d, J = 8.4 Hz, 2H), 5.60 (ddt, J = 16.8, 10.2, 6.6 Hz, 2H), 5.16 – 5.13 (m, 2H), 5.13 – 5.10 (m, 2H), 3.79 (d, J = 6.0 Hz, 4H), 2.42 (s, 3H).

^{13}C -NMR (151 MHz, CDCl_3) δ 143.19, 137.41, 132.65, 129.65, 127.15, 118.92, 49.31, 21.49.

FTIR (neat): 3079, 2982, 2922, 1643, 1597, 1341, 1304, 1153, 1090, 1041, 1017, 991, 925, 903, 887, 814, 801, 761, 706, 659, 592, 545 cm^{-1} .

HSMS (DART+) calcd for $\text{C}_{13}\text{H}_{18}\text{NO}_2\text{S}$ ($[\text{M}+\text{H}]^+$): 252.1058, found: 252.1067.



***tert*-Butyl *N*-3-butenyl-*N*-2-propenylcarbamate 3.81**

Following the representative alkylation procedure, *tert*-butyl *N*-3-butenylcarbamate **3.103** (0.361 g, 2.11 mmol), NaH (0.152 g, 6.33 mmol, 3.0

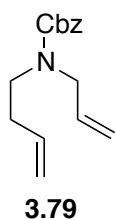
equiv), allyl bromide (0.55 mL, 6.33 mmol, 3.0 equiv) and DMF (1.0 mL for NaH, 2.0 mL for monoalkylamine) were used in the reaction. The crude product was purified by silica gel column chromatography (hexanes: ethyl acetate = 30:1) to afford the title compound as colorless oil (0.319 g, 72%).

¹H-NMR (600 MHz, CDCl₃), carbamate rotamers (peaks become broad, due to slow rotation of N-C(sp²) bond): δ 5.82 – 5.71 (m, 2H), 5.11 (br d, *J* = 10.2 Hz, 2H), 5.05 (d, *J* = 16.8 Hz, 1H), 5.01 (dd, *J* = 10.2, 0.6 Hz, 1H), 3.89 – 3.73 (overlapped broad peaks, m, 2H), 3.28 (br d, *J* = 16.8 Hz, 2H), 2.26 (br d, *J* = 6.0 Hz, 2H), 1.45 (s, 9H).

¹³C-NMR (151 MHz, CDCl₃), carbamate rotamers: δ 155.40, 135.51, 134.31, 116.38, 115.82, 79.37, 49.90, 49.41, 46.17, 33.09, 32.69, 28.38.

FTIR (neat): 3078, 2976, 2928, 1691, 1642, 1460, 1406, 1364, 1245, 1227, 1150, 993, 912, 876, 771 cm⁻¹.

HSMS (DART+) calcd for C₁₂H₂₂NO₂ ([M+H]⁺): 212.1651, found: 212.1657.



Benzyl *N*-3-butenyl-*N*-2-propenylcarbamate 3.79

Following the representative alkylation procedure, Benzyl *N*-3-butenylcarbamate (0.477 g, 2.32 mmol), NaH (0.167 g, 6.96 mmol, 3.0 equiv), allyl bromide (0.60 mL, 6.96 mmol, 3.0 equiv) and DMF (1.0 mL for

NaH, 2.0 mL for monoalkyl amine) were used in the reaction. The crude product was purified by silica gel column chromatography (hexanes: ethyl acetate = 20:1) to afford the title compound as colorless oil (0.539 g, 95%).

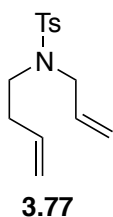
¹H-NMR (600 MHz, CDCl₃), carbamate rotamers (peaks become broad, due to slow rotation of N-C(sp²) bond): δ 7.44 – 7.27 (m, 5H), 5.75 (br s, 2H), 5.24 – 4.94

(overlapped, m, 6 H), 3.98 – 3.83 (overlapped broad peaks, m, 2H), 3.40 – 3.25 (overlapped broad peaks, m, 2H), 2.41 – 2.19 (m, 2H).

^{13}C -NMR (151 MHz, CDCl_3), carbamate rotamers: δ 156.05, 136.87, 135.29, 135.15, 133.87, 133.78, 128.41, 127.87, 127.76, 127.73, 67.01, 50.00, 49.61, 46.65, 45.88, 33.02, 32.51.

FTIR (neat): 3076, 2979, 2943, 1695, 1641, 1497, 1465, 1365, 1235, 1218, 1152, 1089, 992, 913, 767, 733, 696 cm^{-1} .

HSMS (DART+) calcd for $\text{C}_{15}\text{H}_{20}\text{NO}_2$ ($[\text{M}+\text{H}]^+$): 246.1494, found: 246.1502.



***N*-3-butenyl-4-methyl-*N*-2-propenylbenzenesulfonamide 3.77**

Following the representative alkylation procedure, *N*-3-butenyl-4-methylbenzenesulfonamide (0.31 g, 1.38 mmol), NaH (0.099 g, 4.14 mmol, 3.0 equiv), allyl bromide (0.36 mL, 4.14 mmol, 3.0 equiv) and DMF (1.0 mL

for NaH, 2.0 mL for monoalkyl amine) were used in the reaction. The crude product was purified by silica gel column chromatography (hexanes: ethyl acetate = 15:1) to afford the desired product as pale yellow oil (0.352 g, 96%).

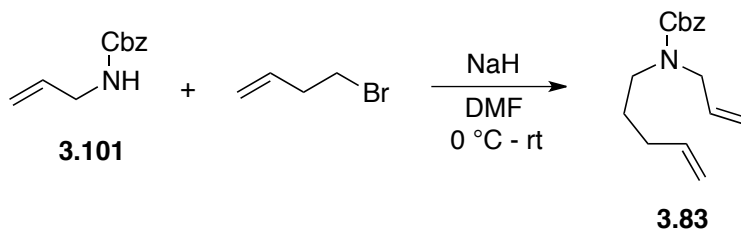
^1H -NMR (600 MHz, CDCl_3) δ 7.68 (d, J = 8.4 Hz, 2H), 7.28 (d, J = 8.4 Hz, 2H), 5.68 (ddt, J = 17.1, 10.2, 6.6 Hz, 1H), 5.63 (ddt, J = 17.1, 10.2, 6.6 Hz, 1H), 5.17 (dq, J = 17.1, 1.2 Hz, 1H), 5.13 (q, J = 10.2, 1.2 Hz, 1H), 5.04 – 4.98 (m, 2H), 5.01 (q, J = 1.8 Hz, 1H), 3.80 (dt, J = 6.0, 1.2 Hz, 2H), 3.20 – 3.14 (m, 2H), 2.41 (s, 3H), 2.29 – 2.23 (m, 2H).

^{13}C -NMR (151 MHz, CDCl_3) δ 143.16, 137.12, 134.69, 133.18, 129.64, 127.11, 118.73, 116.92, 50.67, 46.67, 32.84, 21.47.

FTIR (neat): 3078, 2979, 2922, 2863, 1641, 1597, 1451, 1339, 1304, 1286, 1153, 1089, 992, 913, 814, 746, 659 cm^{-1} .

HSMS (DART+) calcd for $\text{C}_{14}\text{H}_{20}\text{NO}_2\text{S}$ ($[\text{M}+\text{H}]^+$): 266.1215, found: 266.1226.

Benzyl *N*-4-pentenyl-*N*-2-propenylcarbamate **3.83**



Following the representative alkylation procedure, benzyl *N*-allylcarbamate (0.382 g, 2.0 mmol), NaH (0.144 g, 6.0 mmol, 3.0 equiv), 5-bromo-1-pentene (0.47 mL, 4.0 mmol, 2.0 equiv) and DMF (2.0 mL for NaH, 3.0 mL for monoalkyl amine) were used in the reaction. The crude product was purified by silica gel column chromatography (hexanes: ethyl acetate = 25:1) to afford the title compound as pale yellow oil (0.472 g, 91%).

^1H -NMR (600 MHz, CDCl_3), carbamate rotamers (peaks become broad, due to slow rotation of $\text{N}-\text{C}(\text{sp}^2)$ bond): δ 7.42 – 7.27 (m, 5H), 5.78 (br s, 2H), 5.14 (overlapped peaks, s, 4H), 5.07 – 4.91 (m, 2H), 3.96 – 3.81 (overlapped broad peaks, m, 2H), 3.26 (br dd, $J = 13.5, 6.0$ Hz, 2H), 2.04 (broad peaks, m, 2H), 1.70 – 1.57 (m, 2H).

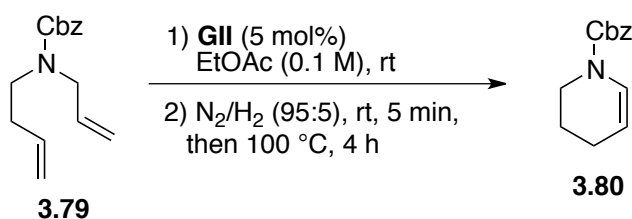
^{13}C -NMR (151 MHz, CDCl_3), carbamate rotamers: δ 156.12, 156.02, 137.90, 137.78, 136.89, 133.92, 133.82, 128.41, 127.85, 127.74, 116.87, 116.40, 114.90, 66.99, 49.90, 49.49, 46.75, 45.90, 30.90, 27.54, 27.13.

FTIR (neat): 3067, 2932, 1696, 1641, 1467, 1455, 1413, 1365, 1233, 1212, 1152, 1092, 991, 911, 767, 734, 696 cm^{-1} .

HSMS (DART+) calcd for $\text{C}_{16}\text{H}_{22}\text{NO}_2$ ($[\text{M}+\text{H}]^+$): 260.1651, found: 260.1653.

The representative procedure of tandem RCM/olefin isomerization reactions

3,4-dihydro-2*H*-pyridine-1-carboxylic acid benzyl ester **3.80**



Benzyl *N*-3-butenyl-*N*-2-propenylcarbamate **3.79** (0.0245 g, 0.1 mmol) was dissolved in ethyl acetate (1.0 mL) in a pressure tube (approximate capacity, 15 mL) containing a stir bar. After **GII** (0.0042 g, 0.005 mmol, 0.05 equiv) was added in one portion, the tube was sealed with a rubber septum and placed under N_2 atmosphere. The reaction mixture was stirred at 22 $^\circ\text{C}$ for 1.5 h until TLC analysis indicated complete consumption of the starting material. A gas mixture of N_2/H_2 ($\text{N}_2:\text{H}_2 = 95:5$, balloon) was then bubbled vigorously into the solution via a cannula at 22 $^\circ\text{C}$ for 5 min. Upon finishing the rubber septum was replaced with a PTFE plug, and the sealed tube was placed in a 100 $^\circ\text{C}$ oil bath. The reaction mixture was stirred at 100 $^\circ\text{C}$ for 4 h before it was allowed to cool down to 22 $^\circ\text{C}$ naturally. The reaction mixture was transferred to a round bottom flask (3 \times 2 mL CH_2Cl_2 was used to rinse the pressure tube), and concentrated *in vacuo*. The obtained dark brown oil residue was purified by silica gel column chromatography

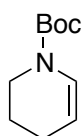
(hexanes: ethyl acetate = 20:1) to afford the title compound **3.80** as colorless oil (0.0195 g, 90%).

¹H-NMR (600 MHz, CDCl₃), two carbamate rotamers in 1:1.5 ratio: δ 7.38 – 7.31 (m, 5H), 6.89 (d, *J* = 8.4 Hz, 0.4H), 6.80 (d, *J* = 8.4 Hz, 0.6H), 5.18 (s, 2H), 4.97 (dt, *J* = 8.4, 3.6 Hz, 0.4H), 4.86 (dt, *J* = 8.4, 4.2 Hz 0.6H), 3.65 – 3.61 (m, 2H), 2.07 – 2.01 (m, 2H), 1.87 – 1.78 (m, 2H).

¹³C-NMR (151 MHz, CDCl₃), two carbamate rotamers: δ 153.53, 153.11, 136.38, 128.50, 128.10, 127.99, 125.34, 124.88, 106.73, 106.39, 67.41, 67.31, 42.39, 42.19, 21.62, 21.43, 21.24.

FTIR (neat): 2937, 2883, 1699, 1650, 1446, 1407, 1343, 1298, 1226, 1181, 1103, 1051, 967, 948, 8190, 761, 741, 716, 696, 447 cm⁻¹.

HSMS (DART+) calcd for C₁₃H₁₆NO₂ ([M+H]⁺): 218.1181, found: 218.1186.



3,4-dihydro-2H-pyridine-1-carboxylic acid *tert*-butyl ester **3.82**

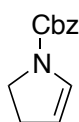
Following the representative procedure, *tert*-butyl *N*-3-butenyl-*N*-2-propenylcarbamate **3.81** (0.0211 g, 0.1 mmol) was used in the reaction. The crude product was purified by silica gel column chromatography (hexanes: ethyl acetate = 35:1) to afford the title compound as colorless oil (0.013 g, 71%).

¹H-NMR (600 MHz, CDCl₃), two carbamate rotamers in 1:1.5 ratio: δ 6.83 (d, *J* = 7.2 Hz, 0.4H), 6.70 (d, *J* = 7.8 Hz, 0.6H), 4.88 (br s, 0.4H), 4.81 – 4.73 (m, 0.6H), 3.58 – 3.47 (m, 2H), 2.00 (qd, *J* = 6.0, 1.8 Hz, 2H), 1.79 (app d, *J* = 4.8 Hz, 2H), 1.47 (s, 9H).

¹³C-NMR (151 MHz, CDCl₃), two carbamate rotamers, δ 152.71, 152.29, 125.60, 125.25, 105.56, 105.11, 80.39, 80.25, 42.54, 41.44, 28.31, 21.72, 21.47, 21.31.

FTIR (neat): 2975, 2930, 1697, 1650, 1475, 1452, 1404, 1354, 1300, 1251, 1163, 1111, 1051, 992, 876, 742, 713, 442 cm^{-1} .

HSMS (DART+) calcd for $\text{C}_{10}\text{H}_{18}\text{NO}_2$ ($[\text{M}+\text{H}]^+$): 184.1338, found: 184.1333.



2,3-dihydro-1H-pyrrole-1-carboxylic acid benzyl ester 3.86

3.86

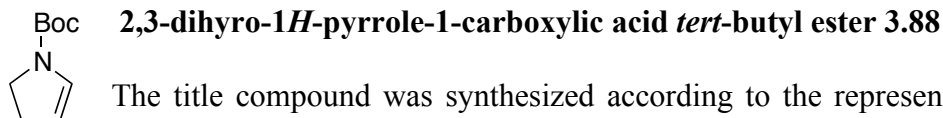
The title compound was synthesized according to the representative procedure with slight modification. Benzyl *N,N*-diallylcarbamate **3.85** (0.0231 g, 0.1 mmol) was used in the reaction. After the sealed tube was placed in a 100 °C oil bath, the reaction mixture was stirred at 100 °C for 2 *h*. Then, it was allowed to cool down to 22 °C naturally. The crude product was purified by silica gel column chromatography (hexanes: ethyl acetate = 12:1) to afford the title compound as colorless oil (0.017 g, 84%).

^1H -NMR (600 MHz, CDCl_3), two carbamate rotamers in 1:1.2 ratio: δ 7.40 – 7.28 (m, 5H), 6.63 (br s, 0.45H), 6.55 (br t, J = 1.8 Hz, 0.55H), 5.17 (s, 2H), 5.09 (br s, 0.45H), 5.04 (br t, J = 1.8 Hz, 0.55H), 3.79 (m, 2H), 2.71 – 2.60 (m, 2H).

^{13}C -NMR (151 MHz, CDCl_3), two carbamate rotamers: δ 152.80, 152.10, 136.60, 136.55, 129.73, 129.03, 128.75, 128.47, 128.05, 128.00, 127.91, 126.10, 108.76, 108.61, 67.02, 66.85, 45.24, 45.05, 29.70, 28.63.

FTIR (neat): 2954, 2892, 1696, 1451, 1404, 1335, 1284, 1210, 1175, 1086, 1043, 969, 914, 849, 770, 736, 696, 603, 559, 458 cm^{-1} .

HSMS (DART+) calcd for $\text{C}_{12}\text{H}_{14}\text{NO}_2$ ($[\text{M}+\text{H}]^+$): 204.1025, found: 204.1026.



The title compound was synthesized according to the representative procedure with slight modification. *tert*-Butyl *N,N*-diallylcarbamate **3.87** (0.0197 g, 0.1 mmol) was used in the reaction. After the sealed tube was placed in a 100 °C oil bath, the reaction mixture was stirred at 100 °C for 2 *h*. Then, it was allowed to cool down to 22 °C naturally. The crude product was purified by silica gel column chromatography (hexanes: ethyl acetate = 25:1) to afford the title compound as pale yellow oil (0.0114 g, 67%).

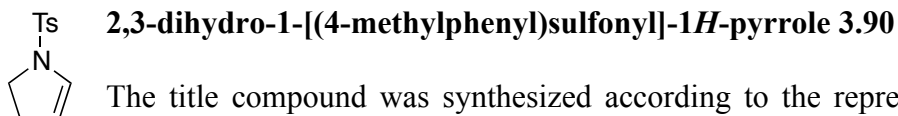
Caution! The title compound is volatile under high vacuum.

¹H-NMR (600 MHz, CDCl₃), two carbamate rotamers in 1:1.3 ratio: δ 6.58 (s, 0.43H), 6.45 (s, 0.57H), 5.01 (partially overlapped s, 0.43H), 4.96 (partially overlapped s, 0.57H), 3.77 – 3.62 (m, 2H), 2.69 – 2.56 (m, 2H), 1.47 (s, 9H).

¹³C-NMR (151 MHz, CDCl₃), two carbamate rotamers, δ 152.31, 151.61, 129.81, 107.48, 79.99, 79.85, 45.26, 44.75, 29.69, 28.67, 28.40.

FTIR (neat): 2974, 2929, 1695, 1617, 1477, 1389, 1364, 1350, 1284, 1165, 1130, 1088, 1039, 999, 969, 879, 762, 702, 453 cm⁻¹.

HSMS (DART+) calcd for C₉H₁₆NO₂ ([M+H]⁺): 170.1181, found: 170.1181.



The title compound was synthesized according to the representative procedure with slight modification. *N,N*-Diallyl-4-methylbenzenesulfonamide **3.89** (0.0251 g, 0.1 mmol) was used in the reaction. After the sealed tube was placed in a 100 °C oil bath, the reaction mixture was stirred at 100 °C for 2 *h*. Then, it was allowed to cool down to 22 °C naturally. The crude product was purified by silica gel column

chromatography (hexanes: ethyl acetate = 8:1) to afford the title compound as a white solid (0.0193 g, 86%).

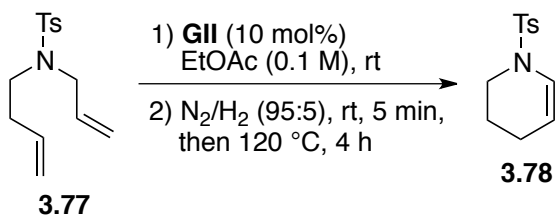
^1H -NMR (600 MHz, CDCl_3) δ 7.66 (d, J = 8.4 Hz, 2H), 7.32 (d, J = 8.4 Hz, 2H), 6.36 (dt, J = 4.2, 2.4 Hz, 1H), 5.11 (dt, J = 4.2, 2.4 Hz, 1H), 3.47 (t, J = 9.0 Hz, 2H), 2.47 (tt, J = 9.0, 2.4 Hz, 2H), 2.43 (s, 3H).

^{13}C -NMR (151 MHz, CDCl_3): δ 143.75, 132.87, 130.69, 129.63, 127.71, 111.21, 47.18, 29.59, 21.55.

FTIR (neat): 3101, 2989, 2919, 2878, 1616, 1593, 1335, 1305, 1288, 1156, 1110, 1085, 1062, 970, 811, 743, 708, 659, 588, 545, 504, 490, 456 cm^{-1} .

HSMS (DART+) calcd for $\text{C}_{11}\text{H}_{14}\text{NO}_2\text{S}$ ($[\text{M}+\text{H}]^+$): 224.0745, found: 224.0741.

1,2,3,4-tetrahydro-1-[(4-methylphenyl)sulfonyl]-pyridine **3.78**



N-3-Butenyl-4-methyl-*N*-2-propenylbenzenesulfonamide **3.77** (0.0133 g, 0.05 mmol) was dissolved in ethyl acetate (0.5 mL) in a pressure tube (approximate capacity, 15 mL) containing a stir bar. **GII** (0.0042 g, 0.005 mmol, 0.1 equiv) was then added in the tube in one portion. The tube was sealed with a rubber septum and placed under N_2 atmosphere. The reaction mixture was stirred at 22 °C for 1.5 h until TLC analysis indicated complete consumption of the starting material. A gas mixture of N_2 and H_2 (N_2/H_2 = 95:5, balloon) was bubbled vigorously into the solution via a cannula at 22 °C

for 5 min. Upon finishing the rubber septum was replaced with a PTFE plug, and the sealed tube was placed in a 120 °C oil bath. The reaction mixture was stirred at 120 °C for 4 h before it was allowed to cool down to 22 °C naturally. The reaction mixture was transferred to a round bottom flask (3×2 mL CH₂Cl₂ was used to rinse the pressure tube), and concentrated *in vacuo*. The obtained dark brown oil residue was purified by silica gel column chromatography (hexanes: ethyl acetate = 10:1) to afford the title compound as a white solid (0.0106 g, 89%).

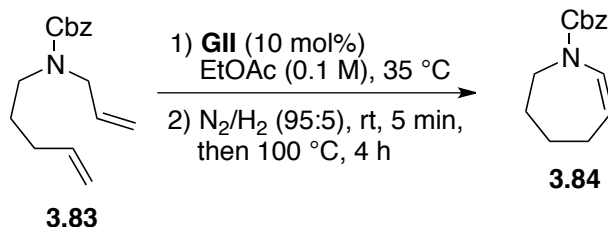
¹H-NMR (600 MHz, CDCl₃) δ 7.66 (d, *J* = 8.4 Hz, 2H), 7.30 (d, *J* = 8.4 Hz, 2H), 6.63 (dt, *J* = 8.4, 2.4 Hz, 1H), 4.96 (dt, *J* = 8.4, 4.2 Hz, 1H), 3.37 – 3.34 (m, 2H), 2.42 (s, 3H), 1.90 (tdd, *J* = 6.6, 3.6, 1.8 Hz, 2H), 1.67 – 1.62 (m, 2H).

¹³C-NMR (151 MHz, CDCl₃) δ 143.49, 135.11, 129.67, 127.04, 125.05, 108.26, 43.82, 21.53, 20.92, 20.88.

FTIR (neat): 2932, 2854, 1646, 1444, 1395, 1336, 1263, 1160, 1101, 1043, 968, 928, 812, 708, 680, 637, 541 cm⁻¹.

HSMS (DART+) calcd for C₁₂H₁₆NO₂S ([M+H]⁺): 238.0902, found: 238.0892.

2,3,4,5-tetrahydro-1H-azepine-1-carboxylic acid benzyl ester **3.84**



Benzyl *N*-4-pentenyl-*N*-2-propenylcarbamate **3.83** (0.026 g, 0.1 mmol) was dissolved in ethyl acetate (1.0 mL) in a pressure tube (approximate capacity, 15 mL)

containing a stir bar. **GII** (0.0085 g, 0.01 mmol, 0.1 equiv) was then added in the tube in one portion. The tube was sealed with a rubber septum, protected under N₂ atmosphere and then placed in a 35 °C oil bath. The reaction mixture was stirred at 35 °C for 1 h until TLC analysis indicated complete consumption of the starting material. The reaction mixture was allowed to cool down to 22 °C. A mixture of N₂ and H₂ (N₂/H₂ = 95:5, balloon) was bubbled vigorously into the solution via a cannula at 22 °C for 5 min. Upon finishing the rubber septum was replaced with a PTFE plug, and the sealed tube was placed in a 100 °C oil bath. The reaction mixture was stirred at 100 °C for 4 h before it was allowed to cool down to 22 °C naturally. The reaction mixture was transferred to a round bottom flask (3×2 mL CH₂Cl₂ was used to rinse the pressure tube), and concentrated *in vacuo*. The obtained dark brown oil residue was purified by silica gel column chromatography (hexanes: ethyl acetate = 25:1) to afford the title compound as colorless oil (0.0157 g, 68%).

¹H-NMR (600 MHz, CDCl₃), two carbamate rotamers in 1:1.8 ratio: δ 7.39 – 7.29 (m, 5H), 6.60 (br d, *J* = 6.6 Hz 0.36H), 6.52 (d, *J* = 8.4 Hz, 0.64H), 5.18 (s, 2H), 5.08 (partially overlapped br s, 0.36H), 5.04 (partially overlapped br s, 0.64H), 3.75 – 3.68 (m, 2H), 2.19 (dd, *J* = 10.2, 5.4 Hz, 2H), 1.87 – 1.64 (m, 4H).

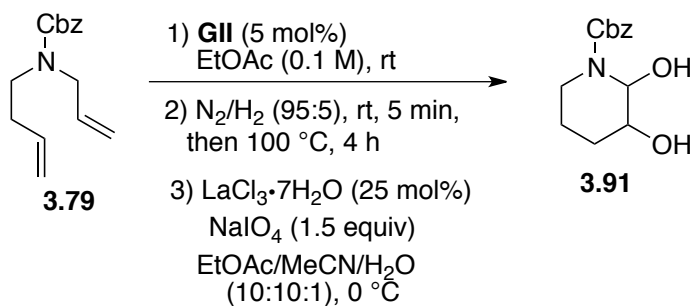
¹³C-NMR (151 MHz, CDCl₃), two carbamate rotamers: δ 154.37, 136.53, 130.63, 129.86, 128.48, 128.01, 127.86, 115.87, 115.71, 67.41, 67.29, 47.68, 28.06, 26.29, 25.97, 25.09.

FTIR (neat): 3033, 2936, 2861, 1699, 1649, 1452, 1407, 1340, 1272, 1251, 1208, 1166, 1109, 1014, 856, 764, 723, 695 cm⁻¹.

HSMS (DART+) calcd for C₁₄H₁₈NO₂ ([M+H]⁺): 232.1338, found: 232.1327.

The representative procedure of tandem RCM/olefin isomerization/olefin dihydroxylation reaction

2,3-Dihydroxy-1-piperidinecarboxylic acid phenymethyl ester 3.91



Tandem RCM/olefin isomerization step

Benzyl *N*-3-butenyl-*N*-2-propenylcarbamate **3.79** (0.098 g, 0.4 mmol) was dissolved in ethyl acetate (4.0 mL) in a pressure tube (approximate capacity, 15 mL) containing a stir bar. **GII** (0.017 g, 0.02 mmol, 5 mol%) was then added in the tube in one portion. The tube was sealed with a rubber septum and placed under N₂ atmosphere. The reaction mixture was stirred at 22 °C for 1.5 h until TLC analysis indicated the complete consumption of the starting material. A gas mixture of N₂/H₂ (N₂/H₂ = 95:5, balloon) was bubbled vigorously into the solution via a cannula at 22 °C for 5 min. Upon finishing the rubber septum was replaced with a PTFE plug, and the sealed tube was placed in a 100 °C oil bath. The reaction mixture was stirred at 100 °C for 4 h before it was allowed to cool down to 22 °C naturally.

Olefin dihydroxylation step

In a 50 mL round bottom flask containing a stir bar $\text{LaCl}_3 \cdot 7\text{H}_2\text{O}$ (0.0371 g, 0.1 mmol), 25 mol%) was dissolved in H_2O (0.4 mL). NaIO_4 (0.128 g, 0.6 mmol, 1.5 equiv) was then added in the flask, and the resulting mixture was stirred vigorously at 22 °C for 5 min until a white slurry was obtained. The flask was cooled to 0 °C with an ice bath. Acetonitrile (0.8 mL) was added in the pressure tube, and the obtained brown solution was added in the cooled flask in one portion via a Pasteur pipette. Acetonitrile (0.2 mL) was used to rinse the pressure tube and then added in the flask as well. The reaction mixture was stirred vigorously at 0 °C for ca. 3 h until TLC analysis indicated complete consumption of ene-carbamate **3.80**. The reaction was quenched with saturated $\text{Na}_2\text{S}_2\text{O}_3$ aqueous solution (5.0 mL) at 0 °C. Then, the ice bath was removed and the mixture was further stirred at 22 °C for 10 min.

Work-up

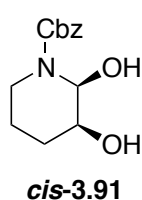
CH_2Cl_2 (15 mL) was added in the quenched reaction mixture, and the resulting biphasic mixture was transferred into a separatory funnel. The organic layer was isolated, and the rest aqueous layer was extracted with CH_2Cl_2 (3×10 mL). The combined organic layers were washed with saturated Na_2SO_3 aqueous solution (15 mL), saturated NaHCO_3 aqueous solution (15 mL) and brine (10 mL) in sequence. The organic phase was dried over anhydrous Na_2SO_4 , filtered and concentrated *in vacuo*. A brown gum was obtained as the crude product.

Purification

The crude product was first purified by silica gel chromatography (hexanes: ethyl acetate = 1:1). R_f = 0.17, developing solvent: hexanes: ethyl acetate = 1:1. The collected compound was loaded on a Biotage Si 12+M pre-packed silica gel column (dimensions:

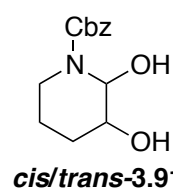
12 mm × 15.0 cm, 8.0 g silica gel), and further purified with a Biotage HPFC system (eluent: dichloromethane: hexanes: ethanol = 2:2.2:0.1). R_f = 0.19, developing solvent: dichloromethane: hexanes: ethanol = 2:2:0.1 (developed three times). The *cis* and *trans* isomers are partially separable under the second purification conditions. The purified title compound was obtained as opaque pale brown gum (0.0609 g, 61% yield)

Cis-3.91 is a known compound.^{9b,10g} Our ^1H -NMR and ^{13}C -NMR data matches the reported literature values.



^1H -NMR (500 MHz, CDCl_3), carbamate rotamers: δ 7.39 – 7.28 (m, 5H), 5.73 (d, J = 3.0 Hz, 1H), 5.12 (s, 2H), 4.19 (br s, 1H), 3.82 (br d, J = 10.5 Hz, 1H), 3.57 (br d, J = 10.0 Hz, 1H), 3.04 (app dt, J = 13.0, 2.5 Hz, 1H), 2.80 (br s, 1H), 1.83 – 1.74 (m, 1H), 1.74 – 1.60 (m, 2H), 1.55 – 1.39 (m, 1H).

^{13}C -NMR (126 MHz, CDCl_3), carbamate rotamers: δ 156.02 (carbonyl carbon, weak signal due to slow relaxation and existence of carbamate rotamers), 136.16, 128.53, 128.16, 127.94, 76.56, 69.02, 67.53, 38.15, 26.74, 23.46.



^1H NMR (500 MHz, CDCl_3), two diastereomers and carbamate rotamers, δ 7.42 – 7.27 (m, 5H), 5.72 (s, 0.6H), 5.59 (s, 0.4H), 5.11 (s, 2H), 4.43 (br s, 1H), 3.97 – 3.73 (m, 1.4H), 3.55 (br d, J = 10.0 Hz, 0.6H), 3.17 (overlapped with a broad peak, app t, J = 11.5 Hz, 1H), 3.03 (overlapped with a broad peak, t, J = 12.5 Hz, 1H), 1.97 – 1.56 (m, 3H), 1.54 – 1.35 (m, 1H).

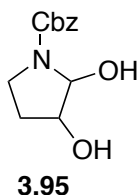
^{13}C NMR (126 MHz, CDCl_3), two diastereomers and carbamate rotamers, δ 156.92 and 155.94 (carbonyl carbon, weak signals due to slow relaxation and existence of carbamate

rotamers), 136.17, 128.52, 128.51, 128.14, 128.10, 127.92, 127.84, 78.19, 76.54, 69.05, 67.52, 67.00, 38.85, 38.13, 26.64, 24.88, 23.50, 18.62.

FTIR (neat): 3384, 2930, 1675, 1423, 1344, 1304, 1255, 1153, 1128, 1070, 1037, 989, 892, 873, 736, 686 cm^{-1} .

HSMS (DART+) calcd for $\text{C}_{13}\text{H}_{16}\text{NO}_3$ ($[\text{M}+\text{H}-\text{H}_2\text{O}]^+$): 234.1130, found: 234.1125.

2,3-Dihydroxy-1-pyrrolidinecarboxylic acid phenymethyl ester **3.95**



The title compound was synthesized according to the representative procedure, except that the tandem RCM/olefin isomerization step followed the procedure of preparation of ene-carbamate **3.86**. Benzyl *N,N*-diallylcarbamate **3.85** (0.0925 g, 0.4 mmol) was used in the reaction. The crude product was first purified by silica gel chromatography (hexanes: ethyl acetate = 1:1.2). R_f = 0.13, developing solvent: hexanes: ethyl acetate = 1:1.2. The collected compound was loaded on a Biotage Si 12+M pre-packed silica gel column (dimensions: 12 mm \times 15.0 cm, 8.0 g silica gel), and further purified with a Biotage HPFC system (eluent: dichloromethane: hexanes: ethanol = 2:1.2:0.1). R_f = 0.12, developing solvent: dichloromethane: hexanes: ethanol = 2:1:0.1 (developed twice). The *cis* and *trans* isomers are inseparable under the two purification conditions. The purified title compound was obtained as opaque pale brown gum (0.0154 g, 16% yield)

Diol **3.95** (a *cis* and *trans* mixture) is a known compound,¹¹ but the reported NMR data does not disclose any defined signal information about the ratio of two diastereomers (the reported NMR data was recorded on a 200 MHz NMR instrument).

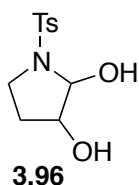
^1H -NMR (600 MHz, CDCl_3), two diastereomers and carbamate rotamers: δ 7.52 – 7.28 (m, 5H), 5.32 (s, 0.67H), 5.27 (s, 0.33H), 5.21 – 5.06 (m, 2H), 4.30 – 4.09 (m, 1.7H), 3.67 – 3.53 (m, 2H), 3.16 (s, 0.3H), 2.80 (s, 0.67H), 2.55 (s, 0.32H), 2.28 – 2.16 (m, 1H), 1.91 – 1.80 (m, 1H).

^{13}C -NMR (151 MHz, CDCl_3), two diastereomers and carbamate rotamers: δ 158.64, 157.33, 138.87, 131.29, 131.17, 130.94, 130.78, 130.55, 130.50, 89.94, 89.30, 78.81, 77.99, 69.97, 69.84, 46.94, 46.64, 45.54, 33.10, 32.66, 32.34.

FTIR (neat): 3391, 2953, 2924, 1679, 1553, 1413, 1351, 1177, 1119, 1096, 1032, 987, 735, 696, 607 cm^{-1} .

HSMS (DART+) calcd for $\text{C}_{12}\text{H}_{14}\text{NO}_3$ ($[\text{M}+\text{H}-\text{H}_2\text{O}]^+$): 220.0974, found: 220.0963.

2,3-Dihydroxy-1-[(4-Methylphenyl)sulfonyl]pyrrolidine **3.96**



The title compound was synthesized according to the representative procedure, except that the tandem RCM/olefin isomerization step followed the procedure of preparation of ene-sulfonamide **3.90**. *N,N*-diallyl-4-methylbenzenesulfonamide **3.89** (0.101 g, 0.4 mmol) was used in the reaction. The crude product was first purified by silica gel chromatography (hexanes: ethyl acetate = 1:1.2). R_f = 0.13, developing solvent: hexanes: ethyl acetate = 1:1.2. The collected compound was loaded on a Biotage Si 12+M pre-packed silica gel column (dimensions: 12 mm \times 15.0 cm, 8.0 g silica gel), and further purified with a Biotage HPFC system (eluent: dichloromethane: hexanes: methanol = 2:1:0.1). R_f = 0.07, developing solvent: dichloromethane: hexanes: methanol = 2:1:0.1. The *cis*- and *trans*-isomers are

inseparable under the two purification conditions. The purified title compound was obtained as opaque pale brown gum (0.0369 g, 36% yield).

Diol **3.96** is a known compound,³⁸ but we have not found any reported characterization data of this compound.

¹H-NMR (500 MHz, CDCl₃), two diastereomers: δ 7.80 – 7.69 (m, 2H), 7.32 – 7.25 (m, 2H), 5.29 (app s, 1H), 4.36 (br s, 0.4H), 4.17 (d, J = 3.0 Hz, 0.6H), 4.03 (br s, 0.6H), 3.96 (br s, 0.4H), 3.50 (td, J = 9.0, 2.0 Hz, 0.6H), 3.45 (ddd, J = 9.0, 8.5, 4.0 Hz, 0.4H), 3.32 – 3.24 (app ddd, J = 10.0, 9.0, 6.5 Hz, 0.6H), 3.16 (br d, J = 5.5 Hz, 0.4H), 3.07 (td, J = 8.5, 7.5 Hz, 0.4H), 2.66 (br d, J = 2.0 Hz, 0.6H), 2.44 – 2.36 (partially overlapped two singlets, 3H), 2.27 – 2.18 (m, 0.6H), 2.05 – 1.97 (m, 0.4H), 1.96 – 1.86 (m, 0.4H), 1.81 (dd, J = 13.5, 7.0 Hz, 0.6H).

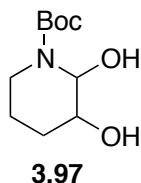
¹³C-NMR (126 MHz, CDCl₃), two diastereomers: δ 143.88, 143.72, 135.36, 135.15, 129.83, 129.68, 127.38, 127.26, 89.31, 81.79, 75.85, 71.39, 45.55, 43.90, 30.64, 30.34, 21.52.

FTIR (neat): 3427, 2954, 1597, 1400, 1326, 1185, 1155, 1090, 1071, 1025, 1012, 985, 963, 837, 814, 706, 663, 586, 547, 504 cm⁻¹.

HSMS (DART+) calcd for C₁₁H₁₄NO₃S ([M+H-H₂O])⁺: 240.0694, found: 240.0693.

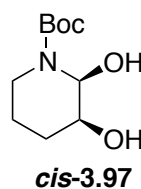
³⁸ Sunose, M.; Anderson, K. M.; Guy Orpen, A.; Gallagher, T.; Macdonald, S. J. F. *Tetrahedron Letters* **1998**, 39, 8885-8888.

2,3-Dihydroxy-1-piperidinecarboxylic acid *tert*-butyl ester **3.97**



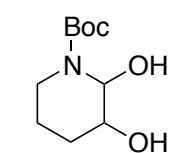
The title compound was synthesized according to the representative procedure. *tert*-Butyl *N*-3-butenyl-*N*-2-propenylcarbamate **3.81** (0.0845 g, 0.4 mmol) was used in the reaction. The crude product was first purified by silica gel column chromatography (hexanes: ethyl acetate = 1.2:1). *R_f* = 0.21, developing solvent: hexanes: ethyl acetate = 1:1. The collected compound was loaded on a Biotage Si 12+M pre-packed silica gel column (dimensions: 12 mm × 15.0 cm, 8.0 g silica gel), and further purified with a Biotage HPFC system (eluent: dichloromethane: hexanes: ethanol = 2:3:0.15). *R_f* = 0.23, developing solvent: dichloromethane: hexanes: ethanol = 2:3:0.15 (developed three times). The *cis* and *trans* isomers are partially separable under the second purification conditions. The purified title compound was obtained as an off-white solid (0.0351 g, 40% yield).

***Cis*-3.91** is a known compound.^{9b} Our ¹H-NMR and ¹³C-NMR data matches the reported literature values.



¹H-NMR (600 MHz, CDCl₃), carbamate rotamers: δ 5.66 (s, 1H), 3.73 (s, 1H), 3.63 – 3.51 (m, 1H), 2.95 (app t, *J* = 10.5 Hz, 1H), 2.59 (s, 1H), 1.94 (s, 1H), 1.86 – 1.75 (m, 1H), 1.74 – 1.53 (m, 3H), 1.53 – 1.36 (a singlet overlapped with other peaks, m, 10H).

¹³C-NMR (151 MHz, CDCl₃), carbamate rotamers: δ 157.92(carbonyl carbon, weak signal due to slow relaxation and existence of carbamate rotamers), 83.29, 79.05, 71.72, 40.68, 30.99, 29.60, 26.13.



cis/trans-3.97

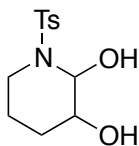
$^1\text{H-NMR}$ (600 MHz, CDCl_3), two diastereomers and carbamate rotamers: δ 5.65 (s, 0.67H), 5.48 (s, 0.33H), 4.11 – 3.39 (m, 2H), 3.10 (dt, $J = 12.6, 2.4$ Hz, 0.33H), 2.95 (app t, $J = 13.2$ HZ, 0.67H), 2.70 (s, 1H), 2.52 (br s, 0.5H), 2.03 (s, 0.5H), 1.95 – 1.58 (m, 3H), 1.53 – 1.36 (a singlet overlapped with other peaks, m, 10H).

$^{13}\text{C-NMR}$ (151 MHz, CDCl_3), two diastereomers and carbamate rotamers: δ 158.93 and 157.97 (carbonyl carbon, weak signals due to slow relaxation and existence of carbamate rotamers), 83.35, 83.28, 80.87, 78.94, 71.73, 69.80, 41.53, 40.70, 31.02, 30.99, 29.57, 27.73, 21.37.

FTIR (neat): 3411, 2975, 2935, 1673, 1415, 1392, 1366, 1268, 1253, 1174, 1149, 1071, 990, 877 cm^{-1} .

HSMS (DART+) calcd for $\text{C}_{10}\text{H}_{18}\text{NO}_3$ ($[\text{M}+\text{H}-\text{H}_2\text{O}]^+$): 200.1287, found: 200.1280.

2,3-Dihydroxy-1-[(4-Methylphenyl)sulfonyl]piperidine **3.98**



3.98

The title compound was synthesized according to the representative procedure, except that the tandem RCM/olefin isomerization step followed the procedure of preparation of ene-sulfonamide **3.78**. *N*-3-Butenyl-4-methyl-*N*-2-propenylbenzenesulfonamide **3.77** (0.106 g, 0.4 mmol) and **GII** (0.034 g, 0.04 mmol) were used in the reaction. The crude product was first purified by silica gel column chromatography (hexanes: ethyl acetate = 1:1). $R_f = 0.15$, developing solvent: hexanes: ethyl acetate = 1:1. The collected compound was further purified with by silica gel column chromatography (dichloromethane: hexanes: ethanol = 2:1.5:0.05). $R_f = 0.12$,

developing solvent: dichloromethane: hexanes: ethanol = 2:1.2:0.05 (developed three times). The *cis* and *trans* isomers are inseparable under the above two purification conditions. The purified title compound was obtained as an off-white solid (0.0806 g, 74% yield).

Diol **3.96** is a known compound,³⁹ but we have not found any reported characterization data of this compound.

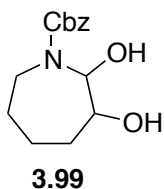
¹H-NMR (500 MHz, acetone-*d*₆), two diastereomers: δ 7.82 – 7.74 (overlapped peaks, m, 2H), 7.40 – 7.32 (overlapped peaks, m, 2H), 5.49 (app t, *J* = 4.0 Hz, 0.86H), 5.41 (dd, *J* = 5.0, 3.0 Hz, 0.14H), 4.82 (app dd, *J* = 5.5, 0.5 Hz, 0.14H), 4.54 – 4.45 (app dd, *J* = 4.5, 0.5 Hz, 0.86H), 3.96 (d, *J* = 5.0 Hz, 0.14H), 3.91 (d, *J* = 6.5 Hz, 0.86H), 3.81 – 3.77 (m, 0.14H), 3.61 – 3.54 (m, 0.86H), 3.41 – 3.34 (m, 1H), 2.77 (td, *J* = 12.0, 2.5 Hz, 1H), 2.45 – 2.38 (two overlapped singlets, 3H), 1.74 – 1.48 (m, 4H).

¹³C-NMR (126 MHz, acetone-*d*₆), two diastereomers: δ 142.97, 137.50, 129.22, 129.11, 127.77, 127.68, 79.46, 78.37, 69.60, 67.30, 39.77, 39.08, 26.12, 24.59, 23.67, 20.46, 18.58.

FTIR (neat): 3460, 2946, 1325, 1305, 1286, 1157, 1108, 1090, 1057, 1019, 991, 927, 889, 814, 761, 660, 586, 563, 542, 511 cm⁻¹.

HSMS (DART+) calcd for C₁₂H₁₆NO₃S ([M+H-H₂O]⁺): 254.0851, found: 254.0858.

Hexahydro-2,3-dihydroxy-1*H*-azepine-1-carboxylic acid phenylmethyl ester **3.99**



The title compound was synthesized according to the representative procedure, except that the tandem RCM/olefin isomerization step followed the procedure of preparation of ene-carbamate **3.84**. Benzyl *N*-4-pentenyl-*N*-2-propenylcarbamate **3.83** (0.052 g, 0.2 mmol) and **GII** (0.017, 0.02 mmol, 10 mol%) were used in the reaction. The crude product was first purified by silica gel column chromatography (hexanes: ethyl acetate = 1:1). R_f = 0.15, developing solvent: hexanes: ethyl acetate = 1:1. The collected compound was loaded on a Biotage Si 12+M pre-packed silica gel column (dimensions: 12 mm \times 15.0 cm, 8.0 g silica gel), and further purified with a Biotage HPFC system (eluent: dichloromethane: hexanes: ethanol = 2:2:0.1). R_f = 0.16, developing solvent: dichloromethane: hexanes: ethanol = 2:1.6:0.1 (developed twice). The *cis* and *trans* isomers are inseparable under the two purification conditions. The purified title compound was obtained as opaque pale brown gum (0.0153 g, 29% yield).

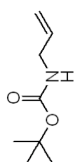
^1H -NMR (600 MHz, CDCl_3), two diastereomers and carbamate rotamers: δ 7.42 – 7.29 (m, 5H), 5.29 – 5.21 (m, 1H), 5.20 – 5.10 (m, 2H), 4.02 (br s, 0.63H), 3.91 (br d, J = 11.4 Hz, 0.5H), 3.81 – 3.72 (m, 1.5H), 3.15 (br s, 0.37H), 2.97 (app dd, J = 15.0, 11.4 Hz, 0.63H), 2.89 (app dd, J = 14.4, 10.8 Hz, 0.37H), 2.71 (br s, 0.63H), 2.63 (br s, 0.37H), 1.90 – 1.75 (m, 2H), 1.75 – 1.66 (m, 1H), 1.62 (app q, J = 11.4 Hz, 1H), 1.53 – 1.37 (m, 2H).

^{13}C -NMR (151 MHz, CDCl_3), two diastereomers and carbamate rotamers: δ 159.38, 158.13, 138.90, 138.79, 131.32, 131.20, 130.98, 130.79, 130.73, 130.42, 87.61, 87.59,

87.11, 77.96, 77.93, 77.63, 77.59, 70.34, 70.13, 45.08, 45.04, 34.84, 34.68, 31.66, 31.31, 28.62, 28.20.

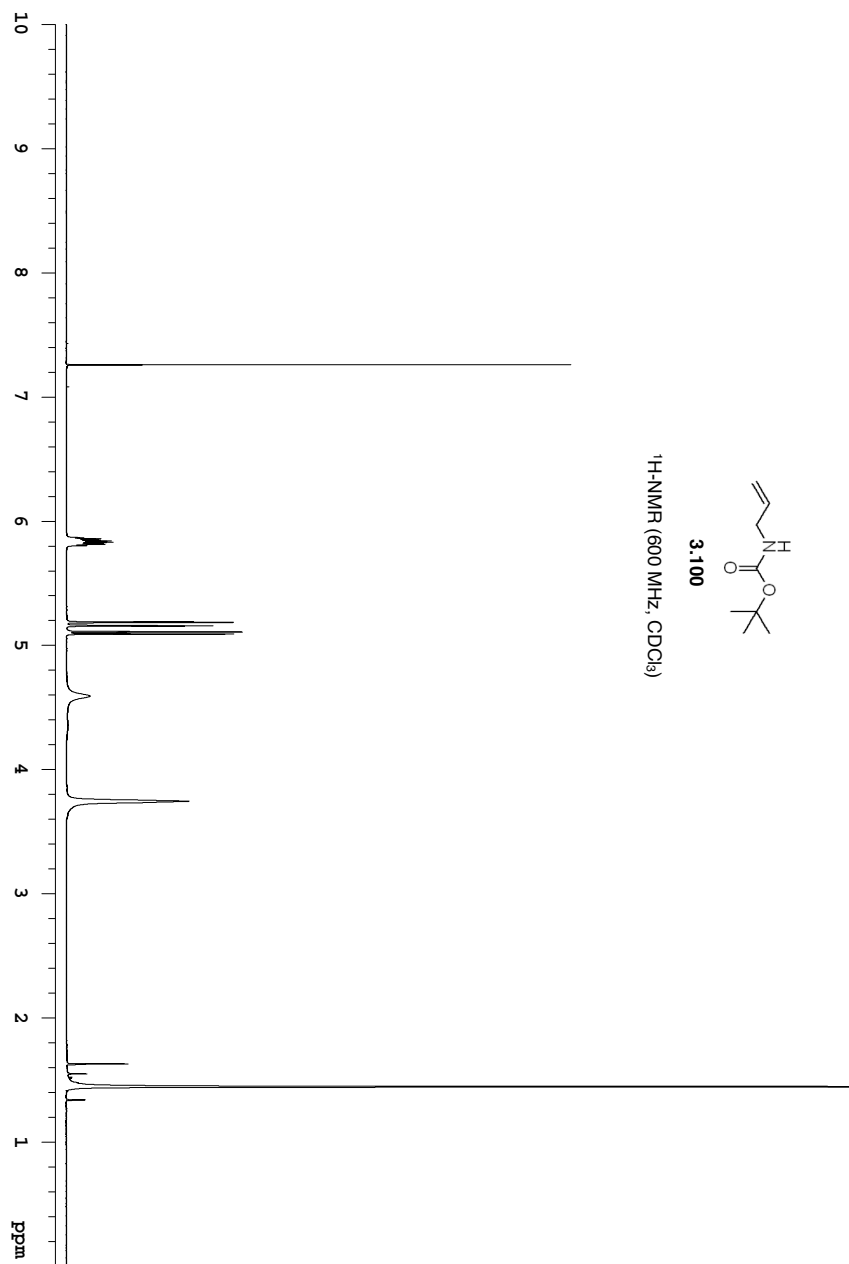
FTIR (neat): 3390, 2931, 2855, 1676, 1453, 1418, 1336, 1278, 1174, 1040, 991, 969, 843, 771, 735, 696 cm^{-1} .

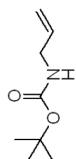
HSMS (DART+) calcd for $\text{C}_{14}\text{H}_{18}\text{NO}_3$ ($[\text{M}+\text{H}-\text{H}_2\text{O}]^+$): 248.1289, found: 248.1285.



3.100

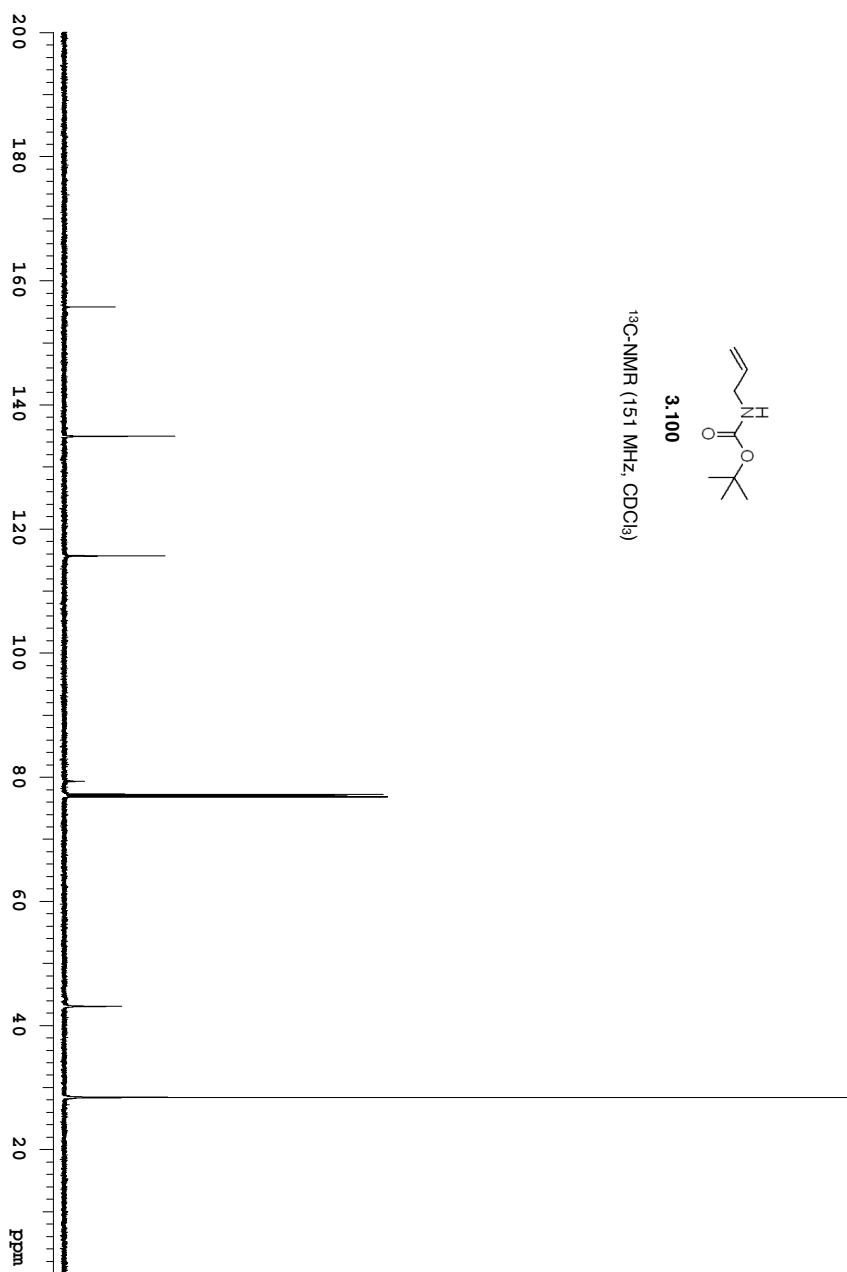
¹H-NMR (600 MHz, CDCl₃)

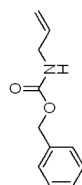




3.100

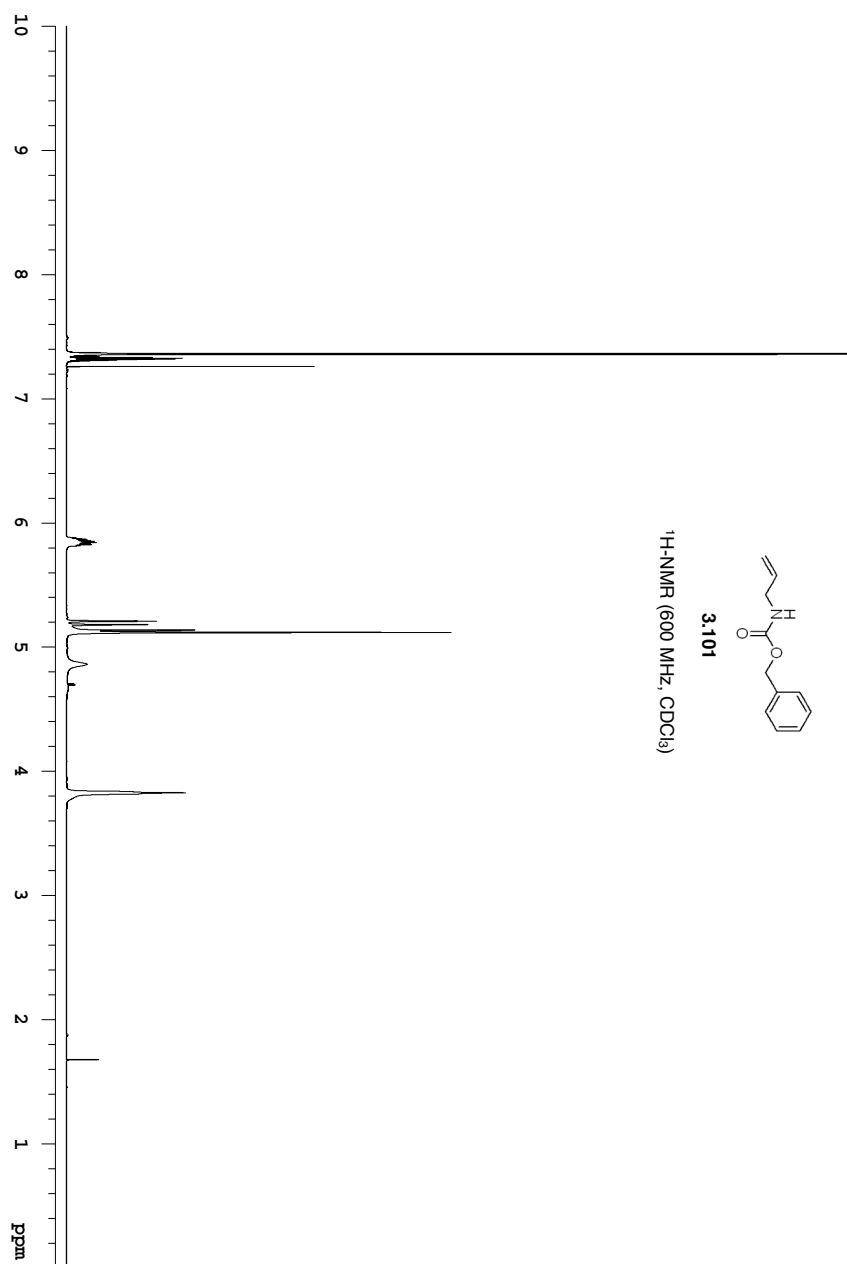
^{13}C -NMR (151 MHz, CDCl_3)

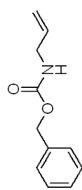




3.101

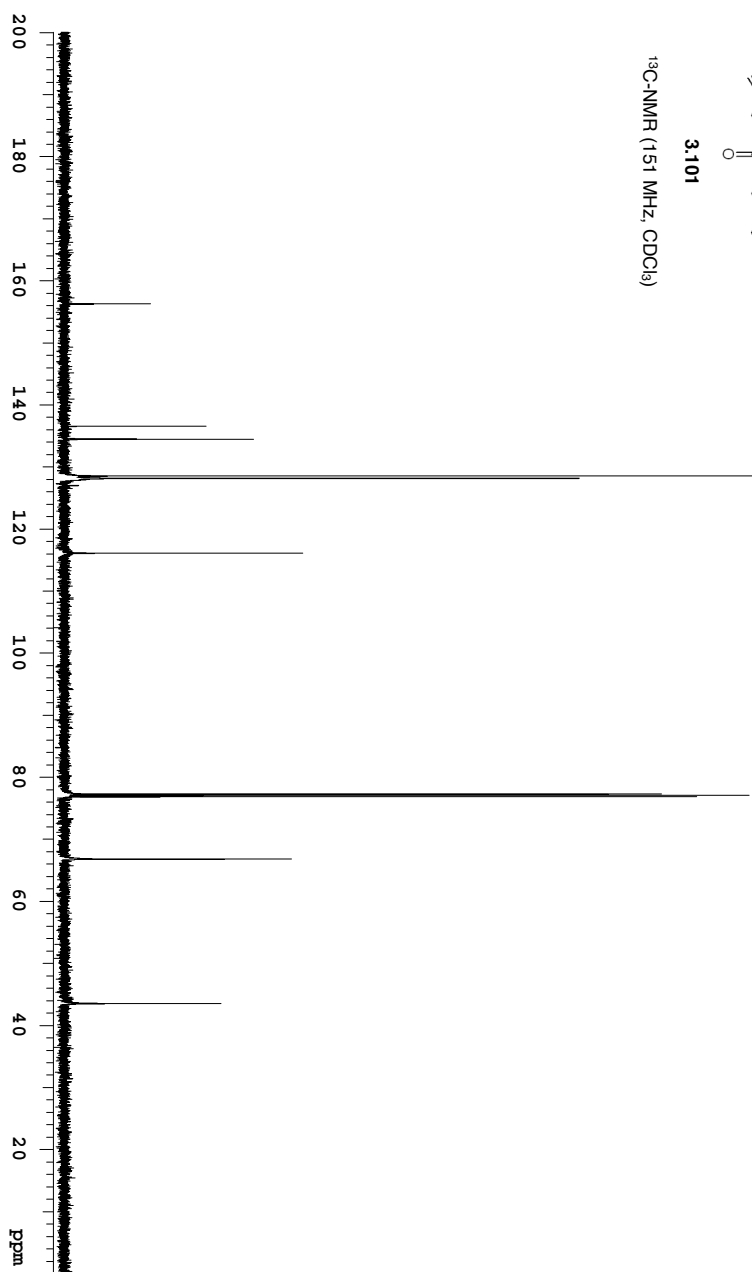
¹H-NMR (600 MHz, CDCl₃)

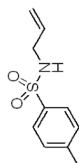




3.101

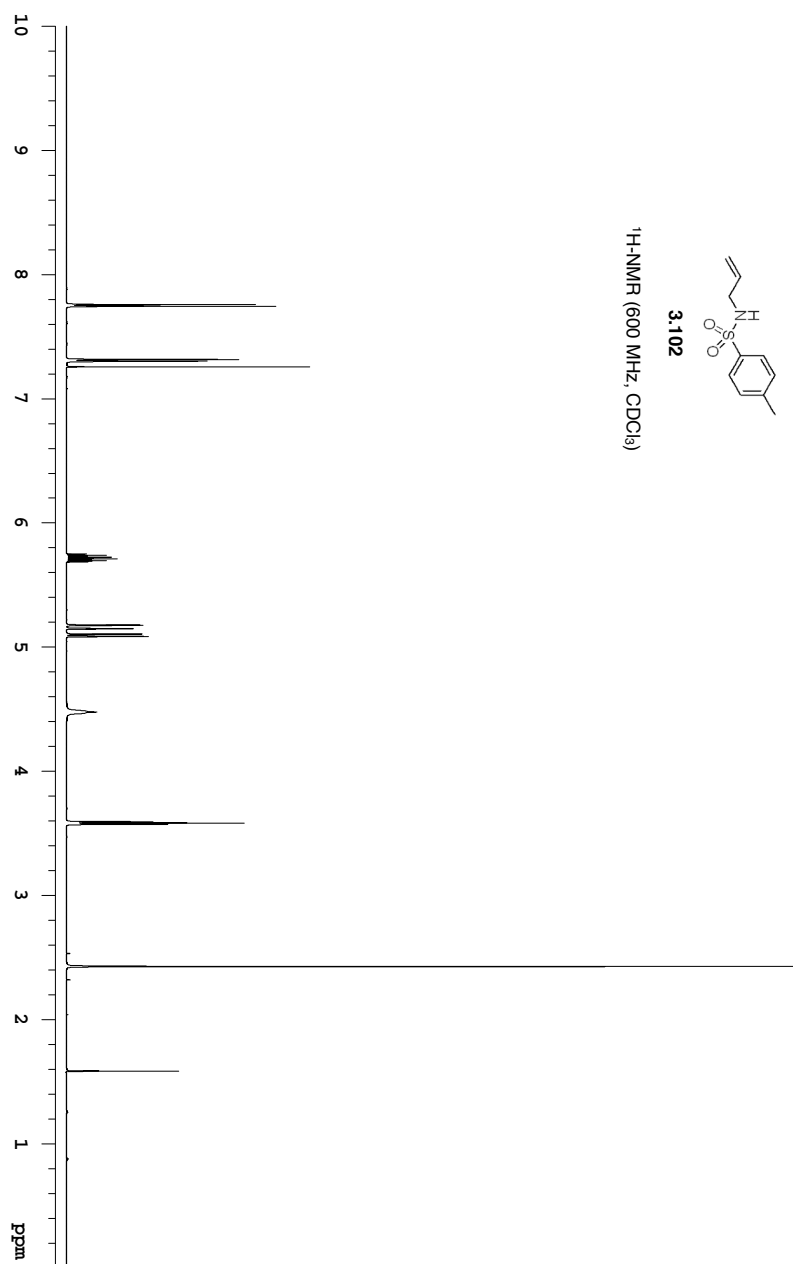
^{13}C -NMR (151 MHz, CDCl_3)

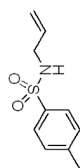




3.102

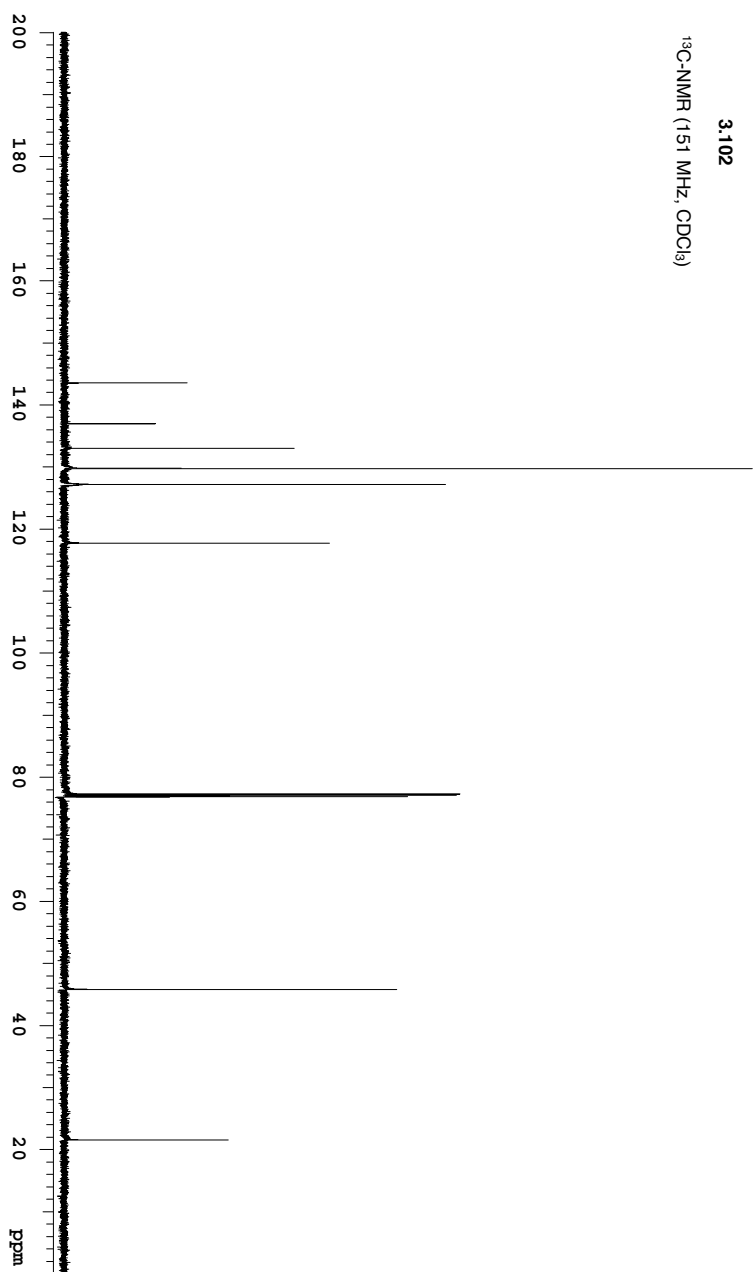
¹H-NMR (600 MHz, CDCl₃)

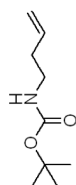




3.102

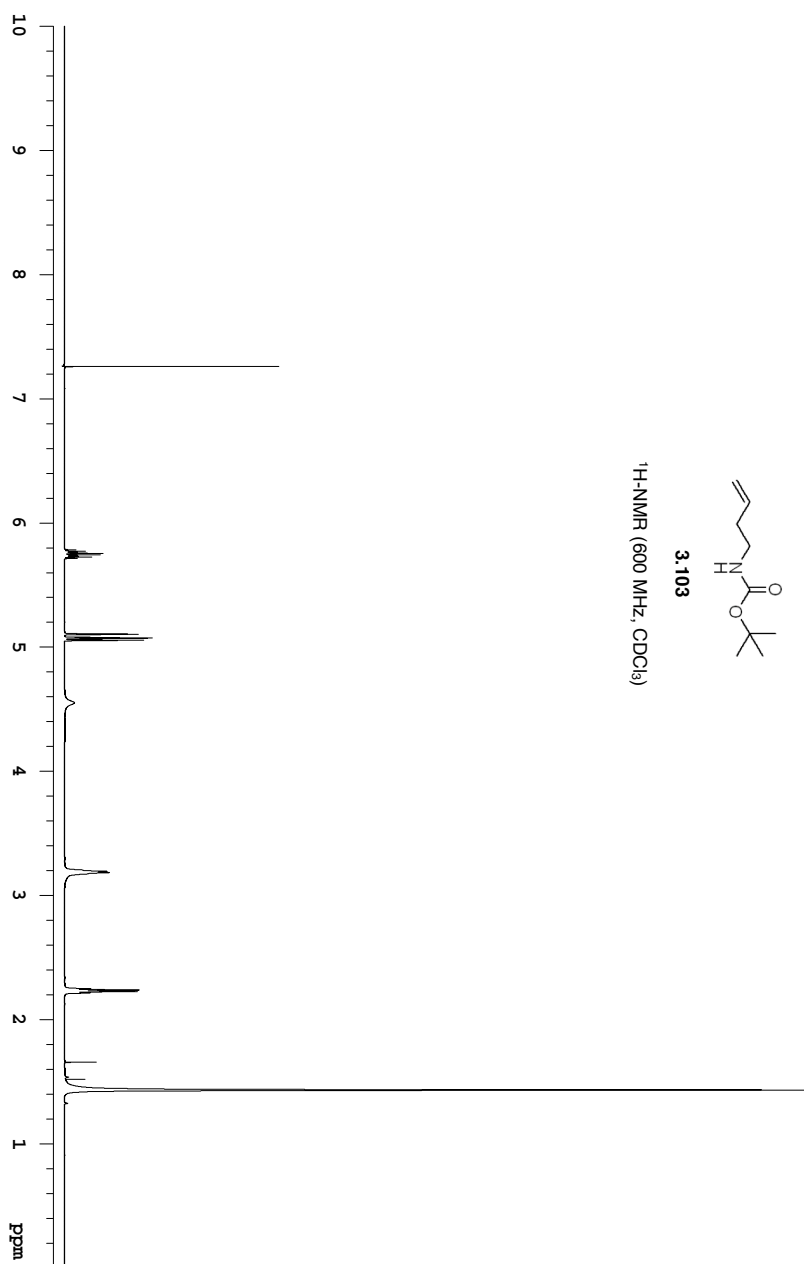
^{13}C -NMR (151 MHz, CDCl_3)

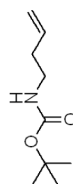




3.103

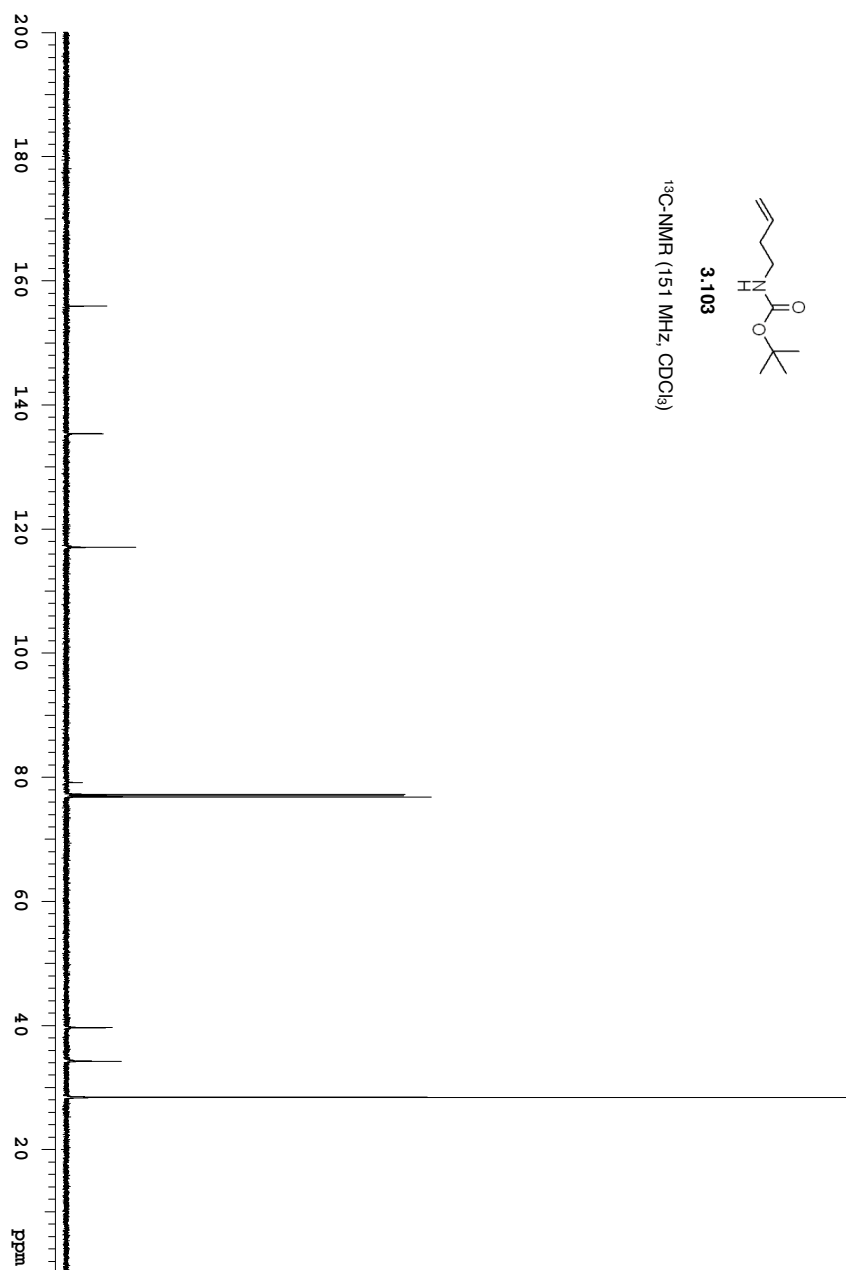
¹H-NMR (600 MHz, CDCl₃)

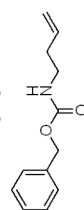




3.103

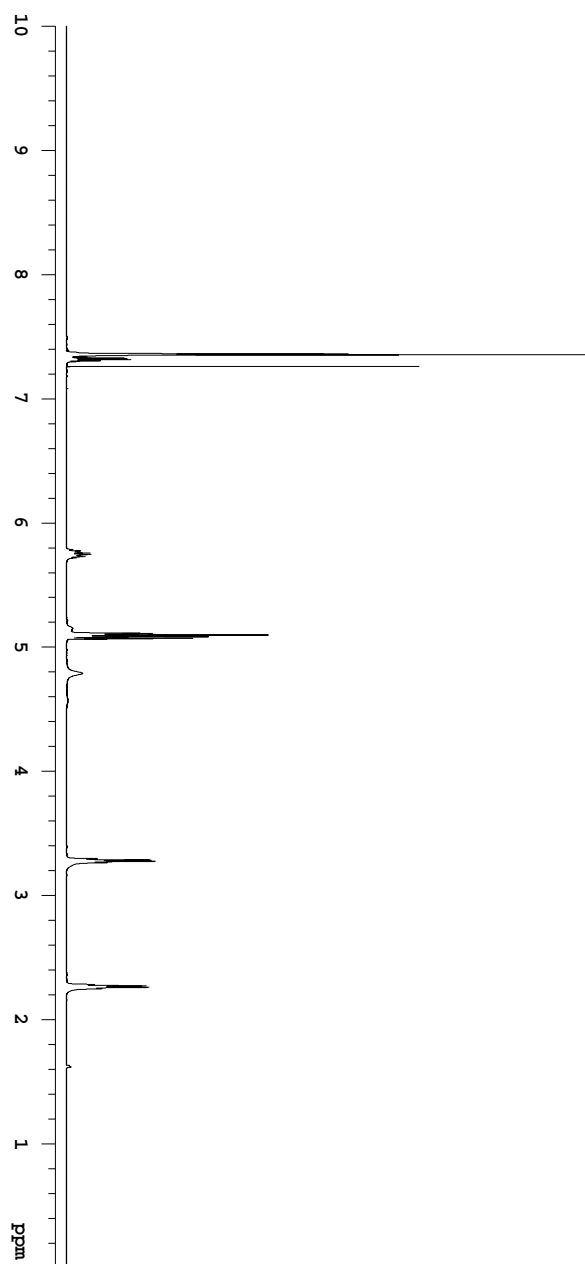
^{13}C -NMR (151 MHz, CDCl_3)

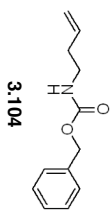




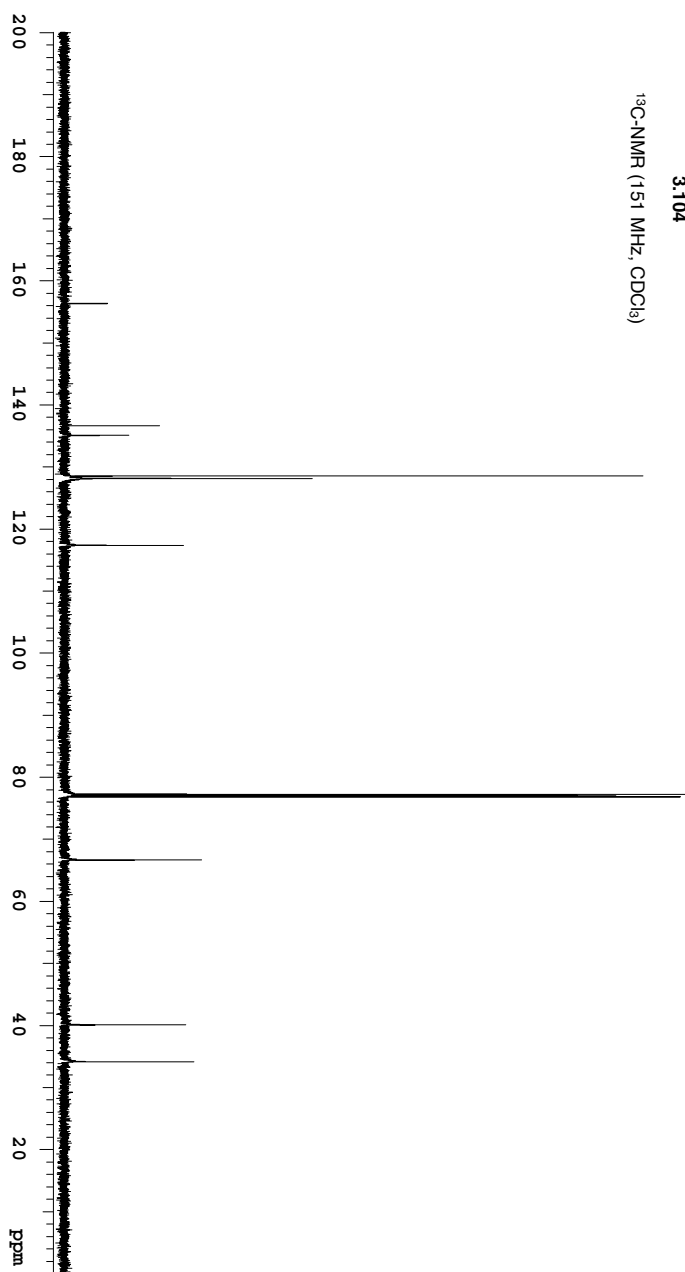
3.104

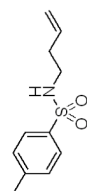
¹H-NMR (600 MHz, CDCl₃)





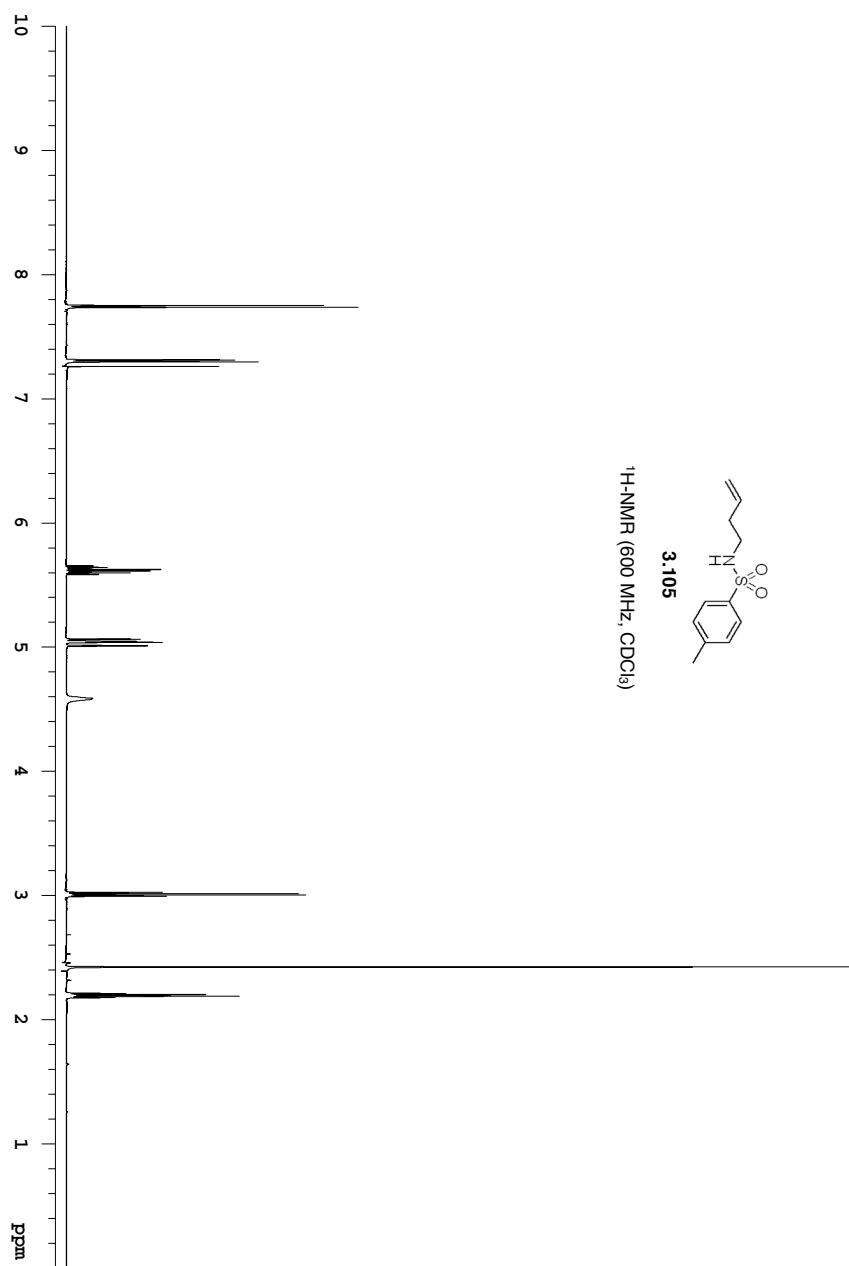
¹³C-NMR (151 MHz, CDCl₃)

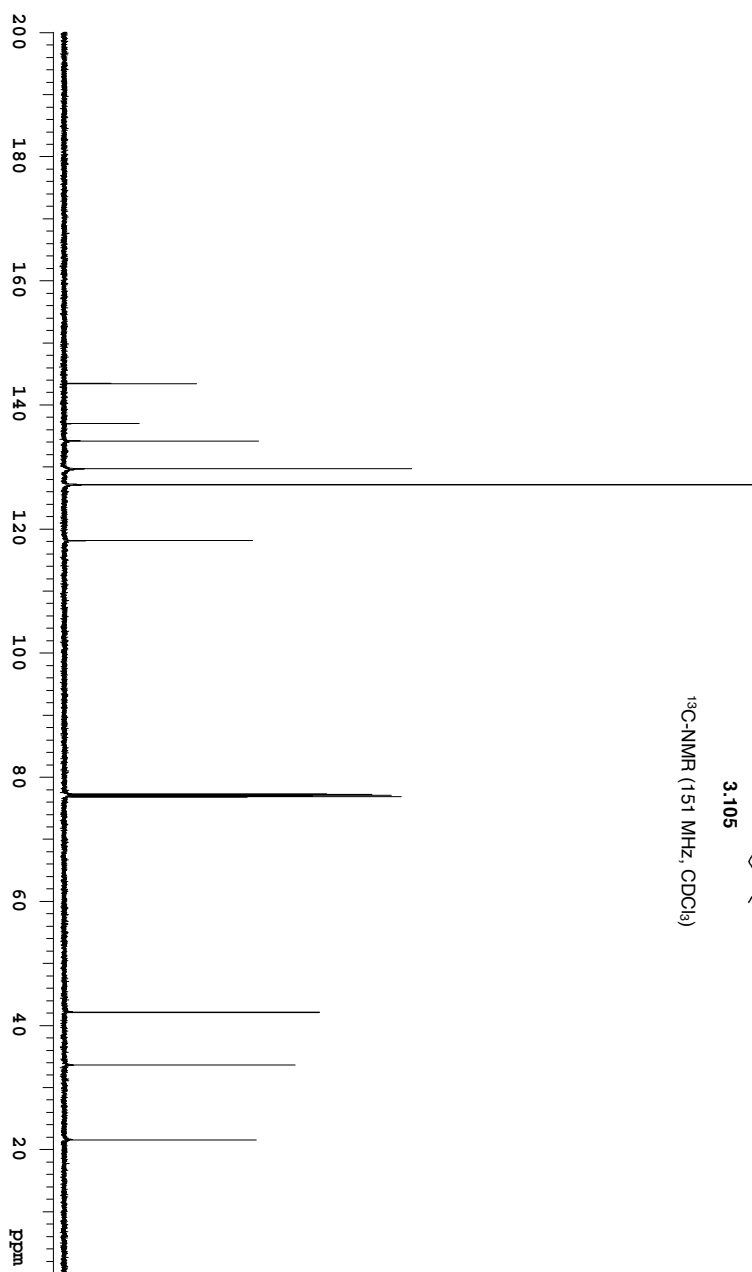
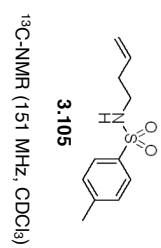


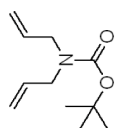


3.105

$^1\text{H-NMR}$ (600 MHz, CDCl_3)

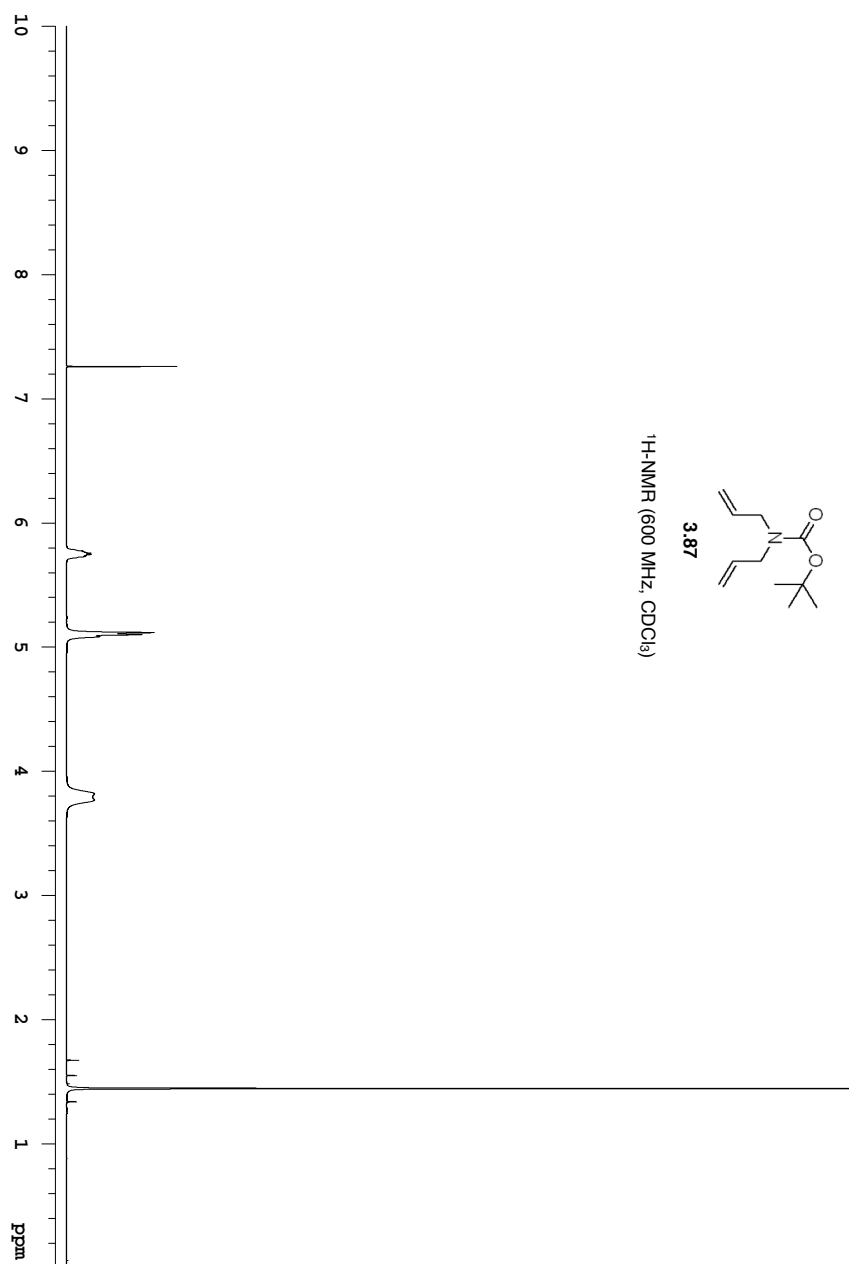


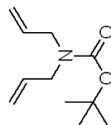




3.87

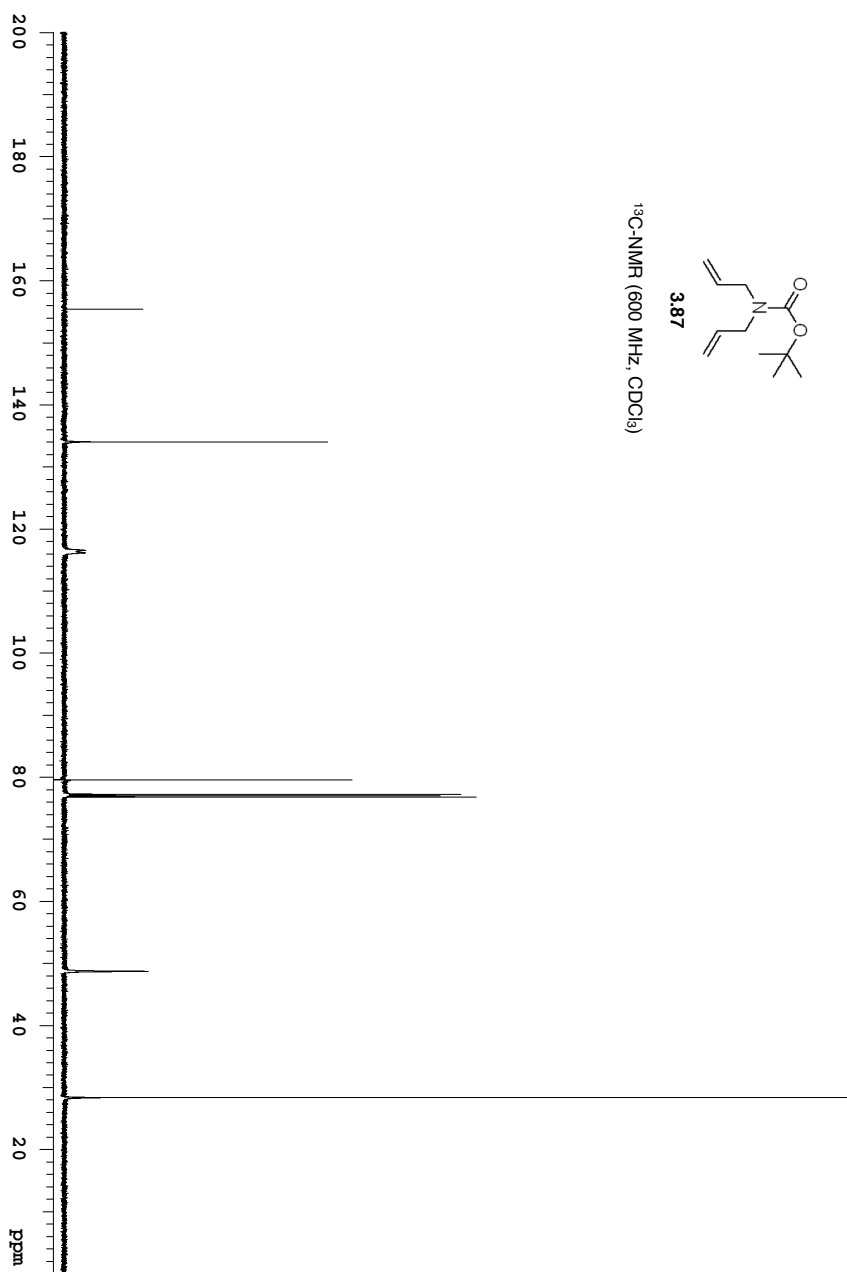
¹H-NMR (600 MHz, CDCl₃)

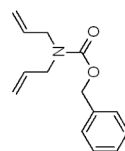




3.87

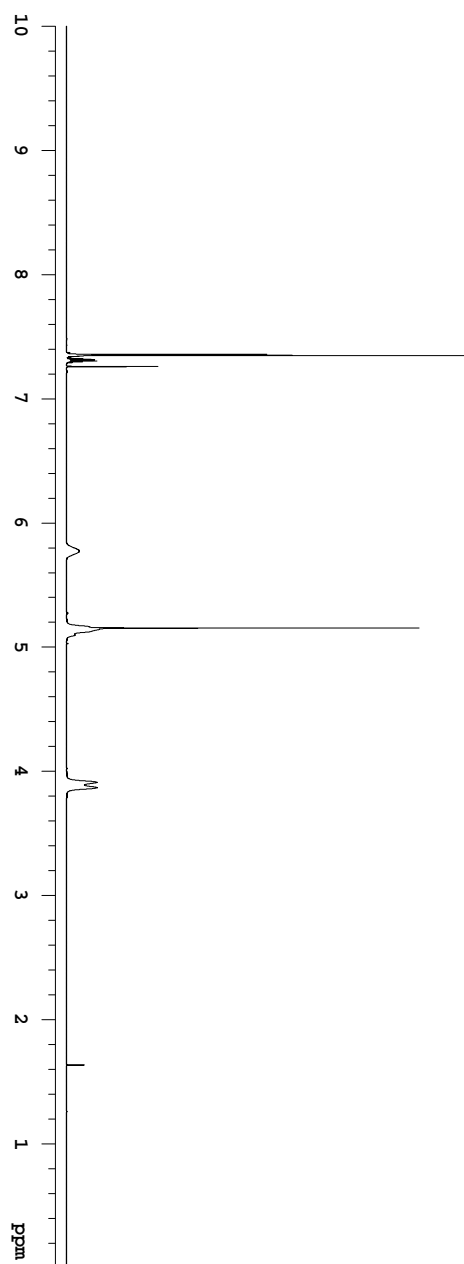
^{13}C -NMR (600 MHz, CDCl_3)

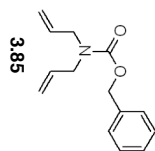




3.85

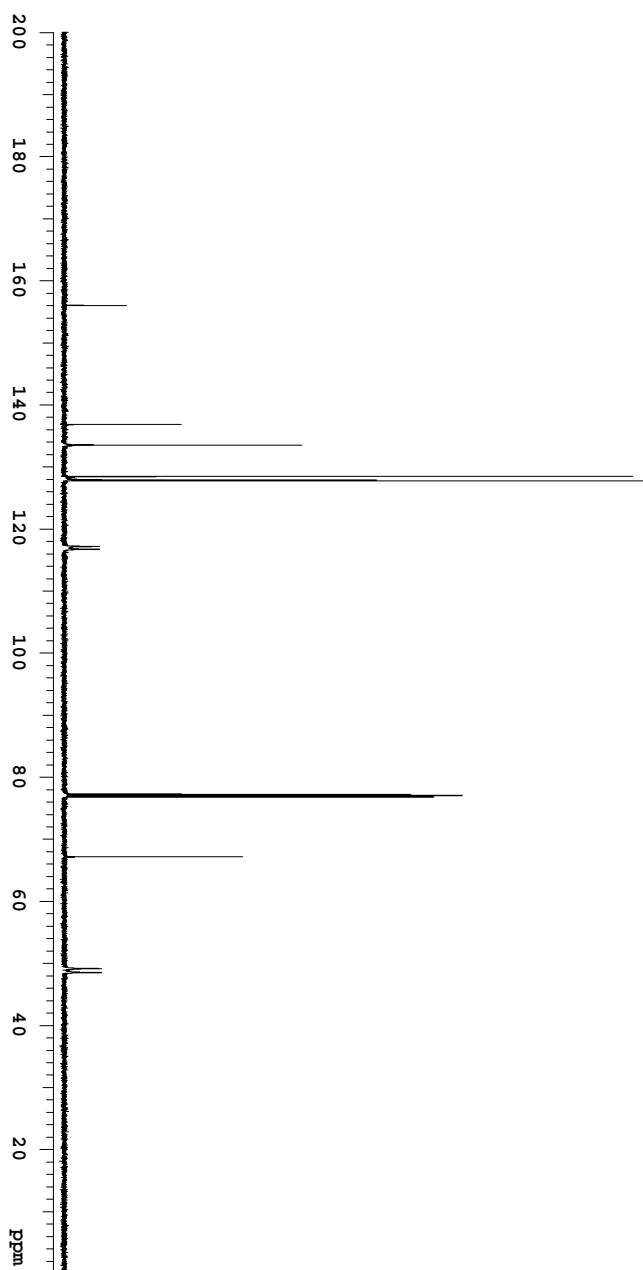
$^1\text{H-NMR}$ (600 MHz, CDCl_3)

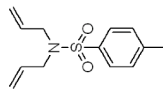




3.85

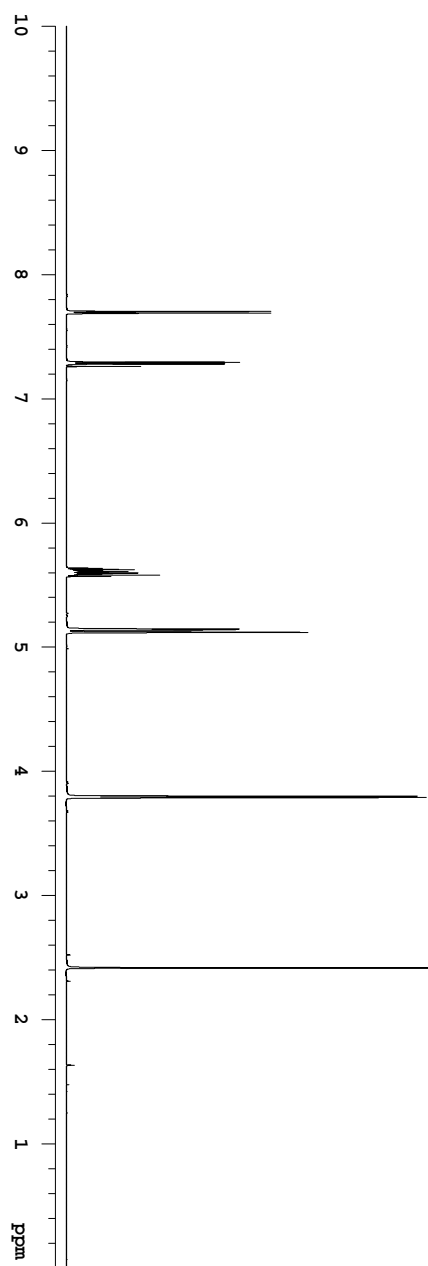
^{13}C -NMR (600 MHz, CDCl_3)

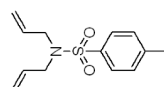




3.89

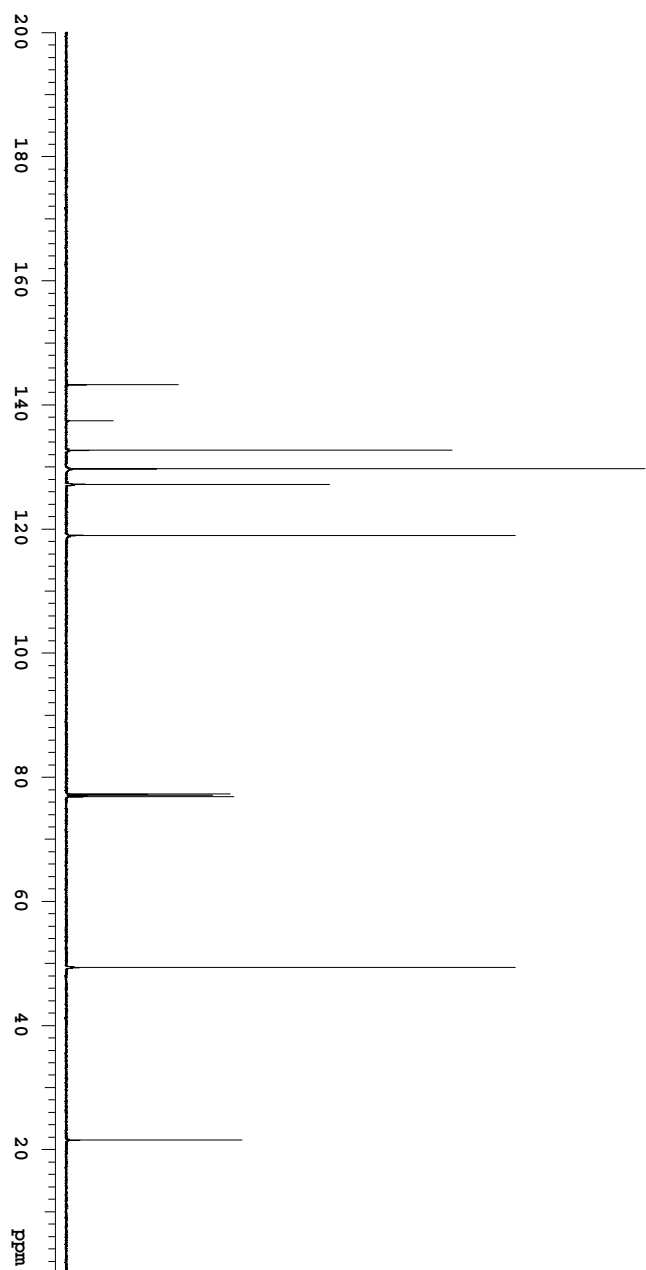
¹H-NMR (600 MHz, CDCl₃)

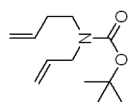




3.89

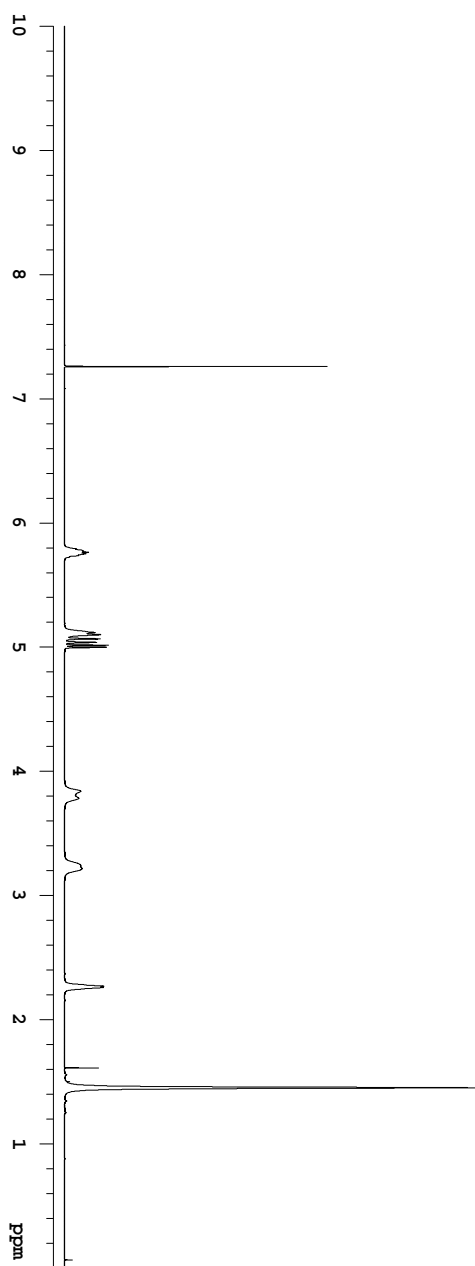
^{13}C -NMR (151 MHz, CDCl_3)

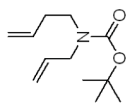




3.81

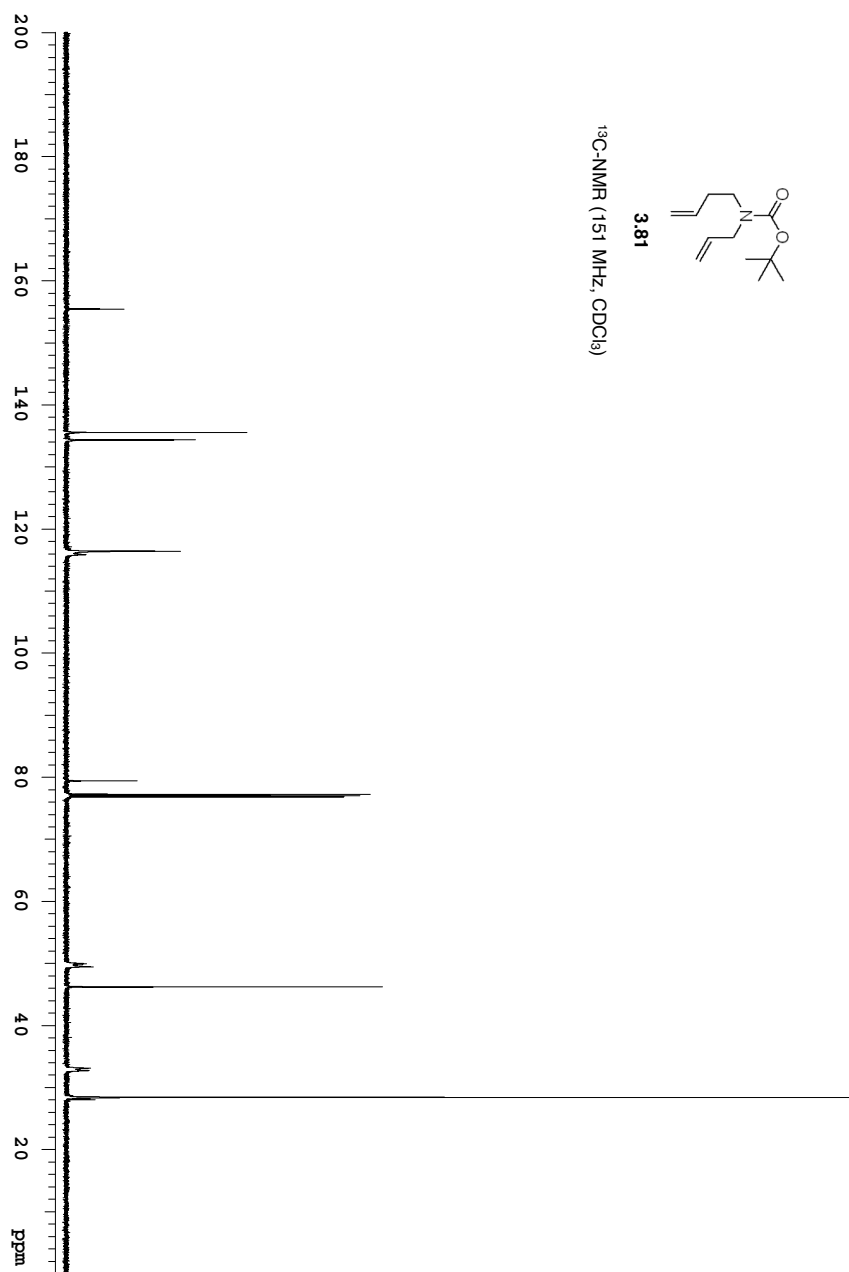
¹H-NMR (600 MHz, CDCl₃)

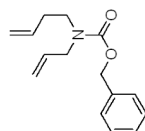




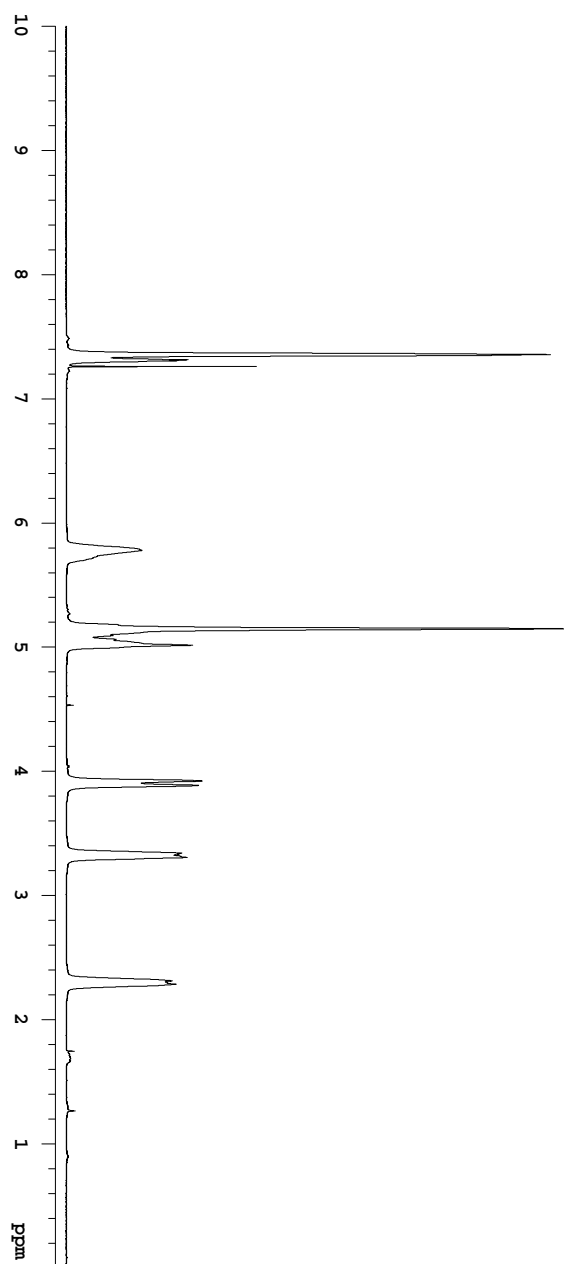
3.81

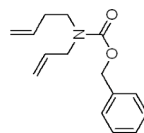
¹³C-NMR (151 MHz, CDCl₃)





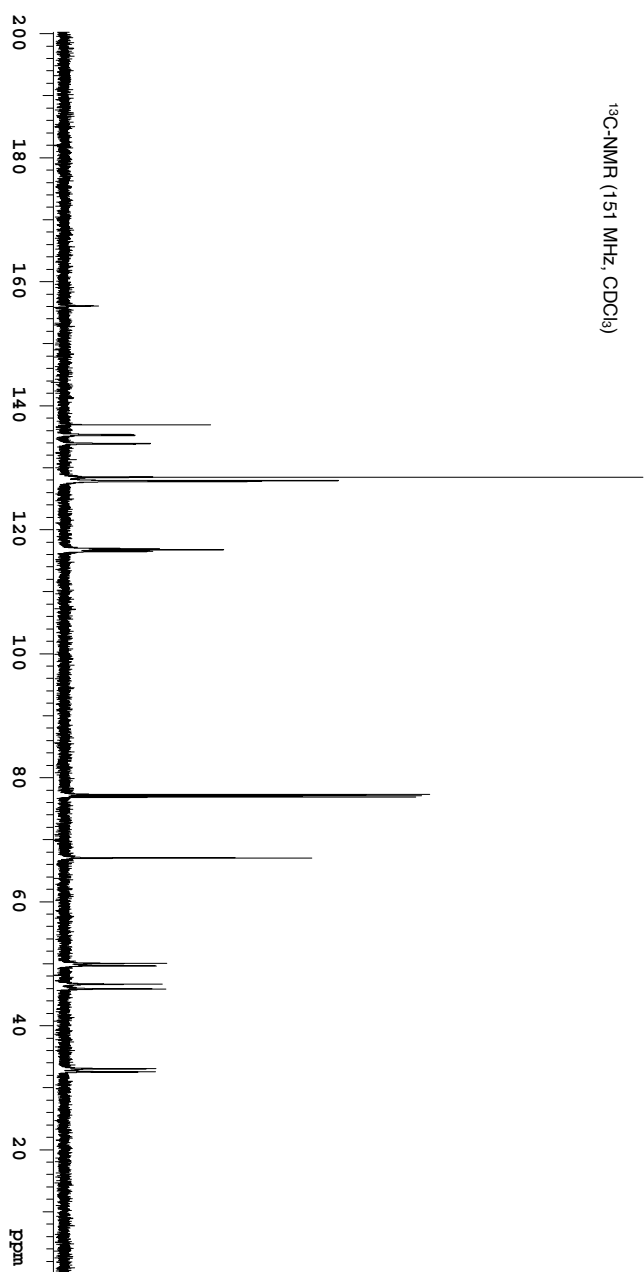
3.79

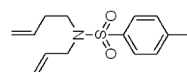
¹H-NMR (600 MHz, CDCl₃)



3.79

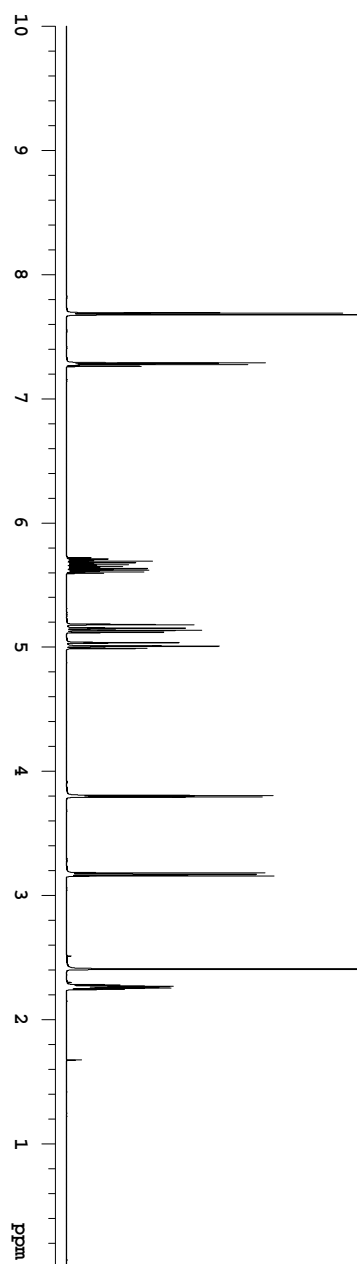
^{13}C -NMR (151 MHz, CDCl_3)

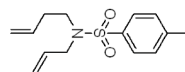




3.77

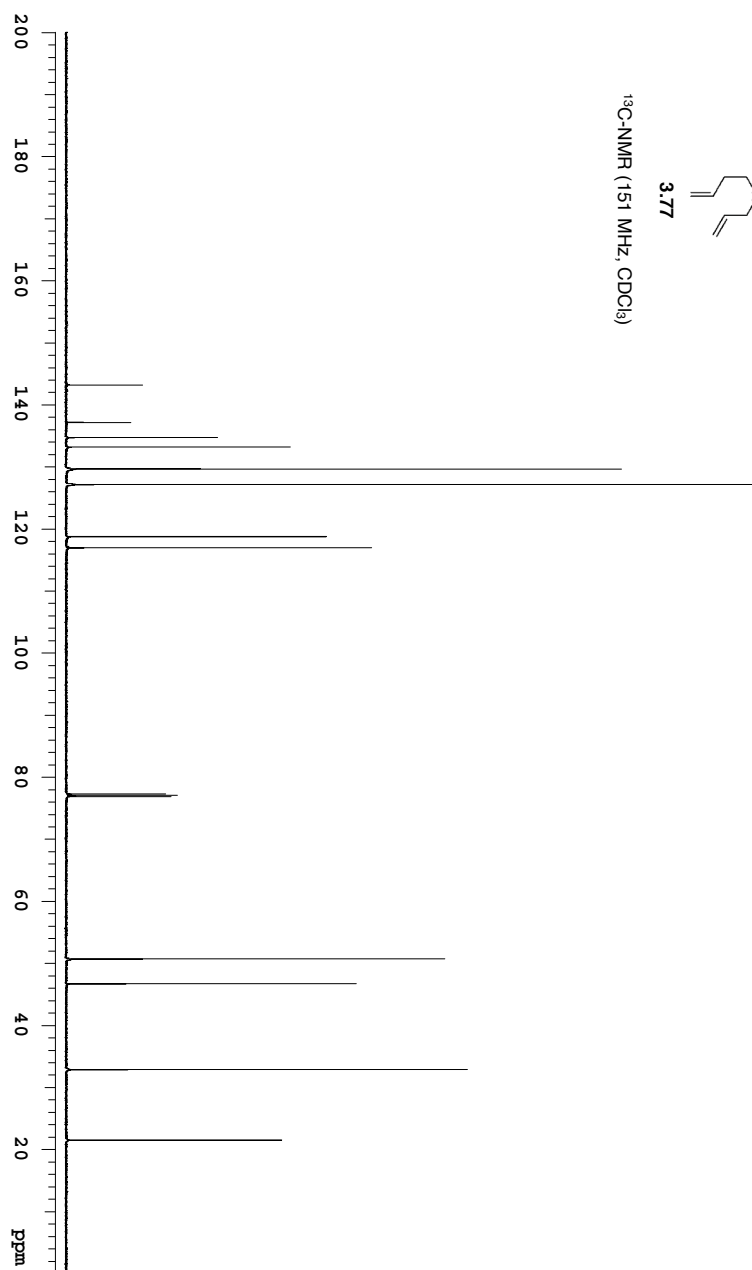
¹H-NMR (600 MHz, CDCl₃)

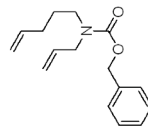




3.77

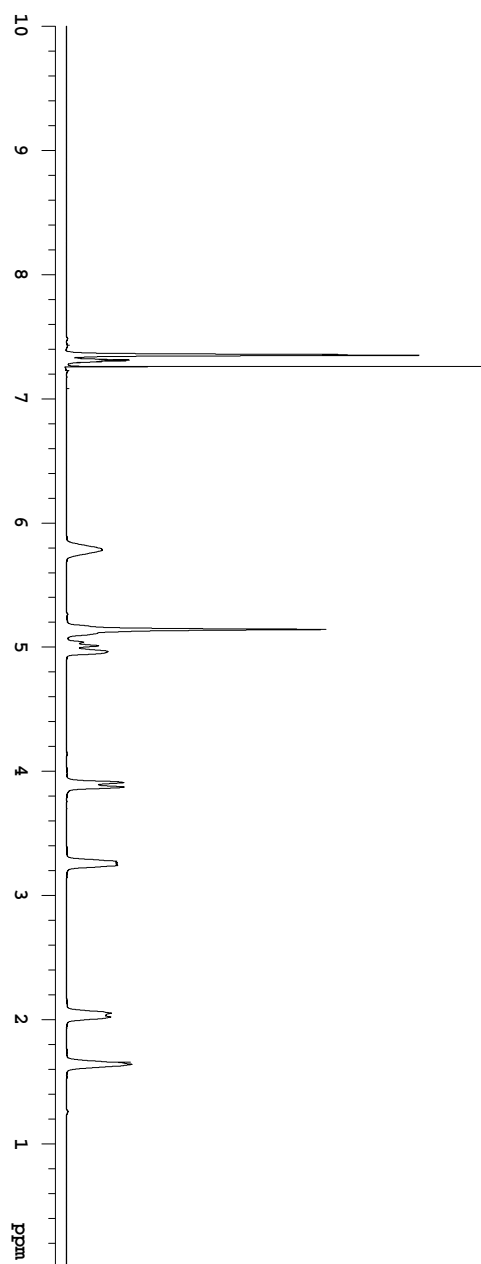
^{13}C -NMR (151 MHz, CDCl_3)

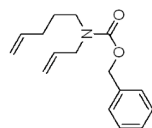




3.83

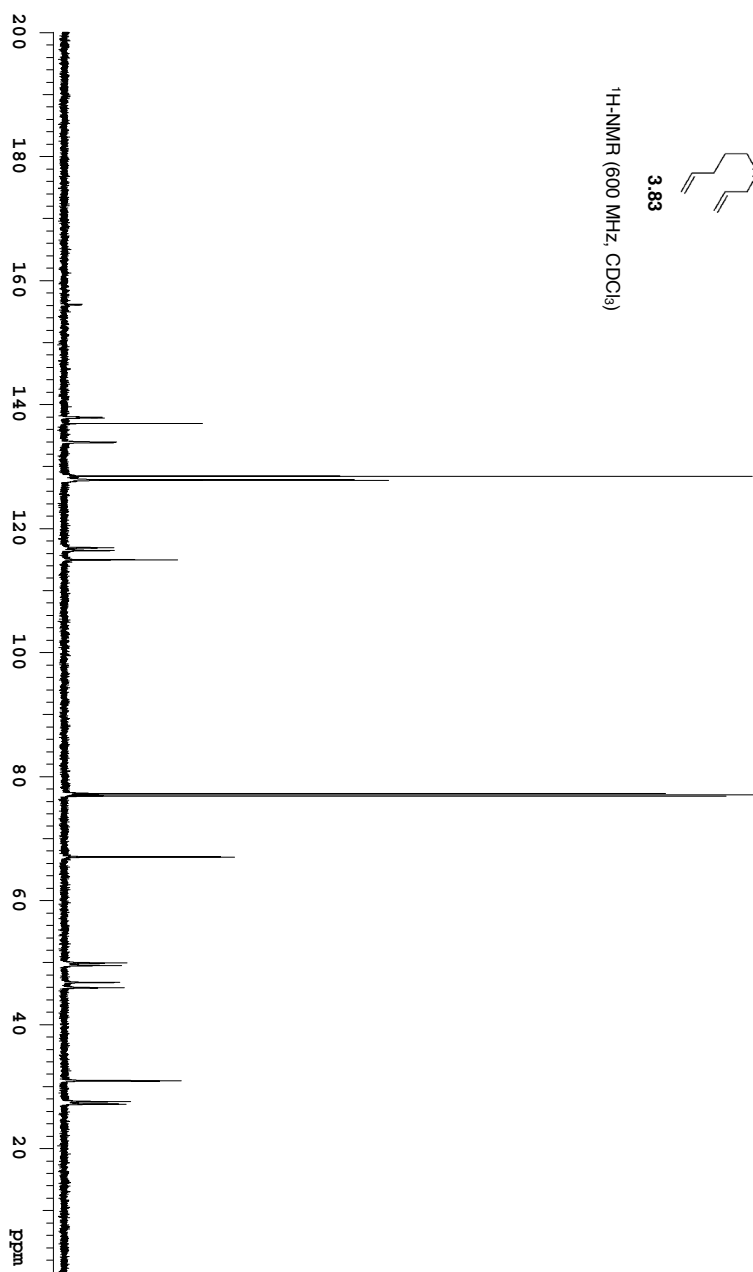
¹H-NMR (600 MHz, CDCl₃)

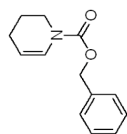




3.83

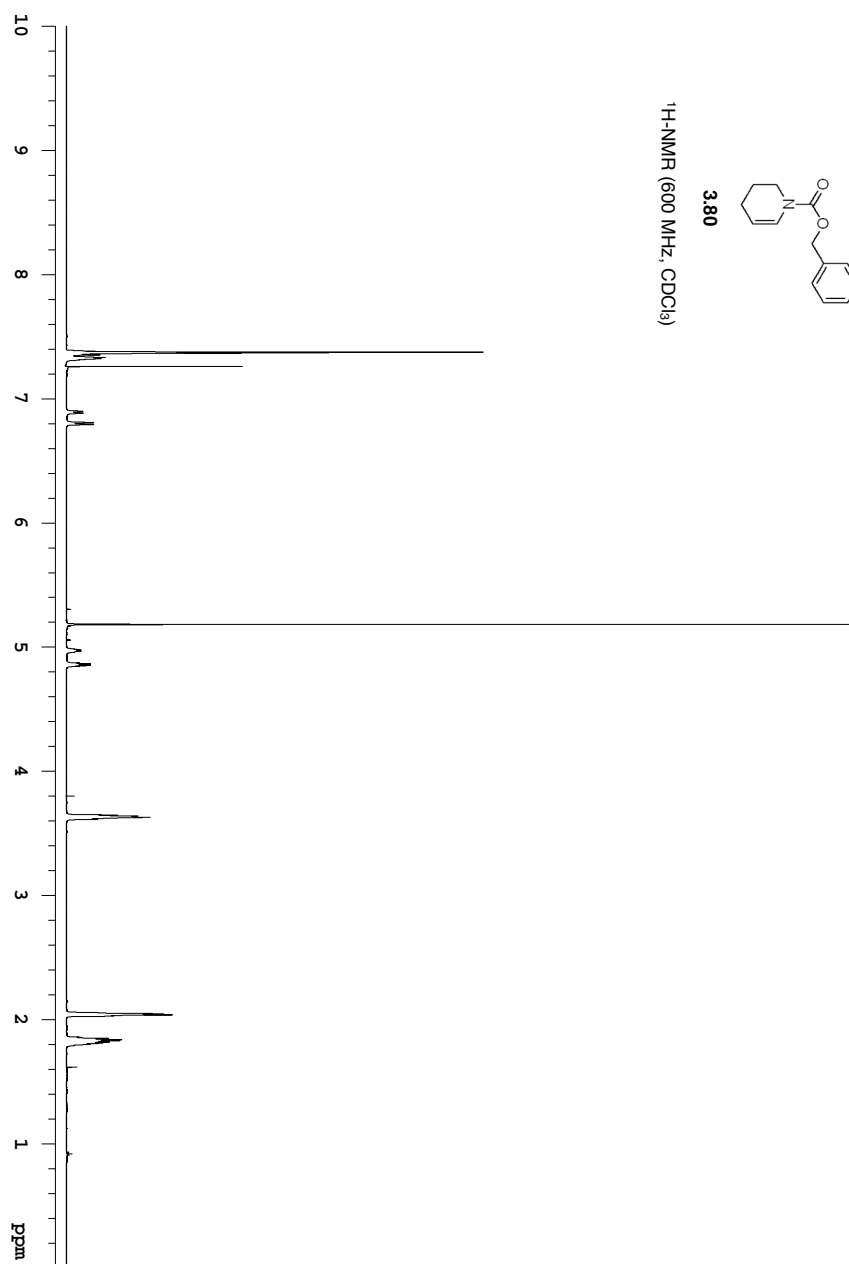
¹H-NMR (600 MHz, CDCl₃)

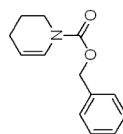




3.80

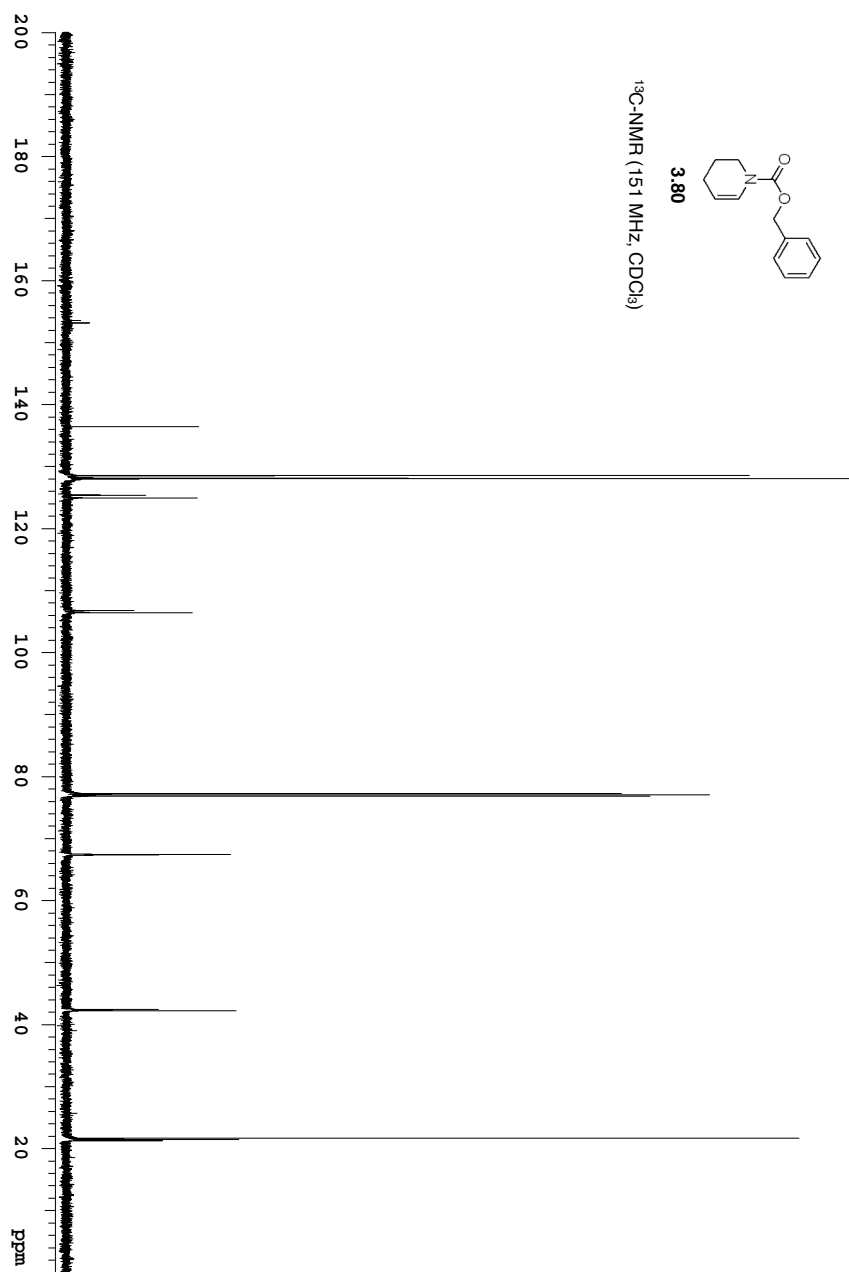
¹H-NMR (600 MHz, CDCl₃)

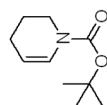




3.80

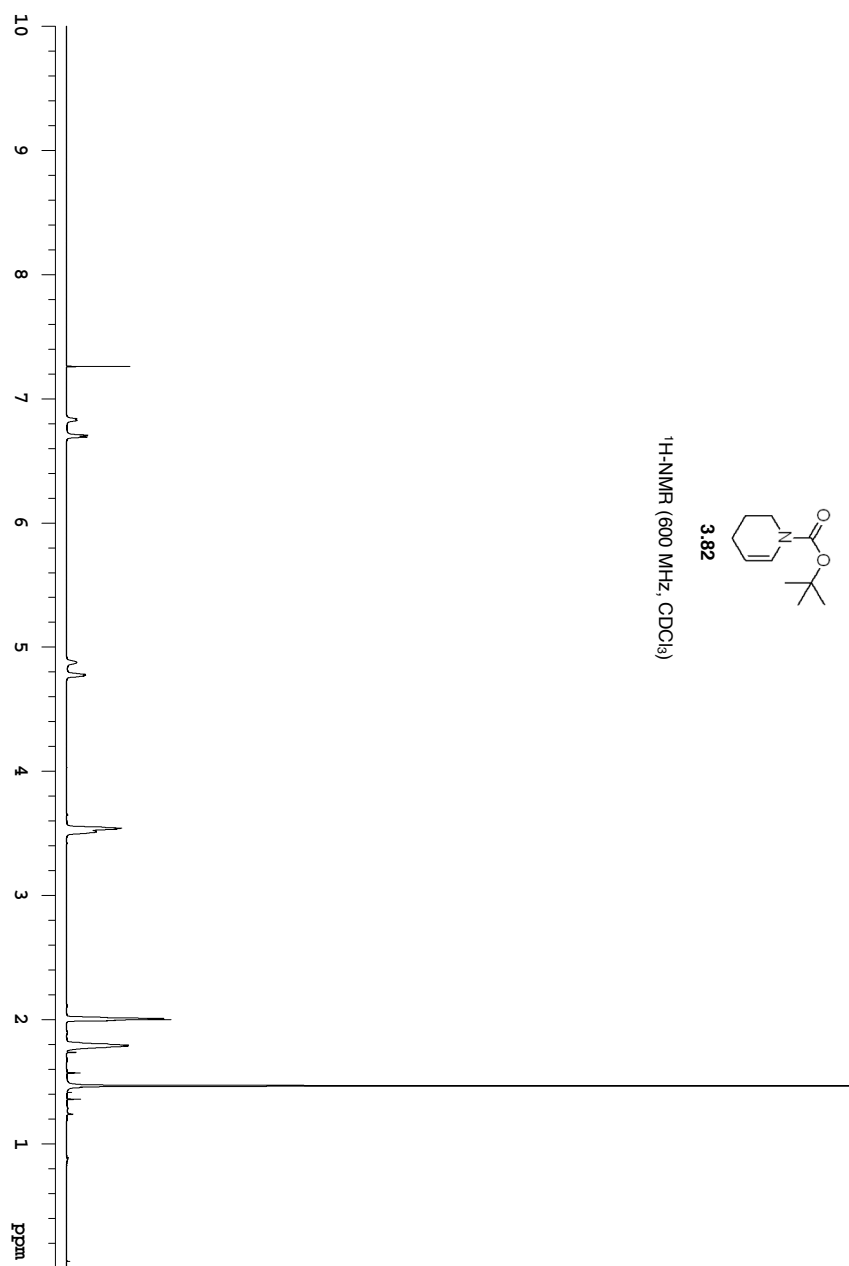
^{13}C -NMR (151 MHz, CDCl_3)

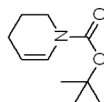




3.82

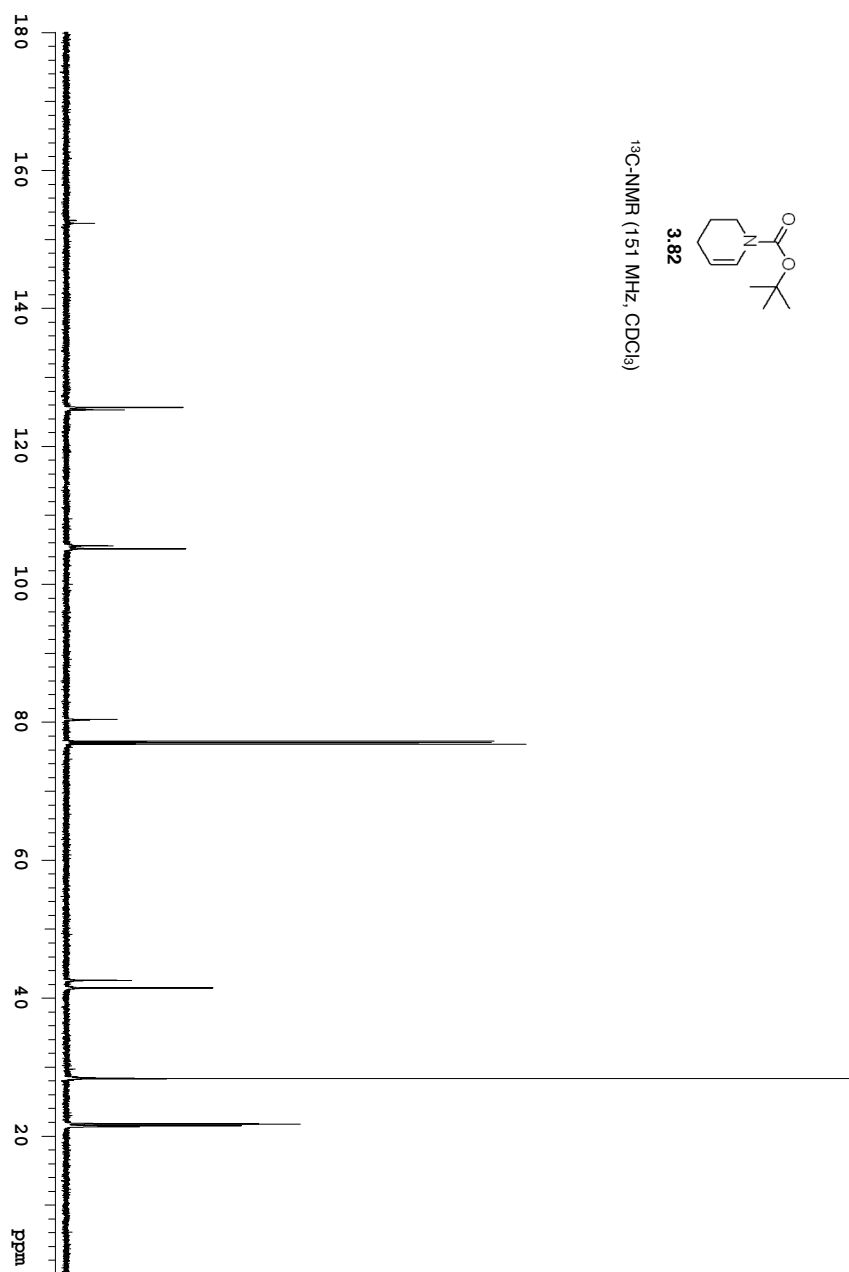
¹H-NMR (600 MHz, CDCl₃)

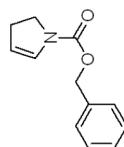




3.82

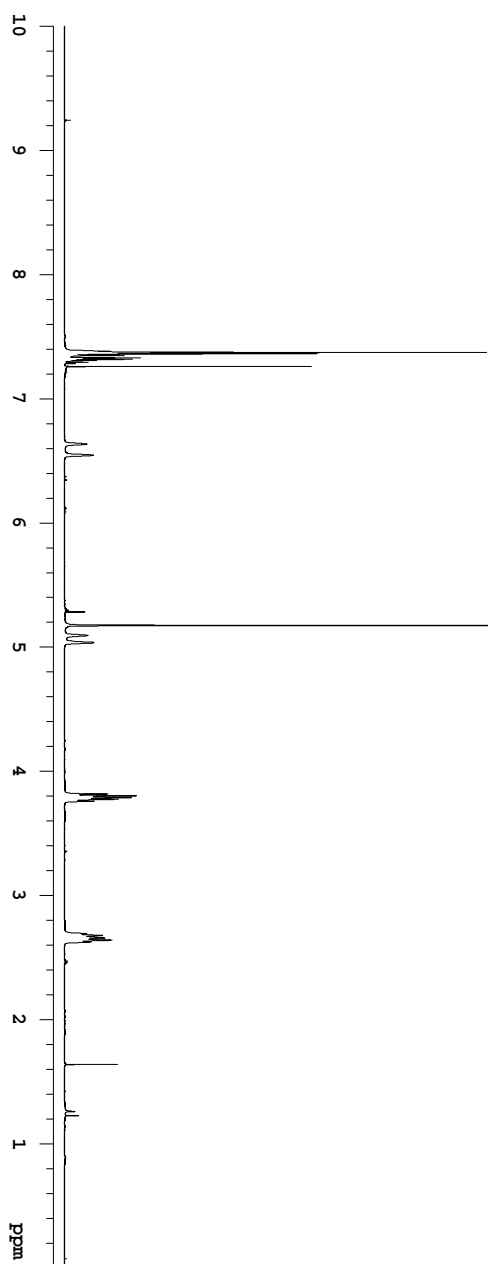
^{13}C -NMR (151 MHz, CDCl_3)

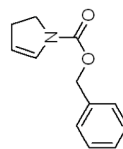




3.86

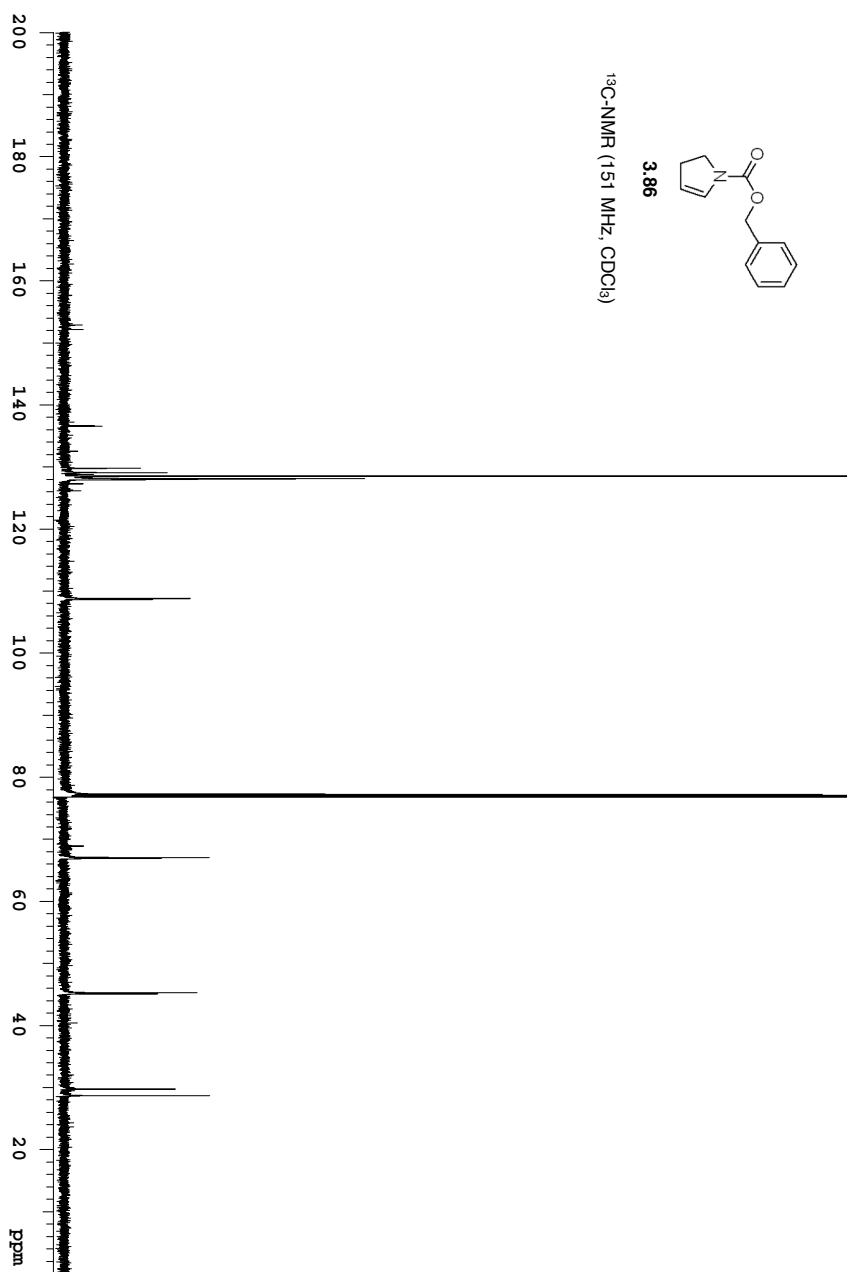
$^1\text{H-NMR}$ (600 MHz, CDCl_3)

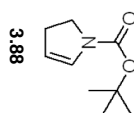




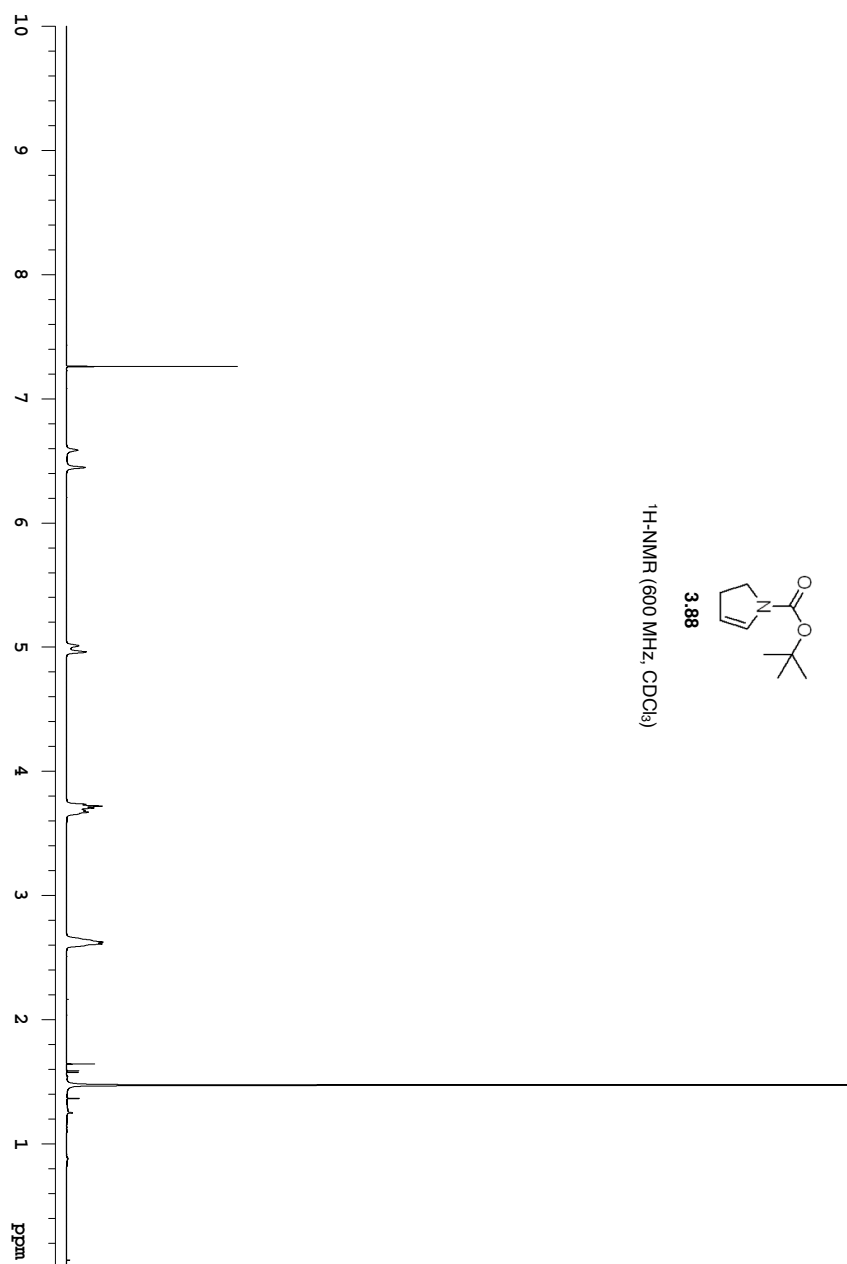
3.86

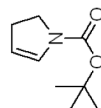
^{13}C -NMR (151 MHz, CDCl_3)





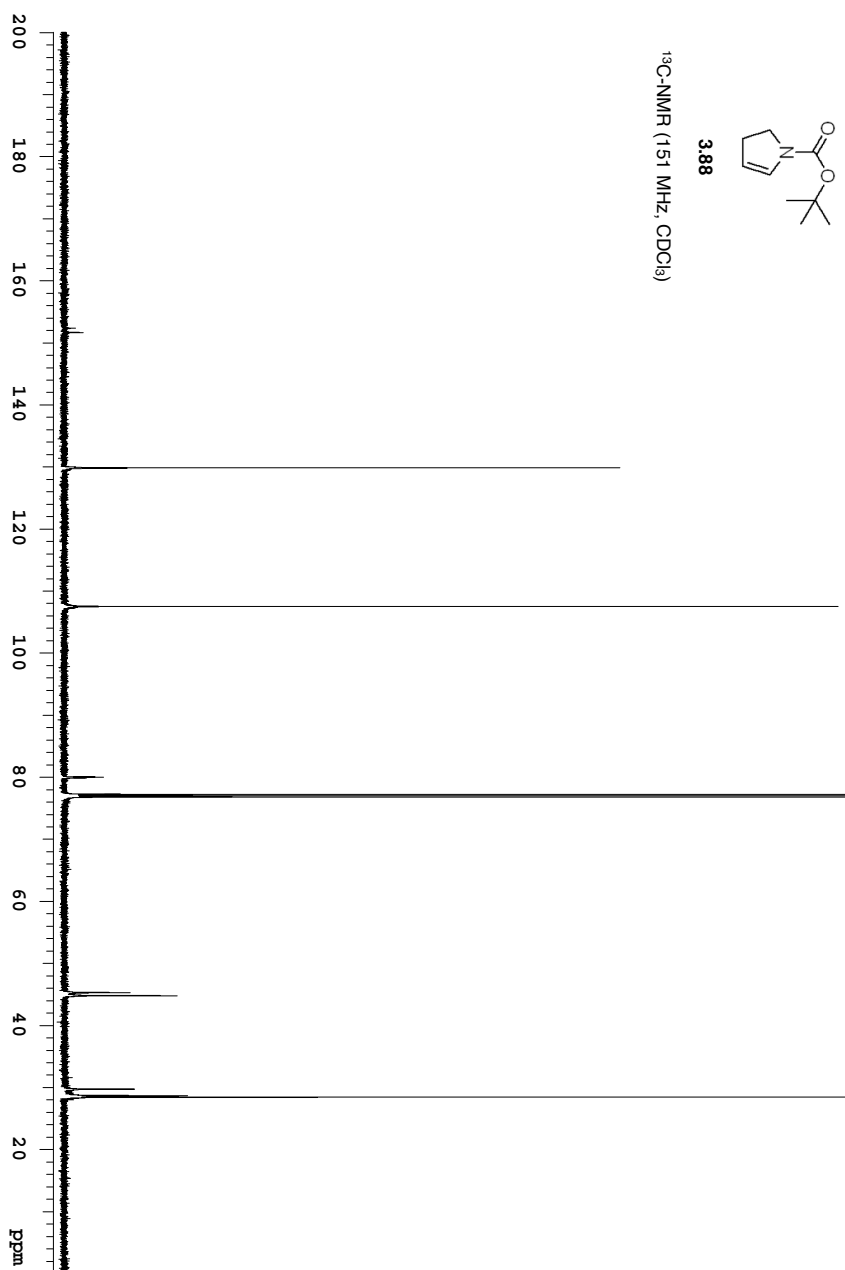
$^1\text{H-NMR}$ (600 MHz, CDCl_3)

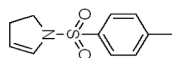




3.88

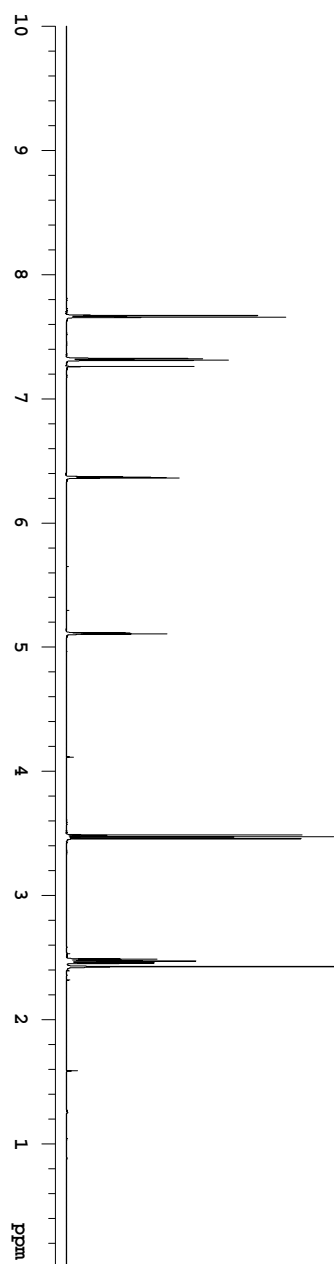
^{13}C -NMR (151 MHz, CDCl_3)

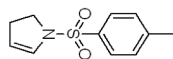




3.90

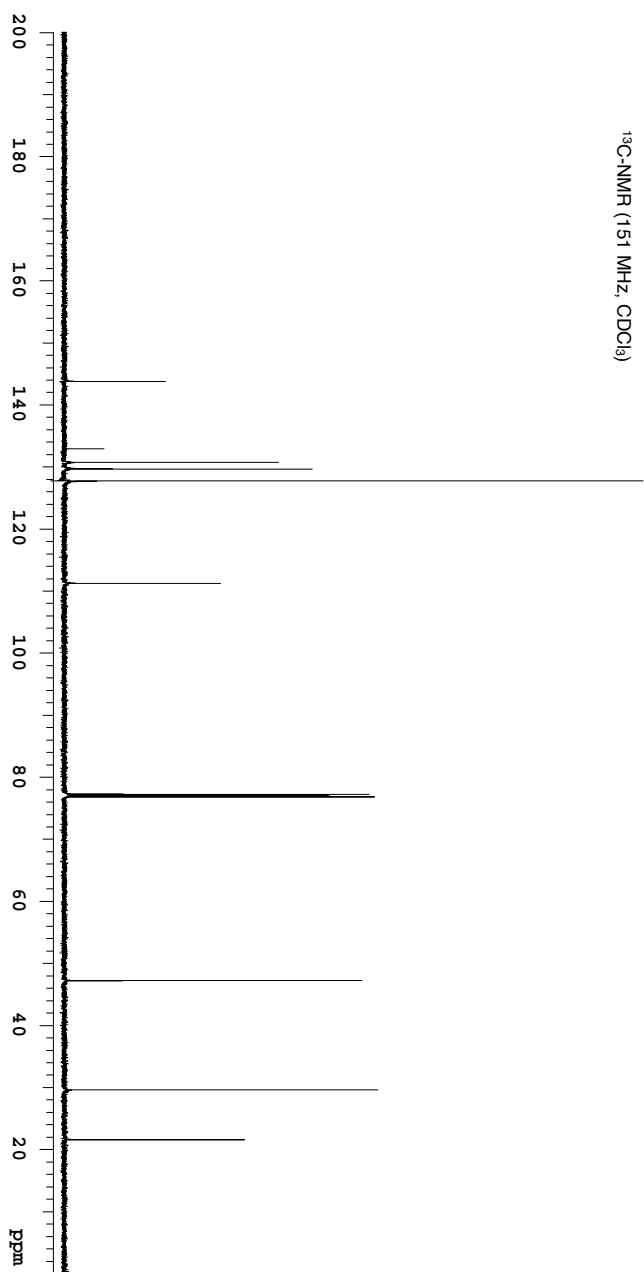
¹H-NMR (600 MHz, CDCl₃)

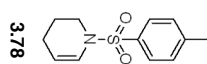




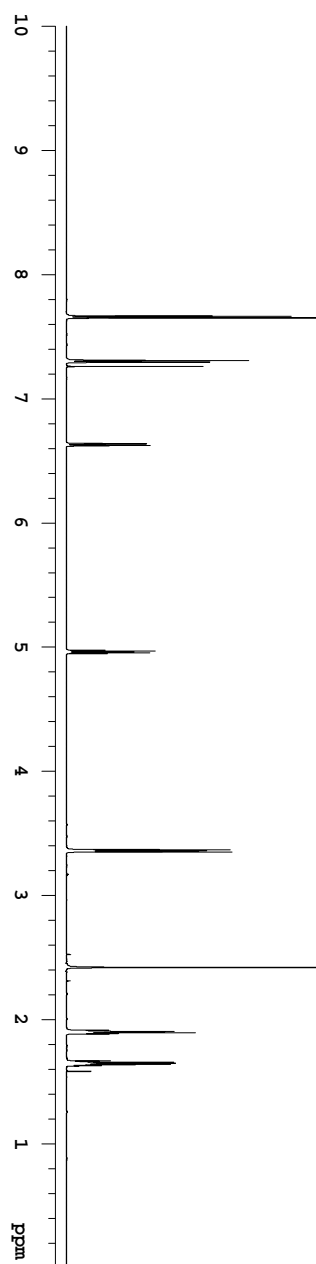
3.90

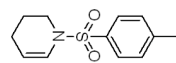
^{13}C -NMR (151 MHz, CDCl_3)





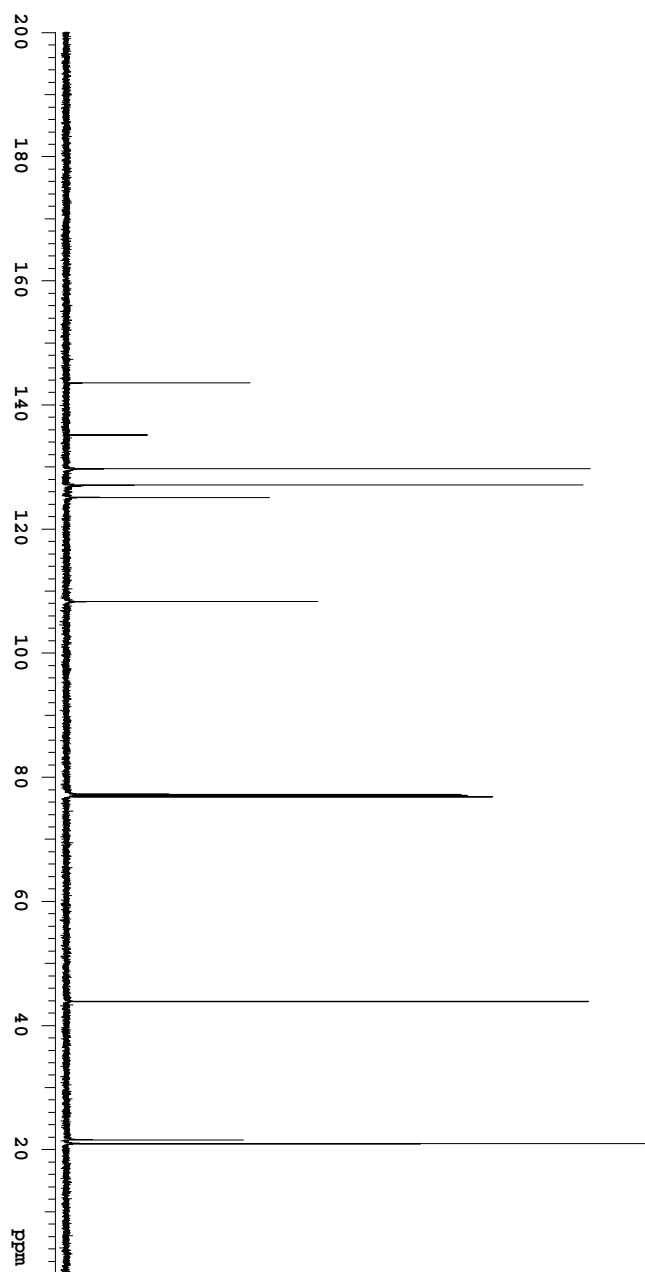
¹H-NMR (600 MHz, CDCl₃)

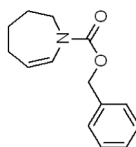




3.78

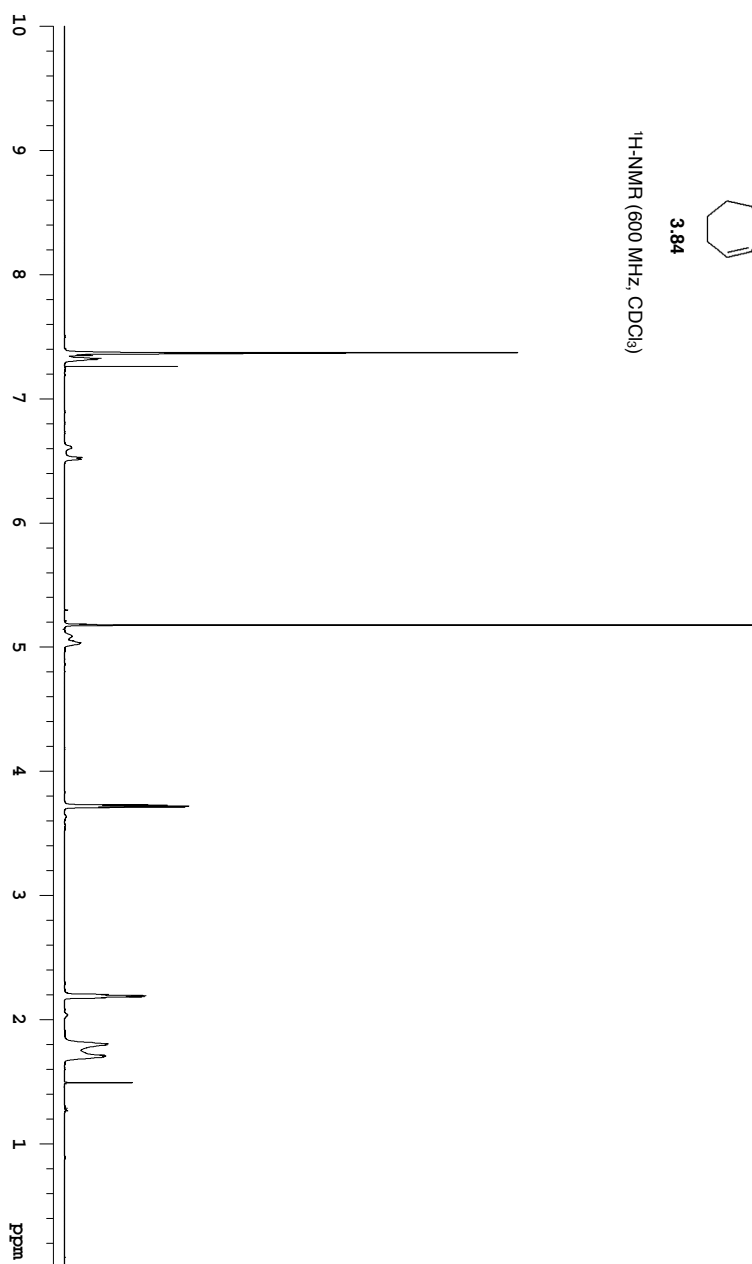
^{13}C -NMR (151 MHz, CDCl_3)

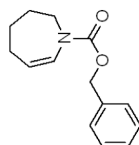




3.84

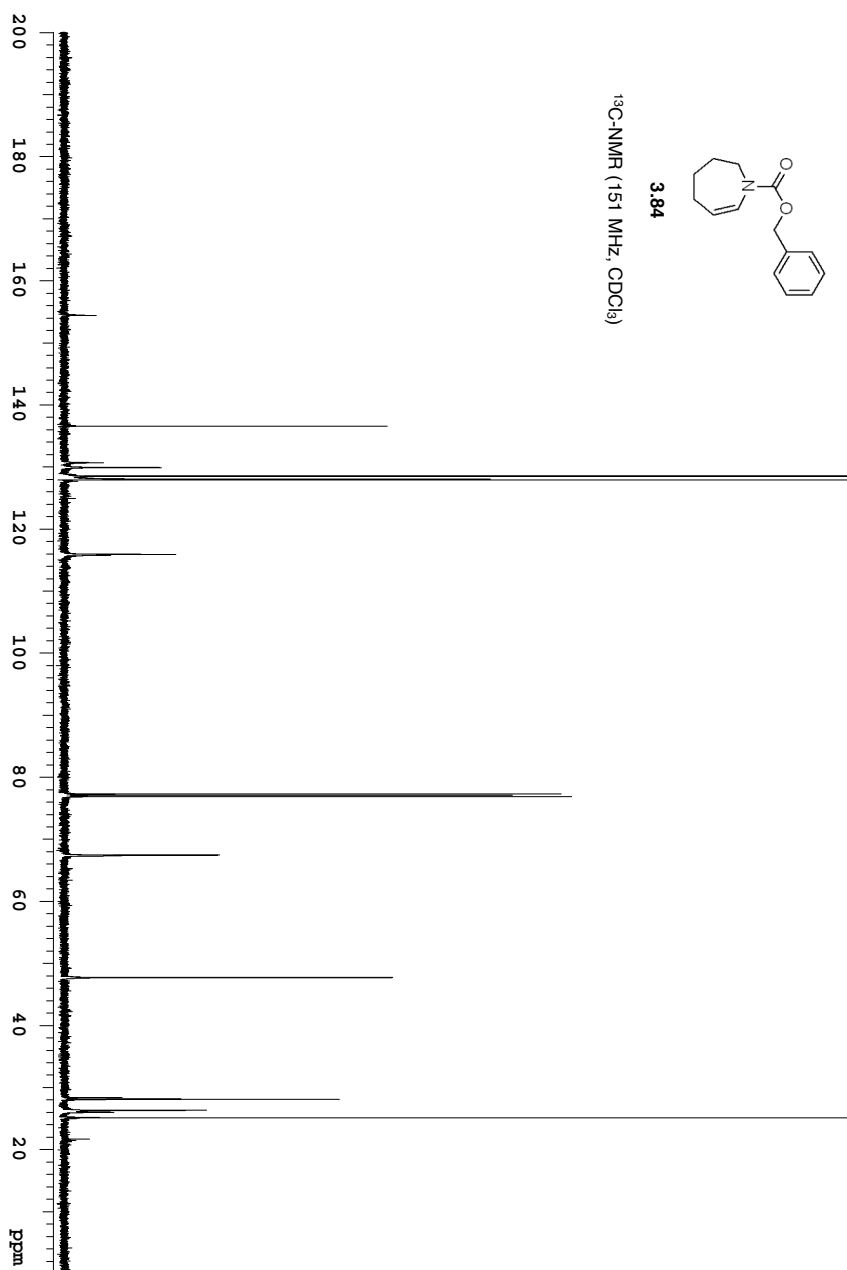
¹H-NMR (600 MHz, CDCl₃)

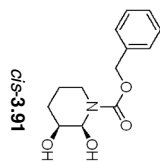




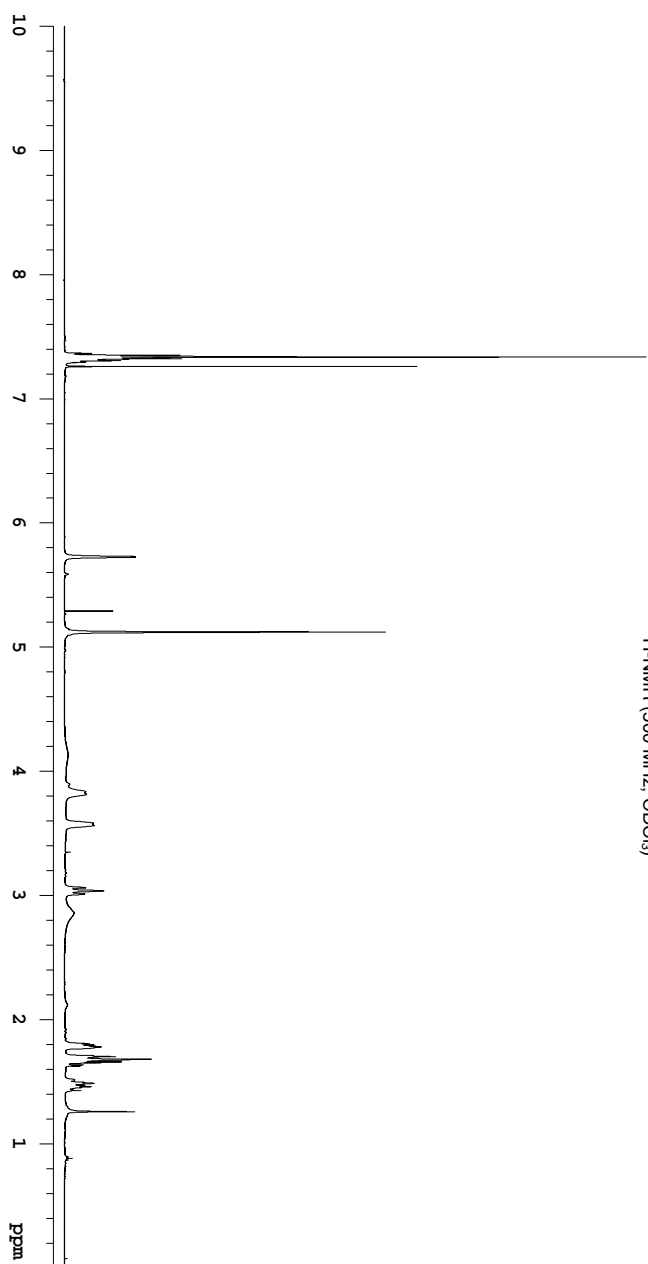
3.84

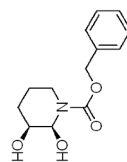
^{13}C -NMR (151 MHz, CDCl_3)





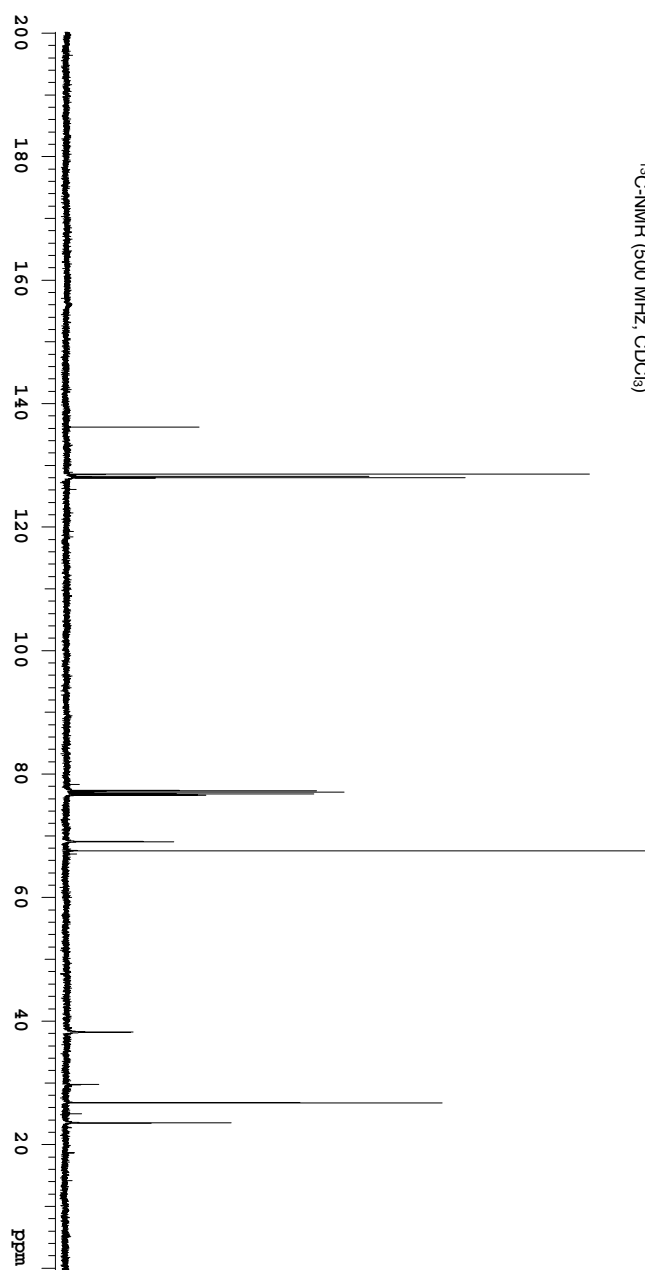
¹H-NMR (500 MHz, CDCl₃)

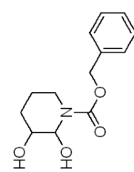




cis-**3.91**

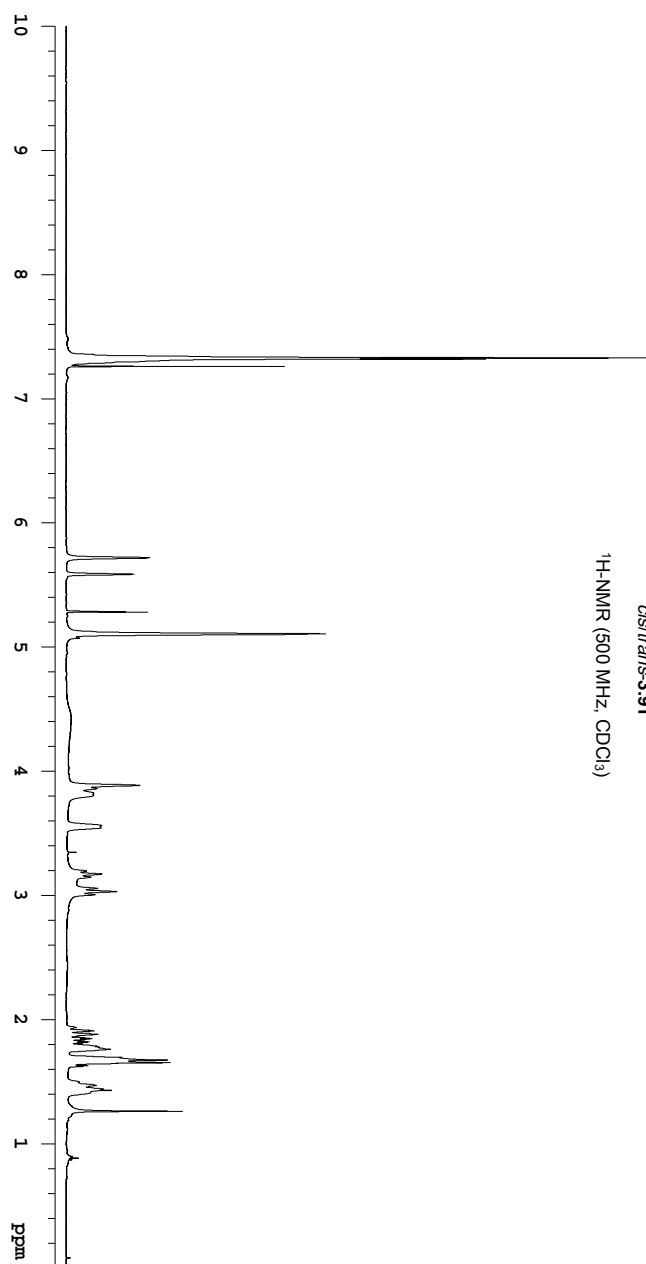
^{13}C -NMR (500 MHz, CDCl_3)

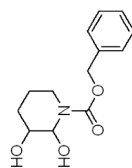




cis/trans-**3.91**

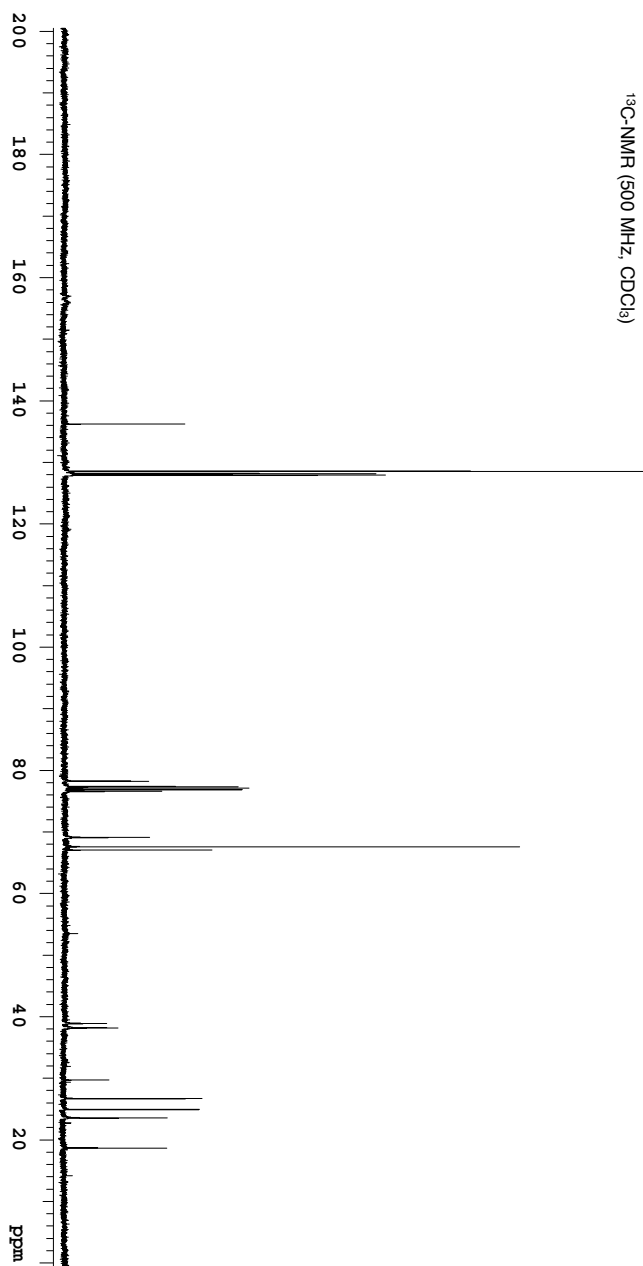
^1H -NMR (500 MHz, CDCl_3)

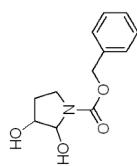




cis/trans-**3.91**

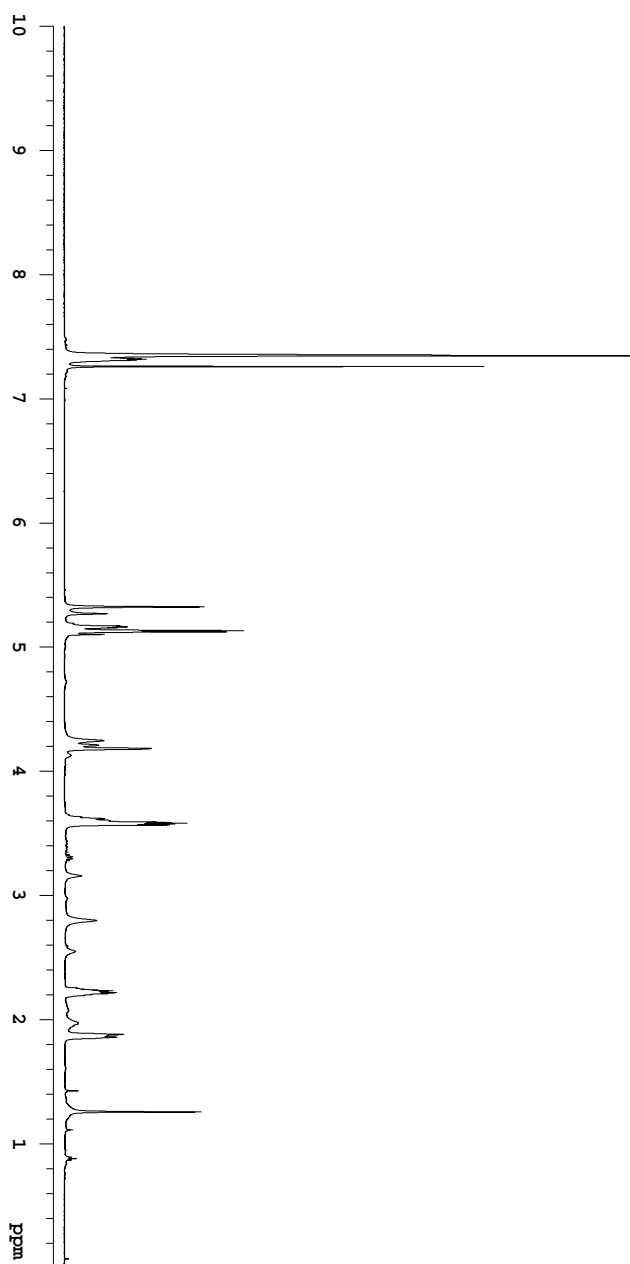
^{13}C -NMR (500 MHz, CDCl_3)

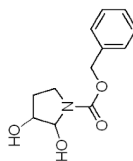




cis/trans-3.95

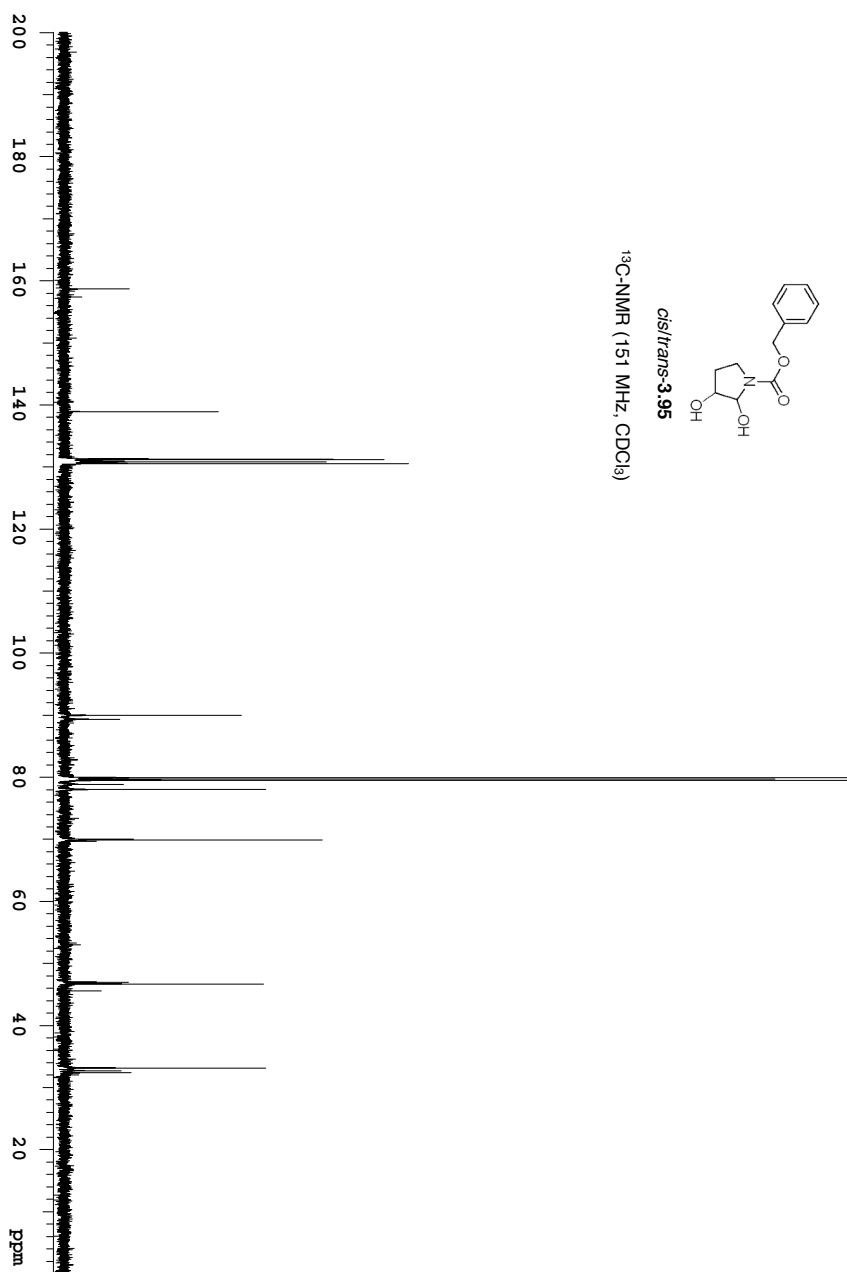
¹H-NMR (600 MHz, CDCl₃)

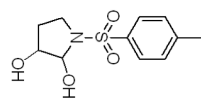




cis/trans-3.95

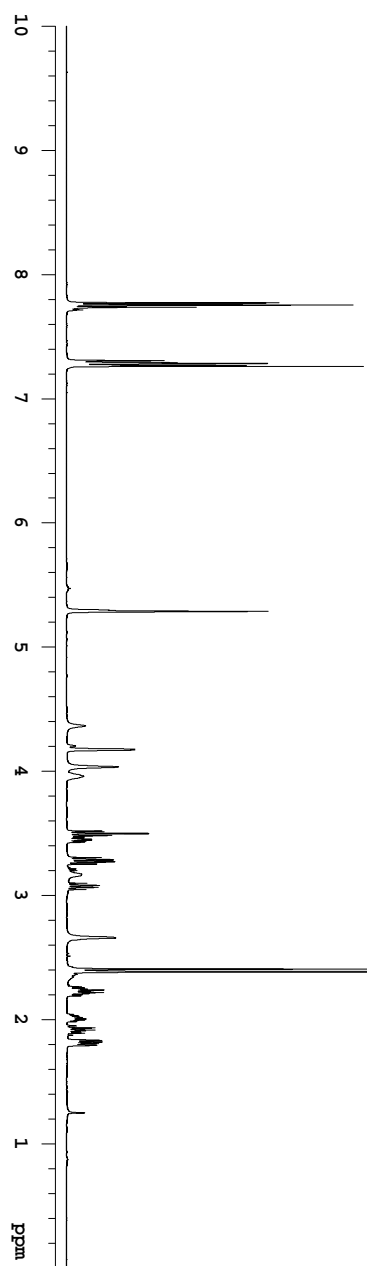
^{13}C -NMR (151 MHz, CDCl_3)

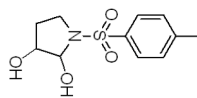




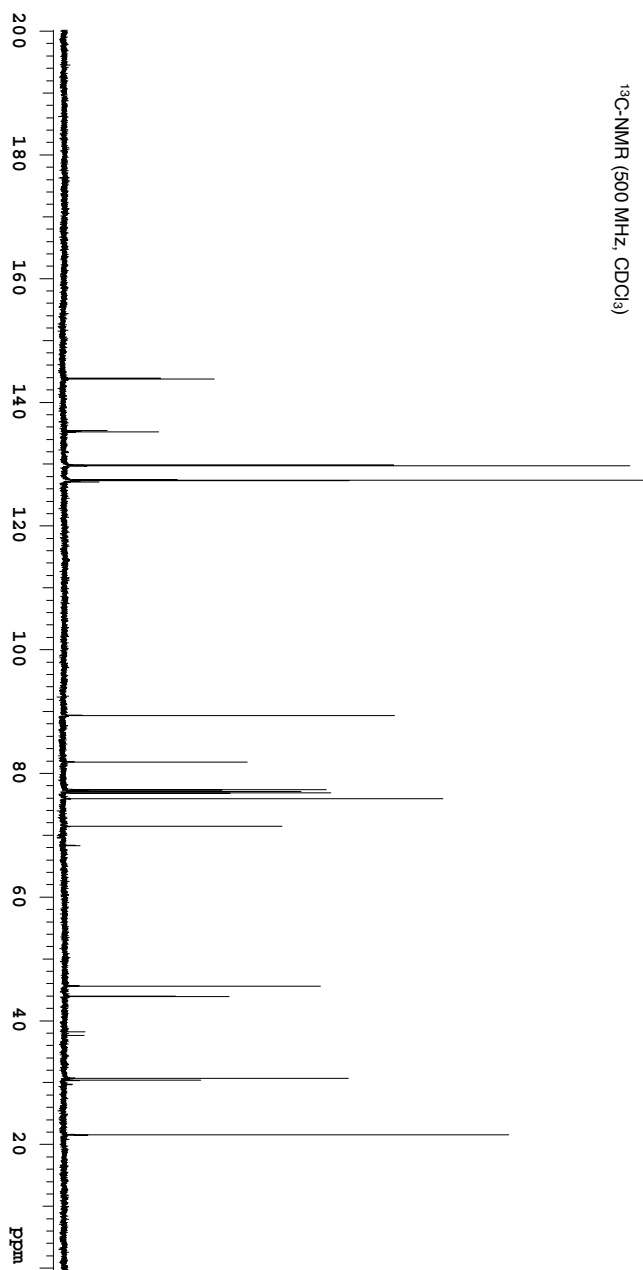
cis/trans-**3.96**

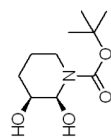
$^1\text{H-NMR}$ (500 MHz, CDCl_3)





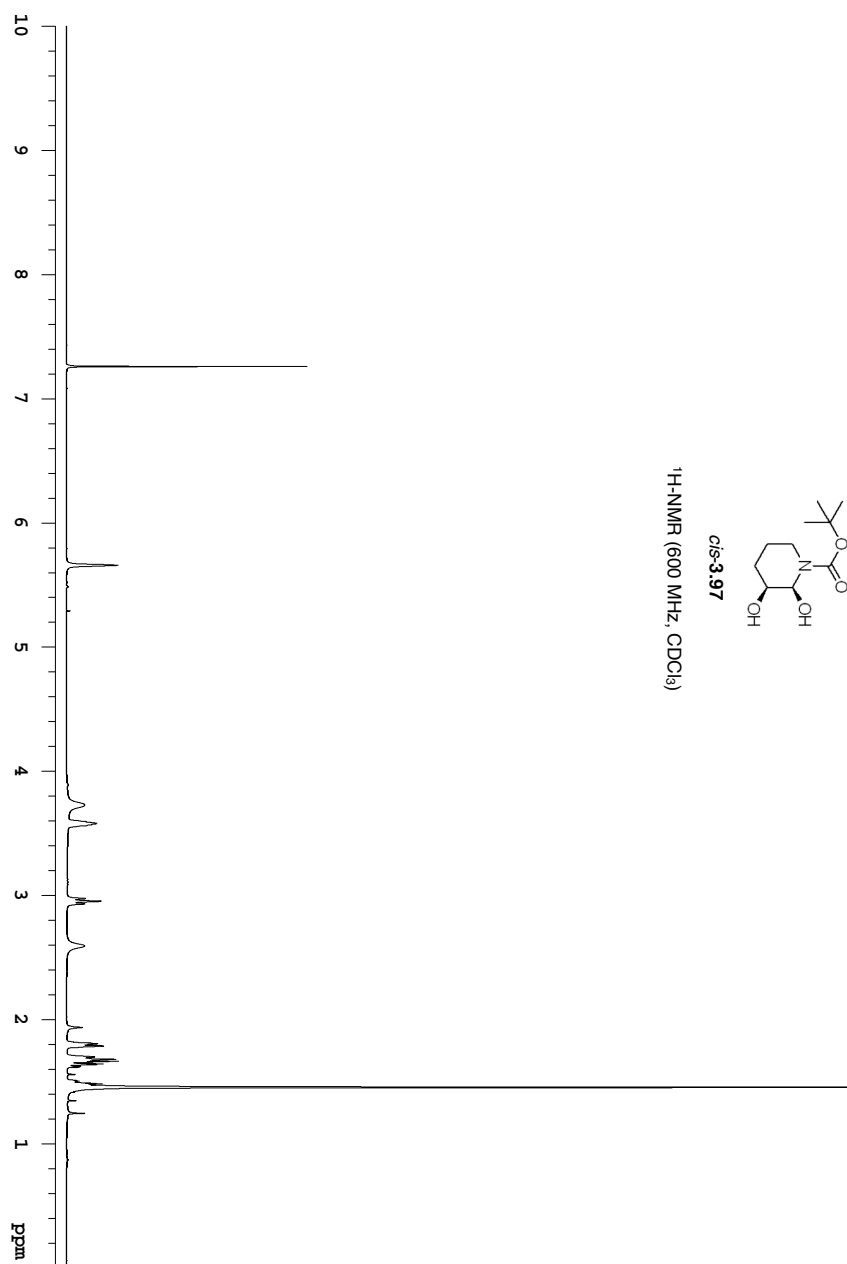
cis/trans-**3,96**
 ^{13}C -NMR (500 MHz, CDCl_3)

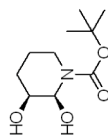




cis-**3.97**

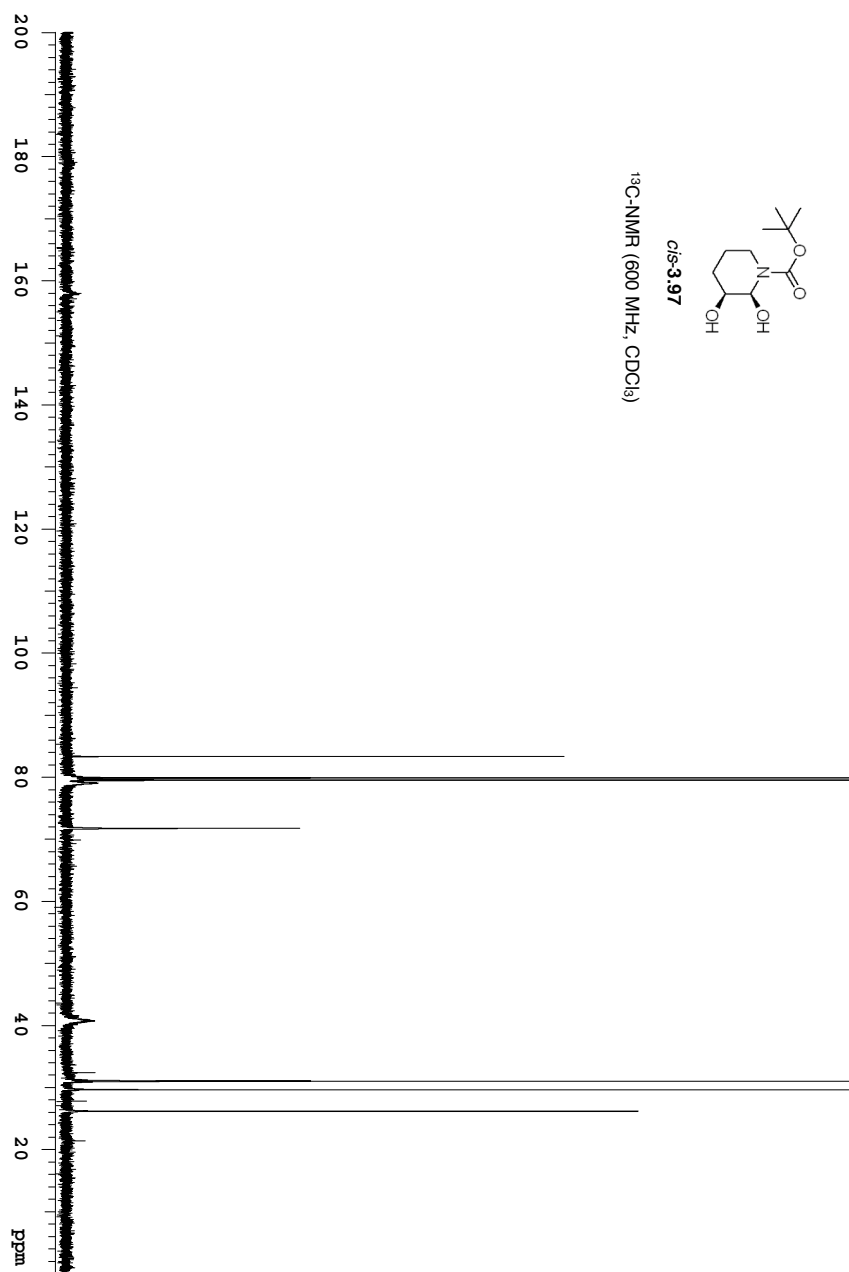
¹H-NMR (600 MHz, CDCl₃)

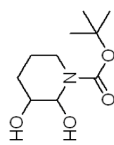




cis-**3.97**

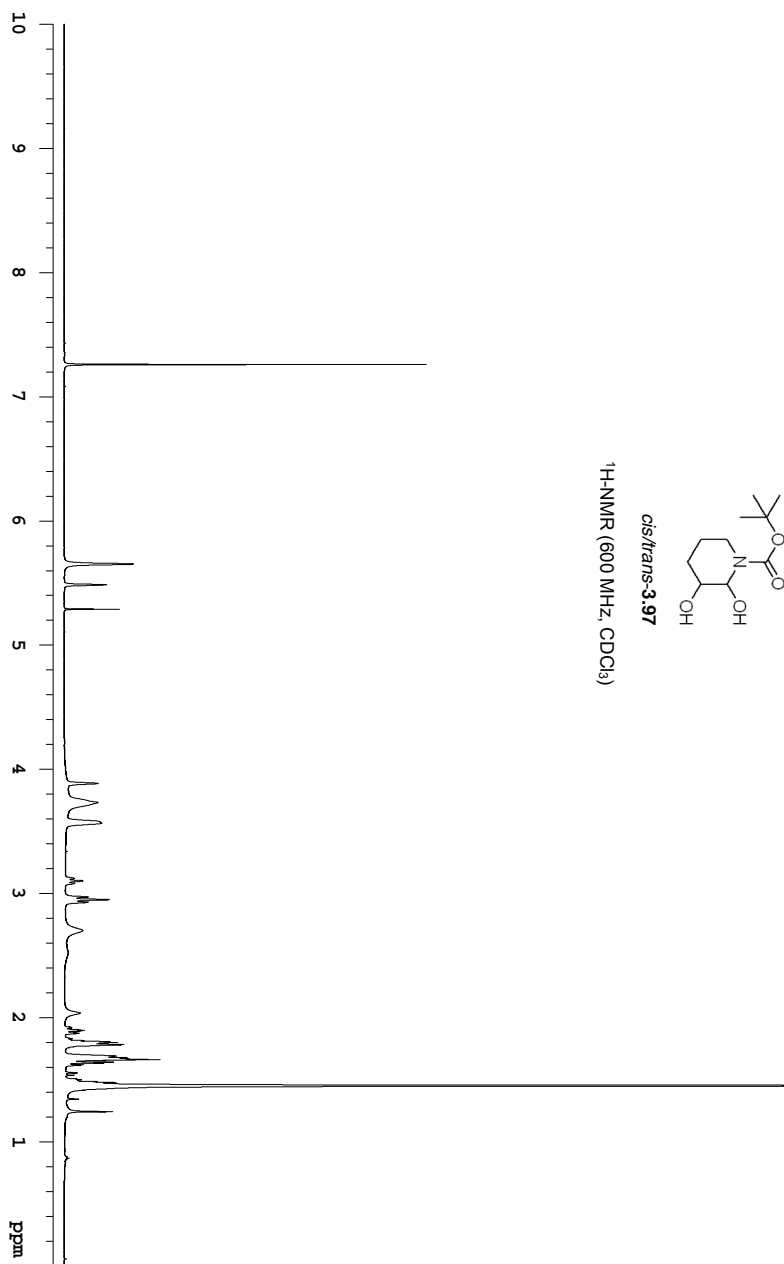
¹³C-NMR (600 MHz, CDCl₃)

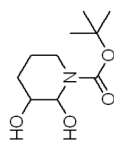




cis/trans-**3.97**

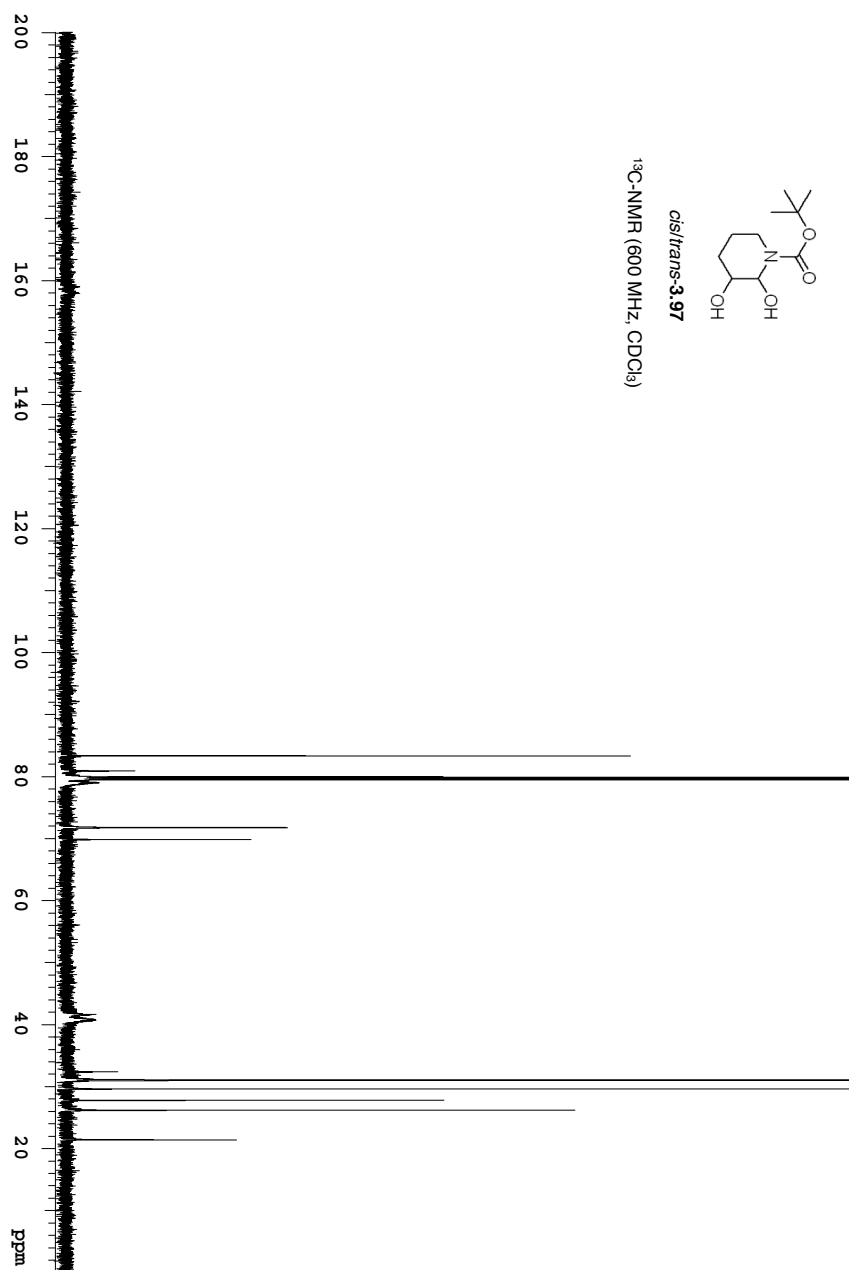
¹H-NMR (600 MHz, CDCl₃)

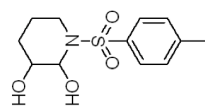




cis/trans-**3.97**

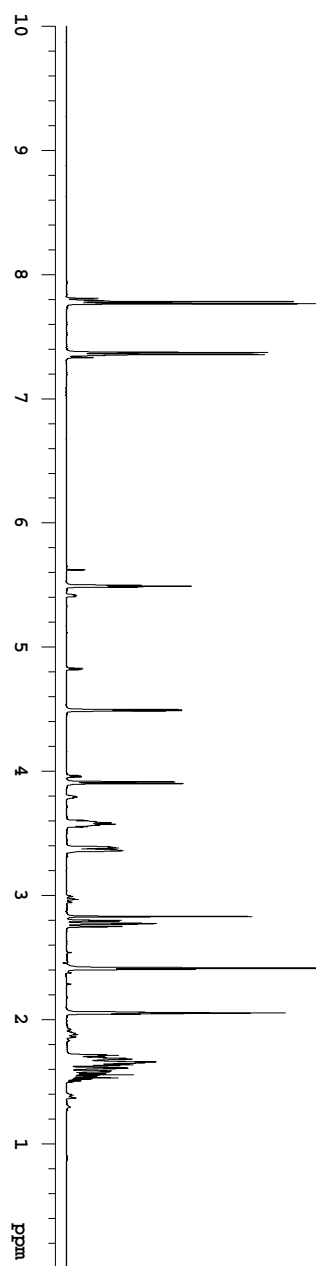
^{13}C -NMR (600 MHz, CDCl_3)

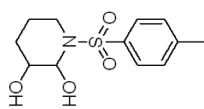




cis/trans-**3,98**

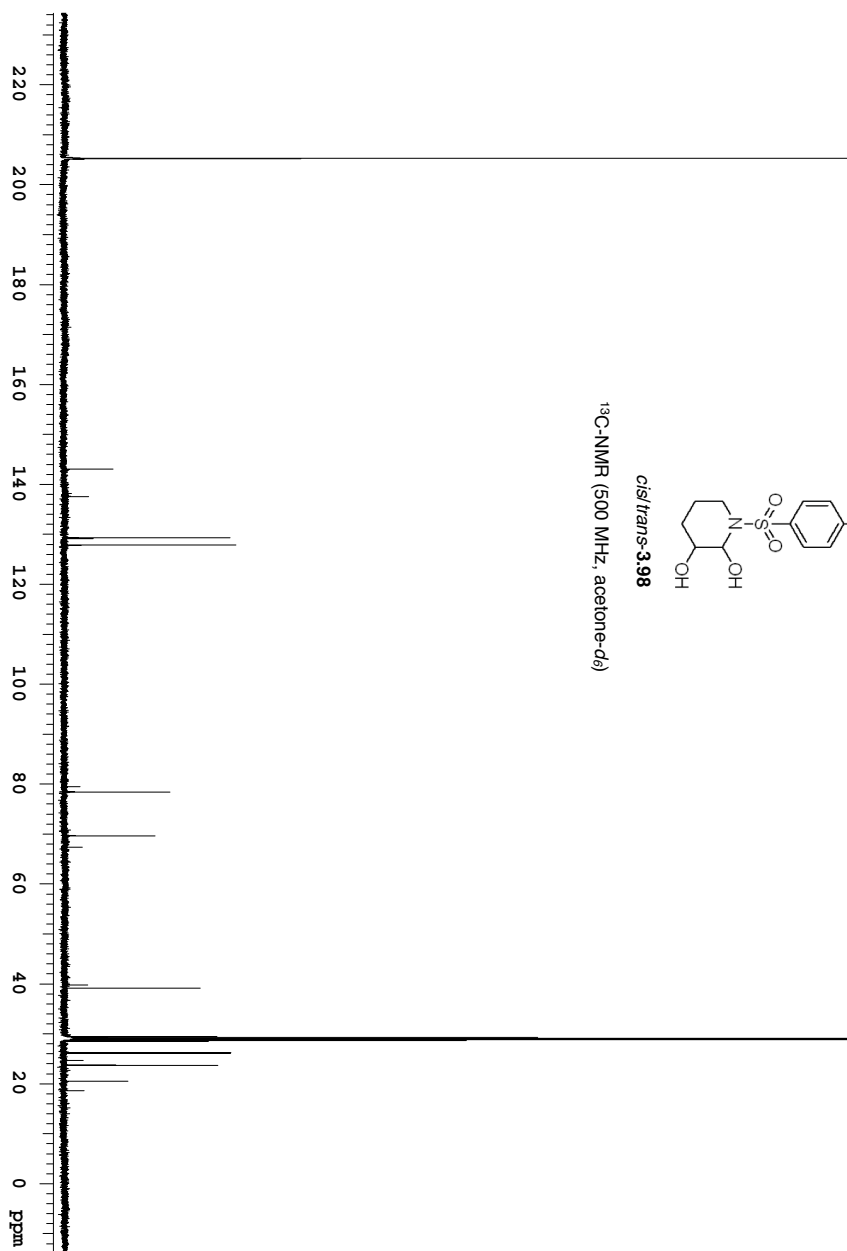
$^1\text{H-NMR}$ (500 MHz, acetone- d_6)

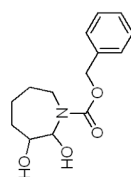




cis/trans-3,98

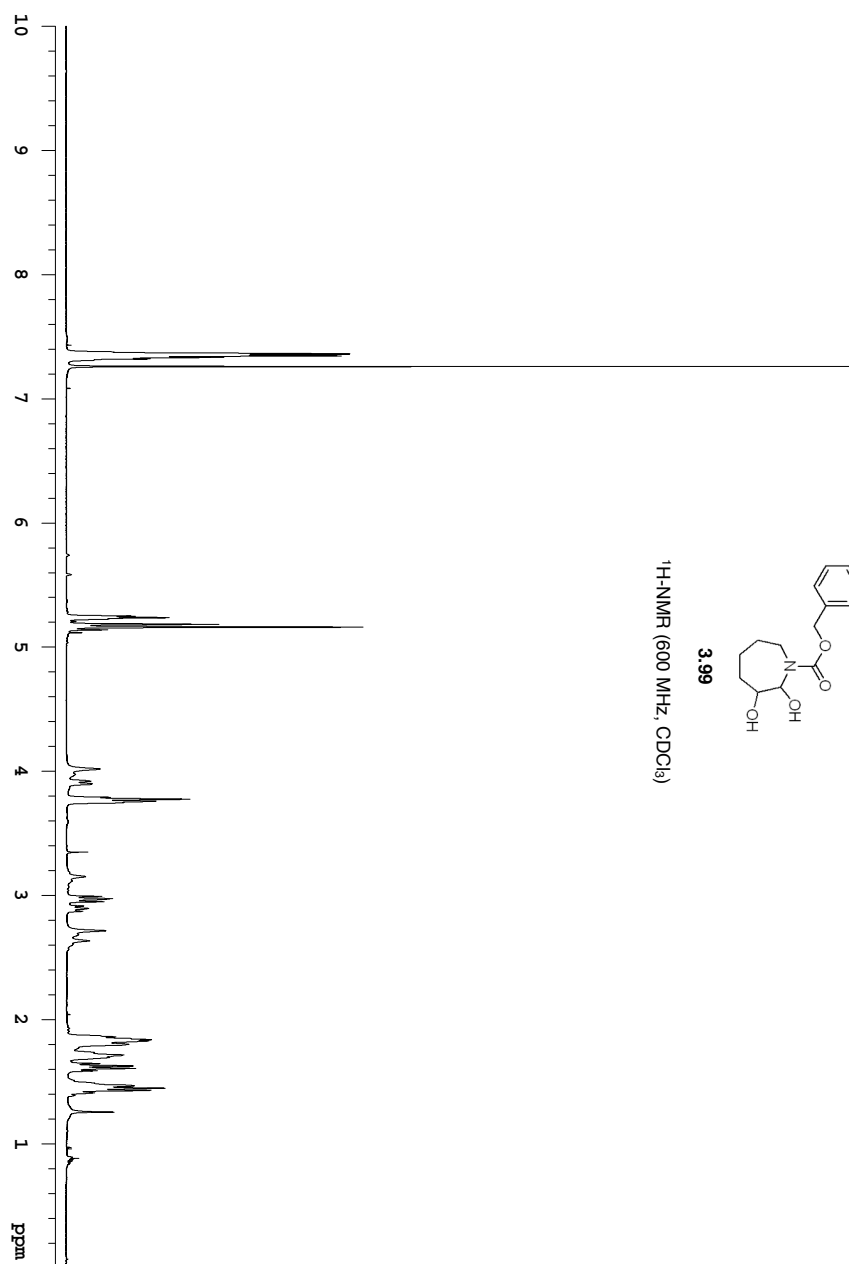
^{13}C -NMR (500 MHz, acetone- d_6)

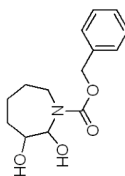




3.99

¹H-NMR (600 MHz, CDCl₃)





3.99

^{13}C -NMR (600 MHz, CDCl_3)

